

Université de Montréal

**Polysaccharide-based Polyion Complex Micelles as New
Delivery Systems for Hydrophilic Cationic Drugs**

par

Ghareb Mohamed Soliman

Faculté de Pharmacie

Thèse présentée à la Faculté des études supérieures
en vue de l'obtention du grade de Philosophiae Doctor (Ph. D.)
en Sciences Pharmaceutiques
option Chimie Médicinale

Août 2009

© Ghareb Mohamed Soliman, 2009

Université de Montréal
Faculté des études supérieures

Cette thèse intitulée :

Polysaccharide-based Polyion Complex Micelles as New Delivery Systems for Hydrophilic
Cationic Drugs

présentée par :

Ghareb Mohamed Soliman

a été évaluée par un jury composé des personnes suivantes :

Dr. Maxime Ranger, président-rapporteur

Dr. Françoise M. Winnik, directeur de recherche

Dr. Grégoire Leclair, membre du jury

Dr. François Ravenelle, examinateur externe

Dr. Martine Raymond, représentant du doyen de la FES

Résumé

Les micelles polyioniques ont émergé comme des systèmes prometteurs de relargage de médicaments hydrophiles ioniques. Le but de cette étude était le développement des micelles polyioniques à base de dextrane pour la relargage de médicaments hydrophiles cationiques utilisant une nouvelle famille de copolymères bloc carboxymethyldextran-poly(éthylène glycol) (CMD-PEG). Quatre copolymères CMD-PEG ont été préparés dont deux copolymères identiques en termes de longueurs des blocs de CMD et de PEG mais différent en termes de densité de charges du bloc CMD; et deux autres copolymères dans lesquels les blocs chargés sont les mêmes mais dont les blocs de PEG sont différents. Les propriétés d'encapsulation des micelles CMD-PEG ont été évaluées avec différentes molécules cationiques: le diminazène (DIM), un médicament cationique modèle, le chlorhydrate de minocycline (MH), un analogue semi-synthétique de la tétracycline avec des propriétés neuro-protectives prometteuses et différents antibiotiques aminoglycosidiques. La cytotoxicité des copolymères CMD-PEG a été évaluée sur différentes lignées cellulaires en utilisant le test MTT et le test du Bleu Alamar. La formation de micelles des copolymères de CMD-PEG a été caractérisée par différentes techniques telles que la spectroscopie RMN ^1H , la diffusion de la lumière dynamique (DLS) et la titration calorimétrique isotherme (ITC). Le taux de relargage des médicaments et l'activité pharmacologique des micelles contenant des médicaments ont aussi été évalués. Les copolymères CMD-PEG n'ont induit aucune cytotoxicité dans les hépatocytes humains et dans les cellules microgliales murines (N9) après 24 h incubation pour des concentrations allant jusqu'à 15 mg/mL. Les interactions électrostatiques entre les copolymères de CMD-PEG et les différentes drogues cationiques ont amorcé la formation de micelles polyioniques avec un cœur composé du complexe CMD-médicaments cationiques et une couronne composée de PEG. Les propriétés des micelles DIM/CMD-PEG ont été fortement dépendantes du degré de carboxyméthylation du bloc CMD. Les micelles de CMD-PEG de degré de carboxyméthylation du bloc CMD $\geq 60\%$, ont incorporé jusqu'à 64 % en poids de DIM et ont résisté à la désintégration induite par les sels et ceci jusqu'à 400 mM NaCl. Par contre, les micelles de CMD-PEG de degré de

II

carboxyméthylation ~ 30% avaient une plus faible teneur en médicament (~ 40 % en poids de DIM) et se désagrégeaient à des concentrations en sel inférieures (~ 100 mM NaCl). Le copolymère de CMD-PEG qui a montré les propriétés micellaires les plus satisfaisantes a été sélectionné comme système de livraison potentiel de chlorhydrate de minocycline (MH) et d'antibiotiques aminoglycosidiques. Les micelles CMD-PEG encapsulantes de MH ou d'aminoglycosides ont une petite taille (< 200 nm de diamètre), une forte capacité de chargement ($\geq 50\%$ en poids de médicaments) et une plus longue période de relargage de médicament. Ces micelles furent stables en solution aqueuse pendant un mois; après lyophilisation et en présence d'albumine sérique bovine. De plus, les micelles ont protégé MH contre sa dégradation en solutions aqueuses. Les micelles encapsulant les drogues ont maintenu les activités pharmacologiques de ces dernières. En outre, les micelles MH réduisent l'inflammation induite par les lipopolysaccharides dans les cellules microgliales murines (N9). Les micelles aminoglycosides ont été quant à elles capable de tuer une culture bactérienne test. Toutefois les micelles aminoglycosides/CMD-PEG furent instables dans les conditions physiologiques. Les propriétés des micelles ont été considérablement améliorées par des modifications hydrophobiques de CMD-PEG. Ainsi, les micelles aminoglycosides/dodecyl-CMD-PEG ont montré une taille plus petite et une meilleure stabilité aux conditions physiologiques. Les résultats obtenus dans le cadre de cette étude montrent que CMD-PEG copolymères sont des systèmes prometteurs de relargage de médicaments cationiques.

Mots-clés : Dextrane, Micelles polyioniques, Diminazène, Médicaments hydrophiles, Minocycline, Neuro-inflammation, Aminoglycosides, Stabilité des micelles.

Abstract

Polyion complex (PIC) micelles have emerged as promising delivery systems of ionic hydrophilic drugs. It was the aim of this study to develop dextran-based PIC micelles for the delivery of hydrophilic cationic drugs using a new family of carboxymethyl-dextran-*block*-poly(ethylene glycol) (CMD-PEG) copolymers. Four CMD-PEG copolymers were prepared: (i) two copolymers identical in terms of the length of CMD and PEG blocks, but different in terms of the charge density of the CMD block; and (ii) two copolymers in which the charged block is the same, but the PEG block is of different molecular weight. The micellization of CMD-PEG copolymers and drug delivery aspects of the resulting micelles were evaluated using different cationic drugs: diminazene (DIM), a model cationic drug, minocycline hydrochloride (MH), a semisynthetic tetracycline antibiotic with promising neuroprotective properties and different aminoglycoside antibiotics. The cytotoxicity of CMD-PEG copolymers was evaluated in different cell lines using MTT and Alamar blue assays. CMD-PEG micelles encapsulating different drugs were characterized using different techniques, such as ^1H NMR spectroscopy, dynamic light scattering (DLS), and isothermal titration calorimetry (ITC). The pattern of drug release and pharmacological activity of micelles-encapsulated drugs were also evaluated. The CMD-PEG copolymers did not induce cytotoxicity in human hepatocytes and murine microglia (N9) in concentrations as high as 15 mg/mL after incubation for 24 h. Electrostatic interactions between CMD-PEG copolymers and different cationic drugs triggered the formation of PIC micelles with a CMD/drug core and a PEG corona. The properties of DIM/CMD-PEG micelles were strongly dependent on the degree of carboxymethylation of the CMD block. Micelles of CMD-PEG copolymers having degree of carboxymethylation $\geq 60\%$, incorporated up to 64 wt% DIM, resisted salt-induced disintegration in solutions up to 400 mM NaCl and sustained DIM release under physiological conditions (pH 7.4, 150 mM NaCl). In contrast, micelles of CMD-PEG of degree of carboxymethylation $\sim 30\%$ had lower drug content (~ 40 wt% DIM) and disintegrated at lower salt concentration (~ 100 mM NaCl). The CMD-PEG copolymer that showed the most satisfactory micellar properties, in terms of high drug loading capacity, sustained drug release and micelles

stability was selected as a potential delivery system of minocycline hydrochloride (MH) and different aminoglycosides. CMD-PEG micelles encapsulating either MH or aminoglycosides had small size (< 200 nm in diameter), high drug loading capacity (≥ 50 wt% drug) and sustained drug release. These micelles were stable in aqueous solution for up to one month, after freeze drying and in the presence of bovine serum albumin. Furthermore, the micelles protected MH against degradation in aqueous solutions. Micelles-encapsulated drugs maintained their pharmacological activity where MH micelles reduced lipopolysaccharides-induced inflammation in murine microglia (N9) cells. And aminoglycosides micelles were able to kill a test micro-organism (*E. coli* X-1 blue strain) in culture. Aminoglycosides/CMD-PEG micelles were unstable under physiological conditions. Micelle properties were greatly enhanced by hydrophobic modification of CMD-PEG. Thus, aminoglycosides/dodecyl-CMD-PEG micelles showed smaller size and better stability under physiological conditions. The results obtained in this study show that CMD-PEG copolymers are promising delivery systems for cationic hydrophilic drugs.

Keywords : Dextran, Polyion complex micelles, Diminazene, Hydrophilic drugs, Minocycline, Neuroinflammation, Aminoglycosides, Micelles stability.

Table of Contents

Résumé	I
Abstract	III
Table of Contents	V
List of figures	XII
List of tables	XVII
Liste of abbreviations	XVIII
Acknowledgments	XXIV
CHAPTER ONE	1
INTRODUCTION	1
An Overview of Polymeric Nanoparticles as Drug Delivery Systems	1
1.1. The need for new drug delivery systems.....	2
1.1.1. The solubility challenge	2
1.1.2. Poor oral absorption	4
1.1.3. The stability challenge	7
1.1.4. Unfavorable pharmacokinetics.....	8
1.2. Polymeric nanoparticulate drug carriers	9
1.3. Advantages of polymeric nanoparticles as drug carriers	10
1.4. Classes of polymeric nanoparticles.....	12
1.4.1. Nanocapsules	12
1.4.2. Nanospheres	14
1.4.3. Polymersomes	15
1.4.4. Dendrimers.....	16
1.4.5. Micelles of amphiphilic copolymers.....	17
1.4.6. Polyion complex (PIC) micelles	20
1.4.6.1. Driving force for PIC micelles formation.....	20
1.4.6.2. Advantages of PIC micelles as drug delivery systems.....	21
1.4.6.3. Preparation methods for PIC micelles	22
1.4.6.4. Classification of copolymers used for PIC micelles formation	23

1.4.6.4.1. Cationic copolymers.....	24
1.4.6.4.2. Anionic copolymers.....	26
1.4.6.5. Properties of PIC micelles.....	26
1.4.6.5.1. Particle size and size distribution	26
1.4.6.5.2. Surface charge	27
1.4.6.5.3. Effect of pH on PIC micelles formation and stability	28
1.4.6.5.4. Effect of ionic strength on PIC micelles stability.....	29
1.4.6.5.5. Colloidal stability of PIC micelles	30
1.4.6.5.6. Critical association concentration (CAC) of PIC micelles.....	30
1.4.6.6. Methods used to characterize PIC micelles	31
1.4.6.6.1. Dynamic light scattering (DLS)	31
1.4.6.6.2. Static light scattering (SLS).....	32
1.4.6.6.3. ζ potential measurements.....	32
1.4.6.6.4. ^1H nuclear magnetic resonance (^1H NMR)	33
1.4.6.6.5. Isothermal titration calorimetry (ITC).....	33
1.4.6.6.6. Other methods	35
1.4.6.7. Applications of PIC micelles as drug delivery systems	36
1.4.6.7.1. PIC micelles as non-viral gene vectors	36
1.4.6.7.2. PIC micelles as delivery systems for anticancer drugs	38
1.4.6.7.3. PIC micelles as delivery systems for other drugs.....	41
1.5. Nanoparticles based on modified dextran as drug carriers	41
1.5.1. Nanoparticles of hydrophobically modified dextran (HM-DEX).....	43
1.5.2. Nanoparticles based on ionic dextran derivatives.....	47
1.6. Thesis rationale and research objectives	48
1.6.1. Rationale	48
1.6.2. Research objectives.....	50
1.7. References.....	51
CHAPTER TWO	84
RESEARCH PAPER	84

Enhancement of Hydrophilic Drug Loading and Release Characteristics through Micellization with New Carboxymethyl-dextran-PEG Block Copolymers of Tunable Charge Density¹	84
2.1. Abstract	85
2.2. Author Keywords	85
2.3. Introduction	85
2.4. Materials and methods	88
2.4.1. Materials	88
2.4.2. Synthesis of carboxymethyl-dextran- <i>block</i> -poly(ethylene glycols) (CMD-PEG)	88
2.4.3. Methods	89
2.4.3.1. General methods	89
2.4.3.2. Light scattering	90
2.4.3.3. Preparation and characterization of the micelles	92
2.4.3.3.1. General method	92
2.4.3.3.2. pH studies	92
2.4.3.3.3. Ionic strength studies	92
2.4.3.3.4. Critical association concentration	93
2.4.3.3.5. Zeta-potential	93
2.4.3.3.6. Stability of micellar solutions upon storage	93
2.4.3.3.7. ¹ H NMR spectra of DIM/CMD-PEG mixtures	93
2.4.3.3.8. Lyophilization/redissolution of DIM/CMD-PEG micelles	94
2.4.3.3.9. Diminazene release studies	94
2.5. Results and discussion	94
2.5.1. Synthesis of carboxymethyl-dextran- <i>block</i> -poly(ethylene glycol)s	94
2.5.2. Preparation and size of diminazene/CMD-PEG micelles	95
2.5.3. Determination of the [+]/[-] ratios corresponding to the onset of micellization and to the maximum drug loading capacity by ¹ H NMR spectroscopy	99
2.5.4. Critical association concentration of diminazene/CMD-PEG micelles	102

2.5.5.	Effect of salt (NaCl) on micelle formation and stability.....	104
2.5.6.	Zeta-potential studies	106
2.5.7.	Effect of solution pH on the stability of diminazene/CMD-PEG micelles.....	106
2.5.8.	Storage stability of diminazene/CMD-PEG micelles	108
2.5.9.	Drug release studies	109
2.6.	Conclusion	110
2.7.	Appendix A. Supplementary data	111
2.8.	Acknowledgments.....	111
2.9.	References.....	111
CHAPTER THREE		117
RESEARCH PAPER.....		117
Minocycline Block Copolymer Micelles and Their Anti-Inflammatory Effects on Microglia².....		117
3.1.	Abstract.....	118
3.2.	Author Keywords.....	118
3.3.	Introduction.....	118
3.4.	Experimental part.....	122
3.4.1.	Materials.....	122
3.4.2.	Preparation of MH-loaded CMD-PEG micelles	123
3.4.3.	Characterization	123
3.4.4.	Stability studies	124
3.4.5.	Drug release studies	125
3.4.6.	Cell survival and nitrite release determinations.....	126
3.5.	Results and Discussion.....	127
3.5.1.	Preparation, characterization, and stability of ternary Ca ²⁺ /MH/CMD-PEG nanoparticles	127
3.5.2.	Stability and release of MH entrapped in Ca ²⁺ /MH/CMD-PEG nanoparticles ([+]/[-] = 1.0, pH 7.4).....	133

3.5.3. Cytotoxicity and anti-inflammatory effects of Ca ²⁺ /MH/CMD-PEG micelles	140
3.6. Conclusions.....	142
3.7. Appendix B. Supplementary data	142
3.8. Acknowledgements.....	142
3.9. References.....	143
CHAPTER FOUR.....	151
RESEARCH PAPER	151
Carboxymethyl-dextran-<i>b</i>-poly(ethylene glycol) Polyion Complex Micelles for the Delivery of Aminoglycoside Antibiotics³	151
4.1. Abstract	152
4.2. Author Keywords.....	152
4.3. Introduction.....	152
4.4. Materials and methods	156
4.4.1. Materials.....	156
4.4.2. Methods.....	156
4.4.2.1. General methods	156
4.4.2.2. Synthesis and characterization of hydrophobically modified CMD-PEG [24]	157
4.4.2.3. Isothermal titration calorimetry (ITC)	159
4.4.2.4. ¹ H NMR spectra of aminoglycosides/CMD-PEG mixtures.....	160
4.4.2.5. Light scattering studies	160
4.4.2.6. Preparation and characterization aminoglycosides/CMD-PEG micelles.....	161
4.4.2.6.1. General method	161
4.4.2.6.2. pH studies	161
4.4.2.6.3. Effect of salt (NaCl) on micelles formation and stability.....	161
4.4.2.7. Effect of freeze-drying on micelles integrity	162
4.4.2.8. Effect of dilution on micelles integrity	162
4.4.2.9. Drug release studies	162

	X
4.4.2.10. Minimal inhibitory concentration (MIC) determination	163
4.5. Results and discussion	163
4.5.1. Isothermal titration calorimetry (ITC) studies	163
4.5.1.1. Buffer and pH dependence of aminoglycosides and CMD-PEG interactions	164
4.5.1.2. Intrinsic thermodynamic parameters for binding of neomycin and paromomycin to CMD-PEG	171
4.5.1.3. Heat capacity change (ΔC_p) determination	172
4.5.2. ^1H NMR studies	173
4.5.3. Size of aminoglycosides/CMD-PEG micelles	176
4.5.4. Effect of salt on micelles formation and stability	179
4.5.5. pH studies.....	182
4.5.5.1. Effect of pH on the self assembly of CMD-PEG and dodecyl-CMD-PEG in aqueous solution.....	182
4.5.5.2. Aminoglycosides/CMD-PEG micelles	183
4.5.6. Effect of freeze drying on micelles integrity.....	185
4.5.7. Effect of dilution on micelles stability	185
4.5.8. Drug release studies	187
4.5.9. Antibacterial activity of micelles-encapsulated aminoglycosides	188
4.6. Conclusion	189
4.7. Acknowledgments.....	190
4.8. References.....	191
CHAPTER FIVE.....	204
GENERAL DISCUSSION	204
5.1. Synthesis of CMD-PEG block copolymers	206
5.2. CMD-PEG copolymers candidates	207
5.3. Preparation of CMD-PEG PIC micelles	207
5.4. Formation, structure and drug loading of CMD-PEG micelles	208
5.5. Size and polydispersity of CMD-PEG micelles.....	212
5.6. Micelles critical association concentration (CAC)	213

5.7.	Effect of salt on CMD-PEG micelles stability	213
5.8.	Effect of pH on micelle formation and stability.....	214
5.9.	Stability of CMD-PEG micelles.....	215
5.10.	Drug release from CMD-PEG micelles	215
5.11.	Cytotoxicity of CMD-PEG copolymers.....	216
5.12.	Pharmacological activity of micelles-encapsulated drugs	216
5.13.	References	217
CHAPTER SIX		220
CONCLUSIONS AND PERSPECTIVES		220
6.1.	Conclusions	221
6.2.	Future work.....	221

List of figures

Figure 1.1. Different problems associated with the administration of poorly water soluble drugs. ^[8]	3
Figure 1.2. Schematic representation of the fluidic mosaic model of the cell membrane. http://lamp.tu-graz.ac.at/~hadley/nanoscience/week4/membrane.jpg	6
Figure 1.3. Different polymeric nanoparticulate drug carriers.....	13
Figure 1.4. Schematic illustration of PIC micelles formation from a pair of oppositely charged species.....	21
Figure 1.5. Architectures of different copolymers used in the preparation of PIC micelles.	24
Figure 1.6. Diagram of ITC showing cells and syringe (left) and representative ITC data (right).	35
Figure 1.7. Chemical structure of dextran showing $\alpha(1-6)$ glycosidic linkages and $\alpha(1-3)$ branching.....	42
Figure 1.8. Chemical structure of dextran sulfate, DEAE-dextran and DEX-SPM.....	48
Figure 2.1. Idealized chemical structure of carboxymethyl dextran- <i>block</i> -poly(ethylene glycol) (CMD-PEG); n represents the number of ethylene glycol units, m is the number of glucopyranose rings of the polysaccharide block, and x represents the fraction of glucose units of the dextran chain that bear a carboxymethyl group. The polysaccharide segment consists of a random distribution of glucopyranose units and carboxymethyl glucopyranose units.....	87
Figure 2.2. (top): Distribution of the hydrodynamic radius (R_H) of micelles in a solution of DIM/60-CMD ₆₈ -PEG ₆₄ ([+]/[-] = 2; polymer concentration: 0.2 g/L; solvent: Tris-HCl buffer, 25 mM, pH 5.3; temperature: 25 °C; θ : 90 °C); (bottom): plots of the changes of R_H (●) and the polydispersity index (PDI, ○) as a function of [+]/[-] in mixtures of DIM and 60-CMD ₆₈ -PEG ₆₄ ; polymer concentration: 0.2 g/L; temperature: 25 °C; θ : 90 °C.....	97

- Figure 2.3.** ^1H NMR spectra recorded for diminazene diacetate (DIM, lower spectra) and solutions of DIM and 60-CMD₆₈-PEG₆₄ of $0 < [+]/[-] < 2$ (left) and $[+]/[-] = 4, 10$ (right); polymer concentration: 3.0 g/L, solvent: D₂O; temperature : 25 °C..... 101
- Figure 2.4.** Plots of the changes as a function of polymer concentration of the ratio ($I_C/I_{0.2}$) of the intensity of light scattered by a solution of DIM and 60-CMD₆₈-PEG₆₄ (\diamond) or 30-CMD₆₈-PEG₆₄ (\blacklozenge) of concentration c to that of a solution of DIM and polymer of concentration 0.2 g/L; solvent: Tris-HCl buffer, 25 mM, pH 5.3; the arrows indicate the critical association concentration. 103
- Figure 2.5.** Plots of the changes of R_H of micelles (\bullet) and the intensity of scattered light (I , \triangle) as a function of NaCl concentration in mixtures of DIM and 30-CMD₆₈-PEG₆₄ (top) or 85-CMD₄₀-PEG₁₄₀ (bottom) in Tris-HCl buffer, 25 mM, pH5.3; polymer concentration: 0.2 g/L; $[+]/[-] = 2$; temperature: 25 °C; θ : 90°; the hatched area corresponds to region II (see text)..... 105
- Figure 2.6.** Plots of the changes of R_H of micelles (\bullet) and of the intensity of scattered light (I , \triangle) as a function of solution pH in mixtures of DIM and 85-CMD₄₀-PEG₁₄₀ in 25 mM Tris-HCl; polymer concentration: 0.2 g/L; $[+]/[-] = 2$; temperature: 25 °C; θ : 90°. 107
- Figure 2.7.** Release of DIM evaluated by the dialysis bag method from (\blacksquare) DIM alone in Tris-HCl 25 mM, $[\text{NaCl}] = 150$ mM, pH 7.4; (\blacktriangledown) DIM/85-CMD₄₀-PEG₁₄₀ micelles, $[+]/[-] = 2$, in 25 mM Tris-HCl, $[\text{NaCl}] = 150$ mM, pH 7.4; (\blacktriangle) DIM/85-CMD₄₀-PEG₁₄₀ micelles, $[+]/[-] = 2$, in 25 mM Tris-HCl $[\text{NaCl}] = 0$ mM, pH 5.3, and (\square) DIM/30-CMD₆₈-PEG₆₄ at $[+]/[-] = 2$, in Tris-HCl, 25 mM $[\text{NaCl}] = 0$ mM, pH 5.3. 110
- Figure 3.1.** Chemical structures of minocycline hydrochloride (left panel) and CMD-PEG block copolymer (right panel)..... 120
- Figure 3.2.** ^1H NMR spectra of MH (A), Ca²⁺/MH, ($[\text{Ca}^{2+}]/[\text{MH}] = 2.0$) (B), CMD-PEG (C), Ca²⁺/MH/CMD-PEG (CMD-PEG concentration = 2.0 mg/mL, $[+]/[-] = 1.0$, $[\text{Ca}^{2+}]/[\text{MH}] = 2.0$) (D) and MH/CMD-PEG ($[+]/[-] = 1.0$) (E) in D₂O, room temperature, pH 7.4 and representative illustrations of the species examined. 129

- Figure 3.3. A:** Hydrodynamic radius (R_H , \blacklozenge) of Ca^{2+} /MH/CMD-PEG micelles as a function of the $[+]/[-]$ ratio; solvent: Tris-HCl buffer (10 mM, pH 7.4; CMD-PEG concentration: 0.2 mg/mL, $[\text{Ca}^{2+}]/[\text{MH}] = 2$). 132
- B:** Scattered light intensity as a function of calcium chloride concentration from solutions of Ca^{2+} /MH/CMD-PEG micelles (\blacksquare), Ca^{2+} /MH (\blacktriangle) and Ca^{2+} /CMD-PEG (\circ); solvent: Tris-HCl buffer (10 mM, pH 7.4), CMD-PEG concentration: 0.2 mg/mL..... 132
- Figure 3.4.** Chromatograms recorded upon storage at room temperature for up to 3 weeks of MH in Tris-HCl buffer (10 mM, pH 7.4) (A), MH/CMD-PEG (B), Ca^{2+} /MH ($[\text{Ca}^{2+}]/[\text{MH}] = 2.0$) (C), Ca^{2+} /MH/CMD-PEG ($[+]/[-] = 1.0$, $[\text{Ca}^{2+}]/[\text{MH}] = 2.0$) (D), $[\text{CMD-PEG}] = 0.1$ mg/mL. For elution conditions: see experimental section. 134
- Figure 3.5.** Release profiles for MH kept at 37 °C in Tris-HCl buffer (10 mM, pH 7.4) in the case of Ca^{2+} /MH (\bullet), Ca^{2+} /MH/CMD-PEG $[\text{NaCl}] = 0$ (\blacksquare) and Ca^{2+} /MH/CMD-PEG $[\text{NaCl}] = 150$ mM (\blacktriangledown). $[+]/[-]$ for micelles = 1.0 and $[\text{Ca}^{2+}]/[\text{MH}] = 2.0$ 137
- Figure 3.6. A:** Normalized size distributions of Ca^{2+} /MH/CMD-PEG micelles upon incubation at 37 °C for 15 h with various amounts of BSA. Also shown are the size distributions recorded for micelles alone (bottom trace) and BSA alone (5 mg/mL) (top trace); $[+]/[-]$ for micelles = 1.0 and $[\text{Ca}^{2+}]/[\text{MH}] = 2.0$ 139
- B:** Normalized size distribution of Ca^{2+} /MH/CMD-PEG micelles upon incubation at 37 °C for 24 h with 5 % serum; also shown are the size distributions of micelles alone after incubation for 24 h at 37 °C (bottom trace) and of 5 % serum alone (top trace); $[+]/[-]$ for micelles = 1.0 and $[\text{Ca}^{2+}]/[\text{MH}] = 2.0$ 139
- Figure 3.7.** Amount of NO released in N9 microglia cells treated with MH alone, Ca^{2+} /MH complex, Ca^{2+} /MH/CMD-PEG micelles or CMD-PEG, all in the presence or absence of 10 $\mu\text{g}/\text{ml}$ of lipopolysaccharide under normal cell culture conditions. Cells were treated for 24 h after which nitrite content in the media was measured using the Griess Reagent. All measurements were done in triplicates in three independent experiments. ** $p < 0.01$, *** $p < 0.001$ 141
- Figure 4.1.** Chemical structures of neomycin, paromomycin (top) and CMD-PEG block copolymer (bottom)..... 155

- Figure 4.2.** ^1H NMR spectra of CMD-PEG block copolymer (top spectrum) and dodecyl₃₈-CMD-PEG copolymer (bottom spectrum) recorded in DMSO-*d*₆ at room temperature..... 158
- Figure 4.3.** Corrected integrated injection heats plotted as a function of the [amine]/[carboxylate] ratio for the titration of either neomycin sulfate (A, B, E) or paromomycin sulphate (C, D, F) into CMD-PEG copolymer in different buffers at pH 7.0 (A, C, E, F) or 8.0 (B, D) at 25 °C (A, B, C, D) or 37 °C (E, F). 165
- Figure 4.4.** ^1H NMR spectra of neomycin sulfate (A), CMD-PEG (B), neomycin/CMD-PEG micelles (pH 7.4, 0 mM NaCl) (C), neomycin/CMD-PEG micelles (pH 7.4, 150 mM NaCl) (D), dodecyl₃₈-CMD-PEG (E), neomycin/dodecyl₃₈-CMD-PEG micelles (pH 7.4, 0 mM NaCl) (F) and neomycin/dodecyl₃₈-CMD-PEG micelles (pH 7.4, 150 mM NaCl) (G). All micelles were prepared in D₂O at polymer concentration of 2.0 g/L, neomycin concentration of 2.1 g/L and [amine]/[carboxylate] = 2.5..... 175
- Figure 4.5.** Effect of the [amine]/[carboxylate] molar ratio on the hydrodynamic radius of paromomycin sulfate (panel A) and neomycin sulfate (panel B) micelles with different polymers: CMD-PEG (▲), dodecyl₁₈-CMD-PEG (●), dodecyl₃₈-CMD-PEG (■). Micelles were prepared in phosphate buffer (10 mM, pH 7.0) at polymer concentration = 0.2 g/L..... 177
- Figure 4.6.** Effect of salt on the intensity of scattered light and hydrodynamic radius of paromomycin (panels A and B) and neomycin (panels C and D) micelles with different CMD-PEG copolymers: dodecyl₃₈-CMD-PEG (■), dodecyl₁₈-CMD-PEG (●), CMD-PEG (▲). Micelles were prepared in phosphate buffer (10 mM, pH 7.0) at final polymer concentration = 0.5 g/L and [amine]/[carboxylate] = 2.5. Relative scattering intensity = intensity at certain salt concentration/ intensity at salt concentration = 0. 180
- Figure 4.7.** Effect of pH on the intensity of light scattered by polymeric solutions of dodecyl₃₈-CMD-PEG (■), dodecyl₁₈-CMD-PEG (▲), and CMD-PEG (●). Solutions were prepared in 10 mM phosphate buffer at polymer concentration of 0.2 mg/mL..... 183

- Figure 4.8.** Effect of pH on the intensity of scattered light (A and B) and hydrodynamic radius (C and D) of CMD-PEG micelles with different aminoglycosides: neomycin (\blacktriangle), paromomycin (Δ), 6"-guanidino-paromomycin (\circ) and 5"-deoxy-5"-guanidino-paromomycin (\bullet). Micelles were prepared in phosphate buffer (10 mM, pH 7.0) at final [CMD-PEG] = 0.5 g/L. Relative scattering intensity = intensity at certain pH/ intensity at pH 7.0..... 184
- Figure 4.9.** Effect of dilution on the hydrodynamic radius (A) and relative intensity of scattered light (B) for neomycin/CMD-PEG micelles (\blacksquare) and paromomycin/CMD-PEG micelles (\bullet). Relative scattering intensity = intensity at certain CMD-PEG concentration/intensity at CMD-PEG concentration of 0.5 g/L..... 186
- Figure 4.10.** Release profiles at 37 °C in 10 mM phosphate buffer of neomycin from: neomycin alone (\blacksquare); neomycin/CMD-PEG micelles, pH 7.0, [NaCl] = 0 mM (\bullet); neomycin/CMD-PEG micelles, pH 7.4, [NaCl] = 0 mM (\blacktriangledown); neomycin/CMD-PEG micelles, pH 7.0, [NaCl] = 150 mM (\blacklozenge); neomycin/CMD-PEG micelles, pH 7.4, [NaCl] = 150 mM (\blacktriangle); neomycin/dodecyl₃₈-CMD-PEG micelles, pH 7.4, [NaCl] = 150 mM (\circ). ([neomycin] = 2.0 g/L, [amine]/[carboxylate] = 2.5)...... 188
- Figure 5.1.** Formation and structure of drug-loaded CMD-PEG PIC micelles..... 209

List of tables

Table 1.1. Polymeric micelles-based formulations in clinical trials. ^[14, 143]	19
Table 1.2. Different cationic copolymers used in the preparation of PIC micelles.....	25
Table 1.3. Different drugs that have been encapsulated into PIC micelles	40
Table 1.4. Different hydrophobic compounds used to modify dextran.....	44
Table 1.5. Methods used for the preparation of drug-loaded HM-DEX nanoparticles.....	46
Table 2.1. Experimental conditions for the carboxymethylation of DEX-PEG copolymers	89
Table 2.2. Molecular properties of the CMD-PEG samples prepared	91
Table 2.3. Characteristics of DIM/CMD-PEG micelles ($[+]/[-] = 2$) ^a in a Tris-HCl buffer (25 mM, pH 5.3) for four different diblock copolymers.....	98
Table 3.1. Residual amount of MH upon storage at room temperature of various formulations of the drug in Tris-HCl buffer of pH 7.4. ^a	135
Table 3.2. Residual amount of MH upon storage at 37 °C of various formulations of the drug in Tris-HCl buffer of pH 7.4 and in the same buffer containing 5% fetal bovine serum. ^a	136
Table 4.1. Thermodynamic parameters for the binding of neomycin sulfate to CMD-PEG at pH 7.0 and 8.0, at 25 °C and a Na ⁺ concentration of 50 mM.....	166
Table 4.2. Thermodynamic parameters for the binding of paromomycin sulfate to CMD- PEG at pH 7.0 and 8.0, at 25 °C and a Na ⁺ concentration of 50 mM.	167
Table 4.3. Thermodynamic parameters for the binding of neomycin sulfate and paromomycin sulfate to CMD-PEG at pH 7.0 and at 37 °C and a Na ⁺ concentration of 50 mM.	168
Table 4.4. Intrinsic thermodynamic parameters and number of uptaken protons for the binding of paromomycin sulfate and neomycin sulfate to CMD-PEG at pH 7.0 (25 °C and 37 °C) and at pH 8.0 (25 °C) and a Na ⁺ concentration of 50 mM.	170
Table 4.5. Characteristics of aminoglycosides/CMD-PEG micelles ($[\text{amine}]/[\text{carboxylate}]$ $= 2.5$) in a phosphate buffer (10 mM, pH 7.0)	176
Table 5.1. Characteristics of different CMD-PEG micelles.....	211

Liste of abbreviations

<i>A</i>	Surface area
Å	Angstrom
Ac-DEX	Acetalated dextran
ADH	Antidiuretic hormone
AFM	Atomic force microscopy
AGs	Aminoglycosides
ASGP	Asialoglycoprotein
ATRA	All-trans retinoic acid
BBB	Blood brain barrier
BCS	Biopharmaceutics classification system
BIC	Block ionomer complexes
BSA	Bovine serum albumin
<i>C</i>	Concentration of the drug in the dissolution medium
°C	Degree Celsius
ΔC	Concentration gradient
CAC	Critical association concentration
CaCl ₂	Calcium chloride
CD	Circular dichroism
CDDP	Cisplatin (<i>cis</i> -dichlorodiammineplatinum) (II)
CMD	Carboxymethyl dextran
CoA	Coenzyme A
C3Ms	Complex coacervates core micelles
ΔC_p	Heat capacity change
<i>C_s</i>	Solubility of the drug in the dissolution medium
CsA	Cyclosporin A
<i>D</i>	Diffusion coefficient

dC/dt	Dissolution rate
DEAE-DEX	Diethylaminoethyl-dextran
DEX	Dextran
DG	Diammonium glycyrrhizinate
DIM	Diminazene diacetate
DLS	Dynamic light scattering
DMF	Dimethyl formamide
DMSO	Dimethyl sulfoxide
DMSO- d_6	Deuterated dimethyl sulfoxide
DNA	Deoxyribonucleic acid
D ₂ O	Deuterium oxide
DS	Degree of substitution
DSC	Differential scanning calorimetry
EPR	Enhanced permeability and retention
FBS	Fetal bovine serum
FRET	Fluorescence resonance energy transfer
ΔG	Free energy change
GI	Gastrointestinal
GPC	Gel permeation chromatography
h	Hour
h	Thickness of the diffusion boundary layer
ΔH	Enthalpy change
HCl	Hydrochloric acid
HM	Hydrophobically modified
¹ H NMR	Proton nuclear magnetic resonance
HPLC	High performance liquid chromatography
IV	Intravenous
IMDM	Iscoe's modified dulbecco's medium
ITC	Isothermal titration calorimetry

K	Binding constant
kDa	Kilo Dalton
MCA	Monochloroacetic acid
MH	Minocycline hydrochloride
M_n	Number average molecular weight
MPS	Mononuclear phagocytic system
MTT	3-(4,5-dimethylthiazol-2-yl)-2,5-diphenyltetrazolium bromide
$M_{w, app}$	Apparent molecular weight
MWCO	Molecular weight cut off
N	Reaction stoichiometry
NaCl	Sodium chloride
N_{agg}	Aggregation number
NaOH	Sodium hydroxide
NIPAM	<i>N</i> -isopropyl acrylamide
NVP	<i>N</i> -vinylpyrrolidone
PAA	Polyacrylic acid
PACA	Poly(alkylcyanoacrylates)
PAMAM	Polyamidoamine
PAsp	Poly(aspartic acid)
PBR	Peripheral benzodiazepine receptor
Pc	Phthalocyanine
PCL	Poly(ϵ -caprolactone)
PDEAEMA	Poly(2-(diethylamino) ethyl methacrylate)
PDI	Polydispersity index
PDMAEMA	Poly(2-(dimethylamino) ethyl methacrylate)
PDMAPA	Poly(3-dimethylamino) propyl aspartamide
PDMAPMA	Poly(<i>N</i> -[3-(dimethyl amino) propyl] methacrylamide)
PDT	Photodynamic therapy
PEDAA	Poly(ethylenediamine aspartamide)

PEG	Poly(ethylene glycol)
PEI	Polyethylenimines
PEOz	Poly(2-ethyl-2-oxazoline)
PGA	Poly(glycolic acid)
PGlu	Poly(glutamic acid)
PHE	Polyhematoporphyrin esters
PHis	Poly(histidine)
PHPMA	Poly- <i>N</i> -(2-hydroxypropyl)methacrylamide
PIC	Polyion complex
PLA	Poly(lactic acid)
PLGA	Poly(lactic- <i>co</i> -glycolic acid)
PLL	Poly(L lysine)
PMAA	Poly(methacrylic acid)
PMMA	Poly(methyl methacrylate)
PPI	Polypropyleneimine
PPBA	Poly(4-phenyl-1-butanoate)l-aspartamide
PQ4VP	Poly(<i>N</i> -methyl-4-vinylpyridinium sulfate)
P2MVP	Poly(2-methyl vinyl pyridinium)
PS	Poly(styrene)
PSMA	Poly(styrene-alter-maleic anhydride)
PSPM	Polyspermine
PTMAEMA	Poly(trimethylammonioethyl methacrylate chloride)
PVP	Poly(<i>N</i> -vinylpyrrolidone)
R_H	Hydrodynamic radius
RNA	Ribonucleic acid
ROS	Reactive oxygen species
rRNA	Ribosomal ribonucleic acid
siRNA	Small interfering RNA
ΔS	Entropy change

SD	Standard deviation
SEM	Scanning electron microscopy
SN-38	7-ethyl-10-hydroxycamptothecin
TEM	Transmission electron microscopy
TMS	Tetramethylsilane
triEGMA	Ethoxytriethylene glycol methacrylate
UK	United Kingdom
US-FDA	United States food and drug administration
UV	Ultraviolet
wt	Weight
λ_{\max}	Wavelength of maximum absorbance
λ_{ex}	Excitation wavelength

*To my daughters, Nada and Sarah and my
wife, Yasmine*

Acknowledgments

This thesis would not have been possible without the support of many people. It is my pleasure to convey my deepest gratitude and sincere appreciation to all of them.

First of all, I am highly indebted to my thesis supervisor, Professor Françoise Winnik, whose dedication, enthusiasm and support have been instrumental in my personal and professional development. During my studies, she has given me the freedom and reliable basis necessary to advance this project and to develop as an independent researcher. I would also like to thank her for giving me the chance to change from a pharmacist who uses ready polymers to one who has the knowledge to synthesize and modify polymers that suit his needs.

Special thanks are due to Professor Dusica Maysinger for giving us the opportunity to test our polymers in her cell culture lab. Her insightful discussions and fruitful collaboration are very much appreciated.

I would also like to express my gratitude and sincere appreciation to Professor Stephen Hanessian for kindly providing us with the modified aminoglycosides used in this study. His availability and thoughtful discussions helped in the rapid progression of my studies.

I would like to extend my thanks to my colleagues Dr. Janek Szychowski and Angela Choi for taking care of the synthesis of modified aminoglycosides and testing our polymers in cell cultures. I am also thankful for my progress report committee members: Drs. Maxime Ranger and Sophie-Dorothée Clas for their availability and thoughtful discussions.

I am also thankful to all my past, present and honorary lab mates in the University of Montreal for their invaluable friendship and collaboration.

A heartfelt thanks goes to my parents, brothers and sisters for their support and encouragement over the years. I extend my heartwarming thankfulness to my wife and my daughters for their unconditional love and support. It is their sacrifice and understanding that allowed me to give my work the attention it needs.

The financial support by the missions department, Ministry of Higher Education, Egypt is gratefully acknowledged.

CHAPTER ONE

INTRODUCTION

An Overview of Polymeric Nanoparticles as Drug Delivery Systems

1.1. The need for new drug delivery systems

Potency and therapeutic effects of many drugs are limited or otherwise reduced because of their unfavorable physiochemical and/or pharmacokinetics properties. For example, instability, limited solubility, accumulation in non-target sites leading to side effects and low bioavailability are just a few of the properties that limit therapeutic benefit of many drugs.^[1] Discovery of new drugs may improve these unfavorable properties. However, discovery and development of new drugs are very long processes with enormous expenditure. In the United States, the average time to discover, develop and approve a new drug is approximately 14.2 years^[2,3] with an average development cost of \$ 802 million.^[4] A large fraction of the rising health care expenses is accounted for by expenses on pharmaceuticals, which have grown rapidly over the last two decades.^[4] Properly designed drug delivery systems can minimize the cost of developing new drugs by optimizing the properties of existing drugs. The search for new drug delivery technologies is also fueled by pharmaceutical companies aiming at registering off-patent or about to be off-patent products. The nano-based drug delivery market is expected to increase from its current value at \$3.4 billion (about 10% of the total drug delivery market) to about \$26 billion by 2012.^[5] The following sections describe the current challenges that face the pharmaceutical formulator and can be overcome through the development of new drug delivery systems.

1.1.1. The solubility challenge

Poor water solubility of drugs presents a challenge for the development of successful drug formulations for either oral or parenteral administration. For orally administered drugs, drug aqueous solubility is a key factor that determines its dissolution rate in the gastrointestinal (GI) fluids and hence, its oral bioavailability. Only soluble drug molecules can be absorbed by the cellular membranes and reach their target after oral administration.^[6] Moreover, oral administration of poorly water soluble drugs quite often leads to low and highly variable bioavailability.

Poor aqueous solubility could also result in serious side effects for drugs administered by intravenous (IV) injection. Water insoluble drugs form aggregates after IV injection leading to blockage of blood vessels and embolism.^[7] Drug aggregates could also lead to local toxicity at the site of accumulation and/or reduced systemic availability. Other problems associated with the administration of poorly water soluble drugs are summarized in Figure 1.1.^[8]

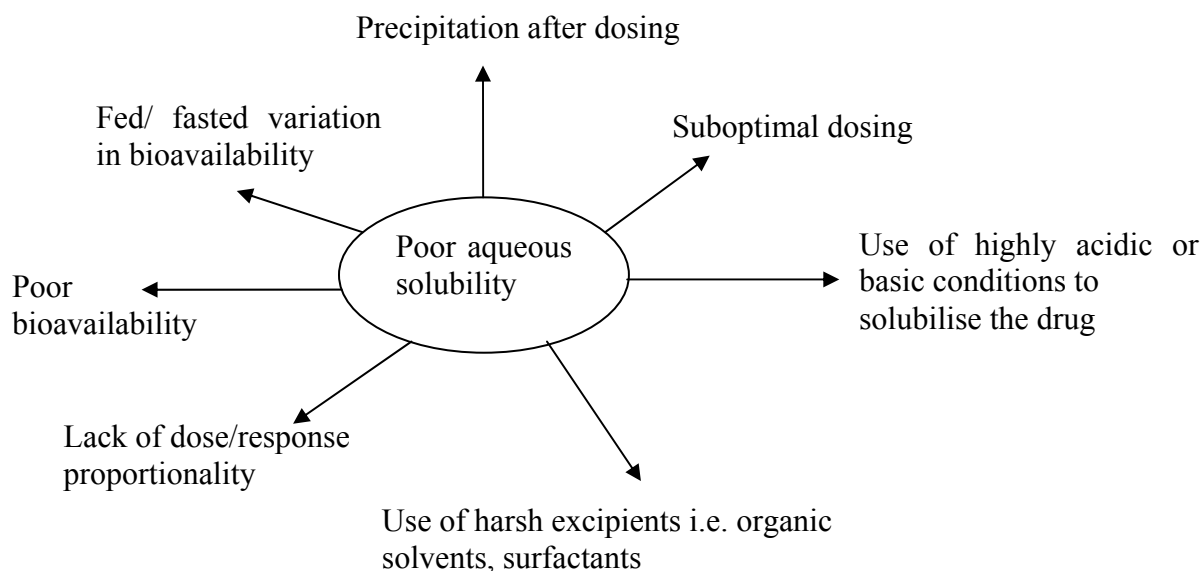


Figure 1.1. Different problems associated with the administration of poorly water soluble drugs.^[8]

A Biopharmaceutics Classification System (BCS) class I drug (high solubility-high permeability) is ideal in terms of solubility and bioavailability.^[9] Advances in the fields of combinatorial chemistry and/or biologically based high-throughput screening have resulted in the availability of large number of new drugs. Most of these newly developed drugs belong to BCS Class II (low solubility-high permeability) or Class IV (low solubility-low permeability).^[10] It is estimated that about 40% of newly developed drug candidates lack adequate water solubility.^[11-13] These insoluble drug candidates are usually rejected by the pharmaceutical industry and never enter a formulation development stage.^[13] Examples of

water insoluble drugs include anticancer drugs since many of them are bulky polycyclic compounds like paclitaxel, tamoxifen, camptothecin, phenytoin, cyclosporine-A, digoxin, nitroglycerin and sulphathiazole.^[14] The modified Noyes-Whitney equation (equation 1) identifies possible parameters that can be modified to enhance the dissolution rate of water insoluble drugs.^[15, 16]

$$\frac{dC}{dt} = \frac{AD(C_s - C)}{h} \quad (1)$$

Where dC/dt is the rate of dissolution, A is the surface area available for dissolution, D is the diffusion coefficient of the compound, C_s is the solubility of the drug in the dissolution medium, C is the concentration of drug in the medium at time t and h is the thickness of the diffusion boundary layer adjacent to the surface of the dissolving particle. The dissolution rate can be increased by increasing the surface area available for dissolution (e.g. by decreasing the particle size of the drug and/or by optimizing the wetting characteristics of the substance surface), by decreasing the boundary layer thickness, by maintaining sink conditions for dissolution and, by improving the apparent solubility of the drug under physiologically relevant conditions. One strategy to increase drug solubility is to create various drug salts, which not only improve drug aqueous solubility but also retain its biological activity. Other approaches to improve drug aqueous solubility include the use of clinically acceptable organic solvents, mixtures of cosolvents, surfactants or pharmaceutical excipients, such as cyclodextrins.^[16] However, these approaches often end-up in serious side effects.^[12, 17] For instance, the water-insoluble anticancer drug paclitaxel (Taxol[®]) is formulated in a 1:1 mixture of Cremophor[®]-EL and ethanol. Cremophor[®] EL causes many side effects, such as hypersensitivity, nephrotoxicity, neurotoxicity, vasodilatation, difficult breathing, lethargy and hypotension.^[17, 18]

1.1.2. Poor oral absorption

Oral dosage forms are, so far, the most preferred drug formulations by the patient, clinician and pharmaceutical manufacturer. In the United States over 80% of drugs administered to produce systemic effects are marketed as oral dosage forms (e.g. tablets,

capsules). From the patient point of view, oral administration is “natural”, easy, safe and less painful than injection. For the clinician, oral administration improves the therapeutic outcome since the patient has more chances to adhere to the prescribed therapeutic regime. Oral drug products are more profitable for the pharmaceutical manufacturer since they require less strict conditions during their manufacturing compared to parenteral products (e.g. sterility etc).

Successful oral drug therapy is faced by several obstacles. The very first prerequisite for successful oral therapy is the adequate drug absorption from its site of administration. Factors affecting oral drug absorption can be broadly divided into three main categories: (i) physicochemical variables, (ii) physiological variables and (iii) dosage form variables.^[19] Rate and extent of drug absorption are governed by a complex interplay of all these factors. Physicochemical properties that influence oral drug absorption include its oil/water partition coefficient (K_o/w), its degree of ionization in biological fluids as determined by its pK_a and pH of the surroundings and its molecular weight. The drug K_o/w is one of the most important physicochemical properties that govern its oral absorption. This is not surprising since the cell membrane is lipidic in nature while the surrounding fluid into which the drug should dissolve is water. Therefore, for a drug to be adequately absorbed it should have enough hydrophilicity to dissolve in the GI fluids and enough lipophilicity to cross the cell membrane.

According to the fluid mosaic model (Figure 1.2), the cell membrane is composed of a lipid bilayer in which the lipid portions (long tails) are arranged inside the bilayer while the polar portions (round head) point outward. The membrane is crossed by transmembrane (or integral) proteins whereas peripheral proteins are attached to the inner surface of the membrane. The outer surface has carbohydrates attached to lipids and proteins.^[19, 20] The cell membrane has small water-filled channels or pores that allow absorption of water, ions or small water soluble molecules. The effective radius of these pores was estimated to be 7-8.5 Å and 3-3.8 Å in human jejunum and ileum, respectively.^[21]

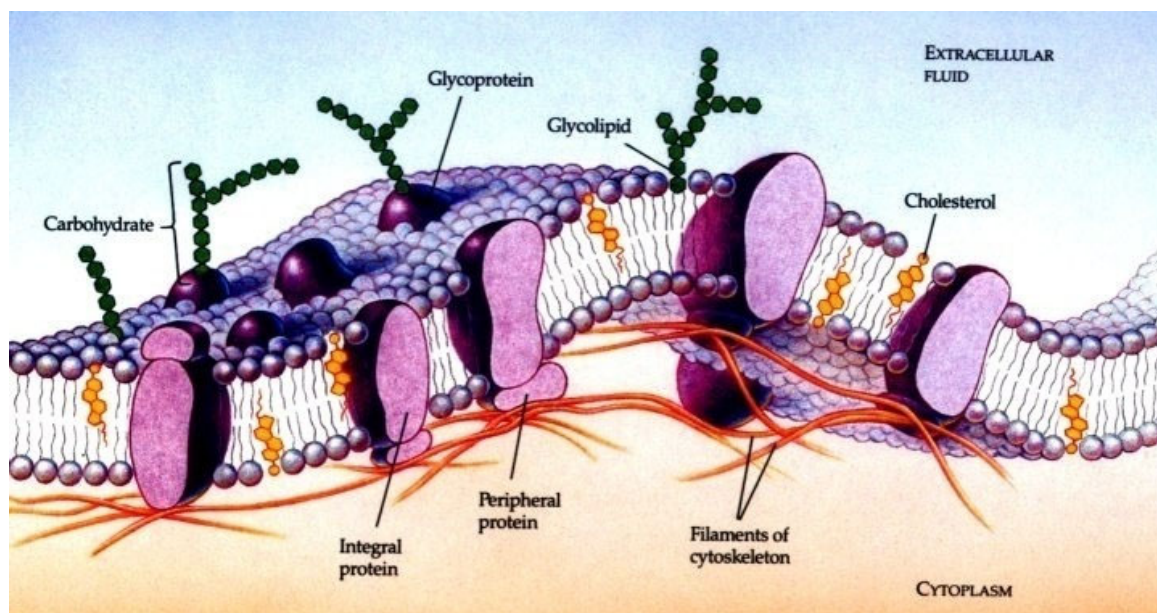


Figure 1.2. Schematic representation of the fluidic mosaic model of the cell membrane.

<http://lamp.tu-graz.ac.at/~hadley/nanoscience/week4/membrane.jpg>

Passive drug absorption through the cellular membranes can take place by either transcellular or paracellular pathways. Transcellular absorption involves passage of the drug through the lipophilic cell membrane, therefore it requires adequate lipophilicity of the drug ($1 < K_{o/w} < 10^5$). In contrast, paracellular absorption takes place by diffusion through space between adjacent cells. The presence of tight junctions between the cells limits the absorption through this pathway to water soluble small molecules ($K_{o/w} < 1$ and molecular weight < 500 g/mol).^[22, 23] In order to correlate the physicochemical properties of drugs to their absorption, Lipinski *et al.* developed the so-called “rule of 5”.^[24] The rule states that a new drug candidate is likely to have poor absorption or membrane permeability if:

1. It has more than 5 hydrogen bond donors.
2. It has more than 10 hydrogen bond acceptors.
3. Its molecular weight is greater than 500 g/mol.
4. Its Log $K_{o/w}$ is greater than 5.

5. The above rules only apply to compounds that undergo passive membrane transport.

The incredible advances in the areas of biotechnology, molecular biology and biochemistry have led to the advent of new classes of therapeutic agents. Peptides, proteins, oligonucleotides, DNA and small interfering RNA (siRNA) are examples of these new therapeutics that present major challenges to drug delivery scientists. For instance, high water solubility and high molecular weight of peptide and protein drugs significantly reduce their permeability through the cell membranes.^[25, 26] Also DNA and siRNA have poor penetration through the cellular membranes due to their high molecular weight and strong anionic charges.^[27-29] The unique physicochemical properties of these therapeutics have motivated drug delivery scientists to develop new delivery systems or explore new routes of drug administration. Thus, nasal, pulmonary and transdermal administration are some of the less conventional routes of drug administration that are currently being explored for the delivery of such new therapeutics.^[30-33]

1.1.3. The stability challenge

Instability in solution, *in vitro* or *in vivo* is one of the hurdles that reduce the usefulness of many therapeutic agents. For instance, instability in solution prevents the development of liquid dosage forms for antibiotics, such as tetracyclines. Instead, these drugs are formulated in solid dosage forms or powders ready for reconstitution at the time of use. Indeed, liquid dosage forms are more desirable in many occasions, such as ophthalmic use, pediatric patients, geriatric patients and patients with difficulty in swallowing.^[34, 35] Moreover, liquid dosage forms are the first choice when rapid onset of action is required like in analgesia and migraine.^[36] Chemical degradation of drugs decreases their potency leading to non effective therapy. The picture is further complicated by the fact that chemical degradation of drugs often results in the formation of toxic degradants with subsequent serious side effects to the patients. For example, epianhydrotetracycline and *m*-aminophenol are toxic degradants of tetracycline and *p*-aminosalicylic acid, respectively.^[37] Chemical instability of drugs in solution could result from hydrolysis, oxidation, photolysis, racemization or decarboxylation.^[37]

Adequate *in vivo* stability in the gastrointestinal fluids and in the blood is a key factor that ensures adequate bioavailability, low clearance and long circulation time. The vast majority of peptide and protein drugs are unstable in the GI tract due to enzymatic degradation and/or instability in the harsh acidic conditions in the stomach.^[38] Consequently, these drugs are given by subcutaneous or IV injections. Injections are not patient friendly and lead to side effects. In addition, DNA instability and degradation by nucleases in the plasma and in the cytoplasm are challenges that need to be addressed for successful gene therapy.^[39] For all these reasons, much effort has been continuously devoted to the development of drug delivery systems that improve drug stability, both *in vitro* and *in vivo*.

1.1.4. Unfavorable pharmacokinetics

The ultimate goal of drug therapy is to achieve and maintain effective drug concentration at its site of action, which is usually located away from the site of administration. As soon as a drug appears in the blood stream, it is subjected to distribution to various organs and tissues. These organs include the liver and kidney, which metabolizes the drug and excretes it from the body, respectively. As a result, drug concentration at the site of action decreases over time and repeated dosing becomes necessary. Moreover, the drug may be metabolized and/or excreted before reaching its site of action leading to therapy failure. Repeated administration usually results in poor compliance and eventually poor therapeutic outcome. In this regard, drug delivery systems that release their cargo in a sustained, controlled, stimuli-responsive or delayed manner are much appreciated. These delivery systems reduce the frequency of administration, enhance drug efficacy by its localization at the site of action and reduce the required dose.^[40]

The lack of “targetability” is another inherent undesirable pharmacokinetic property of most drugs. Following absorption, drugs are usually distributed non-specifically throughout the whole body including healthy tissues. This leads to numerous side effects, which are particularly alarming for cytotoxic drugs whose accumulation in healthy tissues leads to serious adverse effects and limits the allowable dose.^[41] Moreover, the widespread distribution into the whole body dilutes the drug and decreases its concentration at the

target sites. This increases the required doses, which in turn increases the cost of therapy and induces more side effects. Therefore, a delivery system that maximizes drug concentration in pathological tissues and minimizes its concentration in healthy tissues can enhance the drug therapeutic index, reduce the cost of therapy and improve the overall therapeutic outcome. This led to the appearance of the concept of drug targeting, which can be defined as selective drug delivery to certain organ, tissue or cell within the body where its action is needed.^[42] Historically, the 19th century “magic bullet” idea of Paul Ehrlich was the first drug targeting proposal. He proposed that if a substance “magic bullet” would have a specific affinity for disease-causing microorganisms; it would reach these microorganisms and destroy them without affecting healthy tissues. Nowadays drug targeting is a well-known drug delivery strategy that is achieved by either passive or active mechanisms.^[43]

1.2. Polymeric nanoparticulate drug carriers

Scientists ever-expanding knowledge of the human body has led to the identification and understanding of the mechanisms underlying many challenging diseases. Many of these diseases can not be treated by conventional drug delivery systems.^[44] This increases the demand for new drug delivery systems/technologies, which require multidisciplinary collaboration from physical, chemical, biological and engineering scientists.^[45] An ideal drug delivery system should improve aqueous solubility of insoluble drug, enhance its bioavailability, maintain effective drug concentration in the blood over prolonged period of time, reduce side effects associated with drug administration, stabilize the drug both *in vitro* and *in vivo* and deliver the drug, passively or actively to its target.^[46] It should also be cost-effective and acceptable by the patients. To meet all these requirements, the last few decades have witnessed considerable interest in the development of new drug delivery systems.^[44, 47-49] Advances in the fields of polymer chemistry and polymer colloid physico-chemistry have resulted in the availability of many tailor-made polymers. This development changed the conventional role of polymers in drug delivery systems. Polymers were typically used for decades as additives or coatings in conventional drug delivery systems (e.g. tablets, suspensions, capsules) to solubilise, stabilize or control drug release.^[47, 50, 51]

New polymers with tunable properties are now major components of many drug delivery systems.

1.3. Advantages of polymeric nanoparticles as drug carriers

Polymeric nanoparticulate drug carriers hold a promising future due to their superior performance relative to other drug carriers. Firstly, polymers can be designed to be biocompatible and/or biodegradable, which increases the safety of the resulting nanoparticles.^[28] Secondly, polymers physicochemical properties (e.g. hydrophilicity/hydrophobicity balance, charge, molecular weight) can be tuned resulting in nanoparticles with various adjustable properties (e.g. size, surface charge). Moreover, polymeric nanoparticles can be coated with hydrophilic polymers, such as poly(ethylene glycol) (PEG), which decreases the adsorption of opsonin proteins in the blood. This helps nanoparticles escape recognition by the mononuclear phagocytic system (MPS) and circulate longer in the blood.^[52] Polymeric nanoparticles usually have a molecular weight above the threshold for glomerular filtration (42-50 kDa for water soluble synthetic polymers), which is another factor prolonging their residence time in the blood.^[44, 53] Surface of polymeric nanoparticles can be decorated with ligands/antibodies to direct them to certain target in the body.^[54] Some polymeric nanoparticles achieves high drug loading, which maximizes drug/excipients ratio. Incorporation of drugs in polymeric matrices controls their release, which can be sustained or stimuli responsive.^[55] Drug release from the so-called smart nanoparticles can be effected under different external stimuli (i.e. change in pH, temperature or ionic strength).^[56] This allows drug release in certain pathological area in the body.^[57] Absorption of nanoparticles is better than that of microparticles due to their small size.^[58] In addition, nanoparticles small size allows them to accumulate, passively in solid tumors, infarcts and inflamed tissues through the so-called enhanced permeability and retention effect (EPR).^[59] This effect relies on the pathophysiological characteristics of solid tumors, which are characterized by hypervascularity, incomplete vascular architecture, poorly aligned endothelial cells and wide fenestrations.^[14, 60] These characteristics make the vasculature of pathological tissues more “leaky” than that of healthy tissue. Leaky vasculature together with impaired

lymphatic drainage facilitates accumulation of macromolecules and nanoparticles in pathological tissues. The EPR effect is applicable to any macromolecule with molecular weight greater than 40 kDa. Exploiting the EPR effect, drug concentration in the tumor of 10-30 times higher than that in the blood was achieved.^[61] Moreover, the EPR effect results in prolonged drug retention in pathological tissues (e.g. tumor or inflamed tissue) for several weeks.

Despite the great potential of polymer chemistry, the number of synthetic polymers suitable for *in vivo* applications is limited.^[62] A candidate polymer should be biodegradable and/or biocompatible to be considered for *in vivo* drug delivery. In case a polymer is not biodegradable it should be totally eliminated from the body in a reasonable period of time. This allows repeated administration without any risk of uncontrolled accumulation. The polymer and its degradation products, if any, must be non toxic and non immunogenic. Examples of polymers approved by US-FDA (United States Food and Drug Administration) for administration in human beings are poly(lactic acid) (PLA), poly(glycolic acid) (PGA), poly(lactic-*co*-glycolic acid) (PLGA), poly(ethylene glycol) (PEG), and poly(methyl methacrylate) (PMMA).^[63]

Polymeric nanoparticles are colloidal drug carriers that vary in diameter between 10 and 1000 nm. Polymers used in the fabrication of nanoparticles can be categorized, according to their source, into natural, synthetic or semisynthetic. Natural polymers are generally safer and biocompatible, though the synthetic ones are more appealing due to the greater control over their physicochemical properties. Natural polymers that have been used in the formulation of nanoparticles for drug delivery applications include proteins (e.g. collagen, gelatin and albumin) and polysaccharides (e.g. dextran, chitosan, hyaluronic acid, pullulan, cellulose and inulin).^[64, 65] Examples of synthetic polymers used in the manufacture of nanoparticles include aliphatic polyesters, polyanhydrides, polyorthoesters and polycyanoacrylates.^[66] Aliphatic polyesters (e.g. PLA, PGA, PLGA and PCL) are, so far, the most widely used synthetic polymers in the preparation of drug-loaded nanoparticles. One advantage of aliphatic polyesters is their biocompatibility and their controlled degradation to biocompatible monomers.^[65] Controlled polymer degradation results in controlled release of encapsulated drugs. Aliphatic polyesters are degraded by

bulk hydrolysis of their ester bonds.^[67] Their degradation products (e.g. lactic acid or glycolic acid) are removed from the body by normal metabolic pathways.^[68] These degradation products, however, can create acidic microenvironment, which can degrade some acid-labile drugs like protein therapeutics.

1.4. Classes of polymeric nanoparticles

Pharmaceutically interesting polymeric nanoparticulate drug carriers include nanospheres, nanocapsules, polymeric micelles, dendrimers and polymersomes. Each class of these nanocarriers has its own advantages and shortcomings. The type of nanoparticulate carrier obtained from a given polymer depends on the polymer physicochemical properties and the method used to fabricate the nanoparticles. Based on the nanoparticle type, drugs may be encapsulated or dissolved into the nanoparticles core, dispersed in the polymeric matrix or adsorbed to the nanoparticles surface (Figure 1.3).

1.4.1. Nanocapsules

Polymeric nanocapsules are colloidal drug carriers with a solid polymeric shell surrounding a core that is liquid or semisolid at room temperature. The core is used as a reservoir space for encapsulation of different drugs (Figure 1.3). Nanocapsules shell is usually a single polymeric layer formed during polymerization at the interface between the dispersed and continuous phases of the emulsion used in nanocapsules preparation. The shell can also be formed by precipitation of a preformed polymer at the surface of emulsion droplets. Double coated nanocapsules have been prepared through coating of poly(methyl methacrylate) (PMMA) nanocapsules by hydroxypropyl methyl cellulose.^[69] Recently, nanocapsules having a core of liposomes coated by alternating layers of polycation (poly(allylamine hydrochloride)) and polyanion (poly(acrylic acid)) were prepared. This new hybrid system combined the advantages of both liposomes and nanocapsules.^[70]

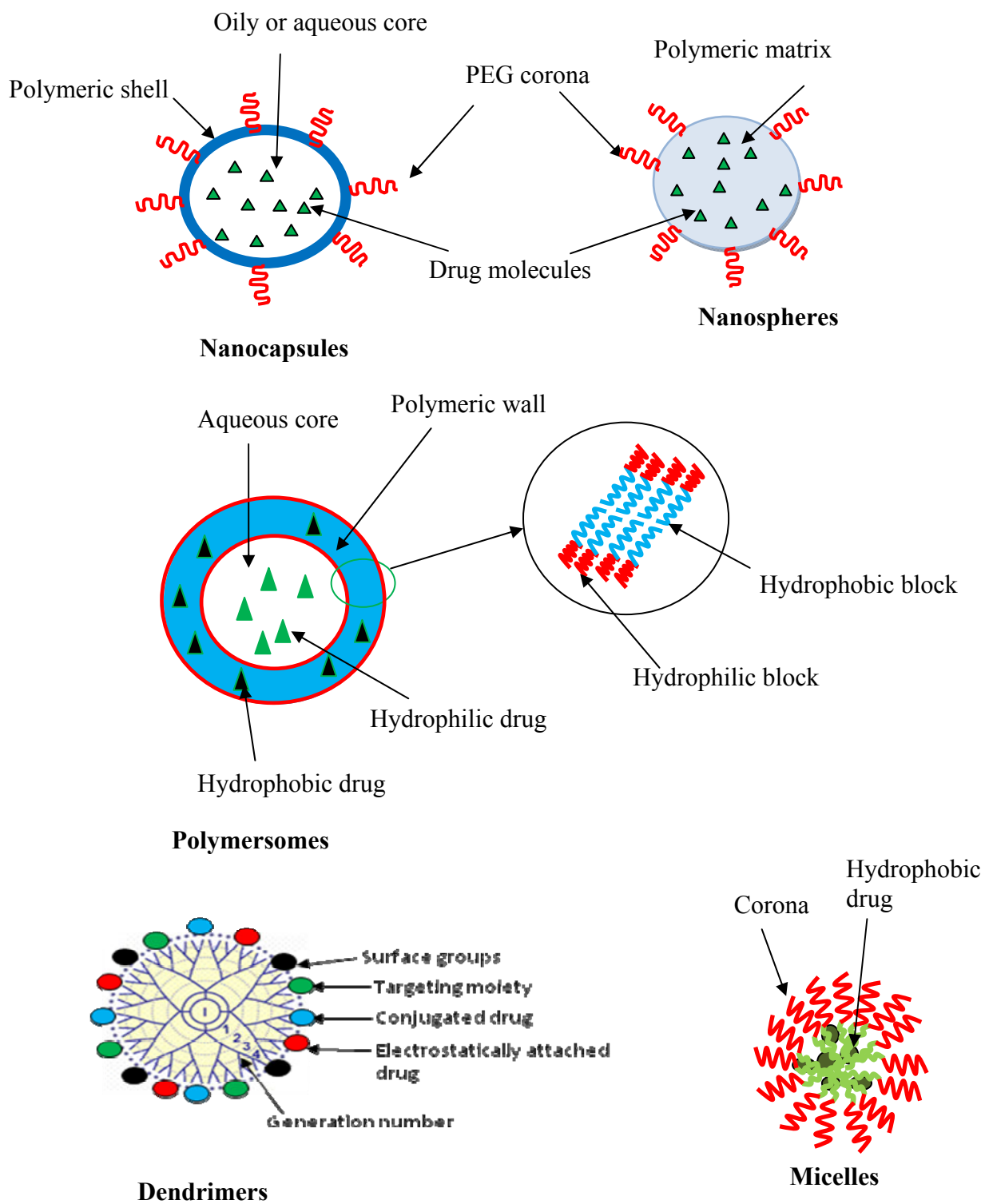


Figure 1.3. Different polymeric nanoparticulate drug carriers.

Traditionally, the nanocapsules core consisted of a lipophilic solvent, usually oil into which hydrophobic drugs were dissolved. The oil type affects drug loading capacity: high drug solubility in the oil gives high drug loading capacity.^[71] Application of nanocapsules with an oily core is limited to encapsulation of hydrophobic drugs.^[72] To overcome this limitation, nanocapsules with aqueous core suitable for encapsulation of water soluble drugs have been developed recently.^[72, 73] Polymeric nanocapsules have been useful in the encapsulation and delivery of hydrophobic drugs (e.g. indomethacin^[74], methotrexate^[75], paclitaxel^[76], spironolactone^[77]), proteins (e.g. insulin^[78], salmon calcitonin^[79]) and water-soluble therapeutics (e.g. oligonucleotides^[72], chlorhexidine digluconate^[80]).

1.4.2. Nanospheres

Contrary to nanocapsules, nanospheres are matrix-type polymeric systems into which the drug is dissolved or entrapped in the matrix or adsorbed to the surface (Figure 1.3). Advantages of nanocapsules over nanospheres include their low polymeric content and high loading capacity for hydrophobic drugs.^[81] Therefore, they have higher drug/polymer ratio. Polymers typically used in the preparation of nanocapsules and nanospheres include aliphatic polyester homopolymers, such as PLA, PLGA and PCL and poly(alkylcyanoacrylates) (PACA).^[82-84] These nanoparticles have found wide spread applications in enhancing *in vivo* performance and delivery of various drugs through different routes of administrations (e.g. IV, oral, ocular).^[85-88]

Following parenteral administration, nanoparticles with hydrophobic surfaces are coated by a group of plasma proteins, of which opsonin proteins facilitate recognition and uptake by the mononuclear phagocytic system (MPS) cells.^[89] Uptake of nanoparticles by these cells depends greatly on their surface chemistry. It is affected by neither the type of the polymer used in nanoparticles preparation nor by their morphology (e.g. nanocapsules or nanospheres). This significantly reduces the residence time of nanoparticles in the blood and results in nanoparticles accumulation in the liver spleen and bone marrow. For instance, bare poly(methyl methacrylate) nanoparticles had a half life in the blood of only 3 min.^[90] Although this phenomenon was found useful in the treatment of liver and spleen

diseases, it is undesirable when drug action is needed in other tissues.^[91, 92] Thus, gentamicin-loaded PLGA nanospheres were designed for the treatment of experimental Brucellosis in mice. Following IV injection, gentamicin-loaded PLGA nanospheres accumulated preferentially in the liver and spleen, the target organs for *Brucella melitensis*.^[93] Adsorption of serum proteins by nanoparticles has also been useful in drug targeting to the brain. Thus, doxorubicin-loaded poly(butyl cyanoacrylate) (PBCA) nanoparticles coated by 1% polysorbate 80 resulted in drug level in the brain that was 60 times higher than that of non-coated nanoparticles.^[94] Polysorbate coat facilitated adsorption of plasma proteins, especially apolipoprotein E (Apo-E), which helped the nanoparticles cross the blood brain barrier (BBB).^[95] When it comes to treating diseases away from the liver and spleen, nanoparticles that evade the uptake by MPS cells are needed. This is usually achieved by coating nanoparticles with hydrophilic polymers. Hydrophilic polymers allow nanoparticles to escape recognition by the cells of the immune system and stay in the circulation for time long enough to target various pathological tissues in the body.^[89] Surface modification with PEG or “pegylation” is the most widely used approach to prepare long circulating or “stealth” nanoparticles.^[96, 97] Thus, copolymers, such as PLA-PEG^[98], PLA-PEG-PLA^[99], PLGA-PEG^[100], chitosan-PEG^[101] and PCL-PEG^[102] have been used in the preparation of drug loaded nanocapsules and nanospheres.

1.4.3. Polymersomes

Polymersomes (polymeric vesicles) are vesicular structures formed by the hydration of amphiphilic block copolymers (Figure 1.3).^[103] They were first introduced by Kunitake *et al.* in 1981 in an attempt to overcome the inherent disadvantages of liposomes.^[104] Polymersomes are analogues of liposomes since both are vesicular structures but they have different composition of the shell, which consists of amphiphilic copolymers in polymersomes and lipids in liposomes. Unlike liposomes which are formed by small molecular weight lipids, polymersomes are formed by high molecular weight amphiphilic copolymers of different architectures (e.g., diblock, triblock, graft and dendritic polymers). This makes polymersomes wall thicker, stronger, tougher and thus, more stable than

conventional liposomes.^[105] Polymersomes presents a number of advantages for biomedical applications: high stability, tunable membrane properties, versatility and ability to encapsulate different types of drugs including hydrophilic, hydrophobic or ionized.^[105] Examples of amphiphilic block copolymers that form polymersomes are poly(butadiene)-PEG^[106], PCL-PEG^[107, 108], polystyrene-dextran^[109], PLA-PEG^[110], poly(propylene sulfide)-PEG^[111], polyphosphazenes containing PEG and ethyl-*p*-aminobenzoate side groups^[112]. For biomedical applications, biodegradable polymers are always preferred. Aqueous core of polymersomes acts as a reservoir space for encapsulating water soluble drugs whereas the thick polymeric shell can be used to integrate hydrophobic molecules (Figure 1.3). This property has been taken advantage of in the preparation of polymersomes loaded with cocktail anticancer drugs. Thus, doxorubicin, a hydrophilic anticancer drug was encapsulated in the aqueous core while the hydrophobic anticancer drug paclitaxel was integrated in the thick polymersomes wall.^[113] Polymersome drug cocktail showed a higher maximum tolerated dose and reduced tumors growth more effectively and for longer durations than free drugs. This shows the potential of polymersomes in mutli-drug therapy and its attractiveness as a carrier for wide range of drugs.

1.4.4. Dendrimers

Dendrimers (from the Greek word *dendron*, meaning tree) are a fairly new class of colloidal drug carriers (Figure 1.3). They are globular branched nanostructures with core-corona architecture. The core is a single atom or a group of atoms having at least two identical chemical functionalities. The branches that stem from the core are composed of repeating units with at least one junction of branching. Branching results in a series of radially concentric layers or generations.^[13, 39] Dendrimers possess several features that make them attractive nanocarriers for drug delivery applications. Firstly, it is possible to fine-tune their properties to suit certain therapeutic needs. Secondly, their surface can be engineered with countless functional groups that are used to attach a drug or targeting moiety. This together with their small size (10-100 nm in diameter) makes them ideal carriers for drug targeting. Thirdly, the cavities or spaces between branches (especially in higher generations) are used for encapsulation of different drugs.^[114, 115] Despite these

numerous advantages, cationic dendrimers, such as polyamidoamine (PAMAM) and polypropyleneimine (PPI) are cytotoxic.^[116] Dendrimers cytotoxicity can be reduced by modifying their surface with hydrophilic polymers, such as PEG. Thus, PEGylated PAMAM and PPI dendrimers not only showed less cytotoxicity, haemolytic activity and immunogenicity compared to the parent compound but also had higher drug loading, stability and longer circulation time in the blood.^[116-119] Another strategy to increase the PAMAM dendrimers biocompatibility while maintaining their ability to encapsulate siRNA involved the synthesis of internally cationic dendrimers with neutral surfaces.^[120] Dendrimers have been used as delivery vehicles for various hydrophobic drugs to improve their aqueous solubility and to enhance their therapeutic efficacy.^[121, 122] Furthermore, surface functional groups have been used for the loading of various hydrophilic drugs. Thus, surface amino groups of dendrimers have been used to encapsulate DNA, oligonucleotides or siRNA through electrostatic interactions.^[123] Dendrimers/oligonucleotides complexes decreased oligonucleotides degradation by RNase and showed improved transfection efficiency.^[123, 124] Some dendrimer-based products have been approved by the FDA. VivaGel™ (Starpharma) is a vaginal microbicide gel for the prevention of sexually transmitted diseases. SuperFect®, developed by Qiagen, is used for gene transfection in a broad range of cell lines.^[125]

1.4.5. Micelles of amphiphilic copolymers

Polymeric micelles are colloidal drug carriers formed in aqueous media through self assembly of amphiphilic copolymers of different architectures (e.g. block, graft, random).^[126] Polymeric micelles have size in the range of 5-100 nm and a core-corona structure (Figure 1.3).^[12] Copolymers that form micelles in water have two segments with different affinities to water: one is hydrophilic while the other is hydrophobic. When these copolymers are dissolved in water, hydrophobic segments tend to aggregate and withdraw from the aqueous environment to minimize system free energy. Above certain concentration of the amphiphile in water, called the critical association concentration (CAC), the copolymer self assemble resulting in the formation of polymeric micelles. The driving force of self assembly is entropy gain of the solvent due to removal of hydrophobic

segments from the aqueous environment.^[127] Self assembly in water of a certain amphiphile results in polymersomes or micelles according to the weight fraction of its hydrophilic block (f), the molecular weight of the amphiphile and the effective interaction parameter of its hydrophobic block with H₂O (χ). For block copolymers with a high χ , polymersomes are formed when $f = 20-40\%$. Worm-like micelles are formed at $40\% < f < 50\%$ whereas spherical micelles are obtained for copolymers with $f = 50-70\%$.^[128, 129]

Polymeric micelles are interesting nanocarriers for drug delivery applications due to their unique segregated core-corona structure that provides them with numerous advantages. The micelles lipophilic core offers a microenvironment for the solubilisation of hydrophobic drugs. In this regard, polymeric micelles are much more efficient and safer than other formulations currently in use. For example, the water-insoluble anesthetic agent propofol is formulated as an oil-in-water microemulsion, which is unstable against dilution, causes pain on injection and poses risk of hyperlipidemia.^[130, 131] To overcome these drawbacks, propofol was encapsulated in polymeric micelles of poly(*N*-vinyl-2-pyrrolidone)-*block*-poly(D,L-lactide).^[132] Sodium deoxycholate used for the solubilisation of amphotericin B is known to be haemolytic, whereas Cremophor[®]EL used for the solubilisation of numerous anticancer drugs has numerous side effects.^[133] In addition to their well-established safety profiles, polymeric micelles are known to remarkably increase the solubility of numerous hydrophobic drugs. Polymeric micelles of PLA-PEG increased aqueous solubility of paclitaxel and doxorubicin, two clinically important anticancer drugs, by 5000-fold and 12 000-fold, respectively.^[134, 135] Encapsulating hydrophobic drugs within the micelles core not only improves their solubility but also sustains their release, protects them against degradation, modifies their biodistribution, decreases their side effects and increases their overall therapeutic efficacy.^[136-139] The hydrophilic corona of polymeric micelles maintains their water solubility and colloidal stability, reduces their uptake by the cells of the immune system and prolongs their circulation time. Micelles corona has also been used to attach targeting ligands so that the micelles accumulate selectively in certain tissue in the body. Thus, certain cancers have over-expression of peripheral benzodiazepine receptor (PBR), which was used to prepare paclitaxel-loaded PBR-targeted micelles. These micelles showed a significantly higher toxicity against human glioblastoma cancer cells *in*

vitro.^[140] Examples of other receptors that are over-expressed by cancer cells and have been used to prepare targeted polymeric micelles are folate and transferrin.^[12]

Poly(ethylene glycol) is the most commonly used corona-forming segment of polymeric micelles, though other hydrophilic polymers, such as poly(*N*-vinyl-2-pyrrolidone) have been used.^[132, 141] Various polymers have been used as core-forming segments of polymeric micelles.^[142] Examples of these polymers include aliphatic polyesters (e.g., PLA, PCL, PLGA), polyethers (e.g., poly(propylene oxide)) and poly(L amino acids).^[60] Poly(L amino acids) commonly used as core-forming segments in polymeric micelles include poly(aspartic acid) (PAsp), poly(glutamic acid) (PGlu), poly(L lysine) (PLL) and poly(histidine) (PHis). Since these amino acids are hydrophilic, they should be hydrophobized in order to form the micelles core.^[44, 60] Many polymeric micelles-based anticancer drug formulations have progressed well beyond experimental/conceptual stages where many formulations are now in clinical trials (Table 1.1).^[14]

Table 1.1. Polymeric micelles-based formulations in clinical trials.^[14, 143]

Trade name	Drug	Polymer	Phase completed	Ref.
NK-911	Doxorubicin	PEG-PAsp-DOX	Phase I	[144]
SP-1049C	Doxorubicin	PEG-PPO-PEG	Phase I	[145]
PAXCEED [®]	Paclitaxel	PEG-PDLLA	Phase II	[146]
Genexol [®] -PM	Paclitaxel	PEG-PDLLA	Phase II	[147]
NK-105	Paclitaxel	PEG-PPBA	Phase I	[148]
NK-012	SN-38	PEG-P(Glu)	Phase I	[149]

PEG: poly (ethylene glycol); PAsp: poly (aspartic acid); PDLLA: poly(_{D,L} lactide); PPBA: poly(4-phenyl-1-butanoate)l-aspartamide; P(Glu): poly(glutamic acid); SN-38: 7-ethyl-10-hydroxycamptothecin.

1.4.6. Polyion complex (PIC) micelles

Polyion complex (PIC) micelles were described for the first time in the mid 90's independently by Kataoka and Kabanov groups.^[150, 151] Since then PIC micelles found applications in various fields including delivery of ionic therapeutics.^[152] This special class of micelles is formed by electrostatic interactions between an ionic-neutral copolymer of different architectures (i.e. block, graft, random) and an oppositely charged species. For drug delivery applications, the oppositely charged species is a therapeutic entity (e.g. drug, DNA or protein). In aqueous media, PIC micelles have a core-corona structure. The neutral water-soluble segment of the polymer forms the corona while the ionic segment-drug complex forms the core. Since their introduction, these colloidal carriers have been given different nomenclatures by different research groups. Thus, the term PIC micelles has been proposed by Kataoka and co-workers^[153], Kabanov and co-workers^[154] have been using the term block ionomer complexes, BIC, while Stuart and co-workers^[155] use the term complex coacervates core micelles, C3Ms. The term PIC micelles will be used throughout the following sections.

1.4.6.1. Driving force for PIC micelles formation

Electrostatic interactions between oppositely charged polyelectrolytes (e.g. a pair of oppositely charged homopolymers, an ionic polymer and an oppositely charged drug) are mainly driven by entropy gain of the system due to release of small molecular weight counter ions.^[156] Charge neutralization due to these interactions creates hydrophobic domains, which leads to precipitation and phase separation in water especially in the vicinity of charge stoichiometric compositions (Figure 1.4).^[157] Replacing one of the interacting polyelectrolytes by an ionic-neutral copolymer endows the system with the amphiphilicity required for self assembly and micelle formation.^[152] The neutral polymer segments that form the PIC micelles corona ensure water solubility of the micelles even under charge stoichiometric conditions (Figure 1.4). Moreover, the hydrophilic shell stabilizes the micelles against aggregation or phase separation. Depending on the chemical nature of the various PIC micelles components, other forces such as metal-ligand

coordination, hydrogen bonding, hydrophobic interactions or van der Waals forces may assist in PIC formation and stabilization.^[158-160]

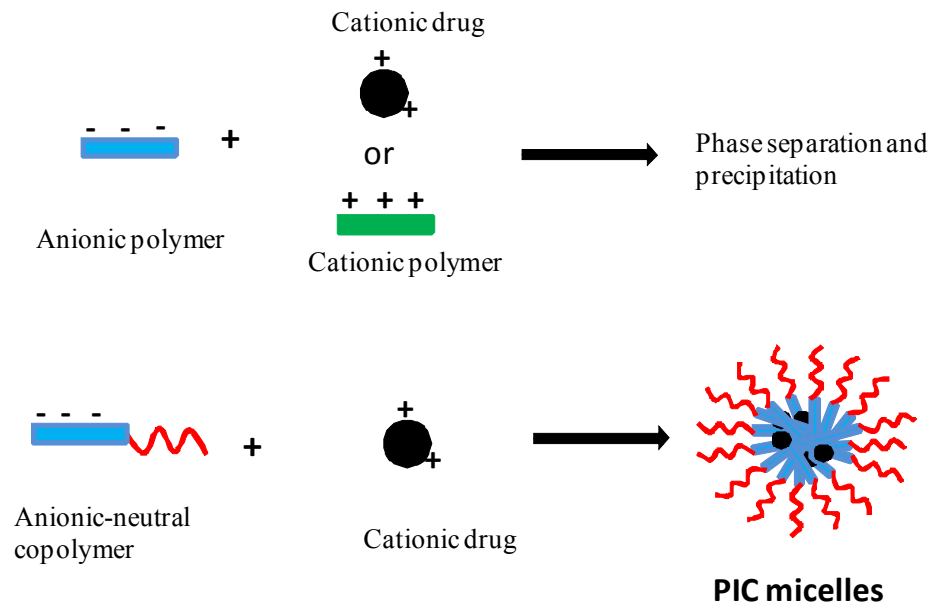


Figure 1.4. Schematic illustration of PIC micelles formation from a pair of oppositely charged species.

1.4.6.2. Advantages of PIC micelles as drug delivery systems

PIC micelles are unique amid colloidal polymeric drug carriers in that they are used exclusively for encapsulation and delivery of ionic drugs. Ionic drugs usually have high water solubility, a property that makes their encapsulation into other nanoparticles tricky.^[161] Moreover, these drugs have low affinity for the hydrophobic core of other nanoparticles and tend to diffuse out in the aqueous medium resulting in very low encapsulation efficiency.^[162, 163] Thus, PLGA nanospheres encapsulated ~ 1 wt% gentamicin, a cationic water soluble aminoglycoside antibiotic.^[92] A given dose of this drug formulation has polymer concentration that is 100 times higher than that of gentamicin. This is not desirable from toxicological point of view since it subjects the body to chemicals that can be avoided by properly selecting the drug carrier. In this regard, PIC micelles have higher drug loading capacity for ionic drugs.^[164] In most cases, PIC micelles have almost complete drug incorporation since micelle formation relies on electrostatic

interactions between the polymer and the oppositely charged drug. For instance, PEG-g-chitosan formed PIC micelles with all-trans retinoic acid that incorporated more than 80 wt% drug.^[165] The same micelles encapsulated another anionic drug, diammonium glycyrrhizinate (DG) with encapsulation efficiency higher than 96%.^[166] PIC micelles are usually prepared in aqueous media limiting the use of organic solvents. Residuals of organic solvents in pharmaceutical preparations should be minimal since they could cause several side effects and pose risk to the human health.^[167] Moreover, organic solvents may inactivate or denature delicate biotherapeutics, such as peptides and proteins.^[168] Fabrication of PIC micelles involves simple mixing in aqueous solvents without the need of vigorous processing conditions, such as heat, sonication, or emulsification. This certainly avoids any deleterious effects on drugs stability and activity. Similar to micelles of amphiphilic copolymers, PIC micelles have excellent colloidal stability, small size and narrow size distribution. Corona forming blocks in PIC micelles are usually selected to provide the micelles with long circulation properties. Moreover, targeting ligands can be attached to the micelles corona to direct them towards certain organ or tissue in the body. Thus, Wakebayashi *et al.*, synthesized α -lactosyl-PEG-poly(2-(dimethylamino) ethyl methacrylate) (lactose-PEG-PDMAEMA) as gene carriers for selective transfection of hepatic cells.^[169] Lactosylated PIC micelles showed substantially higher transfection efficiency compared to non-lactosylated micelles in HepG2 cells having asialoglycoprotein (ASGP) receptors. This higher transfection efficiency was attributed to possible specific interaction between ASGP receptors and lactose moieties of the micelles. Having this in mind, Yang *et al.*, reported the preparation of lactose-conjugated PEG-g-chitosan PIC micelles for liver-targeted delivery of diammonium glycyrrhizinate.^[166] Three drug formulations were administered IV to rats: drug solution in PBS, micelles of PEG-g-chitosan and micelles of lactose-PEG-g-chitosan. Pharmacokinetics analysis showed that the micelles modified with lactose had more ability to deliver the drug to the liver.^[169]

1.4.6.3. Preparation methods for PIC micelles

The most commonly used method for preparation of drug-loaded PIC micelles is simple mixing of the drug and polymer aqueous solutions under proper conditions of

drug/polymer molar charge ratio, polymer concentration, pH and ionic strength.^[170-173] This method is not suitable for the encapsulation of water-insoluble ionic drugs. Other methods, such as dialysis, solvent evaporation and thin film hydration have been adopted for the incorporation of such drugs. Dialysis and solvent evaporation methods typically involve dissolving the polymer in water and dissolving water-insoluble drugs in a water miscible organic solvent, such as dimethyl sulfoxide (DMSO), dimethyl formamide (DMF) or ethanol. The drug and polymer solutions are mixed and the organic solvent is removed by dialysis against water or by evaporation under reduced pressure. Gradual removal of the organic solvent induces micelles formation and drug encapsulation. These two methods have been used for the preparation of all-trans retinoic acid/PEG-*g*-chitosan PIC micelles.^[165, 174] Thin film hydration method was used to prepare amphotericin B-loaded poly(2-ethyl-2-oxazoline)-*b*-poly(aspartic acid) (PEOz-*b*-PAsp) PIC micelles.^[175] Polymer and drug were dissolved in a suitable volatile organic solvent, such as DMF. A thin film is then formed by the evaporation of the organic solvent under reduced pressure followed by hydration with aqueous solvent. The free drug was removed by filtration. PIC micelles preparation by simple mixing of drug and polymer aqueous solutions is advantageous over other methods for scale-up production since it results in high yield and does not involve vigorous processing conditions.

1.4.6.4. Classification of copolymers used for PIC micelles formation

PIC micelles for biomedical applications have been developed using a wide range of ionic-neutral copolymers. Based on their architecture, these copolymers can be divided into 4 main categories (Figure 1.5):

1. Block copolymers: linear copolymers where the end group of one block is covalently linked to the head of another block giving diblock or triblock architectures.^[157]
2. Graft copolymers: branched copolymers with a comb-like architecture where different branches emanate from one main chain.

3. Random copolymers: linear copolymers with the building blocks arranged randomly.^[176]
4. Alternating copolymers: linear copolymers with perfectly alternating arrangement of their building blocks.

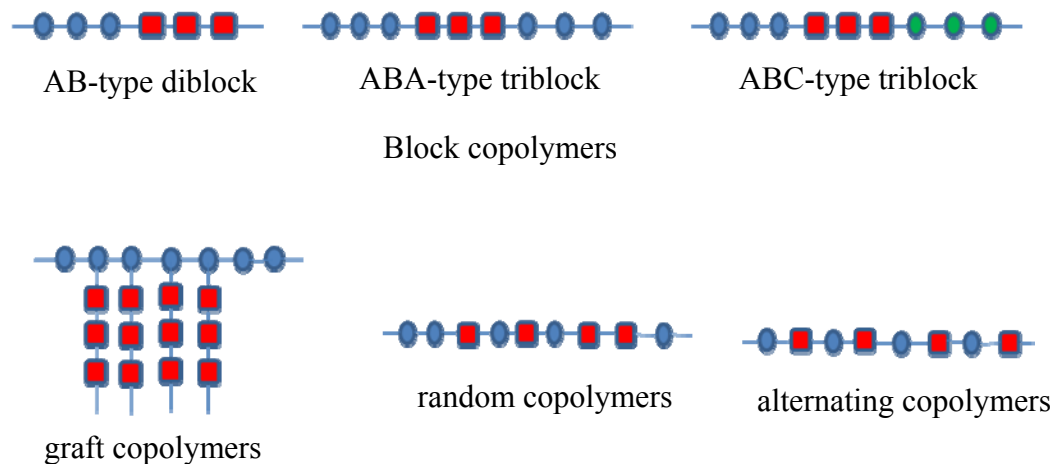


Figure 1.5. Architectures of different copolymers used in the preparation of PIC micelles.

Copolymers used for PIC micelles formation can also be classified according to the charge of their ionic segment into two groups: cationic and anionic copolymers.

1.4.6.4.1. *Cationic copolymers*

Polycation-neutral copolymers as the name implies have two segments; one is neutral while the other contains ionizable cationic functional groups able to interact electrostatically with negatively charged species. The cationic functional groups are primary, secondary, tertiary or quaternary amines. Other ionizable cationic groups, such as amidine and guanidine are also used. According to the chemical nature of the polyamine segment, these copolymers can be classified into: (i) copolymers based on poly(amino acids), (ii) copolymers based on poly(acrylamides), (iii) copolymers based on

polyethylenimines, (iv) copolymers based on polysaccharides and (v) copolymers based on poly(pyridines). Examples of these different cationic copolymers are given in Table 1.2.

Table 1.2. Different cationic copolymers used in the preparation of PIC micelles

Polyamine	Examples	Ref.
Poly(amino acids)	PEG- <i>b</i> -PLL, PLL- <i>b</i> -PEG- <i>b</i> -PLL, PEG- <i>g</i> -PLL, PEG- <i>b</i> -thiol-PLL, PLL- <i>g</i> -DEX, PEG- <i>b</i> -PLL dendrimer, PLL- <i>g</i> -DEX, PLL- <i>g</i> -polysaccharide (dextran, amylose, maltose), PNIPAM- <i>g</i> -PLL, PEG- <i>b</i> -PDMAPA, PEG- <i>b</i> -PEDA	[177-182] [183-191]
Poly(acrylamides)	PHPMA- <i>b</i> -PTMAEMA, PHPMA- <i>b</i> -PDMAEMA, PEG- <i>b</i> -PDEAEMA, random copolymers of 2-(dimethylamino)ethyl methacrylate (DMAEMA) with triEGMA or NVP, PEG- <i>b</i> -PDMAEMA, PVP- <i>b</i> -PDMAEMA, thiol-PEG- <i>b</i> -PDMAEMA, α -lactosyl-PEG- <i>b</i> -PDMAEMA, acetal-PEG- <i>b</i> -PDMAEMA	[169, 179, 192- 203]
Polyethylenimines	PEI- <i>g</i> -PCL, PEG- <i>b</i> -PEI, PEG- <i>g</i> -PEI, PNIPAM- <i>g</i> -PEI	[204-210]
Polysaccharides	PEG- <i>g</i> -chitosan	[165, 166, 168]
Poly(pyridines)	PEG- <i>b</i> -PQ4VP, PEG- <i>b</i> -PQ2VP, PEG- <i>b</i> -P4VP, PEG- <i>b</i> -P2MVP, PS- <i>b</i> -P2VP- <i>b</i> -PEG	[155, 208, 211- 213]
Poly(spermine)	PEG- <i>b</i> -PSPM	[214]

PLL: poly(L lysine); DEX: dextran; PNIPAM: poly(*N*-isopropyl acrylamide); PDMAPA: poly(3-dimethylamino) propyl aspartamide; PEDA: poly(ethylenediamine aspartamide); PHPMA: poly-*N*-(2-hydroxypropyl) methacrylamide; PTMAEMA: poly(trimethylammonioethyl methacrylate); PDMAEMA: poly(*N*-[3-(dimethyl amino) propyl]methacrylamide); PDEAEMA: poly(2-(diethylamino) ethyl methacrylate); PDMAEMA: poly(2-(*N,N*-dimethylamino)ethylmethacrylate); triEGMA: ethoxytriethylene glycol methacrylate, PVP: poly(*N*-vinylpyrrolidone); PEI: polyethylenimine; PQ4VP: poly(*N*-methyl-4-vinylpyridinium sulfate); lyso: lysozyme; PQ2VP: poly(*N*-methyl-2-vinyl

pyridinium iodide); P4VP: poly(4-vinylpyridine); P2MVP: poly(2-methyl vinyl pyridinium); PS-*b*-P2VP-*b*-PEG: poly(styrene-*b*-2-vinyl pyridine-*b*-ethylene glycol).

1.4.6.4.2. Anionic copolymers

Anionic functional groups of the polyanion-neutral copolymers commonly used in PIC micelles preparation are carboxylate and sulfonate. Analogous to polycations, polyanionic copolymers are classified according to the chemical nature of their charged segment into: (i) copolymers based on poly(amino acids) (e.g. PEG-*b*-poly(aspartic acid) (PEG-*b*-PAsp)^[150, 159, 160, 170, 215-217], PEG-*g*-PAsp^[218], poly(2-ethyl-2-oxazoline)-*b*-poly(aspartic acid) (PEOz-*b*-PAsp)^[175], poly(2-isopropyl-2-oxazoline)-*b*-poly(aspartic acid) (PiPrOz-PAsp)^[219], PEG-*b*-poly(L-glutamic acid) (PEG-*b*-PGlu)^[158, 220, 221]); (ii) copolymers based on polyacrylic acid (PAA) (e.g. PEG-*b*-poly(methacrylic acid) (PEG-*b*-PMAA)^[222-225], polystyrene-*b*-PNIPAM-*b*-PAA (PS-*b*-PNIPAM-*b*-PAA)^[226], PNIPAM-*b*-PAA^[227]); and (iii) others (poly(*N*-vinylpyrrolidone)-*b*-poly(styrene-alter-maleic anhydride) (PVP-*b*-PSMA)^[164]).

The vast majority of copolymers used in the formulation of PIC micelles for biomedical applications have PEG as their neutral segment. This derives from its biological inertness, hydrophilicity, biocompatibility and ability to reduce protein adsorption over the micelles surface. Other neutral hydrophilic polymers, such as PVP, PNIPAM, PEOz and PiPrOz have also been used as corona forming blocks in PIC micelles. The attractiveness of PNIPAM, PEOz and PiPrOz as corona forming blocks relies on their thermo-sensitive properties. In aqueous solutions these polymers exhibit reversible thermo-responsive phase transition. This property has been exploited to prepare smart drug carriers that release their payload in certain pathological tissues with abnormally elevated temperature, such as certain types of cancer.^[228, 229]

1.4.6.5. Properties of PIC micelles

1.4.6.5.1. Particle size and size distribution

Most PIC micelles designed for biomedical applications are intended for parenteral administration. Therefore, particle size and size distribution are two crucial parameters

since they affect PIC micelles safety, biodistribution and stability.^[230] Although the smallest capillaries in the body are 5-10 μm in diameter, the size of nanoparticles intended for parenteral administration and any possible aggregates should be far below this size to avoid blocking blood vessels and emboli formation.^[39] Moreover, in order to attain longevity in the blood, nanoparticles diameter should be ≤ 200 nm since the sub-200 nm size along with biocompatibility allows nanoparticles to escape recognition by the MPS cells.^[231, 232]

Particle size of PIC micelles is dependent on many factors including chemical nature of their components, the ratio at which these components are mixed, pH and ionic strength of the medium. The molar charge ratios at which the drug and polymer are mixed greatly influence size and polydispersity index of the resulting PIC micelles. Micelles size is also affected by the order of addition (i.e. drug is added to polymer or vice versa). When a drug is added to an oppositely charged polymer in amounts such that the polymer is in excess, two species usually exist in solution: drug-polymer complex and free polymer. This usually gives micelles with high polydispersity indices where two or more populations exist in solution.^[233] Further increase in drug concentration relative to polymer concentration neutralizes free polymer chains resulting in monodispersed micelles at charge neutrality. For instance, Harada and Kataoka^[153] showed that diameter and polydispersity index of lysozyme/PEG-*b*-PAsp micelles were dependent on their mixing ratio, r (the ratio of the number of aspartic acid residues in PAsp to the total number of arginine and lysine residues in lysozyme). Micelles diameter remained constant ~ 50 nm in the range of $0.125 \leq r \leq 1.0$ and increased almost linearly from ~ 50 to ~ 80 nm when r increased from 1.0 to 4.0. Polydispersity index decreased from 0.1 to 0.05 when r increased from 0.125 to 1.0 and remained constant thereafter. Constant micelles size at $r < 1.0$ was attributed to the formation of stoichiometric micelles ($r = 1.0$) where all PEG-*b*-PAsp in solution participated in micelles formation leaving excess lysozyme free in solution. At $r > 1.0$ thickness of the micelles shell increased due to the increased number of PEG-*b*-PAsp chains in the micelles, which led to increasing the overall micelles size.

1.4.6.5.2. *Surface charge*

Nanoparticles surface charge or zeta potential is one of the key factors that determine their *in vitro* stability, biodistribution and *in vivo* fate.^[97] Nanoparticles with charged surfaces, either positive or negative have better *in vitro* colloidal stability since electrostatic repulsions reduce particle aggregation.^[234, 235] Cell surface is negatively charged due to the presence of sulfated proteoglycans.^[236] Thus, positively charged nanoparticles have a better chance to interact with the cells than neutral or negatively charged ones. Although this improves the cellular uptake of positively charged nanoparticles, it typically results in non-specific distribution and uptake by various non-target tissues. Moreover, positively charged nanoparticles form aggregates with negatively charged serum proteins following IV injection. These aggregates cause transient embolism in the lung capillaries.^[237] Negatively charged liposomes with diameter ~ 200 nm were shown to be cleared from the blood at a rate higher than that of neutral ones.^[238] For all these reasons, PIC micelles for drug delivery applications usually have a neutral PEG corona. The PIC micelles surface charge is determined by measuring their ζ potential (see below).

1.4.6.5.3. *Effect of pH on PIC micelles formation and stability*

The extent to which solution pH affects PIC micelles formation and stability depends on the type of the polyelectrolytes used in the complex formation. Thus, PIC micelles formed by a pair of strong polyelectrolytes are not affected by pH change since the charge density of these polyelectrolytes is fixed.^[152] In contrast, charge density of weak polyelectrolytes is strongly affected by pH change. Consequently, there exists a pH range for which polyelectrolytes have enough charge density to promote PIC micelles formation and stability. The width of this pH range depends on whether the micelles are formed by two weak or one weak and one strong polyelectrolyte. Above or below this pH range, one of the polyelectrolytes becomes neutral resulting in micellar disassembly.^[239-241] This pH responsiveness, although compromises micelles stability, has been taken advantage of in the preparation of PIC micelles that release their payload in response to change in pH of the surroundings. For instance, PIC micelles of PEG-*b*-PMMA/PLL dissociated at pH 5.0 showing their ability to release their cargo in the acidic environment of the endosomes (pH

~ 5-6) following endocytosis.^[223, 242] Yang *et al.*, reported that the release rate of diammonium glycyrrhizinate (an anionic drug) from its PIC micelles with PEG-*g*-chitosan was faster at higher pH values due to the decrease in chitosan degree of ionization.^[166] In addition to its influence on PIC micelles electrostatic interactions, pH affects other forces that contribute to PIC micelles formation and stability, such as hydrogen bonding. Thus, Gohy *et al.*, reported that poly (2-vinylpyridine)-*b*-poly(ethylene glycol) (P2VP-*b*-PEG) and poly(methacrylic acid)-*b*-poly(ethylene glycol) (PMAA-*b*-PEG) did not form PIC micelles at low pH values, instead they formed micelles with a core formed by the hydrogen bonding between neutral PMAA and PEG chains.^[243]

1.4.6.5.4. Effect of ionic strength on PIC micelles stability

PIC micelles are strongly sensitive to changes in ionic strength of the medium since salts cause charge screening and weakening of electrostatic interactions between oppositely charged polyelectrolytes.^[168, 244] Therefore, PIC micelles dissociate above certain salt concentration called critical ionic strength, *I_{cr}*. Critical ionic strength is dependent on the nature of PIC micelles constituents, their charge density, p*K*_a, pH, mixing ratio, micellar concentration and the type of added salt.^[225] PIC micelles formed by a combination of driving forces, such as electrostatic, hydrophobic and metal coordination are much more resistant to increase in salinity than those formed by electrostatic interactions only.^[245, 246] For biomedical applications, PIC micelles should be stable under physiological conditions (NaCl concentration of 0.15 M and pH 7.4). These conditions are challenging for many PIC micelles formulations. Thus, Yuan *et al.*, reported that PIC micelles of lysozyme/PEG-*b*-PAsp disintegrated after NaCl concentration of 0.05 M at pH 7.4.^[241] In addition, Nishiyama *et al.*, reported that PIC micelles of cisplatin/PEG-*b*-PAsp were stable at physiological salt concentration and 37 °C for 10 h, after which the micelles disassembled.^[247] Accordingly, several strategies have been proposed to improve PIC micelles stability under physiological conditions. Two eminent approaches include core-cross linking and hydrophobic modification of the ionic polymers. Thus, siRNA/PEG-*b*-PLL micelles with disulfide cross-linked core were stable against increase in salt concentration up to 0.3 M, well above the physiological salt concentration.^[173] In addition,

lysozyme/PEG-*b*-PAsp micelles cross linked by glutaraldehyde resisted increase in salinity up to 0.2 M.^[241] Hydrophobic modification of the ω end of PEG-*b*-PAsp by different hydrophobic groups (e.g. phenyl, naphthyl and pyrenyl) improved the stability of lysozyme/PEG-*b*-PAsp micelles against increase in salinity. However, non of these hydrophobized derivatives yielded stable micelles under physiological conditions.^[248]

1.4.6.5.5. Colloidal stability of PIC micelles

PIC micelles colloidal stability refers to their ability to remain stable in solution without macroscopic phase separation. At charge neutrality ratios, electrostatic interactions between oppositely charged polyelectrolytes result in phase separation and precipitation. In contrast, if a neutral segment is linked to one of the interacting polyelectrolytes, soluble colloidal particles (PIC micelles) are formed instead. Therefore, PIC micelles colloidal stability is determined by the balance between the tendency of the interacting species to phase separate and the tendency of the neutral blocks to stabilize the micelles and keep them in solution.^[152] Hence, PIC micelles colloidal stability is governed by the factors affecting the strength of electrostatic interactions (e.g. pH, ionic strength, charge density) and the factors affecting neutral blocks stabilizing effect (e.g. block length, molecular architecture, temperature, block length ratio of corona to core forming monomers, $N_{\text{corona}}/N_{\text{core}}$). For pharmaceutical applications, PIC micelles should be colloidally stable in solution for periods long enough to permit accurate dosing *in vitro* and delivery of the drug to its target *in vivo* without precipitation or phase separation. Moreover, these micelles should maintain their integrity and colloidal stability after freeze drying and reconstitution since freeze dried formulations have enhanced shelf life and are easy to handle and transfer.^[249] PIC micelles of lysozyme/PEG-*b*-PAsp prepared at charge neutrality showed no precipitation even after one month of storage at room temperature.^[153] Size of heparin/PEG-*b*-PDMAEMA PIC micelles was not affected by freeze drying and reconstitution.^[233]

1.4.6.5.6. Critical association concentration (CAC) of PIC micelles

Critical association concentration (CAC) or the concentration below which PIC micelles dissociate is one of the factors that determine their *in vivo* stability due to micelles

dilution in the body.^[177] CAC of PIC micelles prepared at charge neutrality is usually very low and affected by the nature of their constituents, their charge density, $N_{\text{corona}}/N_{\text{core}}$ and whether there are additional forces that participate in micelles formation (e.g. hydrophobic interactions).^[250] For instance, CAC of antisense-oligonucleotides/PEG-*b*-PLL micelles was ~ 0.2 mg/mL whereas that of PEG-*b*-PLL/PEG-*b*-PAsp micelles was below 0.01 mg/mL.^[177, 251]

1.4.6.6. Methods used to characterize PIC micelles

1.4.6.6.1. Dynamic light scattering (DLS)

DLS has been the method of choice to determine PIC micelles hydrodynamic radius (R_H). DLS measurements involve determining the time dependence of the light scattered from a small region of solution over a certain period of time.^[252] In case of coherent and monochromatic light, such as the light of a laser beam, it is possible to observe the time-dependent fluctuations of the scattered intensity. These fluctuations are due to Brownian motion of the particles in solution, which makes the distance between them constantly changing with time. Scattered light then undergoes either constructive or destructive interference by the surrounding particles and within this intensity fluctuation, information is obtained about the time scale of particles movement. Scattered light intensity is measured with a detector, such as a photomultiplier tube capable of operating in the photon counting mode. Analysis of the time dependence of intensity fluctuation gives the diffusion coefficient (D). The diffusion coefficient of the particles is used to calculate R_H from the Stokes Einstein equation (equation 2). R_H is the radius of a hypothetical hard sphere having the same diffusion coefficient as the particle in question.

$$R_H = \frac{kT}{6\pi\eta D} \quad (2)$$

Where R_H is the hydrodynamic radius, k is the Boltzmann's constant, T is the absolute temperature, η is the solvent viscosity and D is the diffusion coefficient.

DLS data is analyzed by the cumulant method or inverse Laplace transform (ILT) programs, such as CONTIN. R_H obtained from the cumulant method of analysis is the weighted distribution of all objects present in solution, weighted with their relative scattering power. Therefore, cumulant analysis is best suited for solutions having monodispersed particles. CONTIN analysis is preferred for heterodisperse or polydispersed systems.^[152]

1.4.6.6.2. *Static light scattering (SLS)*

In a typical SLS experiment, one measures the intensity of light scattered by a given solution as a function of the scattering angle and concentration of the solution. The light scattered by a dilute polymer solution can be expressed by equation 3^[177]:

$$\frac{\Delta R(\Theta)}{KC} = \frac{1}{M_{w, app}} (1 + q^2 R_g^2/3) + 2A_2C \quad (3)$$

Where C is the concentration of the polymer, $\Delta R(\Theta)$ is the difference between the Rayleigh ratio of the solution and that of the solvent, $M_{w, app}$ is the apparent weight average molecular weight of the polymer, q is the magnitude of the scattering vector, R_g is the radius of gyration, A_2 is the second virial coefficient, and $K = (4\pi^2 n^2 (dn/dc)^2)/(N_A \lambda^4)$ (N is Avogadro's number and dn/dc is the refractive index increments). The $M_{w, app}$ of the PIC micelles is obtained from Zimm plot of the data. The association number of the micelles is obtained by dividing micelles $M_{w, app}$ by molecular weight of a single polyanion/polycation constituting chain, assuming that PIC micelles have composition equal to the mixing ratio.^[177] SLS measurements have also been used to determine CAC of PIC micelles since the scattering intensity is a sensitive function of the weight average molecular weight of the micelles.^[253] Intensity of light scattered by PIC micelles at a fixed angle (i.e. 90°) has been frequently used to monitor micelles stability as a function of solution pH, ionic strength and storage under different conditions.^[170, 233, 247]

1.4.6.6.3. *ζ potential measurements*

ζ potential of PIC micelles is usually determined via light scattering detection in the so-called Zetasizer. ζ potential is calculated from micelles electrophoretic mobility in response to an applied external electric field using Smoluchowski equation. ζ potential measurements are used to determine PIC micelles surface charge and to confirm the formation of PIC micelles with core-corona structure. Thus, neutral ζ potential values observed for lysozyme/PEG-*b*-PAsp micelles were taken as an indirect evidence for the formation of PIC micelles with lysozyme/PAsp core coated by neutral PEG corona.^[153] Furthermore, ζ potential measurements have been used to confirm drug encapsulation into PIC micelles. Drug incorporation into the micelles neutralizes both the polymer and drug charges, which decreases the absolute value of micelles ζ potential. For instance, the encapsulation of all-trans retinoic acid into PEG-*g*-chitosan PIC micelles resulted in decreasing their ζ potential.^[165]

1.4.6.6.4. ¹H nuclear magnetic resonance (¹H NMR)

In the PIC micelles literature, ¹H NMR studies have been used to confirm the formation of micelles with core-corona structures. This takes advantage of the restricted motion of the drug and polymer segments forming the core, which results in significant line broadening and/or disappearance of the signals due to corresponding protons. In contrast, protons of the polymer segments forming the corona maintain their mobility and thus, appear well resolved.^[254] Thus, for all-trans retinoic acid (ATRA)/PEG-*g*-chitosan micelles, the specific ¹H NMR signals of ATRA and chitosan were not visible in either D₂O or DMSO. This was in contrast to the signals of PEG, which were visible in both solvents. These results confirmed that the PIC micelles have ATRA/chitosan core and a PEG corona.^[165]

1.4.6.6.5. Isothermal titration calorimetry (ITC)

Electrostatic interactions taking place during PIC micelles formation can be characterized by isothermal titration calorimetry (ITC) if they are associated with generation (exothermic reaction) or absorption (endothermic reaction) of heat. ITC monitors heat change due to these interactions and determines thermodynamic parameters of the binding. ITC is the only instrument that in a single experiment determines

thermodynamic parameters of the binding including binding constant (K), reaction stoichiometry (N), enthalpy change (ΔH) and entropy change (ΔS).^[255, 256]

ITC is composed of two cells (reference and sample) and an injection syringe (Figure 1.6, left). The reference and sample cells are made of a thermally conducting material, surrounded by an adiabatic jacket. A typical ITC experiment involves addition at a constant temperature of aliquots of known volume of ligand solution from the syringe into the sample cell containing macromolecule solution. Addition of ligand is automated by a highly precise syringe stirred at desired speed by a computer-controlled stepper motor. Each injection of the syringe solution triggers the binding reaction and, depending on the binding affinity and the concentration of reactants in the cell, a certain amount of ligand/macromolecule complex is formed. Heat released or absorbed during complex formation causes a difference in temperature between the reference and sample cells. Consequently, ITC raises or lowers the thermal power ($\mu\text{cal/sec}$) required to keep a constant temperature difference (close to zero) between the sample and the reference cell. After each injection, the system reaches equilibrium and the temperature balance is restored. The recorded signal shows a typical deflection pattern in the form of a peak (raw data). Integrating the area under the peak with respect to time provides the heat change per injection (Figure 1.6, right). As the interaction in the cell finishes, the heat signal diminishes until only the background heat due to ligand dilution is observed. The heat change profile as a function of the ligand/macromolecule molar ratio can be analyzed to give thermodynamic parameters of the interaction under investigation. Thermodynamics of binding between poly(ethylene glycol)-*b*-poly(2-(diethylamino)ethyl methacrylate) and Plasmid DNA were studied by ITC.^[195]

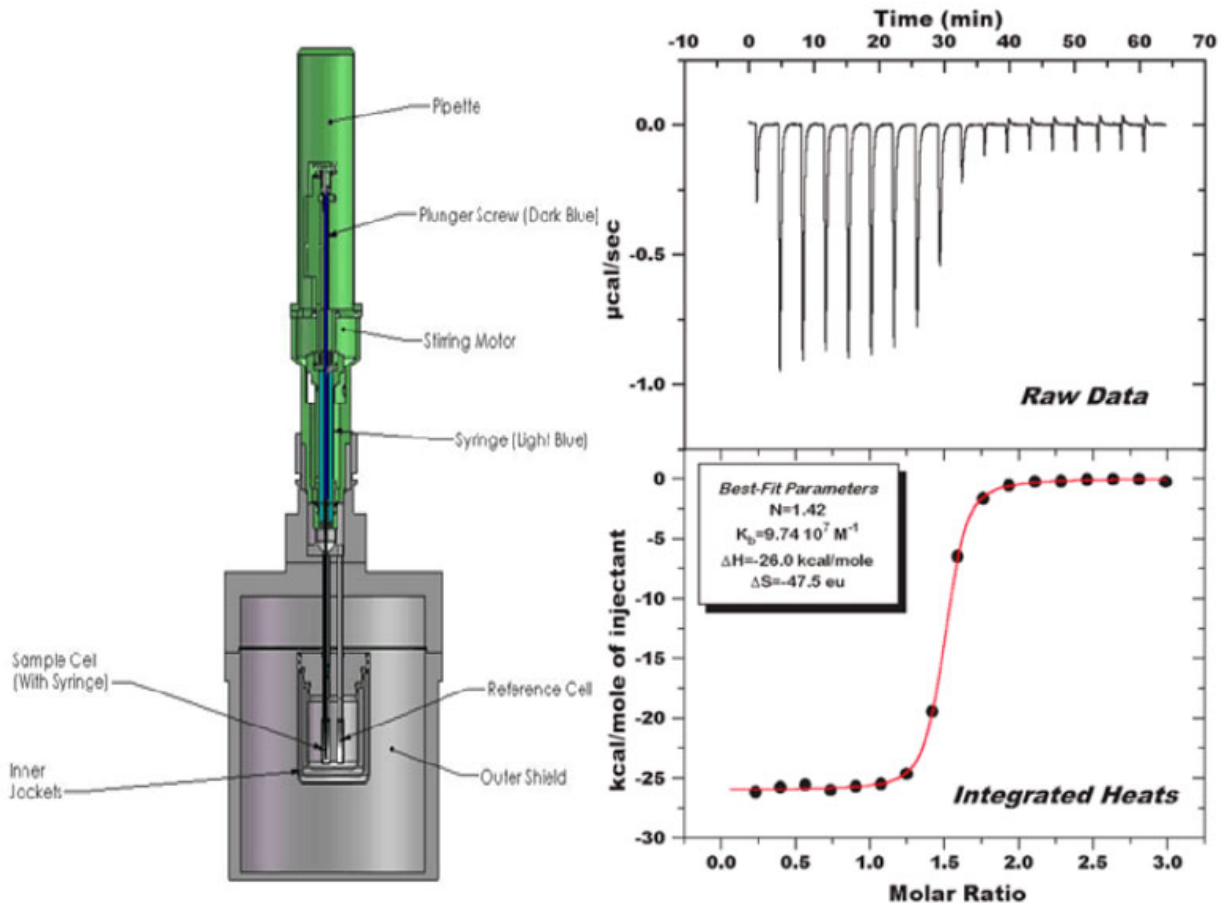


Figure 1.6. Diagram of ITC showing cells and syringe (left) and representative ITC data (right).

www.microcalorimetry.com

1.4.6.6.6. Other methods

In addition to the previously described methods, many other techniques have been used to characterize PIC micelles and study their formation, structure, dynamics and functions. Thus, gel retardation assays have been used to detect complex formation between siRNA and polycations and to qualitatively confirm the absence of free siRNA.^[173, 257] Fluorescence resonance energy transfer (FRET)^[258] and circular dichroism (CD)^[216] have

been used to study secondary structures of DNA and protein/peptide entrapped in PIC micelles. Imaging techniques that have been used to visualize PIC micelles include atomic force microscopy (AFM)^[233], transmission electron microscopy (TEM)^[165], scanning electron microscopy (SEM)^[259] and cryogenic transmission electro microscopy (cryo-TEM)^[260]. Enthalpy changes associated with the complexation in PIC micelles have been studied by differential scanning calorimetry (DSC)^[261].

1.4.6.7. Applications of PIC micelles as drug delivery systems

1.4.6.7.1. PIC micelles as non-viral gene vectors

Gene therapy is the delivery of genes to cells and tissues to treat a disease, such as hereditary diseases in which a non-functional mutant gene is replaced by a functional one. Gene therapy has a great potential not only in the treatment of hereditary diseases but also in the treatment of acquired diseases, such as cancer and infectious diseases. In addition to delivery of functional genes, silencing of defective genes can be achieved by the conventional antisense technology or more recently by sequence specific gene silencing using small interfering RNA (siRNA).^[27, 262] Efficient gene delivery is hindered by many obstacles including poor tissue penetration due to large molecular weight and anionic nature of the genes, difficulty of targeting genes to the nucleus, instability and rapid *in vivo* elimination and poor transfection efficiency.

In order to overcome these obstacles either viral or non viral gene vectors are used. Although viral vectors have the advantage of high transfection efficiency, their potential safety risks, as well as immunogenicity justify the search for alternative non-viral vectors. Among different non-viral gene vectors, those based on electrostatic interactions between DNA and cationic lipids (i.e. lipoplexes)^[263] or DNA and cationic polymers (i.e. polyplexes)^[264] are the most studied systems. Lipoplexes and polyplexes are not soluble at charge stoichiometric ratios due to charge neutralization. Water solubility of lipoplexes and polyplexes is preserved by using an excess of the cationic species resulting in numerous side effects after *in vivo* administration.^[262] In contrast, PIC micelles, as polyplexes, have the ability to condense DNA and maintain their water solubility at stoichiometric ratios, thanks to their neutral corona (usually PEG). To be viable gene vectors, PIC micelles

should be stable under physiological conditions, their DNA payload should be kept encapsulated as long as the micelles are circulating in the blood and it should be released once the micelles are inside the target cells.

The literature shows numerous examples of PIC micelles being used as non-viral gene vectors. For instance, PEG-*b*-poly(amino acids) copolymers (e.g. PEG-*b*-PLL, PEG-*b*-PGlu) have been frequently used for the delivery of DNA, oligonucleotides and siRNA. Plasmid DNA (pDNA) encapsulated in PIC micelles of PEG-*b*-PLL was more resistant to degradation by nucleases than free pDNA.^[180] Moreover, pDNA was more tolerable to physiological conditions when encapsulated in PIC micelles than pDNA encapsulated in polyplexes (pDNA/PLL) or lipoplexes (pDNA/lipofectamine).^[258] Transfection efficiency of pDNA/PEG-*b*-PLL PIC micelles in cultured 293 cells increased with increasing the length of PLL segment or the mixing charge ratio (PLL/pDNA) suggesting that the transfection efficiency is related to the degree of pDNA condensation.^[265] Following IV injection, naked pDNA was cleared from the blood stream within 5 minutes. In contrast, pDNA/PEG-*b*-PLL micelles had a considerably higher blood retention time. Moreover, *in vivo* gene expression was observed for up to 3 days post-injection of the micelles.^[266]

Despite these advantages of PIC micelles as gene vectors, their stability in the blood was not enough to permit their clinical application. To address this issue, the core of PEG-*b*-PLL micelles entrapping DNA was cross linked by disulfide bonds, which are stable in the blood and readily hydrolyzed in the cytoplasm due to the presence of high concentrations of glutathione.^[267] Interestingly, core-cross linked PIC micelles were stable under physiologic conditions and showed 100-fold higher siRNA transfection efficiency compared to non cross-linked micelles, which were not stable at physiological ionic strength.^[173]

In addition to PIC micelles of PEG-*b*-poly(amino acids), those based on cationic aliphatic polyesters were used as delivery vectors for siRNA. Thus, Xiong *et al.*, evaluated a novel family of PEG-*b*-PCL based copolymers with polyamine side chains on the PCL block for siRNA delivery. Polymers studied were PEG-*b*-PCL with grafted spermine (PEG-*b*-P(CL-*g*-SP)), grafted tetraethylenepentamine (PEG-*b*-P(CL-*g*-TP)), or grafted *N,N*-dimethyldipropylenetriamine (PEG-*b*-P(CL-*g*-DP)).^[257] The siRNA formulated in PEG-*b*-

P(CL-*g*-SP) and PEG-*b*-P(CL-*g*-TP) micelles demonstrated effective endosomal escape and efficient gene silencing. Another PCL-based copolymer for siRNA delivery was a cationic triblock copolymer consisting of PEG, PCL and poly(2-aminoethyl ethylene phosphate) (PEG-*b*-PCL-*b*-PAEEP).^[268] Based on MTT assays, these new polymers were not cytotoxic even at polymer concentration of 1 mg/mL. PIC micelles of siRNA/PEG-*b*-PCL-*b*-PPEEA were effectively internalized into HEK293 cells, resulting in significant gene silencing activity. These studies demonstrated the promise of PIC micelles as efficient non-viral gene vectors.

1.4.6.7.2. PIC micelles as delivery systems for anticancer drugs

Cisplatin (*cis*-dichlorodiammineplatinum(II); CDDP) is an anticancer drug that is widely used for the treatment of many malignancies, including testicular, ovarian, bladder, head and neck, small-cell, and non-small-cell lung cancers.^[269] However, its clinical use is limited due to emergence of intrinsic and acquired resistance and severe side effects.^[270, 271] Moreover, it is cleared from the body by glomerular filtration within 15 min following IV injection.^[44] PIC micelles of CDDP and PEG-*b*-poly(amino acids) copolymers have been developed in order to increase the drug half life in the blood and to enhance its accumulation in solid tumors.

When aqueous solutions of CDDP and poly(amino acids) are mixed, metal complexation between platinum of CDDP and carboxylic acid groups of the poly(amino acid) segment of the copolymer trigger formation of PIC micelles. CDDP/PEG-*b*-PAsp micelles sustained drug release for over 50 h in the presence of 150 mM NaCl. Following IV injection to Lewis lung carcinoma-bearing mice, micelles showed a 4.6-fold higher CDDP accumulation in tumor sites compared to free CDDP. However, *in vivo* anti-tumor activity of micelles-encapsulated drug was similar to that of the free drug.^[272] To improve micelles stability under physiological conditions and increase their blood circulation time, PEG-*b*-PAsp was replaced by PEG-*b*-PGlu. PGlu has a more hydrophobic backbone due to the presence of one additional CH₂ group, which can increase micelles stability. This modification resulted in better control over drug release from the micelles under physiological conditions. Thus, 50% CDDP was released after 30 h and 90 h from PEG-*b*-

PAsp and PEG-*b*-PGlu micelles, respectively.^[158] Furthermore, CDDP/PEG-*b*-PGlu micelles showed longer circulation in the blood, 11% of the injected dose was detected in the blood at 24 h post injection, compared to 1.5% in the case of CDDP/PEG-*b*-PAsp micelles at the same time. Tumor accumulation of CDDP/PEG-*b*-PGlu micelles was 20-fold higher than that of free CDDP, indicating tumor-selective targeting by the EPR effect. Intravenous injection of CDDP/PEG-*b*-PGlu micelles to tumor bearing mice showed complete tumor regression for more than 80% of the treated mice, with only minimal body weight loss (within 5% of the initial weight). In contrast, treatment with free CDDP at the same dose exhibited tumor regression for only 15% of treated mice and significant body weight loss (20% of the initial weight). The CDDP/PEG-*b*-PGlu micelles are now undergoing a phase I/II clinical trial as NC-6004 in the UK.^[273, 274]

Photodynamic therapy (PDT), which involves photosensitizers accumulation in solid tumors followed by local photoirradiation of solid tumors with light of a specific wavelength, is a promising physical approach of cancer treatment.^[275, 276] Following photoirradiation, PSs generate reactive oxygen species (ROS), such as singlet oxygen, which results in photochemical destruction of tumor tissues. However, PSs readily form aggregates, resulting in self quenching and significant reduction in singlet oxygen production.^[277] Moreover, PDT causes skin hyperphotosensitivity requiring the patient to stay in a darkened room away from light for at least 2 weeks. These side effects result from lack of tumor selectivity of currently approved PSs, such as Photofrin® (polyhematoporphyrin esters, PHE).^[278] To overcome these drawbacks and enhance the efficacy of PDT, phthalocyanine (Pc), an anionic photosensitizer dendrimer was encapsulated into PIC micelles of PEG-*b*-PLL.^[275] The micelles showed significantly higher *in vivo* PDT efficacy than Photofrin® in mice bearing human lung adenocarcinoma A549 cells. Micelles-treated mice did not show skin phototoxicity, which was apparently observed for Photofrin®-treated mice, under identical conditions. Other anticancer drugs that have been successfully encapsulated into PIC micelles are shown in Table 1.3.

Table 1.3. Different drugs that have been encapsulated into PIC micelles

Polymer	Drug	Application	Ref.
PEG- <i>b</i> -PMAA	cisplatin	anticancer	[224]
PEG- <i>g</i> -chitosan	ATRA	anticancer	[165]
PEG- <i>b</i> -PLL	dendrimer phthalocyanine	PDT	[279]
PEG- <i>b</i> -PLL	anionic porphyrin	PDT	[181]
PEG- <i>b</i> -PAsp	cationic porphyrin	PDT	[215]
PS- <i>b</i> -PNIPAM- <i>b</i> -PAA/ PEG- <i>b</i> -P4VP	ibuprofen	anti-inflammatory, analgesic	[226]
PEG- <i>b</i> -PAsp	vasopressin	ADH	[160]
PLL- <i>g</i> -DEX	DNA	gene therapy	[187]
PEG- <i>b</i> -MAA/PDMAEMA	DNA	gene therapy	[280]
PAA- <i>b</i> -pluronic- <i>b</i> -PAA	doxorubicin	anticancer	[281]
PEG- <i>b</i> -PDMAEMA	heparin	anticoagulant	[233]
PEG- <i>g</i> -chitosan	DG	anti-inflammatory	[166]

PEG-*b*-PMAA: PEG-*b*-poly(methacrylic acid); ATRA: all-trans retinoic acid; PEG-*b*-PLL: PEG-*b*-poly(L lysine); PDT: Photodynamic therapy; PEG-*b*-PAsp: PEG-*b*-poly(aspartic acid); PS-*b*-PNIPAM-*b*-PAA: poly(styrene)-*b*-poly(N-isopropyl acrylamide)-*b*-poly(acrylic acid); PEG-*b*-P4VP: PEG-*b*-poly(4-vinylpyridine); PLL-*g*-DEX: poly(L lysine)-*g*-dextran; ADH: antidiuretic hormone; PDMAEMA: poly(2-(*N,N*-dimethylamino) ethyl methacrylate); DG: diammonium glycyrrhizinate.

1.4.6.7.3. PIC micelles as delivery systems for other drugs

In addition to their usefulness in gene and cancer therapy, PIC micelles have found applications as delivery systems for other drugs (Table 1.3). Thus, the antifungal drug amphotericin B (AmB) was encapsulated into PIC micelles of PEOz-*b*-PAsp to reduce its cytotoxicity and enhance its efficacy.^[175] Prolonged release of the drug from micelles effectively inhibited the growth of *Candida albicans* even after three days of administration. Moreover, AmB-loaded micelles showed lower cytotoxicity, *in vitro* and higher potency than the commercial AmB formulation, Fungizone®. PIC micelles of poly(*N*-vinylpyrrolidone)-*b*-poly(styrene-*alt*-maleic anhydride/chitosan were used as a delivery vehicle for coenzyme A (CoA).^[164] CoA was released from the micelles in response to change in solution pH and ionic strength showing the potential of these micelles for drug delivery applications.

1.5. Nanoparticles based on modified dextran as drug carriers

From toxicological point of view, biopolymers are ideal for pharmaceutical applications since they are biocompatible and biodegradable. Amongst biopolymers, the polysaccharides class offers the advantages of structural diversity, functional versatility and abundance in nature. According to their charge, polysaccharides can be classified into neutral, cationic or anionic. Chitosan (cationic), hyaluronic acid (anionic) and dextran (neutral) are the most frequently used biopolymers in the preparation of polysaccharides-based nanoparticles.

Dextran (Figure 1.7) is synthesized from sucrose by different bacterial strains. It is consisting of α -(1-6) linked D-glucose units with varying degrees of α -(1-3) branching depending on the bacteria used in its preparation.^[282] The degree of branching may vary between 0.5 and 60%. Branching at α -(1-2) and α -(1-4) is also possible.^[283] Dextran obtained from *Leuconostoc mesenteroids* NRRL B-512 are of particular pharmaceutical interest.^[282] They are characterized by their content of 95% α -1,6-glucofuranosidic linkages and 5% 1,3-linkages.

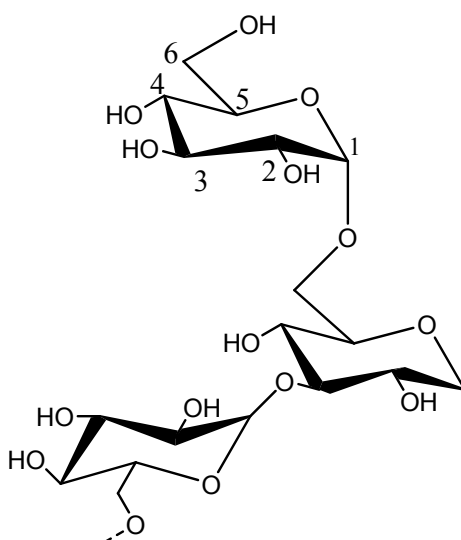


Figure 1.7. Chemical structure of dextran showing $\alpha(1-6)$ glycosidic linkages and $\alpha(1-3)$ branching.

Dextran is soluble in many solvents including water, mild acidic and alkaline conditions^[284], dimethyl sulfoxide, formamide, glycerol, and ethylene glycol.^[285] Dextran is not absorbed orally since its hydrophilicity prevents its transcellular absorption while its size prevents its paracellular absorption in the GI tract.^[286] It is degraded into low molecular weight fractions during passage through the GI tract.^[287] Dextran is depolymerized by various α -1-glucosidases (dextranases) available in various organs, including the liver, kidney, spleen and the lower part of the GI tract.^[288] The presence of high concentrations of dextranases in the colon allowed the preparation of colon-targeted dextran-based drug delivery systems for the local treatment of various colon disorders, such as irritable bowel syndrome, colon cancer and ulcerative colitis.^[289-292]

The pharmacokinetics of intravenously administered dextran are dependent on its molecular weight. Mehvar *et al.*^[286] studied molecular weight dependence of dextran pharmacokinetics in rats by measuring dextran concentrations in serum and urine after IV injection of five different molecular weights: 4, 20, 40, 70, and 150 kDa. Dextran of high molecular weights (i.e. 40, 70 and 150 kDa) was detectable in the blood for up to 12 h post-dosing. In contrast, dextran having molecular weights of 4 and 20 kDa was rapidly eliminated so that it was undetectable in the blood 1.5 and 3 h post-dosing, respectively.

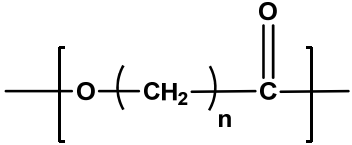
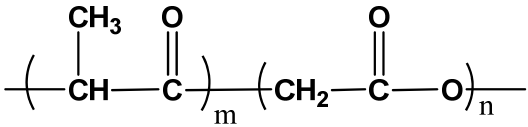
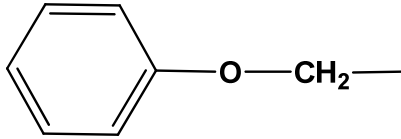
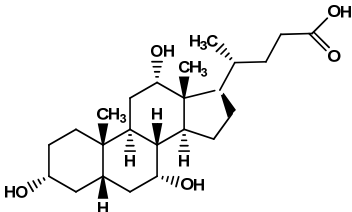
Chang *et al.*^[293] showed that neutral dextran is eliminated in rats by glomerular filtration without any tubular secretion or reabsorption. Therefore, renal clearance of dextran is reported as a fraction of the glomerular filtration rate.

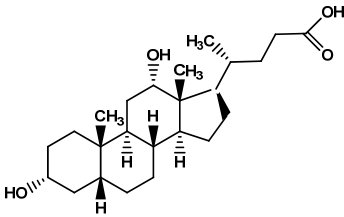
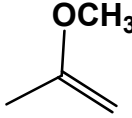
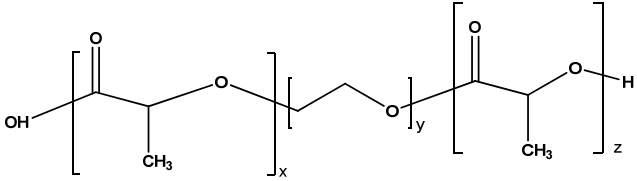
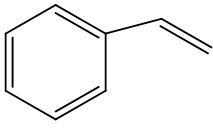
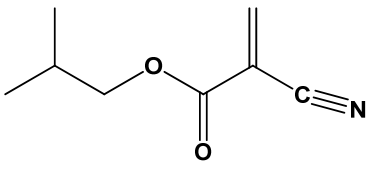
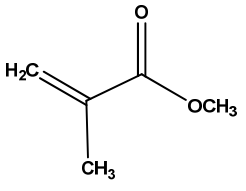
Dextran is clinically used as plasma volume expander, peripheral flow promoter and antithrombolytic agent for more than 5 decades.^[294, 295] Other biomedical applications of dextran include its use as a drug carrier system. Thus, dextran hydrogels have been used for the delivery of various drugs, such as salmon calcitonin and vitamin E and as scaffolds for vascular tissue engineering.^[296-298] Dextran has also been used for the preparation of macromolecular prodrugs through conjugation with different drugs and proteins either directly or through a spacer.^[295] Furthermore, dextran-based nanoparticles served as delivery vehicles for several hydrophobic and hydrophilic drugs. Native dextran lacks the amphiphilicity required to form nanoparticles since it is highly water soluble and neutral. Therefore, dextran-based nanoparticles are obtained either by hydrophobic modification of dextran or by electrostatic interactions between ionic dextran derivatives and oppositely charged drugs.

1.5.1. Nanoparticles of hydrophobically modified dextran (HM-DEX)

Hydrophobic modification of dextran facilitates its self assembly into nanoparticles and creates microreservoirs suitable for solubilization of hydrophobic drugs. The structural features of dextran (Figure 1.7) with numerous hydroxyl groups along its backbone gives diversity in the type of bonds that can be used to attach a hydrophobic moiety. Thus, different hydrophobic moieties have been linked to dextran by ester, ether, amide and many others bonds. Table 1.4 gives examples of the various hydrophobic moieties that have been used to modify dextran.

Table 1.4. Different hydrophobic compounds used to modify dextran.

Hydrophobic moiety	Resulting polymer	Ref.
PCL 	PCL- <i>g</i> -DEX	[299-301]
PLGA 	PLGA- <i>g</i> -DEX	[302]
Polyethyleneglycolalkyl ether $C_nH_{2n+1}-(O-CH_2-CH_2)_m-$	PEG- <i>C_n</i> - <i>g</i> -DEX	[303]
Phenoxy, C6 and C10 alkyl chains  $CH_3-(CH_2)_5-$ $CH_3-(CH_2)_9-$	DEX-P _x , DEX-C6 _x , DEX-C10 _x	[304]
Cholic acid 	Cholate and deoxycholate esters of dextran	[305]

<p>Deoxycholic acid</p> 		
<p>2-methoxypropene</p> 	Ac-DEX	[306]
<p>PLA</p> 	PLA- <i>g</i> -DEX	[307]
<p>Styrene</p> 	PS- <i>g</i> -DEX PS- <i>b</i> -DEX	[308, 309]
<p>IBCA</p> 	PIBCA- <i>g</i> -DEX PIBCA- <i>b</i> -DEX	[310]
<p>MMA</p> 	PMMA- <i>b</i> -DEX	[311]

PLGA: poly(lactic-*co*-glycolic acid); PCL: poly(ϵ -caprolactone); PLA: poly(lactic acid); IBCA: isobutyl cyanoacrylate; MMA: methyl methacrylate; PS: polystyrene; Ac-DEX: acetalated dextran.

Drug-loaded nanoparticles of HM-DEX have been prepared by different methods based on the solubility characteristics of HM-DEX and the drug. For instance, cyclosporin A(CsA)-loaded PEG-*Cn-g*-DEX micelles were prepared by the dialysis method.^[303] CsA solution in ethanol was mixed with aqueous solution of PEG-*Cn-g*-DEX followed by dialysis against water. Gradual replacement of the organic solvent with water induces micelles formation and simultaneous drug incorporation in micelles core. Other examples of drug-loaded HM-DEX nanoparticles and their preparation methods are given in Table 1.5.

Table 1.5. Methods used for the preparation of drug-loaded HM-DEX nanoparticles

Polymer	Drug	Preparation method	Drug content^a (% w/w)	Ref.
PLGA- <i>g</i> -DEX	amphotericin B	dilaysis	4.2	[312]
PLGA- <i>g</i> -DEX	clonazepam	dialysis	10.2	[313]
PLGA- <i>g</i> -DEX	amphotericin B	dialysis	4.8-18.9	[314]
PLGA- <i>g</i> -DEX	doxorubicin	dialysis	5.7-7.5	[302]
PCL- <i>g</i> -DEX	tamoxifen	nanoprecipitation	3.8-43.5	[315]
PCL- <i>g</i> -DEX	indomethacin	dialysis	ND	[299]
PCL- <i>g</i> -DEX	coumarin-6	oil/water emulsion	ND	[316]
PEG- <i>Cn-g</i> -DEX	cyclosporin A	dialysis	1.5-4.8	[303]
Ac-DEX	ovalbumin	double emulsion	3.7	[306]

^a: Drug content = weight of drug in nanoparticles X 100 / total weight of nanoparticles.

ND: not determined.

Nanoparticles of HM-DEX usually have a core-corona structure with the hydrophobic chains forming the core and dextran forming the corona. Nanoparticles core is used to solubilise hydrophobic drugs (Table 1.5) whereas the dextran shell reduces protein adsorption and uptake by the MPS cells and thus, prolong the nanoparticles circulation in the blood. The configuration of dextran chains over nanoparticles surface had a crucial role in determining their interaction with biological systems.^[317, 318] Thus, PCL-g-DEX nanoparticles with dextran chains organized as larger and looser loops adsorbed higher amounts of bovine serum albumin compared to nanoparticles having dextran chains arranged in dense and compact configuration.^[319] Moreover, PMMA nanoparticles with dense brush-like dextran shell had significantly higher blood circulation time than uncoated PMMA nanoparticles. Uncoated PMMA nanoparticles were eliminated from the blood in few minutes whereas DEX-PMMA nanoparticles were slowly eliminated over a period of more than 48 h.^[90]

1.5.2. Nanoparticles based on ionic dextran derivatives

These nanoparticles are formed by electrostatic interactions between ionic dextran derivatives, either anionic or cationic and an oppositely charged polymer, protein, drug or DNA. Contrary to nanoparticles of HM-DEX where dextran forms the nanoparticles shell, nanoparticles of ionic dextran have a core of dextran electrostatically linked to a drug. Dextran sulfate (anionic), diethylaminoethyl-dextran (DEAE-DEX) (cationic) and dextran-spermine (DEX-SPM) (cationic) are the most commonly used ionic dextrans for nanoparticles formation (Figure 1.8). Dextran sulfate forms nanoparticles by strong electrostatic interactions with positively charged polymers, such as chitosan^[259, 320, 321], polyethylenimine (PEI)^[322, 323], poly(L lysine) (PLL)^[324] and polyallylamine.^[325] Nanoparticles of dextran sulfate/chitosan have been used to encapsulate several drugs, such as insulin, amphotericin B and doxorubicin.^[321, 326, 327] Cationic dextrans (e.g. DEAE-DEX and DEX-SPM) have been used as non-viral gene vectors due to their ability to condense DNA.^[328, 329]

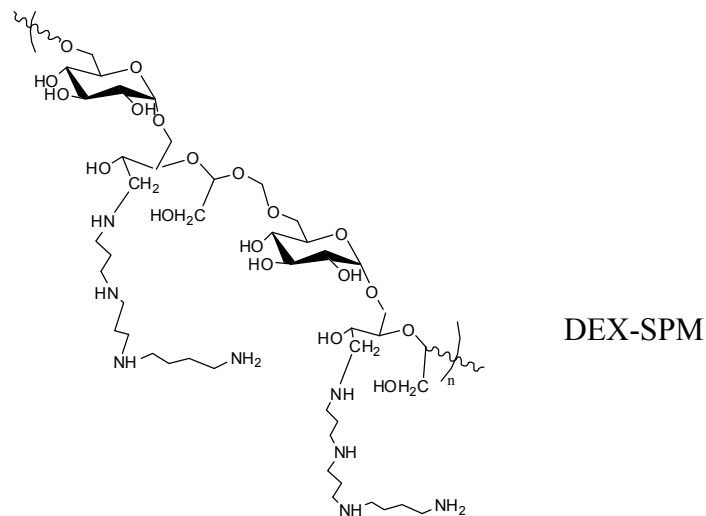
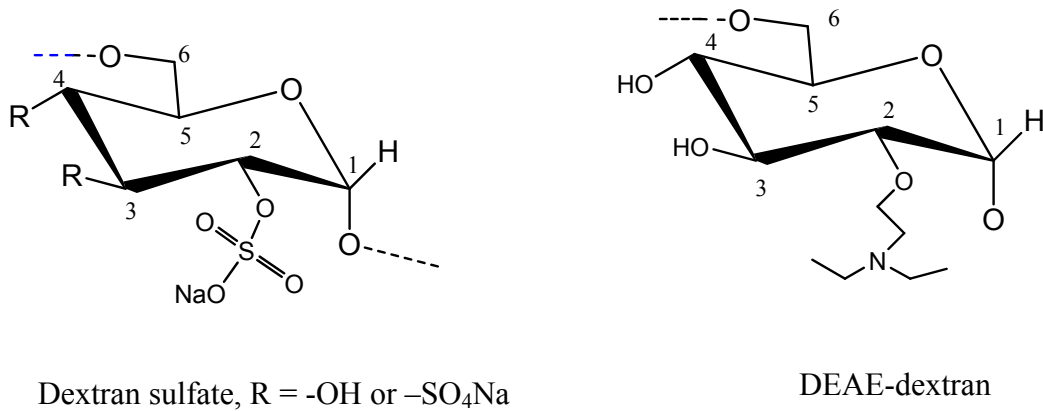


Figure 1.8. Chemical structure of dextran sulfate, DEAE-dextran and DEX-SPM.

1.6. Thesis rationale and research objectives

1.6.1. Rationale

Dextran is a well-known biocompatible and biodegradable polysaccharide that has been in clinical use for more than 5 decades.^[295] Different kinds of dextran-based drug carrier systems, such as nanoparticles, microparticles and hydrogels have been prepared and evaluated for the delivery of numerous drugs. Among these different carriers,

nanoparticles are, on many levels, the most promising ones because of their outstanding performance, both *in vitro* and *in vivo*. Most of these drug carriers were designed to encapsulate hydrophobic drugs. Little work was devoted to the development of dextran-based nanoparticles for the delivery of ionic water soluble drugs. PIC micelles are formed by electrostatic interactions between an ionic drug and oppositely charged copolymer. PIC micelles have found several applications in drug delivery due to their unique characteristics of straightforward preparation, small size, high drug loading capacity and excellent colloidal stability.^[153, 164, 177] However, very few PIC micelles were based on polysaccharides, such as chitosan and none at all was based on dextran. This, together with the success of PEGylated nanoparticles and the favorable properties of dextran prompted us to develop dextran-*block*-PEG copolymers suitable for drug delivery applications. Dextran block of these copolymers was functionalized by connecting carboxymethyl groups at different degrees of substitution to give a new family of carboxymethyl-dextran-PEG (CMD-PEG) block copolymers.^[330] When CMD-PEG copolymers are mixed with cationic drugs, PIC micelles are expected to form by electrostatic interactions between CMD segment of the copolymer and the cationic drug. These micelles are expected to have a CMD/cationic drug core surrounded by a PEG corona. Drug incorporation into the micelles core should sustain its release and protect it against degradation in solution. PEG corona of the micelles should prevent aggregation in solution and prolong their circulation in the blood. It was the overall aim of this project to develop PIC micelles based on CMD-PEG block copolymers for the encapsulation of different cationic drugs, such as aminoglycoside antibiotics and tetracycline antibiotics.

Physicochemical properties of PIC micelles, as well as their performance as drug delivery systems are affected; to a great extent by the properties of the copolymers used to formulate them.^[251, 331] Thus, relative block length of the ionic-neutral copolymer segments, charge density of the ionic block and the presence of other forces that assist in PIC micelles formation (e.g. hydrophobic interactions, metal coordination or hydrogen bonding) have been shown to affect PIC micelles properties.^[152] To reveal the effect of these parameters on the properties of CMD-PEG micelles, we developed four CMD-PEG copolymers: (i) two copolymers identical in terms of the length of CMD and PEG blocks, but different in

terms of the charge density of the CMD block; and (ii) two copolymers in which the charged block is the same, but the PEG block is of different molecular weight. The micellization of these four copolymers with a model water soluble cationic drug, diminazene diacetate was studied. The polymer that showed the most satisfactory results in terms of various drug delivery aspects, such as high drug loading, controlled drug release and micelles stability was chosen for encapsulation of other cationic drugs, such as aminoglycoside and tetracycline antibiotics (different properties of the drugs used in this thesis are given in appendix D).

1.6.2. Research objectives

1. To synthesize and characterize a series of CMD-PEG copolymers of different relative block lengths and ionic charge densities.
2. To study the effect of CMD-PEG relative block length and ionic charge density on the properties of PIC micelles formed with a model water soluble cationic drug, diminazene diacetate.
3. To develop and characterize a CMD-PEG micelle formulation encapsulating minocycline hydrochloride, a neuroprotective tetracycline as a potential treatment of several diseases, such as stroke, amyotrophic lateral sclerosis and Parkinson's disease.
4. To develop and characterize CMD-PEG PIC micelles formulations encapsulating various aminoglycoside antibiotics, such as neomycin and paromomycin for the treatment of bacterial infections caused by gram negative bacteria.
5. To improve the stability of aminoglycosides/CMD-PEG micelles against increase in salinity by hydrophobic modification of the CMD block.

1.7. References

- [1] José Alonso M. Nanomedicines for overcoming biological barriers. *Biomed. Pharmacother.* **2004**, *58*: 168-72.
- [2] MiMasi J. New drug development in the United States from 1963 to 1999. *Clin. Pharmacol. Ther.* **2001**, *69*: 286-96.
- [3] Devalapally H, Chakilam A, Amiji MM. Role of nanotechnology in pharmaceutical product development. *J. Pharm. Sci.* **2007**, *96*: 2547-65.
- [4] DiMasi JA, Hansen RW, Grabowski HG. The price of innovation: new estimates of drug development costs. *J. Health Econ.* **2003**, *22*: 151-85.
- [5] Sosnik A, Carcaboso AM, Chiappetta DA. Polymeric nanocarriers: new endeavors for the optimization of the technological aspects of drugs. *Recent Pat. Biomed. Eng.* **2008**, *1*: 43-59.
- [6] Mallick S, Pattnaik S, Swain K. Current perspectives of solubilization: Potential for improved bioavailability. *Drug Dev. Ind. Pharm.* **2007**, *33*: 865-73.
- [7] Fernandez AM, Van Derpoorten K, Dasnois L, Lebtahi K, Dubois V, Lobl TJ, Gangwar S, Oliyai C, Lewis ER, Shochat D, Trouet A. N-succinyl-(beta-alanyl-L-leucyl-L-alanyl-L-leucyl)doxorubicin: An extracellularly tumor-activated prodrug devoid of intravenous acute toxicity. *J. Med. Chem.* **2001**, *44*: 3750-3.
- [8] Merisko-Liversidge EM, Liversidge GG. Drug Nanoparticles: Formulating Poorly Water-Soluble Compounds. *Toxicol. Pathol.* **2008**, *36*: 43-8.
- [9] Amidon GL, Lennernas H, Shah VP, Crison JR. A theoretical basis for a biopharmaceutic drug classification-the correlation of in-vitro drug product dissolution and in-vivo bioavailability. *J. Pharm. Res.* **1995**, *12*: 413-20.
- [10] Klein S, Wempe MF, Zoeller T, Buchanan NL, Lambert JL, Ramsey MG, Edgar KJ, Buchanan CM. Improving glyburide solubility and dissolution by complexation with hydroxybutenyl-beta-cyclodextrin. *J. Pharm. Pharmacol.* **2009**, *61*: 23-30.
- [11] Lipinski CA. Drug-like properties and the causes of poor solubility and poor permeability. *J. Pharmacol. Toxicol. Methods* **2000**, *44*: 235-49.
- [12] Torchilin VP. Targeted polymeric micelles for delivery of poorly soluble drugs. *Cell. Mol. Life Sci.* **2004**, *61*: 2549-59.

- [13] Svenson S. Dendrimers as versatile platform in drug delivery applications. *Eur. J. Pharm. Biopharm.* **2009**, *71*: 445-62.
- [14] Matsumura Y. Polymeric micellar delivery systems in oncology. *Jpn. J. Clin. Oncol.* **2008**, *38*: 793-802.
- [15] Noyes AA, Whitney WR. The rate of solution of solid substances in their own solutions. *JACS* **1897**, *19*: 930-4.
- [16] Leuner C, Dressman J. Improving drug solubility for oral delivery using solid dispersions. *Eur. J. Pharm. Biopharm.* **2000**, *50*: 47-60.
- [17] Weiss RB, Donehower RC, Wiernik PH, Ohnuma T, Gralla RJ, Trump DL, Baker JR, Jr., Van Echo DA, Von Hoff DD, Leyland-Jones B. Hypersensitivity reactions from taxol. *J. Clin. Oncol.* **1990**, *8*: 1263-8.
- [18] Danhier F, Lecouturier N, Vroman B, Jérôme C, Marchand-Brynaert J, Feron O, Préat V. Paclitaxel-loaded PEGylated PLGA-based nanoparticles: In vitro and in vivo evaluation. *J. Controlled Release* **2009**, *133*: 11-7.
- [19] Mayersohn M. Principles of drug absorption. In: Banker GS, Rhodes CT, editors. *Modern Pharmaceutics*. New York: Marcel Dekker, Inc., 2002.
- [20] Danielli JF, Davson H. A contribution to the theory of permeability of thin films. *J. Cell Comp. Physiol.* **1935**, *5*: 495-508.
- [21] Fordtran JS. Permeability characteristics of the human small intestine. *J. Clin. Invest.* **1965**, *44*: 1935-44.
- [22] Hayashi M, Sakai T, Hasegawa Y, Nishikawahara T, Tomioka H, Iida A, Shimizu N, Tomita M, Awazu S. Physiological mechanism for enhancement of paracellular drug transport. *J. Controlled Release* **1999**, *62*: 141-8.
- [23] He YL, Murby S, Warhurst G, Gifford L, Walker D, Ayrton J, Eastmond R, Rowland M. Species differences in size discrimination in the paracellular pathway reflected by oral bioavailability of poly(ethylene glycol) and D-peptides. *J. Pharm. Sci.* **1998**, *87*: 626-33.
- [24] Lipinski CA, Lombardo F, Dominy BW, Feeney PJ. Experimental and computational approaches to estimate solubility and permeability in drug discovery and development settings. *Adv. Drug Deliv. Rev.* **1997**, *23*: 3-25.

- [25] Ghassemi AH, van Steenberg MJ, Talsma H, van Nostrum CF, Jiskoot W, Crommelin DJA, Hennink WE. Preparation and characterization of protein loaded microspheres based on a hydroxylated aliphatic polyester, poly(lactic-co-hydroxymethyl glycolic acid). *J. Controlled Release* **2009**, *138*: 57-63.
- [26] Corbo DC, Huang YC, Chien YW. Nasal delivery of progestational steroids in ovariectomized rabbits. II. Effect of penetrant hydrophilicity. *Int. J. Pharm.* **1989**, *50*: 253-60.
- [27] Kim W, Kim S. Efficient siRNA delivery with non-viral polymeric vehicles. *Pharm. Res.* **2009**, *26*: 657-66.
- [28] Luten J, van Nostrum CF, De Smedt SC, Hennink WE. Biodegradable polymers as non-viral carriers for plasmid DNA delivery. *J. Controlled Release* **2008**, *126*: 97-110.
- [29] Grimm D. Small silencing RNAs: State-of-the-art. *Adv. Drug Deliv. Rev.* **2009**, *61*: 672-703.
- [30] Csaba N, Garcia-Fuentes M, Alonso MJ. Nanoparticles for nasal vaccination. *Adv. Drug Deliv. Rev.* **2009**, *61*: 140-57.
- [31] Klingler C, Müller BW, Steckel H. Insulin-micro- and nanoparticles for pulmonary delivery. *Int. J. Pharm.* **2009**, *377*: 173-9.
- [32] Ungaro F, d'Emmanuele di Villa Bianca R, Giovino C, Miro A, Sorrentino R, Quaglia F, La Rotonda MI. Insulin-loaded PLGA/cyclodextrin large porous particles with improved aerosolization properties: In vivo deposition and hypoglycaemic activity after delivery to rat lungs. *J. Controlled Release* **2009**, *135*: 25-34.
- [33] Li G, Badkar A, Nema S, Kolli CS, Banga AK. In vitro transdermal delivery of therapeutic antibodies using maltose microneedles. *Int. J. Pharm.* **2009**, *368*: 109-15.
- [34] Dowson AJ, Almquist P. Part III: The convenience of, and patient preference for, zolmitriptan orally disintegrating tablet. *Curr. Med. Res. Opin.* **2005**, *21*: S13-S7.
- [35] Carnaby-Mann G, Crary M. Pill Swallowing by Adults With Dysphagia. *Arch. Otolaryngol. Head Neck Surg.* **2005**, *131*: 970-5.

- [36] Barbanti P, Le Pera D, Cruccu G. Sumatriptan fast-disintegrating/rapid-release tablets in the acute treatment of migraine. *Expert Rev. Neurother.* **2007**, *7*: 927-34.
- [37] Guillory JK, Poust RI. chemical kinetics and drug stability. In: Banker GS, Rhodes CT, editors. *Modern Pharmaceutics*. New York: Marcel Dekker Inc, 2002.
- [38] Yamanaka YJ, Leong KW. Engineering strategies to enhance nanoparticle-mediated oral delivery. *J. Biomater. Sci., Polym. Ed.* **2008**, *19*: 1549-70.
- [39] Dutta T, Jain NK, McMillan NAJ, Parekh HS. Dendrimer nanocarriers as versatile vectors in gene delivery. *Nanomed. Nanotechnol. Biol. Med.* **2009**, *In Press*, *uncorrected proof*.
- [40] Robinson J, Jantzen G. Sustained- and controlled-release drug-delivery systems. In: Banker GS, Rhodes CT, editors. *Modern Pharmaceutics*. New York: Marcel Dekker, Inc., 2002.
- [41] Sinha R, Kim GJ, Nie S, Shin DM. Nanotechnology in cancer therapeutics: bioconjugated nanoparticles for drug delivery. *Mol. Cancer Ther.* **2006**, *5*: 1909-17.
- [42] Yokoyama M. Drug targeting with polymeric micelle drug carriers. In: Yui N, editor. *Supramolecular design for biological applications* CRC Press, 2002. p. 245-68.
- [43] Huwylar J, Drewe J, Krahenbuhl S. Tumor targeting using liposomal antineoplastic drugs. *Int. J. Nanomed.* **2008**, *3*: 21-9.
- [44] Osada K, Christie RJ, Kataoka K. Polymeric micelles from poly(ethylene glycol)-poly(amino acid) block copolymer for drug and gene delivery. *J. R. Soc. Interface* **2009**, *6*: S325-S39.
- [45] Martin del Valle EM, Galan MA, Carbonell RG. Drug delivery technologies: the way forward in the new decade. *Ind. Eng. Chem. Res.* **2009**, *48*: 2475-86.
- [46] Torchilin V. Multifunctional and stimuli-sensitive pharmaceutical nanocarriers. *Eur. J. Pharm. Biopharm.* **2009**, *71*: 431-44.
- [47] Kim S, Kim JH, Jeon O, Kwon IC, Park K. Engineered polymers for advanced drug delivery. *Eur. J. Pharm. Biopharm.* **2009**, *71*: 420-30.
- [48] Patil A, Shaikh IM, Kadam VJ, Jadhav KR. Nanotechnology in therapeutics - current technologies and applications. *Curr. Nanosci.* **2009**, *5*: 141-53.

- [49] Kurtoglu YE, Navath RS, Wang B, Kannan S, Romero R, Kannan RM. Poly(amidoamine) dendrimer-drug conjugates with disulfide linkages for intracellular drug delivery. *Biomaterials* **2009**, *30*: 2112-21.
- [50] Kumar V, Banker GS. Chemically-modified cellulosic polymers. *Drug Dev. Ind. Pharm.* **1993**, *19*: 1-31.
- [51] Kumar M, Kumar N. Polymeric controlled drug-delivery systems: Perspective issues and opportunities. *Drug Dev. Ind. Pharm.* **2001**, *27*: 1-30.
- [52] Gref R, Minamitake Y, Peracchia MT, Trubetskoy V, Torchilin V, Langer R. Biodegradable long-circulating polymeric nanospheres. *Science* **1994**, *263*: 1600-3.
- [53] Seymour LW, Duncan R, Strohaln J, Kopecek J. Effect of molecular-weight (MBARW) of n-(2-hydroxypropyl) methacrylamide copolymers on body distribution and rate of excretion after subcutaneous, intraperitoneal, and intravenous administration to rats. *J. Biomed. Mater. Res.* **1987**, *21*: 1341-58.
- [54] Kabanov AV, Batrakova EV, Meliknubarov NS, Fedoseev NA, Dorodnich TY, Alakhov VY, Chekhonin VP, Nazarova IR, Kabanov VA. A new class of drug carriers - micelles of poly(oxyethylene)-poly(oxypropylene) block copolymers as microcontainers for drug targeting from blood in brain. *J. Controlled Release* **1992**, *22*: 141-57.
- [55] Italia JL, Yahya MM, Singh D, Kumar M. Biodegradable nanoparticles improve oral bioavailability of amphotericin B and show reduced nephrotoxicity compared to intravenous FungizoneA (R). *Pharm. Res.* **2009**, *26*: 1324-31.
- [56] Litzinger DC, Huang L. Phosphatidylethanolamine liposomes: drug delivery, gene transfer and immunodiagnostic applications. *BBA* **1992**, *1113*: 201-27.
- [57] Makhof A, Tozuka Y, Takeuchi H. pH-Sensitive nanospheres for colon-specific drug delivery in experimentally induced colitis rat model. *Eur. J. Pharm. Biopharm.* **2009**, *72*: 1-8.
- [58] McClean S, Prosser E, Meehan E, O'Malley D, Clarke N, Ramtoola Z, Brayden D. Binding and uptake of biodegradable poly-lactide micro- and nanoparticles in intestinal epithelia. *Eur. J. Pharm. Sci.* **1998**, *6*: 153-63.

- [59] Matsumura Y, Maeda H. A new concept for macromolecular therapeutics in cancer-chemotherapy - mechanism of tumorotropic accumulation of proteins and the antitumor agent smancs. *Cancer Res.* **1986**, *46*: 6387-92.
- [60] Gaucher G, Dufresne M-H, Sant VP, Kang N, Maysinger D, Leroux J-C. Block copolymer micelles: Preparation, characterization and application in drug delivery. *J. Controlled Release* **2005**, *109*: 169-88.
- [61] Maeda H, Bharate GY, Daruwalla J. Polymeric drugs for efficient tumor-targeted drug delivery based on EPR-effect. *Eur. J. Pharm. Biopharm.* **2009**, *71*: 409-19.
- [62] Vauthier C, Bouchemal K. Methods for the preparation and manufacture of polymeric nanoparticles. *Pharm. Res.* **2009**, *26*: 1025-58.
- [63] Mishra B, Patel BB, Tiwari S. Colloidal nanocarriers: A review on formulation technology, types and applications towards targeted drug delivery. *Nanomed. Nanotechnol. Biol. Med. In Press, Accepted Manuscript*.
- [64] Dang JM, Leong KW. Natural polymers for gene delivery and tissue engineering. *Adv. Drug Deliv. Rev.* **2006**, *58*: 487-99.
- [65] Singh R, Singh S, Lillard JW. Past, present, and future technologies for oral delivery of therapeutic proteins. *J. Pharm. Sci.* **2008**, *97*: 2497-523.
- [66] Rabinow B, Chaubal M. Injectable nanoparticles for efficient drug delivery. In: Gupta R, Kompella U, editors. Nanoparticle technology for drug delivery. New York: Taylor & Francis Group, 2006.
- [67] Sinha VR, Bansal K, Kaushik R, Kumria R, Trehan A. Poly- ϵ -caprolactone microspheres and nanospheres: an overview. *Int. J. Pharm.* **2004**, *278*: 1-23.
- [68] Alexis F, Rhee J-W, Richie JP, Radovic-Moreno AF, Langer R, Farokhzad OC. New frontiers in nanotechnology for cancer treatment. *Urol. Oncol. Sem. Ori.* **2008**, *26*: 74-85.
- [69] Nassar T, Rom A, Nyska A, Benita S. Novel double coated nanocapsules for intestinal delivery and enhanced oral bioavailability of tacrolimus, a P-gp substrate drug. *J. Controlled Release* **2009**, *133*: 77-84.

- [70] Jain P, Jain S, Prasad KN, Jain SK, Vyas SP. Polyelectrolyte coated multilayered liposomes (nanocapsules) for the treatment of *Helicobacter pylori* infection. *Mol. Pharm.* **2009**, *6*: 593-603.
- [71] Couvreur P, Barratt G, Fattal E, Legrand P, Vauthier C. Nanocapsule technology: A review. *Crit. Rev. Ther. Drug Carr. Syst.* **2002**, *19*: 99-134.
- [72] Lambert G, Fattal E, Pinto-Alphandary H, Gulik A, Couvreur P. Polyisobutylcyanoacrylate nanocapsules containing an aqueous core as a novel colloidal carrier for the delivery of oligonucleotides. *Pharm. Res.* **2000**, *17*: 707-14.
- [73] Crespy D, Stark M, Hoffmann-Richter C, Ziener U, Landfester K. Polymeric nanoreactors for hydrophilic reagents synthesized by interfacial polycondensation on miniemulsion droplets. *Macromolecules* **2007**, *40*: 3122-35.
- [74] Miyazaki S, Takahashi A, Kubo W, Bachynsky J, Lobenberg R. Poly n-butylcyanoacrylate (PNBCA) nanocapsules as a carrier for NSAIDs: in vitro release and in vivo skin penetration. *J. Pharm. Pharm. Sci.* **2003**, *6*: 238-45.
- [75] de Faria TJ, de Campos AM, Senna EL. Preparation and characterization of poly(D,L-lactide) (PLA) and poly(D,L-lactide)-poly(ethylene glycol) (PLA-PEG) nanocapsules containing antitumoral agent methotrexate. *Macromol. Symp.* **2005**, *229*: 228-33.
- [76] Zhang Y, Zhu SY, Yin LC, Qian F, Tang C, Yin CH. Preparation, characterization and biocompatibility of poly(ethylene glycol)-poly(n-butyl cyanoacrylate) nanocapsules with oil core via miniemulsion polymerization. *Eur. Polym. J.* **2008**, *44*: 1654-61.
- [77] Blouza IL, Charcosset C, Sfar S, Fessi H. Preparation and characterization of spironolactone-loaded nanocapsules for paediatric use. *Int. J. Pharm.* **2006**, *325*: 124-31.
- [78] Pinto-Alphandary H, Aboubakar M, Jaillard D, Couvreur P, Vauthier C. Visualization of insulin-loaded nanocapsules: in vitro and in vivo studies after oral administration to rats. *Pharm. Res.* **2003**, *20*: 1071-84.
- [79] Prego C, Torres D, Alonso MJ. Chitosan nanocapsules: a new carrier for nasal peptide delivery. *J. Drug Deliv. Sci. Technol.* **2006**, *16*: 331-7.

- [80] Paiphansiri U, Tangboriboonrat P, Landfester K. Polymeric nanocapsules containing an antiseptic agent obtained by controlled nanoprecipitation onto water-in-oil miniemulsion droplets. *Macromol. Biosci.* **2006**, *6*: 33-40.
- [81] Gref R, Couvreur P. Nanocapsules: preparation, characterization and therapeutic applications. In: Torchilin V, editor. Nanoparticulates as drug carriers. London: Imperial College Press, 2006.
- [82] Graf A, Rades T, Hook SM. Oral insulin delivery using nanoparticles based on microemulsions with different structure-types: Optimisation and in vivo evaluation. *Eur. J. Pharm. Sci.* **2009**, *37*: 53-61.
- [83] Legrand P, Barratt G, Mosqueira V, Fessi H, Devissaguet JP. Polymeric nanocapsules as drug delivery systems - A review. *STP Pharma Sci.* **1999**, *9*: 411-8.
- [84] Letchford K, Burt H. A review of the formation and classification of amphiphilic block copolymer nanoparticulate structures: micelles, nanospheres, nanocapsules and polymersomes. *Eur. J. Pharm. Biopharm.* **2007**, *65*: 259-69.
- [85] Limayem Blouza I, Charcosset C, Sfar S, Fessi H. Preparation and characterization of spironolactone-loaded nanocapsules for paediatric use. *Int. J. Pharm.* **2006**, *325*: 124-31.
- [86] Nagarwal RC, Kant S, Singh PN, Maiti P, Pandit JK. Polymeric nanoparticulate system: A potential approach for ocular drug delivery. *J. Controlled Release* **2009**, *136*: 2-13.
- [87] Záviová V, Koneracká M, Múcková M, Kopcanský P, Tomasovicová N, Lancz G, Timko M, Pätoprstá B, Bartos P, Fabián M. Synthesis and characterization of polymeric nanospheres loaded with the anticancer drug paclitaxel and magnetic particles. *J. Magn. Magn. Mater.* **2009**, *321*: 1613-6.
- [88] Chauvierre C, Leclerc L, Labarre D, Appel M, Marden MC, Couvreur P, Vauthier C. Enhancing the tolerance of poly(isobutylcyanoacrylate) nanoparticles with a modular surface design. *Int. J. Pharm.* **2007**, *338*: 327-32.
- [89] Aggarwal P, Hall JB, McLeland CB, Dobrovolskaia MA, McNeil SE. Nanoparticle interaction with plasma proteins as it relates to particle biodistribution, biocompatibility and therapeutic efficacy. *Adv. Drug Deliv. Rev.* **2009**, *61*: 428-37.

- [90] Passirani C, Barratt G, Devissaguet J-P, Labarre D. Long-circulating nanoparticles bearing heparin or dextran covalently bound to poly(methyl methacrylate). *Pharm. Res.* **1998**, *15*: 1046-50.
- [91] Patil A, Shaikh IM, Kadam VJ, Jadhav KR. Nanotechnology in therapeutics - current technologies and applications. *Curr. Nanosci.* **2009**, *5*: 141-53.
- [92] Lecaroz MC, Blanco-Prieto MJ, Campanero MA, Salman H, Gamazo C. Poly(D,L-lactide-co-glycolide) particles containing gentamicin: Pharmacokinetics and pharmacodynamics in *Brucella melitensis*-infected mice. *Antimicrob. Agents Chemother.* **2007**, *51*: 1185-90.
- [93] Lecaroz MC, Blanco-Prieto MJ, Campanero MA, Salman H, Gamazo C. Poly(D,L-Lactide-Coglycolide) Particles Containing Gentamicin: Pharmacokinetics and Pharmacodynamics in *Brucella melitensis*- Infected Mice. *Antimicrob. Agents Chemother.* **2007**, *51*: 1185-90.
- [94] Gulyaev AE, Gelperina SE, Skidan IN, Antropov AS, Kivman GY, Kreuter J. Significant transport of doxorubicin into the brain with polysorbate 80-coated nanoparticles. *Pharm. Res.* **1999**, *16*: 1564-9.
- [95] Kreuter J. Nanoparticulate systems for brain delivery of drugs. *Adv. Drug Deliv. Rev.* **2001**, *47*: 65-81.
- [96] Otsuka H, Nagasaki Y, Kataoka K. PEGylated nanoparticles for biological and pharmaceutical applications. *Adv. Drug Deliv. Rev.* **2003**, *55*: 403-19.
- [97] Owens DE, Peppas NA. Opsonization, biodistribution, and pharmacokinetics of polymeric nanoparticles. *Int. J. Pharm.* **2006**, *307*: 93-102.
- [98] Nguyen A, Marsaud V, Bouclier C, Top S, Vessieres A, Pigeon P, Gref R, Legrand P, Jaouen G, Renoir J-M. Nanoparticles loaded with ferrocenyl tamoxifen derivatives for breast cancer treatment. *Int. J. Pharm.* **2008**, *347*: 128-35.
- [99] Quesnel R, Hildgen P. Synthesis of PLA-b-PEG multiblock copolymers for stealth drug carrier preparation. *Molecules* **2005**, *10*: 98-104.
- [100] Ishihara T, Kubota T, Choi T, Takahashi M, Ayano E, Kanazawa H, Higaki M. Polymeric nanoparticles encapsulating betamethasone phosphate with different release profiles and stealthiness. *Int. J. Pharm.* **2009**, *375*: 148-54.

- [101] Prego C, Torres D, Fernandez-Megia E, Novoa-Carballal R, Quinoa E, Alonso MJ. Chitosan-PEG nanocapsules as new carriers for oral peptide delivery - Effect of chitosan pegylation degree. *J. Controlled Release* **2006**, *111*: 299-308.
- [102] Kim SY, Lee YM. Taxol-loaded block copolymer nanospheres composed of methoxy poly(ethylene glycol) and poly(epsilon-caprolactone) as novel anticancer drug carriers. *Biomaterials* **2001**, *22*: 1697-704.
- [103] Christian DA, Cai S, Bowen DM, Kim Y, Pajerowski JD, Discher DE. Polymersome carriers: From self-assembly to siRNA and protein therapeutics. *Eur. J. Pharm. Biopharm.* **2009**, *71*: 463-74.
- [104] Kunitake T, Nakashima N, Takarabe K, Nagai M, Tsuge A, Yanagi H. Vesicles of polymeric bilayer and monolayer membranes *JACS* **1981**, *103*: 5945-7.
- [105] Meng F, Zhong Z, Feijen J. Stimuli-responsive polymersomes for programmed drug delivery. *Biomacromolecules* **2009**, *10*: 197-209.
- [106] Li SL, Byrne B, Welsh J, Palmer AF. Self-assembled poly(butadiene)-b-poly(ethylene oxide) polymersomes as paclitaxel carriers. *Biotechnol. Prog.* **2007**, *23*: 278-85.
- [107] Katz JS, Levine DH, Davis KP, Bates FS, Hammer DA, Burdick JA. Membrane stabilization of biodegradable polymersomes. *Langmuir* **2009**, *25*: 4429-34.
- [108] Pang ZQ, Lu W, Gao HL, Hu KL, Chen J, Zhang CL, Gao XL, Jiang XG, Zhu CQ. Preparation and brain delivery property of biodegradable polymersomes conjugated with OX26. *J. Controlled Release* **2008**, *128*: 120-7.
- [109] Houga C, Giermanska J, Lecommandoux Sb, Borsali R, Taton D, Gnanou Y, Le Meins J-Fo. Micelles and polymersomes obtained by self-assembly of dextran and polystyrene based block copolymers. *Biomacromolecules* **2009**, *10*: 32-40.
- [110] Zhou W, Feijen J. Biodegradable polymersomes for controlled drug release. *J. Controlled Release* **2008**, *132*: e35-e6.
- [111] Napoli A, Boerakker MJ, Tirelli N, Nolte RJM, Sommerdijk NAJM, Hubbell JA. Glucose-oxidase based self-destructing polymeric vesicles. *Langmuir* **2004**, *20*: 3487-91.

- [112] Zheng C, Qiu LY, Zhu KJ. Novel polymersomes based on amphiphilic graft polyphosphazenes and their encapsulation of water-soluble anti-cancer drug. *Polymer* **2009**, *50*: 1173-7.
- [113] Ahmed F, Pakunlu RI, Brannan A, Bates F, Minko T, Discher DE. Biodegradable polymersomes loaded with both paclitaxel and doxorubicin permeate and shrink tumors, inducing apoptosis in proportion to accumulated drug. *J. Controlled Release* **2006**, *116*: 150-8.
- [114] Bawarski WE, Chidlowsky E, Bharali DJ, Mousa SA. Emerging nanopharmaceuticals. *Nanomed. Nanotechnol. Biol. Med.* **2008**, *4*: 273-82.
- [115] Svenson S, Chauhan AS. Dendrimers for enhanced drug solubilization. *Nanomedicine* **2008**, *3*: 679-702.
- [116] Mishra V, Gupta U, Jain NK. Surface-engineered dendrimers: a solution for toxicity issues. *J. Biomater. Sci., Polym. Ed.* **2009**, *20*: 141-66.
- [117] Wang W, Xiong W, Wan JL, Sun XH, Xu HB, Yang XL. The decrease of PAMAM dendrimer-induced cytotoxicity by PEGylation via attenuation of oxidative stress. *Nanotechnology* **2009**, *20*: 7.
- [118] Bai SH, Ahsan F. Synthesis and evaluation of PEGylated dendrimeric nanocarrier for pulmonary delivery of low molecular weight heparin. *Pharm. Res.* **2009**, *26*: 539-48.
- [119] Gajbhiye V, Kumar PV, Tekade RK, Jain NK. PEGylated PPI dendritic architectures for sustained delivery of H-2 receptor antagonist. *Eur. J. Med. Chem.* **2009**, *44*: 1155-66.
- [120] Patil ML, Zhang M, Taratula O, Garbuzenko OB, He HX, Minko T. Internally cationic polyamidoamine PAMAM-OH dendrimers for siRNA delivery: effect of the degree of quaternization and cancer targeting. *Biomacromolecules* **2009**, *10*: 258-66.
- [121] Liu MJ, Kono K, Frechet JMJ. Water-soluble dendritic unimolecular micelles: Their potential as drug delivery agents. *J. Controlled Release* **2000**, *65*: 121-31.
- [122] Wang F, Bronich TK, Kabanov AV, Rauh RD, Roovers J. Synthesis and evaluation of a star amphiphilic block copolymer from poly(epsilon-caprolactone) and

- poly(ethylene glycol) as a potential drug delivery carrier. *Bioconjugate Chem.* **2005**, *16*: 397-405.
- [123] Weber N, Ortega P, Clemente MI, Shcharbin D, Bryszewska M, de la Mata FJ, Gomez R, Munoz-Fernandez MA. Characterization of carbosilane dendrimers as effective carriers of siRNA to HIV-infected lymphocytes. *J. Controlled Release* **2008**, *132*: 55-64.
- [124] Kang HM, DeLong R, Fisher MH, Juliano RL. Tat-conjugated PAMAM dendrimers as delivery agents for antisense and siRNA oligonucleotides. *Pharm. Res.* **2005**, *22*: 2099-106.
- [125] Yang H, Kao WJ. Dendrimers for pharmaceutical and biomedical applications. *J. Biomater. Sci., Polym. Ed.* **2006**, *17*: 3-19.
- [126] Mahmud A, Xiong X-B, Aliabadi HM, Lavasanifar A. Polymeric micelles for drug targeting. *J. Drug Target.* **2007**, *15*: 553 - 84.
- [127] Bromberg L. Polymeric micelles in oral chemotherapy. *J. Controlled Release* **2008**, *128*: 99-112.
- [128] Won Y-Y, Davis HT, Bates FS. Giant wormlike rubber micelles. *Science* **1999**, *283*: 960-3.
- [129] Discher BM, Won Y-Y, Ege DS, Lee JCM, Bates FS, Discher DE, Hammer DA. Polymersomes: tough vesicles made from diblock copolymers. *Science* **1999**, *284*: 1143-6.
- [130] Glen JB, Hunter SC. Pharmacology of an emulsion formulation of ICI 35 868. *Br. J. Anaesth.* **1984**, *56*: 617-26.
- [131] Marik PE. Propofol: Therapeutic indications and side-effects. *Curr. Pharm. Design* **2004**, *10*: 3639-49.
- [132] Ravenelle F, Gori S, Le Garrec D, Lessard D, Luo L, Palusova D, Sneyd J, Smith D. Novel Lipid and Preservative-free Propofol Formulation: Properties and Pharmacodynamics. *Pharm. Res.* **2008**, *25*: 313-9.
- [133] Yu BG, Okano T, Kataoka K, Kwon G. Polymeric micelles for drug delivery: solubilization and haemolytic activity of amphotericin B. *J. Controlled Release* **1998**, *53*: 131-6.

- [134] Piskin E, Kaitian X, Denkbaz EB, Kucukyavuz Z. Novel PDLLA/PEG copolymer micelles as drug carriers. *J. Biomater. Sci., Polym. Ed.* **1995**, *7*: 359-73.
- [135] Zhang X, Jackson JK, Burt HM. Development of amphiphilic diblock copolymers as micellar carriers of taxol. *Int. J. Pharm.* **1996**, *132*: 195-206.
- [136] Aliabadi HM, Elhasi S, Brocks DR, Lavasanifar A. Polymeric micellar delivery reduces kidney distribution and nephrotoxic effects of cyclosporine A after multiple dosing. *J. Pharm. Sci.* **2008**, *97*: 1916-26.
- [137] Chu HY, Liu N, Wang X, Jiao Z, Chen ZM. Morphology and in vitro release kinetics of drug-loaded micelles based on well-defined PMPC-b-PBMA copolymer. *Int. J. Pharm.* **2009**, *371*: 190-6.
- [138] Ma ZS, Haddadi A, Molavi O, Lavasanifar A, Lai R, Samuel J. Micelles of poly(ethylene oxide)-b-poly(epsilon-caprolactone) as vehicles for the solubilization, stabilization, and controlled delivery of curcumin. *J. Biomed. Mater. Res., Part A* **2008**, *86A*: 300-10.
- [139] Hamaguchi T, Matsumura Y, Suzuki M, Shimizu K, Goda R, Nakamura I, Nakatomi I, Yokoyama M, Kataoka K, Kakizoe T. NK105, a paclitaxel-incorporating micellar nanoparticle formulation, can extend in vivo antitumour activity and reduce the neurotoxicity of paclitaxel. *Br. J. Cancer* **2005**, *92*: 1240-6.
- [140] Musacchio T, Laquintana V, Latrofa A, Trapani G, Torchilin VP. PEG-PE micelles loaded with paclitaxel and surface-modified by a PBR-Ligand: synergistic anticancer effect. *Mol. Pharm.* **2009**, *6*: 468-79.
- [141] Gaucher G, Asahina K, Wang JH, Leroux JC. Effect of Poly(N-vinylpyrrolidone)-block-poly(D,L-lactide) as Coating Agent on the Opsonization, Phagocytosis, and Pharmacokinetics of Biodegradable Nanoparticles. *Biomacromolecules* **2009**, *10*: 408-16.
- [142] Lavasanifar A, Samuel J, Kwon GS. Poly(ethylene oxide)-block-poly(-amino acid) micelles for drug delivery. *Adv. Drug Deliv. Rev.* **2002**, *54*: 169-90.
- [143] Aliabadi HM, Lavasanifar A. Polymeric micelles for drug delivery. *Expert Opin. Drug Deliv.* **2006**, *3*: 139-62.

- [144] Matsumura Y, Hamaguchi T, Ura T, Muro K, Yamada Y, Shimada Y, Shirao K, Okusaka T, Ueno H, Ikeda M, Watanabe N. Phase I clinical trial and pharmacokinetic evaluation of NK911, a micelle-encapsulated doxorubicin. *Br. J. Cancer* **2004**, *91*: 1775-81.
- [145] Danson S, Ferry D, Alakhov V, Margison J, Kerr D, Jowle D, Brampton M, Halbert G, Ranson M. Phase I dose escalation and pharmacokinetic study of pluronic polymer-bound doxorubicin (SP1049C) in patients with advanced cancer. *Br. J. Cancer* **2004**, *90*: 2085-91.
- [146] <http://clinicaltrials.gov/ct2/show/NCT00055133>.
- [147] Lee KS, Chung HC, Im SA, Park YH, Kim CS, Kim SB, Rha SY, Lee MY, Ro J. Multicenter phase II trial of Genexol-PM, a Cremophor-free, polymeric micelle formulation of paclitaxel, in patients with metastatic breast cancer. *Breast Cancer Res. Treat.* **2008**, *108*: 241-50.
- [148] Hamaguchi T, Kato K, Yasui H, Morizane C, Ikeda M, Ueno H, Muro K, Yamada Y, Okusaka T, Shirao K, Shimada Y, Nakahama H, Matsumura Y. A phase I and pharmacokinetic study of NK105, a paclitaxel-incorporating micellar nanoparticle formulation. *Br. J. Cancer* **2007**, *97*: 170-6.
- [149] Burris HA, Infante JR, Spigel DR, Greco FA, Thompson DS, Matsumoto S, Kawamura S, Jones SF. A phase I dose-escalation study of NK012. *J. Clin. Oncol.* **2008**, *26*: May 20 suppl; abstr 2538.
- [150] Harada A, Kataoka K. Formation of polyion complex micelles in an aqueous milieu from a pair of oppositely-charged block copolymers with poly(ethylene glycol) segments. *Macromolecules* **1995**, *28*: 5294-9.
- [151] Kabanov AV, Bronich TK, Kabanov VA, Yu K, Eisenberg A. Soluble stoichiometric complexes from poly(N-ethyl-4-vinylpyridinium) cations and poly(ethylene oxide)-block-polymethacrylate anions. *Macromolecules* **1996**, *29*: 6797-802.
- [152] Voets IK, de Keizer A, Stuart MAC. Complex coacervate core micelles. *Adv. Colloid Interface Sci.* **2009**, *147-148*: 300-18.

- [153] Harada A, Kataoka K. Novel polyion complex micelles entrapping enzyme molecules in the core: Preparation of narrowly-distributed micelles from lysozyme and poly(ethylene glycol)-poly(aspartic acid) block copolymer in aqueous medium. *Macromolecules* **1998**, *31*: 288-94.
- [154] Bronich TK, Kabanov AV, Kabanov VA, Yu K, Eisenberg A. Soluble complexes from poly(ethylene oxide)-block-polymethacrylate anions and N-alkylpyridinium cations. *Macromolecules* **1997**, *30*: 3519-25.
- [155] Danial M, Klok H-A, Norde W, Cohen Stuart MA. Complex coacervate core micelles with a lysozyme-modified corona. *Langmuir* **2007**, *23*: 8003-9.
- [156] Harada A, Kataoka K. Supramolecular assemblies of block copolymers in aqueous media as nanocontainers relevant to biological applications. *Prog. Polym. Sci.* **2006**, *31*: 949-82.
- [157] Kakizawa Y, Kataoka K. Block copolymer micelles for delivery of gene and related compounds. *Adv. Drug Deliv. Rev.* **2002**, *54*: 203-22.
- [158] Nishiyama N, Okazaki S, Cabral H, Miyamoto M, Kato Y, Sugiyama Y, Nishio K, Matsumura Y, Kataoka K. Novel cisplatin-incorporated polymeric micelles can eradicate solid tumors in mice. *Cancer Res.* **2003**, *63*: 8977-83.
- [159] Prompruk K, Govender T, Zhang S, Xiong CD, Stolnik S. Synthesis of a novel PEG-block-poly(aspartic acid-stat-phenylalanine) copolymer shows potential for formation of a micellar drug carrier. *Int. J. Pharm.* **2005**, *297*: 242-53.
- [160] Aoyagi T, Sugi K-i, Sakurai Y, Okano T, Kataoka K. Peptide drug carrier: studies on incorporation of vasopressin into nano-associates comprising poly(ethylene glycol)-poly(-aspartic acid) block copolymer. *Colloids Surf., B* **1999**, *16*: 237-42.
- [161] Barichello JM, Morishita M, Takayama K, Nagai T. Encapsulation of hydrophilic and lipophilic drugs in PLGA nanoparticles by the nanoprecipitation method. *Drug Dev. Ind. Pharm.* **1999**, *25*: 471-6.
- [162] Li X, Zhang Y, Yan R, Jia W, Yuan M, Deng X, Huang Z. Influence of process parameters on the protein stability encapsulated in poly--lactide-poly(ethylene glycol) microspheres. *J. Controlled Release* **2000**, *68*: 41-52.

- [163] Ricci M, Giovagnoli S, Blasi P, Schoubben A, Perioli L, Rossi C. Development of liposomal capreomycin sulfate formulations: Effects of formulation variables on peptide encapsulation. *Int. J. Pharm.* **2006**, *311*: 172-81.
- [164] Luo Y, Wang A, Yuan J, Gao Q. Preparation, characterization and drug release behavior of polyion complex micelles. *Int. J. Pharm.* **2009**, *374*: 139-44.
- [165] Jeong YI, Kim SH, Jung TY, Kim IY, Kang SS, Jin YH, Ryu HH, Sun HS, Jin SG, Kim KK, Ahn KY, Jung S. Polyion complex micelles composed of all-trans retinoic acid and poly (ethylene glycol)-grafted-chitosan. *J. Pharm. Sci.* **2006**, *95*: 2348-60.
- [166] Yang KW, Li XR, Yang ZL, Li PZ, Wang F, Liu Y. Novel polyion complex micelles for liver-targeted delivery of diammonium glycyrrhizinate: *In vitro* and *in vivo* characterization. *J. Biomed. Mater. Res. Part A* **2009**, *88A*: 140-8.
- [167] Witschi C, Doelker E. Residual solvents in pharmaceutical products: acceptable limits, influences on physicochemical properties, analytical methods and documented values. *Eur. J. Pharm. Biopharm.* **1997**, *43*: 215-42.
- [168] Mao SR, Bakowsky U, Jintapattanakit A, Kissel T. Self-assembled polyelectrolyte nanocomplexes between chitosan derivatives and insulin. *J. Pharm. Sci.* **2006**, *95*: 1035-48.
- [169] Wakebayashi D, Nishiyama N, Yamasaki Y, Itaka K, Kanayama N, Harada A, Nagasaki Y, Kataoka K. Lactose-conjugated polyion complex micelles incorporating plasmid DNA as a targetable gene vector system: their preparation and gene transfecting efficiency against cultured HepG2 cells. *J. Controlled Release* **2004**, *95*: 653-64.
- [170] Govender T, Stolnik S, Xiong C, Zhang S, Illum L, Davis SS. Drug-polyionic block copolymer interactions for micelle formation: Physicochemical characterisation. *J. Controlled Release* **2001**, *75*: 249-58.
- [171] Cheng H, Zhu JL, Zeng X, Jing Y, Zhang XZ, Zhuo RX. Targeted gene delivery mediated by folate-polyethylenimine-block-poly(ethylene glycol) with receptor selectivity. *Bioconjugate Chem.* **2009**, *20*: 481-7.

- [172] Yessine M-A, Dufresne M-H, Meier C, Petereit H-U, Leroux J-C. Proton-actuated membrane-destabilizing polyion complex micelles. *Bioconjugate Chem.* **2007**, *18*: 1010-4.
- [173] Matsumoto S, Christie RJ, Nishiyama N, Miyata K, Ishii A, Oba M, Koyama H, Yamasaki Y, Kataoka K. Environment-Responsive Block Copolymer Micelles with a Disulfide Cross-Linked Core for Enhanced siRNA Delivery. *Biomacromolecules* **2009**, *10*: 119-27.
- [174] Kim DG, Jeong YI, Nah JW. All-trans retinoic acid release from polyion-complex micelles of methoxy poly(ethylene glycol) grafted chitosan. *J. Appl. Polym. Sci.* **2007**, *105*: 3246-54.
- [175] Wang C-H, Wang W-T, Hsiue G-H. Development of polyion complex micelles for encapsulating and delivering amphotericin B. *Biomaterials* **2009**, *30*: 3352-8.
- [176] Qiu LY, Bae YH. Polymer architecture and drug delivery. *Pharm. Res.* **2006**, *23*: 1-30.
- [177] Harada A, Togawa H, Kataoka K. Physicochemical properties and nuclease resistance of antisense-oligodeoxynucleotides entrapped in the core of polyion complex micelles composed of poly(ethylene glycol)-poly(-Lysine) block copolymers. *Eur. J. Pharm. Sci.* **2001**, *13*: 35-42.
- [178] Kataoka K, Togawa H, Harada A, Yasugi K, Matsumoto T, Katayose S. Spontaneous formation of polyion complex micelles with narrow distribution from antisense oligonucleotide and cationic block copolymer in physiological saline. *Macromolecules* **1996**, *29*: 8556-7.
- [179] Wolfert MA, Schacht EH, Toncheva V, Ulbrich K, Nazarova O, Seymour LW. Characterization of vectors for gene therapy formed by self-assembly of DNA with synthetic block co-polymers. *Hum. Gene Ther.* **1996**, *7*: 2123-33.
- [180] Katayose S, Kataoka K. Remarkable increase in nuclease resistance of plasmid DNA through supramolecular assembly with poly(ethylene glycol) poly(L-lysine) block copolymer. *J. Pharm. Sci.* **1998**, *87*: 160-3.

- [181] Stapert HR, Nishiyama N, Jiang D-L, Aida T, Kataoka K. Polyion complex micelles encapsulating light-harvesting ionic dendrimer zinc porphyrins. *Langmuir* **2000**, *16*: 8182-8.
- [182] Peng Y, Lin P, Lin J, Xu G, Zhang H, Shi J. Cationic triblock copolymer micelles deliver anionic spacer chains substituted aluminum phthalocyanine for enhancement intracellular photodynamic efficacy. *Mater. Lett.* **2009**, *63*: 914-6.
- [183] Kakizawa Y, Harada A, Kataoka K. Glutathione-sensitive stabilization of block copolymer micelles composed of antisense DNA and thiolated poly(ethylene glycol)-block-poly(l-lysine): A potential carrier for systemic delivery of antisense DNA. *Biomacromolecules* **2001**, *2*: 491-7.
- [184] Miyata K, Kakizawa Y, Nishiyama N, Harada A, Yamasaki Y, Koyama H, Kataoka K. Block cationer polyplexes with regulated densities of charge and disulfide cross-linking directed to enhance gene expression. *JACS* **2004**, *126*: 2355-61.
- [185] Choi JS, Lee EJ, Choi YH, Jeong YJ, Park JS. Poly(ethylene glycol)-block-poly(l-lysine) dendrimer: Novel linear polymer/dendrimer block copolymer forming a spherical water-soluble polyionic complex with DNA. *Bioconjugate Chem.* **1999**, *10*: 62-5.
- [186] Kim WJ, Akaike T, Maruyama A. DNA strand exchange stimulated by spontaneous complex formation with cationic comb-type copolymer. *JACS* **2002**, *124*: 12676-7.
- [187] Maruyama A, Watanabe H, Ferdous A, Katoh M, Ishihara T, Akaike T. Characterization of interpolyelectrolyte complexes between double-stranded DNA and polylysine comb-type copolymers having hydrophilic side chains. *Bioconjugate Chem.* **1998**, *9*: 292-9.
- [188] Maruyama A, Ishihara T, Kim J-S, Kim SW, Akaike T. Nanoparticle DNA carrier with poly(l-lysine) grafted polysaccharide copolymer and poly(d,l-lactic acid). *Bioconjugate Chem.* **1997**, *8*: 735-42.
- [189] Oupicky D, Reschel T, Konak C, Oupicka L. Temperature-controlled behavior of self-assembly gene delivery vectors based on complexes of DNA with poly(l-lysine)-graft-poly(N-isopropylacrylamide). *Macromolecules* **2003**, *36*: 6863-72.

- [190] Itaka K, Kanayama N, Nishiyama N, Jang W-D, Yamasaki Y, Nakamura K, Kawaguchi H, Kataoka K. Supramolecular nanocarrier of siRNA from PEG-based block cationic copolymer carrying diamine side chain with distinctive pKa directed to enhance intracellular gene silencing. *JACS* **2004**, *126*: 13612-3.
- [191] Akagi D, Oba M, Koyama H, Nishiyama N, Fukushima S, Miyata T, Nagawa H, Kataoka K. Biocompatible micellar nanovectors achieve efficient gene transfer to vascular lesions without cytotoxicity and thrombus formation. *Gene Ther.* **2007**, *14*: 1029-38.
- [192] Scales CW, Huang F, Li N, Vasilieva YA, Ray J, Convertine AJ, McCormick CL. Corona-stabilized interpolyelectrolyte complexes of siRNA with nonimmunogenic, hydrophilic/cationic block copolymers prepared by aqueous RAFT polymerization. *Macromolecules* **2006**, *39*: 6871-81.
- [193] van de Wetering P, Schuurmans-Nieuwenbroek NME, van Steenberg MJ, Crommelin DJA, Hennink WE. Copolymers of 2-(dimethylamino)ethyl methacrylate with ethoxytriethylene glycol methacrylate or N-vinyl-pyrrolidone as gene transfer agents. *J. Controlled Release* **2000**, *64*: 193-203.
- [194] van de Wetering P, Cherng JY, Talsma H, Crommelin DJA, Hennink WE. 2-(dimethylamino)ethyl methacrylate based (co)polymers as gene transfer agents. *J. Controlled Release* **1998**, *53*: 145-53.
- [195] Tan JF, Too HP, Hatton TA, Tam KC. Aggregation behavior and thermodynamics of binding between poly(ethylene oxide)-block-poly(2-(diethylamino)ethyl methacrylate) and plasmid DNA. *Langmuir* **2006**, *22*: 3744-50.
- [196] Tamura A, Oishi M, Nagasaki Y. Enhanced cytoplasmic delivery of siRNA using a stabilized polyion complex based on PEGylated nanogels with a cross-linked polyamine structure. *Biomacromolecules* **2009**, *in press*:
- [197] Bromberg L, Deshmukh S, Temchenko M, Iourtchenko L, Alakhov V, Alvarez-Lorenzo C, Barreiro-Iglesias R, Concheiro A, Hatton TA. Polycationic block copolymers of poly(ethylene oxide) and poly(propylene oxide) for cell transfection. *Bioconjugate Chem.* **2005**, *16*: 626-33.

- [198] Alvarez-Lorenzo C, Barreiro-Iglesias R, Concheiro A, Iourtchenko L, Alakhov V, Bromberg L, Temchenko M, Deshmukh S, Hatton TA. Biophysical characterization of complexation of DNA with block copolymers of poly(2-dimethylaminoethyl) methacrylate, poly(ethylene oxide), and poly(propylene oxide). *Langmuir* **2005**, *21*: 5142-8.
- [199] Caputo A, Betti M, Altavilla G, Bonaccorsi A, Boarini C, Marchisio M, Buttò S, Sparnacci K, Laus M, Tondelli L, Ensoli B. Micellar-type complexes of tailor-made synthetic block copolymers containing the HIV-1 tat DNA for vaccine application. *Vaccine* **2002**, *20*: 2303-17.
- [200] Luo Y, Yao X, Yuan J, Ding T, Gao Q. Preparation and drug controlled-release of polyion complex micelles as drug delivery systems. *Colloids Surf., B* **2009**, *68*: 218-24.
- [201] Dufresne M-H, Gauthier MA, Leroux J-C. Thiol-functionalized polymeric micelles: From molecular recognition to improved mucoadhesion. *Bioconjugate Chem.* **2005**, *16*: 1027-33.
- [202] Wakebayashi D, Nishiyama N, Itaka K, Miyata K, Yamasaki Y, Harada A, Koyama H, Nagasaki Y, Kataoka K. Polyion complex micelles of pDNA with acetal-poly(ethylene glycol)-poly(2-(dimethylamino)ethyl methacrylate) block copolymer as the gene carrier system: Physicochemical properties of micelles relevant to gene transfection efficacy. *Biomacromolecules* **2004**, *5*: 2128-36.
- [203] Kataoka K, Harada A, Wakebayashi D, Nagasaki Y. Polyion complex micelles with reactive aldehyde groups on their surface from plasmid DNA and end-functionalized charged block copolymers. *Macromolecules* **1999**, *32*: 6892-4.
- [204] Qiu LY, Bae YH. Self-assembled polyethylenimine-graft-poly([epsilon]-caprolactone) micelles as potential dual carriers of genes and anticancer drugs. *Biomaterials* **2007**, *28*: 4132-42.
- [205] Vinogradov SV, Bronich TK, Kabanov AV. Self-assembly of polyamine-poly(ethylene glycol) copolymers with phosphorothioate oligonucleotides. *Bioconjugate Chem.* **1998**, *9*: 805-12.

- [206] Vinogradov SV, Batrakova E, Li S, Kabanov A. Polyion complex micelles with protein-modified corona for receptor-mediated delivery of oligonucleotides into cells. *Bioconjugate Chem.* **1999**, *10*: 851-60.
- [207] Nguyen HK, Lemieux P, Vinogradov SV, Gebhart CL, Guerin N, Paradis G, Bronich TK, Alakhov VY, Kabanov AV. Evaluation of polyether-polyethyleneimine graft copolymers as gene transfer agents. *Gene Ther.* **2000**, *7*: 126-38.
- [208] Bronich TK, Nguyen HK, Eisenberg A, Kabanov AV. Recognition of DNA topology in reactions between plasmid DNA and cationic copolymers. *JACS* **2000**, *122*: 8339-43.
- [209] Howard KA, Dong MD, Oupicky D, Bisht HS, Buss C, Besenbacher F, Kjems J. Nanocarrier stimuli-activated gene delivery. *Small* **2007**, *3*: 54-7.
- [210] Bisht HS, Manickam DS, You Y, Oupicky D. Temperature-controlled properties of DNA complexes with poly(ethylenimine)-graft-poly(N-isopropylacrylamide). *Biomacromolecules* **2006**, *7*: 1169-78.
- [211] Ma R, Wang B, Liu X, An Y, Li Y, He Z, Shi L. Pyranine-induced micellization of poly(ethylene glycol)-block-poly(4-vinylpyridine) and pH-triggered release of pyranine from the complex micelles. *Langmuir* **2007**, *23*: 7498-504.
- [212] Lindhoud S, de Vries R, Schweins R, Cohen Stuart MA, Norde W. Salt-induced release of lipase from polyelectrolyte complex micelles. *Soft Matter* **2009**, *5*: 242-50.
- [213] Khanal A, Nakashima K. Incorporation and release of cloxacillin sodium in micelles of poly(styrene-b-2-vinyl pyridine-b-ethylene oxide). *J. Controlled Release* **2005**, *108*: 150-60.
- [214] Kabanov AV, Vinogradov SV, Suzdaltseva YG, Alakhov VY. Water-soluble block polycations as carriers for oligonucleotide delivery. *Bioconjugate Chem.* **1995**, *6*: 639-43.
- [215] Zhang G-D, Harada A, Nishiyama N, Jiang D-L, Koyama H, Aida T, Kataoka K. Polyion complex micelles entrapping cationic dendrimer porphyrin: effective

- photosensitizer for photodynamic therapy of cancer. *J. Controlled Release* **2003**, *93*: 141-50.
- [216] Harada A, Kataoka K. Chain length recognition: Core-shell supramolecular assembly from oppositely charged block copolymers. *Science* **1999**, *283*: 65-7.
- [217] Jaturanpinyo M, Harada A, Yuan X, Kataoka K. Preparation of bionanoreactor based on core-shell structured polyion complex micelles entrapping trypsin in the core cross-linked with glutaraldehyde. *Bioconjugate Chem.* **2004**, *15*: 344-8.
- [218] Chen W, Chen HR, Hu JH, Yang WL, Wang CC. Synthesis and characterization of polyion complex micelles between poly(ethylene glycol)-grafted poly(aspartic acid) and cetyltrimethyl ammonium bromide. *Colloids Surf., A* **2006**, *278*: 60-6.
- [219] Park JS, Akiyama Y, Yamasaki Y, Kataoka K. Preparation and characterization of polyion complex micelles with a novel thermosensitive poly(2-isopropyl-2-oxazoline) shell via the complexation of oppositely charged block ionomers. *Langmuir* **2007**, *23*: 138-46.
- [220] Thunemann AF, Schutt D, Sachse R, Schlaad H, Mohwald H. Complexes of poly(ethylene oxide)-block-poly(L-glutamate) and diminazene. *Langmuir* **2006**, *22*: 2323-8.
- [221] Luo K, Yin J, Song Z, Cui L, Cao B, Chen X. Biodegradable interpolyelectrolyte complexes based on methoxy poly(ethylene glycol)-b-poly(α ,L-glutamic acid) and chitosan. *Biomacromolecules* **2008**, *9*: 2653-61.
- [222] Ranger M, Jones MC, Yessine MA, Leroux JC. From well-defined diblock copolymers prepared by a versatile atom transfer radical polymerization method to supramolecular assemblies. *J. Polym. Sci. Pol. Chem.* **2001**, *39*: 3861-74.
- [223] Boudier A, Aubert-Pouëssel A, Louis-Plence P, Gérardin C, Jorgensen C, Devoisselle J-M, Bégu S. The control of dendritic cell maturation by pH-sensitive polyion complex micelles. *Biomaterials* **2009**, *30*: 233-41.
- [224] Bontha S, Kabanov AV, Bronich TK. Polymer micelles with cross-linked ionic cores for delivery of anticancer drugs. *J. Controlled Release* **2006**, *114*: 163-74.

- [225] Solomatin SV, Bronich TK, Bargar TW, Eisenberg A, Kabanov VA, Kabanov AV. Environmentally Responsive Nanoparticles from Block Ionomer Complexes: Effects of pH and Ionic Strength. *Langmuir* **2003**, *19*: 8069-76.
- [226] Wang H, An Y, Huang N, Ma R, Li J, Shi L. Contractive polymeric complex micelles as thermo-sensitive nanopumps. *Macromol. Rapid Commun.* **2008**, *29*: 1410-4.
- [227] Voets IK, Moll PM, Aqil A, Jérôme C, Detrembleur C, Waard P, Keizer A, Stuart MAC. Temperature responsive complex coacervate core micelles with a PEO and PNIPAAm corona. *J. Phys. Chem. B* **2008**, *112*: 10833-40.
- [228] Cheng C, Wei H, Zhang XZ, Cheng SX, Zhuo RX. Thermo-triggered and biotinylated biotin-P(NIPAAm-co-HMAAm)-b-PMMA micelles for controlled drug release. *J. Biomed. Mater. Res., Part A* **2009**, *88A*: 814-22.
- [229] Ambade AV, Savariar EN, Thayumanavan S. Dendrimeric micelles for controlled drug release and targeted delivery. *Mol. Pharm.* **2005**, *2*: 264-72.
- [230] Sun X, Rossin R, Turner JL, Becker ML, Joralemon MJ, Welch MJ, Wooley KL. An assessment of the effects of shell cross-linked nanoparticle size, core composition, and surface PEGylation on in vivo biodistribution. *Biomacromolecules* **2005**, *6*: 2541-54.
- [231] Stolnik S, Illum L, Davis SS. Long circulating microparticulate drug carriers. *Adv. Drug Deliv. Rev.* **1995**, *16*: 195-214.
- [232] Nishiyama N, Kataoka K. Current state, achievements, and future prospects of polymeric micelles as nanocarriers for drug and gene delivery. *Pharmacol. Ther.* **2006**, *112*: 630-48.
- [233] Dufresne MH, Leroux JC. Study of the micellization behavior of different order amino block copolymers with heparin. *Pharm. Res.* **2004**, *21*: 160-9.
- [234] Astete CE, Sabliov CM. Synthesis and characterization of PLGA nanoparticles. *J. Biomater. Sci., Polym. Ed.* **2006**, *17*: 247-89.
- [235] Trimaille T, Pichot C, Elaissari A, Fessi H, Briancon S, Delair T. Poly(D,L-lactic acid) nanoparticle preparation and colloidal characterization. *Colloid Polym. Sci.* **2003**, *281*: 1184-90.

- [236] Bernfield M, Gotte M, Park PW, Reizes O, Fitzgerald ML, Lincecum J, Zako M. Functions of cell surface heparan sulfate proteoglycans. *Annu. Rev. Biochem.* **1999**, *68*: 729-77.
- [237] Zhang J-S, Liu F, Huang L. Implications of pharmacokinetic behavior of lipoplex for its inflammatory toxicity. *Adv. Drug Deliv. Rev.* **2005**, *57*: 689-98.
- [238] Levchenko TS, Rammohan R, Lukyanov AN, Whiteman KR, Torchilin VP. Liposome clearance in mice: the effect of a separate and combined presence of surface charge and polymer coating. *Int. J. Pharm.* **2002**, *240*: 95-102.
- [239] Gohy J-F, Varshney SK, Antoun S, Jerome R. Water-soluble complexes formed by sodium poly(4-styrenesulfonate) and a poly(2-vinylpyridinium)-block-poly(ethyleneoxide) copolymer. *Macromolecules* **2000**, *33*: 9298-305.
- [240] Serefoglou E, Oberdisse J, Staikos G. Characterization of the soluble nanoparticles formed through coulombic interaction of bovine serum albumin with anionic graft copolymers at low pH. *Biomacromolecules* **2007**, *8*: 1195-9.
- [241] Yuan X, Yamasaki Y, Harada A, Kataoka K. Characterization of stable lysozyme-entrapped polyion complex (PIC) micelles with crosslinked core by glutaraldehyde. *Polymer* **2005**, *46*: 7749-58.
- [242] Murphy RF, Powers S, Cantor CR. Endosome pH measured in single cells by dual fluorescence flow cytometry: rapid acidification of insulin to pH 6. *J. Cell Biol.* **1984**, *98*: 1757-62.
- [243] Gohy J-F, Varshney SK, Jerome R. Water-soluble complexes formed by sodium poly(4-styrenesulfonate) and a poly(2-vinylpyridinium)-block-poly(ethyleneoxide) copolymer. *Macromolecules* **2001**, *34*: 3361-6.
- [244] Koji A, Hiroyuki O, Eishun T. Phase changes of polyion complex between poly(methacrylic acid) and a polycation carrying charges in the chain backbone. *Makromol. Chem.* **1977**, *178*: 2285-93.
- [245] Voets IK, de Keizer A, Stuart MAC, Justynska J, Schlaad H. Irreversible structural transitions in mixed micelles of oppositely charged diblock copolymers in aqueous solution. *Macromolecules* **2007**, *40*: 2158-64.

- [246] Bouyer F, Gérardin C, Fajula F, Putaux JL, Chopin T. Role of double-hydrophilic block copolymers in the synthesis of lanthanum-based nanoparticles. *Colloids Surf., A* **2003**, *217*: 179-84.
- [247] Nishiyama N, Yokoyama M, Aoyagi T, Okano T, Sakurai Y, Kataoka K. Preparation and characterization of self-assembled polymer-metal complex micelle from cis-dichlorodiammineplatinum(II) and poly(ethylene glycol)-poly(α,β -aspartic acid) block copolymer in an aqueous medium. *Langmuir* **1999**, *15*: 377-83.
- [248] Yuan X, Harada A, Yamasaki Y, Kataoka K. Stabilization of lysozyme-incorporated polyion complex micelles by the ω -end derivatization of poly(ethylene glycol)-poly(α,β -aspartic acid) block copolymers with hydrophobic groups. *Langmuir* **2005**, *21*: 2668-74.
- [249] Choi K-C, Bang J-Y, Kim C, Kim P-I, Lee S-R, Chung W-T, Park W-D, Park J-S, Lee YS, Song C-E, Lee H-Y. Antitumor effect of adriamycin-encapsulated nanoparticles of poly(DL-lactide-co-glycolide)-grafted dextran. *J. Pharm. Sci.* **2008**, *98*: 2104-12.
- [250] Yan Y, de Keizer A, Cohen Stuart MA, Drechsler M, Besseling NAM. Stability of complex coacervate core micelles containing metal coordination polymer. *J. Phys. Chem. B* **2008**, *112*: 10908-14.
- [251] Harada A, Kataoka K. Effect of charged segment length on physicochemical properties of core-shell type polyion complex micelles from block ionomers. *Macromolecules* **2003**, *36*: 4995-5001.
- [252] Chu B. laser light scattering. New York: Academic Press, 1991.
- [253] Khougaz K, Gao Z, Eisenberg A. Determination of the critical micelle concentration of block copolymer micelles by static light scattering. *Macromolecules* **1994**, *27*: 6341-6.
- [254] Walderhaug H, Söderman O. NMR studies of block copolymer micelles. *Curr. Opin. Colloid Interface Sci.* **2009**, *14*: 171-7.
- [255] Ababou A, Ladbury JE. Survey of the year 2005: literature on applications of isothermal titration calorimetry. *J. Mol. Recognit.* **2007**, *20*: 4-14.

- [256] Andujar-Sanchez M, Camara-Artigas A, Jara-Perez V. A calorimetric study of the binding of lisinopril, enalaprilat and captopril to angiotensin-converting enzyme. *Biophys. Chem.* **2004**, *111*: 183-9.
- [257] Xiong X-B, Uludag H, Lavasanifar A. Biodegradable amphiphilic poly(ethylene oxide)-block-polyesters with grafted polyamines as supramolecular nanocarriers for efficient siRNA delivery. *Biomaterials* **2009**, *30*: 242-53.
- [258] Itaka K, Harada A, Nakamura K, Kawaguchi H, Kataoka K. Evaluation by fluorescence resonance energy transfer of the stability of nonviral gene delivery vectors under physiological conditions. *Biomacromolecules* **2002**, *3*: 841-5.
- [259] Schatz C, Lucas J-M, Viton C, Domard A, Pichot C, Delair T. Formation and properties of positively charged colloids based on polyelectrolyte complexes of biopolymers. *Langmuir* **2004**, *20*: 7766-78.
- [260] Yan Y, Besseling, de Keizer A, Drechsler M, Fokkink R, Cohen Stuart MA. Wormlike aggregates from a supramolecular coordination polymer and a diblock copolymer. *J. Phys. Chem. B* **2007**, *111*: 11662-9.
- [261] Nisha CK, Manorama SV, Ganguli M, Maiti S, Kizhakkedathu JN. Complexes of poly(ethylene glycol)-based cationic random copolymer and calf thymus DNA: A complete biophysical characterization. *Langmuir* **2004**, *20*: 2386-96.
- [262] Osada K, Kataoka K. Drug and gene delivery based on supramolecular assembly of PEG-polypeptide hybrid block copolymers. *Adv. Polym. Sci.* **2006**, *202*: 113-53.
- [263] Koynova R, Tenchov B, Wang L, MacDonald RC. Hydrophobic moiety of cationic lipids strongly modulates their transfection activity. *Mol. Pharm.* **2009**, *6*: 951-8.
- [264] Kim TI, Bai CZ, Nam K, Park JS. Comparison between arginine conjugated PAMAM dendrimers with structural diversity for gene delivery systems. *J. Controlled Release* **2009**, *136*: 132-9.
- [265] Itaka K, Yamauchi K, Harada A, Nakamura K, Kawaguchi H, Kataoka K. Polyion complex micelles from plasmid DNA and poly(ethylene glycol)-poly(-lysine) block copolymer as serum-tolerable polyplex system: physicochemical properties of micelles relevant to gene transfection efficiency. *Biomaterials* **2003**, *24*: 4495-506.

- [266] Harada-Shiba M, Yamauchi K, Harada A, Takamisawa I, Shimokado K, Kataoka K. Polyion complex micelles as vectors in gene therapy - pharmacokinetics and in vivo gene transfer. *Gene Ther.* **2002**, *9*: 407-14.
- [267] Kakizawa Y, Harada A, Kataoka K. Environment-sensitive stabilization of core-shell structured polyion complex micelle by reversible cross-linking of the core through disulfide bond. *JACS* **1999**, *121*: 11247-8.
- [268] Sun T-M, Du J-Z, Yan L-F, Mao H-Q, Wang J. Self-assembled biodegradable micellar nanoparticles of amphiphilic and cationic block copolymer for siRNA delivery. *Biomaterials* **2008**, *29*: 4348-55.
- [269] Rosenberg B. Platinum complexes for the treatment of cancer. *Interdiscip. Sci. Rev.* **1978**, *3*: 134-47.
- [270] Kartalou M, Essigmann JM. Mechanisms of resistance to cisplatin. *Mutat. Res.-Fundam. Mol. Mech. Mutagen.* **2001**, *478*: 23-43.
- [271] Pinzani V, Bressolle F, Haug IJ, Galtier M, Blayac JP, Balmes P. Cisplatin-induced renal toxicity and toxicity-modulating strategies - a review. *Cancer Chemother. Pharmacol.* **1994**, *35*: 1-9.
- [272] Nishiyama N, Kato Y, Sugiyama Y, Kataoka K. Cisplatin-loaded polymer-metal complex micelle with time-modulated decaying property as a novel drug delivery system. *Pharm. Res.* **2001**, *18*: 1035-41.
- [273] Uchino H, Matsumura Y, Negishi T, Koizumi F, Hayashi T, Honda T, Nishiyama N, Kataoka K, Naito S, Kakizoe T. Cisplatin-incorporating polymeric micelles (NC-6004) can reduce nephrotoxicity and neurotoxicity of cisplatin in rats. *Br. J. Cancer* **2005**, *93*: 678-87.
- [274] Wilson RH, Plummer R, Adam J, Eatock MM, Boddy AV, Griffin M, Miller R, Matsumura Y, Shimizu T, Calvert H. Phase I and pharmacokinetic study of NC-6004, a new platinum entity of cisplatin-conjugated polymer forming micelles. *J. Clin. Oncol.* **2008**, *26*: abstr 2573.
- [275] Nishiyama N, Nakagishi Y, Morimoto Y, Lai PS, Miyazaki K, Urano K, Horie S, Kumagai M, Fukushima S, Cheng Y, Jang WD, Kikuchi M, Kataoka K. Enhanced

- photodynamic cancer treatment by supramolecular nanocarriers charged with dendrimer phthalocyanine. *J. Controlled Release* **2009**, *133*: 245-51.
- [276] Dougherty TJ, Marcus SL. Photodynamic therapy. *Eur. J. Cancer* **1992**, *28*: 1734-42.
- [277] Matsumura Y, Kataoka K. Preclinical and clinical studies of anticancer agent-incorporating polymer micelles. *Cancer Sci.* **2009**, *100*: 572-9.
- [278] Macdonald IJ, Dougherty TJ. Basic principles of photodynamic therapy. *J. Porphyrins Phthalocyanines* **2001**, *5*: 105-29.
- [279] Jang WD, Nakagishi Y, Nishiyama N, Kawauchi S, Morimoto Y, Kikuchi M, Kataoka K. Polyion complex micelles for photodynamic therapy: Incorporation of dendritic photosensitizer excitable at long wavelength relevant to improved tissue-penetrating property. *J. Controlled Release* **2006**, *113*: 73-9.
- [280] Gu Z, Yuan Y, He J, Zhang M, Ni P. Facile approach for DNA encapsulation in functional polyion complex for triggered intracellular gene delivery: Design, synthesis, and mechanism. *Langmuir* **2009**, *25*: 5199-208.
- [281] Tian Y, Ravi P, Bromberg L, Hatton TA, Tam KC. Synthesis and aggregation behavior of pluronic F87/poly(acrylic acid) block copolymer in the presence of doxorubicin. *Langmuir* **2007**, *23*: 2638-46.
- [282] Larsen C. Dextran prodrugs -- structure and stability in relation to therapeutic activity. *Adv. Drug Deliv. Rev.* **1989**, *3*: 103-54.
- [283] Taylor C, Cheetham NWH, Walker GJ. Application of high-performance liquid chromatography to a study of branching in dextrans. *Carbohydr. Res.* **1985**, *137*: 1-12.
- [284] Schacht E. Polysaccharide macromolecules as drug carriers. In: Illum L, Davis SS, editors. *Polymers in controlled drug delivery*. Bristol: Wright, 1987. p. 131-51.
- [285] Heinze T, Liebert T, Heublein B, Hornig S. Functional Polymers Based on Dextran. *Polysaccharides II*, 2006. p. 199-291.
- [286] Mehvar R, Shepard TL. Molecular-weight-dependent pharmacokinetics of fluorescein-labeled dextrans in rats. *J. Pharm. Sci.* **1992**, *81*: 908-12.

- [287] Koyama Y, Miyagawa T, Kawaide A, Kataoka K. Receptor-mediated absorption of high molecular weight dextrans from intestinal tract. *J. Controlled Release* **1996**, *41*: 171-6.
- [288] Larsen C. Dextran prodrugs -structure and stability in relation to therapeutic activity. *Adv. Drug Deliv. Rev.* **1989**, *3*: 103-54.
- [289] Jain A, Gupta Y, Jain SK. Perspectives of biodegradable natural polysaccharides for site-specific drug delivery to the colon. *J. Pharm. Pharm. Sci.* **2007**, *10*: 86-128.
- [290] Harboe E, Larsen C, Johansen M, Olesen HP. Macromolecular prodrugs. XV. Colon targeted delivery. bioavailability of naproxen from orally administered dextran-naproxen ester prodrugs varying in molecular size in the pig. *Pharm. Res.* **1989**, *6*: 919-23.
- [291] Hovgaard L, Brondsted H. Dextran hydrogels for colon-specific drug delivery. *J. Controlled Release* **1995**, *36*: 159-66.
- [292] Varshosaz J, Emami J, Tavakoli N, Fassihi A, Minaiyan M, Ahmadi F, Dorkoosh F. Synthesis and evaluation of dextran-budesonide conjugates as colon specific prodrugs for treatment of ulcerative colitis. *Int. J. Pharm.* **2009**, *365*: 69-76.
- [293] Chang RL, Ueki IF, Troy JL, Deen WM, Robertson CR, Brenner BM. Permselectivity of the glomerular capillary wall to macromolecules. II. Experimental studies in rats using neutral dextran. *Biophys. J.* **1975**, *15*: 887-906.
- [294] de Jonge E, Levi M. Effects of different plasma substitutes on blood coagulation: A comparative review. *Crit. Care Med.* **2001**, *29*: 1261-7.
- [295] Mehvar R. Dextrans for targeted and sustained delivery of therapeutic and imaging agents. *J. Controlled Release* **2000**, *69*: 1-25.
- [296] Cassano R, Trombino S, Muzzalupo R, Tavano L, Picci N. A novel dextran hydrogel linking trans-ferulic acid for the stabilization and transdermal delivery of vitamin E. *Eur. J. Pharm. Biopharm.* **2009**, *72*: 232-8.
- [297] Basan H, Gümüsderelioglu M, Tevfik Orbey M. Release characteristics of salmon calcitonin from dextran hydrogels for colon-specific delivery. *Eur. J. Pharm. Biopharm.* **2007**, *65*: 39-46.

- [298] Liu Y, Chan-Park MB. Hydrogel based on interpenetrating polymer networks of dextran and gelatin for vascular tissue engineering. *Biomaterials* **2009**, *30*: 196-207.
- [299] Lu H-W, Zhang L-M, Liu J-Y, Chen R-F. Synthesis of an amphiphilic polysaccharide derivative and its micellization for drug release. *J. Bioact. Compat. Polym.* **2008**, *23*: 154-70.
- [300] Liu J-Y, Zhang L-M. Preparation of a polysaccharide-polyester diblock copolymer and its micellar characteristics. *Carbohydr. Polym.* **2007**, *69*: 196-201.
- [301] Gref R, Rodrigues J, Couvreur P. Polysaccharides grafted with polyesters: Novel amphiphilic copolymers for biomedical applications. *Macromolecules* **2002**, *35*: 9861-7.
- [302] Jeong Y, Choi K, Song C. Doxorubicin release from core-shell type nanoparticles of poly(DL-lactide-co-glycolide)-grafted dextran. *Arch. Pharmacol Res.* **2006**, *29*: 712-9.
- [303] Francis MF, Lavoie L, Winnik FM, Leroux J-C. Solubilization of cyclosporin A in dextran-g-polyethyleneglycolalkyl ether polymeric micelles. *Eur. J. Pharm. Biopharm.* **2003**, *56*: 337-46.
- [304] Aumelas A, Serrero A, Durand A, Dellacherie E, Leonard M. Nanoparticles of hydrophobically modified dextrans as potential drug carrier systems. *Colloids Surf., B* **2007**, *59*: 74-80.
- [305] Nichifor M, Carpov A. Bile acids covalently bound to polysaccharides 1. Esters of bile acids with dextran. *Eur. Polym. J.* **1999**, *35*: 2125-9.
- [306] Bachelder EM, Beaudette TT, Broaders KE, Dashe J, Fréchet JMJ. Acetal-derivatized dextran: An acid-responsive biodegradable material for therapeutic applications. *JACS* **2008**, *130*: 10494-5.
- [307] Li Y, Nothnagel J, Kissel T. Biodegradable brush-like graft polymers from poly(-lactide) or poly(-lactide-co-glycolide) and charge-modified, hydrophilic dextrans as backbone-Synthesis, characterization and in vitro degradation properties. *Polymer* **1997**, *38*: 6197-206.

- [308] Ladaviere C, Averlant-Petit MC, Fabre O, Durand A, Dellacherie E, Marie E. Preparation of polysaccharide-coated nanoparticles by emulsion polymerization of styrene. *Colloid Polym. Sci.* **2007**, 285: 621-30.
- [309] Houga C, Meins J-FL, Borsali R, Taton D, Gnanou Y. Synthesis of ATRP-induced dextran-b-polystyrene diblock copolymers and preliminary investigation of their self-assembly in water. *Chem. Commun.* **2007**, 3063-5.
- [310] Bertholon I, Lesieur S, Labarre D, Besnard M, Vauthier C. Characterization of dextran-poly(isobutylcyanoacrylate) copolymers obtained by redox radical and anionic emulsion polymerization. *Macromolecules* **2006**, 39: 3559-67.
- [311] Passirani C, Barratt G, Devissaguet J-P, Labarre D. Interactions of nanoparticles bearing heparin or dextran covalently bound to poly(methyl methacrylate) with the complement system. *Life Sci.* **1998**, 62: 775-85.
- [312] Bang J-Y, Song C-E, Kim C, Park W-D, Cho K-R, Kim P-I, Lee S-R, Chung W-T, Choi K-C. Cytotoxicity of amphotericin B-incorporated polymeric micelles composed of poly(DL-lactide-co-glycolide)/dextran graft copolymer. *Arch. Pharmacol Res.* **2008**, 31: 1463-9.
- [313] Jung S-W, Jeong Y-I, Kim Y-H, Choi K-C, Kim S-H. Drug release from core-shell type nanoparticles of poly(DL-lactide-co-glycolide)-grafted dextran. *J. Microencapsulation* **2005**, 22: 901 - 11.
- [314] Choi K-C, Bang J-Y, Kim P-I, Kim C, Song C-E. Amphotericin B-incorporated polymeric micelles composed of poly(d,l-lactide-co-glycolide)/dextran graft copolymer. *Int. J. Pharm.* **2008**, 355: 224-30.
- [315] Villemson A, Couvreur P, Gillet B, Larionova N, Gref R. Dextran-poly-epsilon-caprolactone micro- and nanoparticles: preparation, characterization and tamoxifen solubilization. *J. Drug Deliv. Sci. Technol.* **2006**, 16: 307-13.
- [316] Prabu P, Chaudhari A, Aryal S, Dharmaraj N, Park S, Kim W, Kim H. In vitro evaluation of poly(caprolactone) grafted dextran (PGD) nanoparticles with cancer cell. *J. Mater. Sci. Mater. Med.* **2008**, 19: 2157-63.

- [317] Jaulin N, Appel M, Passirani C, Barratt G, Labarre D. Reduction of the uptake by a macrophagic cell line of nanoparticles bearing heparin or dextran covalently bound to poly(methyl methacrylate). *J. Drug Target.* **2000**, *8*: 165 - 72.
- [318] Lemarchand C, Gref R, Passirani C, Garcion E, Petri B, Müller R, Costantini D, Couvreur P. Influence of polysaccharide coating on the interactions of nanoparticles with biological systems. *Biomaterials* **2006**, *27*: 108-18.
- [319] Lemarchand C, Gref R, Lesieur S, Hommel H, Vacher B, Besheer A, Maeder K, Couvreur P. Physico-chemical characterization of polysaccharide-coated nanoparticles. *J. Controlled Release* **2005**, *108*: 97-111.
- [320] Drogoz A, David L, Rochas C, Domard A, Delair T. Polyelectrolyte complexes from polysaccharides: Formation and stoichiometry monitoring. *Langmuir* **2007**, *23*: 10950-8.
- [321] Tiyaboonchai W, Limpeanchob N. Formulation and characterization of amphotericin B-chitosan-dextran sulfate nanoparticles. *Int. J. Pharm.* **2007**, *329*: 142-9.
- [322] Tiyaboonchai W, Woiszwillo J, Middaugh CR. Formulation and characterization of amphotericin B-polyethylenimine-dextran sulfate nanoparticles. *J. Pharm. Sci.* **2001**, *90*: 902-14.
- [323] Tiyaboonchai W, Woiszwillo J, Middaugh CR. Formulation and characterization of DNA-polyethylenimine-dextran sulfate nanoparticles. *Eur. J. Pharm. Sci.* **2003**, *19*: 191-202.
- [324] Huang M, Vitharana SN, Peek LJ, Coop T, Berkland C. Polyelectrolyte complexes stabilize and controllably release vascular endothelial growth factor. *Biomacromolecules* **2007**, *8*: 1607-14.
- [325] Nimesh S, Kumar R, Chandra R. Novel polyallylamine-dextran sulfate-DNA nanoplexes: Highly efficient non-viral vector for gene delivery. *Int. J. Pharm.* **2006**, *320*: 143-9.
- [326] Janes KA, Fresneau MP, Marazuela A, Fabra A, Alonso MJ. Chitosan nanoparticles as delivery systems for doxorubicin. *J. Controlled Release* **2001**, *73*: 255-67.

- [327] Sarmiento B, Martins S, Ribeiro A, Veiga F, Neufeld R, Ferreira D. Development and comparison of different nanoparticulate polyelectrolyte complexes as insulin carriers. *Int. J. Pept. Res. Ther.* **2006**, *12*: 131-8.
- [328] Eliyahu H, Siani S, Azzam T, Domb AJ, Barenholz Y. Relationships between chemical composition, physical properties and transfection efficiency of polysaccharide-spermine conjugates. *Biomaterials* **2006**, *27*: 1646-55.
- [329] Kaplan JM, Pennington SE, George JAS, Woodworth LA, Fasbender A, Marshall J, Cheng SH, Wadsworth SC, Gregory RJ, Smith AE. Potentiation of gene transfer to the mouse lung by complexes of adenovirus vector and polycations improves therapeutic potential. *Hum. Gene Ther.* **1998**, *9*: 1469-79.
- [330] Hernandez OS, Soliman GM, Winnik FM. Synthesis, reactivity, and pH-responsive assembly of new double hydrophilic block copolymers of carboxymethyl dextran and poly(ethylene glycol). *Polymer* **2007**, *48*: 921-30.
- [331] Adams DJ, Rogers SH, Schuetz P. The effect of PEO block lengths on the size and stability of complex coacervate core micelles. *J. Colloid Interface Sci.* **2008**, *322*: 448-56.

CHAPTER TWO

RESEARCH PAPER

Enhancement of Hydrophilic Drug Loading and Release Characteristics through Micellization with New Carboxymethyldextran-PEG Block Copolymers of Tunable Charge Density¹

Ghareb Mohamed Soliman, Françoise M. Winnik

Faculty of Pharmacy and Department of Chemistry, Université de Montréal, CP 6128,
Succursale Centre Ville, Montréal, QC, Canada, H3C 3J7

International Journal of Pharmaceutics 356 (2008) 248-258

¹ My contribution included designing the experiments, polymer synthesis, micelles preparation and characterization, interpreting the results and writing the paper. Dr. Françoise M. Winnik supervised the research.

2.1. Abstract

The micellization of a model cationic drug, diminazene diacetate (DIM) and a series of new diblock copolymers, carboxymethyl-dextran-poly(ethylene glycol) (CMD-PEG), were evaluated as a function of the ionic charge density or degree of substitution (DS) of the carboxymethyl-dextran block and the molar ratio, $[+]/[-]$, of positive charges provided by the drug to negative charges provided by CMD-PEG. Micelles ($[+]/[-] = 2$) incorporated up to 64% (w/w) DIM and ranged in hydrodynamic radius (R_H) from 36 to 50 nm, depending on the molecular weight and DS of CMD-PEG. The critical association concentration (CAC) was on the order of 15–50 mg/L for CMD-PEG of DS > 60%, and ca. 100 mg/L for CMD-PEG of DS \sim 30%. The micelles were stable upon storage in solution for up to 2 months and after freeze-drying in the presence of trehalose. They remained intact within the $4 < \text{pH} < 11$ range and for solutions of pH 5.3, they resisted increases in salinity up to ~ 0.4 M NaCl in the case of CMD-PEG of high DS. However, micelles of DIM and a CMD-PEG of low DS (30%) disintegrated in solutions containing more than 0.1 M NaCl, setting a minimum value to the DS of copolymers useful in *in vivo* applications. Sustained *in vitro* DIM release was observed for micelles of CMD-PEG of high DS ($[+]/[-] = 2$).

2.2. Author Keywords

Polyion complex micelles; Dextran; Electrostatic interactions; Polyelectrolytes; Diminazene diacetate; Hydrophilic drug

2.3. Introduction

Polysaccharides are ubiquitous components of traditional pharmaceutical formulations where they act as coatings or suspending agents, tablet binders and extended-release matrix formers.^[1, 2] They are also known to possess self-assembling qualities and to undergo stimuli-responsive transformations, such as heat- or salt-triggered gelation. More recently, polysaccharide-based nanostructures have emerged as promising materials for

biological and medical applications.^[3] Micellar systems based on dextran^[4], cellulose ethers^[5], poly(ethylene glycol)(PEG)-grafted chitosans^[6], hyaluronan-*block*-poly(2-ethyl-2-oxazoline)^[7] or pullulans, have been shown effective nanocarriers for various drugs and proteins.^[6-9] In most cases polysaccharide nanoparticles were designed for the delivery of hydrophobic drugs. Fewer studies have been devoted to polysaccharide-based nanoparticles for the delivery of highly water soluble drugs. To address this issue, we developed a straightforward synthesis of carboxymethyl-dextran-*block*-poly(ethylene glycol)s (CMD-PEG, Figure 2.1).^[10] The CMD-PEG copolymers were designed specifically as substrates of *tunable charge density*, able to form polyion complex (PIC) micelles upon interaction with an oppositely charged drug. The charge density of the ionic segment cannot be adjusted readily in the case of diblock copolymers used in most PIC-micelle-based drug delivery systems, in which the ionic fragment is usually a poly(amino acid) bearing a charge on each repeat unit. Since the number of charged groups linked to the ionic segment determines the loading efficiency and drug release characteristics of PIC micelles, the control of charge density adds a new dimension in the design of drug-loaded PIC micelles which we set about to explore.

We compare the properties of PIC micelles formed by four CDM-PEG copolymers: (i) two copolymers identical in terms of the length of each block, but different in terms of the charge density of the CMD block and (ii) two copolymers in which the charged block is the same, but the neutral block is of different molecular weight. This strategy enabled us to determine the optimal charge density required to form stable micelles with high drug loading efficiency, small size, and suitable drug release profiles of diminazene diacetate(DIM), a dicationic molecule used as model drug. DIM is effective in the treatment of trypanosomiasis in animals.^[11] It has been used previously to demonstrate the formation of PIC micelles with poly(aspartic acid)-*block*-poly(ethylene glycol)^[12] and poly(ethylene oxide)-*block*-poly(L-glutamate).^[13]

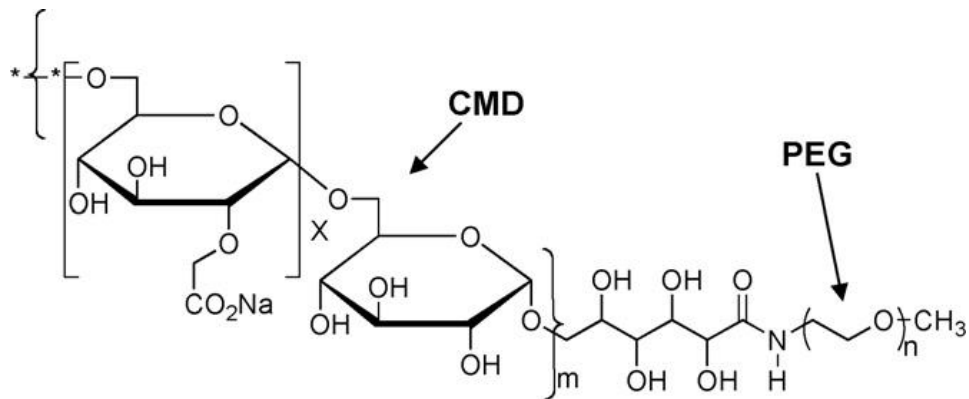


Figure 2.1. Idealized chemical structure of carboxymethyl-dextran-*block*-poly(ethylene glycol) (CMD-PEG); n represents the number of ethylene glycol units, m is the number of glucopyranose rings of the polysaccharide block, and x represents the fraction of glucose units of the dextran chain that bear a carboxymethyl group. The polysaccharide segment consists of a random distribution of glucopyranose units and carboxymethyl glucopyranose units.

We characterize the micelles formed between diminazene and the four CMD-PEG copolymers and assess the effect of charge density on the physico-chemical properties of the micelles, on their stability as a function of salinity, pH, and storage time, and on the drug release kinetics. In order to determine the level of drug loading as a function of charge density, we used static and dynamic light scattering which, together with ^1H NMR spectroscopy, allow one to characterize drug-loaded micelles and to detect drug molecules dissolved in the aqueous medium (free drug).

2.4. Materials and methods

2.4.1. Materials

Trizma[®] hydrochloride (Tris-HCl), diminazene diacetate ($\geq 90\%$ pure, as stated by the supplier), d(+) trehalose dihydrate, Amberlite[®] IR-120 and all other chemicals were purchased from Sigma-Aldrich Chemicals (St. Louis, MO, USA). The drug (m.p. = 215–217 °C) was used without further purification. The purity of DIM was estimated to be $\geq 96\%$ on the basis of the ¹H NMR spectrum of DIM in D₂O. Dextran-PEG (DEX-PEG) samples were synthesized as described previously.^[10] Dialysis tubing (SpectraPore, MWCO: 1000 or 3500 g/mol) was purchased from Fisher Scientific (Rancho Dominguez, CA, USA). All solvents were reagent grade and used as received.

2.4.2. Synthesis of carboxymethyldextran-*block*-poly(ethylene glycols) (CMD-PEG)

CMD-PEG samples of high charge density were obtained according to the protocol previously reported.^[10] The method is described briefly below and the amounts of reagents and solvents employed in each synthesis are given in Table 2.1. Sodium hydroxide was added to a solution of DEX-PEG in an isopropanol–water mixture (85:15 v:v) kept at room temperature. The reaction mixture was heated to 60 °C and kept at this temperature for 30 min. Monochloroacetic acid was added portion-wise to the mixture while stirring. The reaction mixture was kept at 60 °C for 90 min. It was cooled to room temperature, transferred in a dialysis bag and dialyzed against water for 24 h. The purified copolymers were isolated by lyophilization and characterized by ¹H NMR (D₂O, 400 MHz) δ /ppm: 5.07 (anomeric proton on glucopyranose bearing a carboxymethyl group at C₂), 4.89 (anomeric proton on glucopyranose unsubstituted at C₂), 4.15–4.08 (–CH₂COONa), 3.97–3.36 (CMD C-2 to C-6 glucopyranosyl protons), 3.61 (PEG, –CH₂CH₂O–), 3.29 (–OCH₃). It was found advantageous to carry out the carboxymethylation of DEX₄₀-PEG₁₄₀ copolymer on the crude mixture of DEX₄₀-PEG₁₄₀/PEG-NH₂ (Table 2.2) since the separation of this

copolymer resulted in low yield (~30 %) due to the partial solubility of DEX₄₀-PEG₁₄₀ in hot ethanol.

To prepare samples of low degree of carboxymethylation, such as 30-CMD₆₈-PEG₆₄, the carboxymethylation was achieved by adding monochloroacetic acid to a stirred solution of DEX₆₈-PEG₆₄ in aqueous NaOH kept in an ice/water bath, followed by treatment at 60 °C for 1 h. The resulting polymer was purified as described above. ¹H NMR (D₂O, 400 MHz) δ/ppm: 5.07 (anomeric proton on glucopyranose bearing a carboxymethyl group at C₂), 4.88 (anomeric proton on glucopyranose unsubstituted at C₂), 4.15–4.08 (–CH₂COONa), 3.95–3.36 (CMD C-2 to C-6 glucopyranosyl protons), 3.61 (PEG,–CH₂CH₂O–), 3.29 (–OCH₃).

Table 2.1. Experimental conditions for the carboxymethylation of DEX-PEG copolymers

Polymer	DEX _n -PEG _m		NaOH (mmol)	MCA ^a (mmol)	Isopropanol / Water (mL)
	g	mmol Glu ^b			
85-CMD ₄₀ -PEG ₁₄₀ ^c	2.20 ^d	-	16.51	8.80	9.95 / 1.75
80-CMD ₄₀ -PEG ₆₄	0.50	2.19	10.68	5.69	6.43 / 1.17
60-CMD ₆₈ -PEG ₆₄	0.27	1.6	7.50	4.00	4.53 / 0.80
30-CMD ₆₈ -PEG ₆₄	0.50	3.0	24.00	14.0	0.00 / 4.00

^a MCA: monochloroacetic acid.

^b Glu: glucopyranosyl.

^c: The prefix denotes the degree of carboxymethylation of the dextran block.

^d: Mixture of DEX₄₀-PEG₁₄₀ and unreacted PEG-NH₂.

2.4.3. Methods

2.4.3.1. General methods

¹H NMR spectra were recorded for solutions in D₂O (25 °C) using a Bruker AV-400

MHz spectrometer operating at 400 MHz. Chemical shifts are given relative to external tetramethylsilane (TMS = 0 ppm). Gel permeation chromatography (GPC) measurements were carried out using a GPC system with an Agilent 1100 isocratic pump, a Dawn EOS multiangle laser light scattering detector (Wyatt Technology Corp., Santa Barbara, USA) and an Optilab DSP interferometric refractometer (Wyatt Technology Corp.) using PL-aquagel-OH 40 (8 μm) and PL-aquagel-OH 30 (8 μm) columns (Polymer Laboratories, Amherst, MA, USA) eluted with a pH 7.02 buffer composed of 0.2 M NaNO_3 , 0.01 M NaH_2PO_4 , 0.08 mM NaN_3 at a flow rate of 0.5 mL/min. Solutions for analysis had a polymer concentration of 10.0 mg/mL and the injection volume was set at 100 μL . For dn/dc measurements, solutions of each polymer of concentration ranging from 0.2 to 1.0 mg/mL were prepared in the same buffer. UV-vis absorption spectra were recorded with an Agilent 8452A photodiode array spectrometer. Zeta-potential measurements were carried out with a Malvern ZetaSizer Nanoseries ZS (Malvern Instruments, Worcestershire, UK). Lyophilizations were performed with a Virtis (Gardiner, NY, USA) Sentry Benchtop (3L) freeze-dryer. Melting point was measured with a Büchi 535 capillary melting point apparatus (Büchi, Switzerland).

2.4.3.2. Light scattering

Static (SLS) and dynamic (DLS) light scattering experiments were performed on a CGS-3 goniometer (ALV GmbH) equipped with an ALV/LSE-5003 multiple- τ digital correlator (ALV GmbH), a He-Ne laser ($\lambda = 632.8$ nm), and a C25P circulating water bath (Thermo Haake). The SLS data were analyzed according to the Zimm method.^[14] The refractive index increment (dn/dc) values of the CMD-PEG samples (Table 2.2) and of diminazene diaceturate (0.2543 mL/g) in Tris-HCl buffer, pH 5.3 were measured using an Optilab DSP interferometric refractometer (Wyatt Technology Corp.). The dn/dc value of the micelles was calculated from Eq. (1).^[15, 16]

$$\left(\frac{dn}{dc}\right)_{micelle} = W_{CMD-PEG} \left(\frac{dn}{dc}\right)_{CMD-PEG} + W_{drug} \left(\frac{dn}{dc}\right)_{drug} \quad (1)$$

Where $(dn/dc)_{\text{CMD-PEG}}$ and $(dn/dc)_{\text{drug}}$ are the refractive index increments of CMD-PEG and diminazene diacetate, respectively, and $W_{\text{CMD-PEG}}$ and W_{drug} are the weight fractions of CMD-PEG and diminazene diacetate, respectively. A cumulant analysis was applied to obtain the diffusion coefficient (D) of the micelles in solution. The hydrodynamic radius (R_H) of the micelles was obtained using the Stokes-Einstein Eq. (2),

$$D = \frac{k_B T}{6\pi\eta_s R_H} \quad (2)$$

Where η_s is the viscosity of the solvent, k_B is the Boltzmann constant, and T is the absolute temperature. The constrained regularized CONTIN method was used to obtain the particle size distribution.^[17] The data presented are the mean of six measurements \pm S.D. Solutions for analysis were filtered through a 0.45 μm Millex Millipore PVDF membrane prior to measurements.

Table 2.2. Molecular properties of the CMD-PEG samples prepared

Polymer	dn/dc^a (mL/mg)	M_w^b (g mol ⁻¹)	M_n^b (g mol ⁻¹)	DS ^c
85-CMD ₄₀ -PEG ₁₄₀ ^d	0.1416	14,800	10,800	0.86 \pm 0.09
80-CMD ₄₀ -PEG ₆₄	0.1434	12,200	10,200	0.76 \pm 0.08
60-CMD ₆₈ -PEG ₆₄	0.1376	16,800	13,400	0.62 \pm 0.06
30-CMD ₆₈ -PEG ₆₄	0.1392	15,900	12,000	0.31 \pm 0.03

^a: Values recorded for polymer solutions in 25 mM Tris-HCl pH 5.3, 25 °C.

^b: From GPC measurements in aqueous NaNO₃ (0.2 M)/NaH₂PO₄ (0.01 M)/NaN₃ (0.8 mM); pH 7.02.

^c: Degree of substitution: mol fraction of glucopyranose units carrying a -CH₂-COONa group; determined by potentiometric titration.

^d: In this nomenclature, the prefix denotes the degree of carboxymethylation of the dextran block; the subscripts designate the average number of glucopyranosyl and -CH₂-CH₂-O-repeat units of the CMD and PEG segments, respectively.

2.4.3.3. Preparation and characterization of the micelles

2.4.3.3.1. General method

Stock solutions of the diblock copolymers (1.0 g/L) and diminazene diaceturate (4.0 g/L) were prepared in Tris–HCl buffer (25 mM, pH 5.3). Specified volumes of the diminazene diaceturate solution were added dropwise to a magnetically stirred polymer solution over a 10-min period to obtain solutions with a $[+]/[-]$ ratio ranging from 0.2 to 5.0. For simplicity reasons the $[+]/[-]$ ratio was calculated assuming a drug purity of 100%. The uncertainty of the ratio is estimated to be ~ 0.08 knowing that the purity of the drug is $\geq 96\%$. The volume of each sample was adjusted to 5.0 mL by addition of the same buffer. The final CMD-PEG concentration was 0.2 g/L in all samples.

2.4.3.3.2. pH studies

A micellar solution (CMD-PEG: 0.2 g/L; $[+]/[-] = 2.0$) was prepared in 25 mM Tris-HCl buffer, pH 5.3. Aliquots of this solution were treated either with 1.0 N NaOH or with 1.0 N HCl to obtain solutions ranging in pH from 11 to 2. After each pH adjustment, the sample was stirred for 5 min prior to measurement. The hydrodynamic radius, polydispersity index and scattered light intensity of an aliquot of the sample were determined by DLS. A control experiment was carried out with CMD-PEG solutions (0.2 g/L) treated in the same pH range. The mean \pm S.D. of six measurements was determined.

2.4.3.3.3. Ionic strength studies

Micellar solutions (CMD-PEG: 0.2 g/L; $[+]/[-] = 2.0$) were prepared in a 25 mM Tris–HCl buffer of pH 5.3. Aliquots of a NaCl stock solution (2.5 M) in the same buffer were added to the micellar solutions in volumes such that $[\text{NaCl}]$ in the sample ranged from 50 to 600 mM. The mixture was stirred for 5 min and the volume of each sample was adjusted to 5.0 mL with Tris–HCl buffer, pH 5.3. The hydrodynamic radius, polydispersity index and scattered light intensity of an aliquot of each sample were determined by DLS measurements. The mean \pm S.D. of six measurements was determined.

2.4.3.3.4. *Critical association concentration*

Micellar solutions were prepared using the general procedure described above, with a polymer concentration of 0.2 g/L and $[+]/[-] = 2$. The micellar solutions were serially diluted with Tris-HCl (25 mM, pH 5.3) and the intensity of light scattered by the solutions was determined by DLS at a scattering angle of 90° . Six consecutive scattered light intensity measurements were performed. Their average value is reported. Normalized intensities, $I_C/I_{0.2}$ where I_C is the intensity of the light scattered by a solution of concentration c and $I_{0.2}$ is the intensity of the light scattered by a solution of polymer concentration 0.2 g/L were plotted against polymer concentration. The CAC was determined from the plot, following methods reported previously.^[18]

2.4.3.3.5. *Zeta-potential*

The ζ -potential of polymer micelles (CMD-PEG concentration: 0.2 g/L) of various $[+]/[-]$ molar ratios, prepared in Tris-HCl buffer (25 mM, pH 5.3) following the general procedure described above, was measured for solutions kept at 25 °C. Each sample was measured four times and the mean \pm S.D. is presented. The ζ -potential of the particles was calculated from the electrophoretic mobility values using Smoluchowski equation.

2.4.3.3.6. *Stability of micellar solutions upon storage*

The R_H and size distribution of polymer micelles (CMD-PEG concentration: 0.2 g/L), $[+]/[-] = 2$, prepared in Tris-HCl buffer (25 mM, pH 5.3) following the general procedure described above, were measured by DLS as described above at various time intervals up to 60 days. Solutions were kept at 25 °C between measurements.

2.4.3.3.7. *^1H NMR spectra of DIM/CMD-PEG mixtures*

Specified volumes of a DIM stock solution in D_2O (10 g/L) were added dropwise to a magnetically stirred solution of CMD-PEG in D_2O over a period of 10 min in amounts necessary to prepare mixed solutions of CMD-PEG (3.0 g/L) with $[+]/[-]$ ranging from 0.2 to 10.0. ^1H NMR spectra of the mixed solutions were recorded as described above.

2.4.3.3.8. *Lyophilization/redissolution of DIM/CMD-PEG micelles*

Micellar solutions of DIM/85-CMD₄₀-PEG₁₄₀ (10 mL, polymer concentration: 0.2 g/L; [+]/[-] = 2.0) in a Tris-HCl buffer (25 mM, pH 5.3) or in aqueous trehalose (5%, w/v) were frozen by placing the glass vials containing the samples in a dry ice/acetone mixture (temperature: -78 °C). After 30 min the vials were placed in the freeze-dryer and lyophilized for 48 h. The resulting powder was rehydrated with deionized water (10 mL) to reach a polymer concentration of 0.2 g/L. The resulting mixture was stirred at room temperature for 10 min and analyzed by DLS.

2.4.3.3.9. *Diminazene release studies*

The release of diminazene diacetate from micelles (3.0 mL, [DIM] = 1.2 g/L, [+]/[-] = 2) in a Tris-HCl buffered saline (25 mM, pH 5.3, 0 mM NaCl or 25 mM, pH 7.4, 150 mM NaCl) was evaluated by the dialysis bag method at 37 °C against the buffer (200 mL) used to prepare the micelles and using a dialysis membrane of MWCO = 3500 g/mol).^[19, 20] The concentration of diminazene in the dialyate was determined from the absorbance at 370 nm using a calibration curve. A control experiment to determine diminazene diffusion through the membrane in the absence of the polymer was carried out using a solution of diminazene (1.2 g/L, 3 mL) in the same Tris-HCl buffer. The concentration of diminazene released from the micelles is expressed as the cumulative percentage of the total drug available and plotted as a function of dialysis time.

2.5. Results and discussion

2.5.1. Synthesis of carboxymethyldextran-*block*-poly(ethylene glycol)s

The ionic diblock copolymers CMD-PEG were obtained by reaction of monochloroacetic acid (MCA) with DEX-PEG in the presence of sodium hydroxide.^[10] Reaction conditions were adjusted in order to obtain copolymers of desired degree of substitution (DS), defined as the molar fraction of glucopyranose rings bearing a -CH₂COO- group. To obtain a high substitution level (DS > 0.50), solutions of DEX-PEG

in a 85/15 (v/v) isopropanol/water mixture were treated with aqueous NaOH (9.0 M) at 60 °C.^[21] To achieve moderate carboxymethylation yields ($DS \leq 0.30$), MCA was added to a solution of DEX-PEG in aqueous NaOH cooled to ~ 0 °C, with subsequent treatment at 60 °C for 1 h.^[22] All CMD-PEG samples were isolated as their sodium salts. The successful incorporation of carboxylate groups onto the dextran block was ascertained by analysis of the ^1H NMR spectrum of the CMD-PEG samples, which exhibits two doublets (δ 4.89 and 5.07 ppm) ascribed to the resonance of the anomeric protons, a series of signals between δ 4.08 and 4.15 ppm, due to the methylene protons α to the carboxylate group, and two signals characteristic of the PEG block: a singlet at δ 3.28 ppm due to the methoxy end group of the PEG block and a broad signal at δ 3.60 ppm due to the $-\text{CH}_2-\text{CH}_2-\text{O}-$ groups.^[10] The average molar mass of the CMD-PEG diblock copolymers measured by gel permeation chromatography are listed in Table 2.2, together with the degree of substitution (DS) of the polymers determined by potentiometric titration carried out following the procedure reported previously.^[10]

2.5.2. Preparation and size of diminazene/CMD-PEG micelles

Simple mixing of diminazene diacetate ($\text{pK}_a = 11$)^[23] and CMD-PEG in a Tris-HCl buffer (25 mM) of pH 5.3 should trigger the formation of micellar complexes via electrostatic interactions, since both DIM and CMD-PEG are fully ionized at this solution pH. These conditions were used throughout, unless specified otherwise. Evidence for the formation of nanoparticles was provided by dynamic light scattering (DLS) measurements, exemplified in Figure 2.2 (top) which presents the size distribution recorded for a solution of diminazene/60-CMD₆₈-PEG₆₄ of charge ratio $[+]/[-] = 2.0$, where $[+]/[-]$ is the ratio of the molar concentration of positive charges provided by the drug to that of the negative charges provided by the polymer. The changes in the particles hydrodynamic radius (R_H) and polydispersity index (PDI) as a function of the ratio $[+]/[-]$ are shown in Figure 2.2 (bottom) for the same drug/CMD-PEG system. Particles of $R_H \sim 50$ nm with a PDI of ~ 0.5 were detected in mixed solutions containing a large excess of polymer ($[+]/[-] < 0.2$) signaling the formation of loose polymer/drug aggregates as a result of the competition

between drug/polymer attractive forces and repulsive forces between the negative charges on the CMD segments. The hydrodynamic radius and polydispersity index of the scattering objects reached minimum values, ~ 20 nm and 0.05, respectively, in mixed solutions of $[+]/[-] \sim 1$, i.e., when charge neutralization is achieved. Further increase in drug concentration, with respect to polymer concentration, resulted in a gradual increase in the size of the nanoparticles until $[+]/[-] \sim 2$, implying further incorporation of diminazene within the micellar core, as observed also by ^1H NMR spectroscopy (see below). No changes in R_H or PDI took place upon further addition of drug, signifying that micelles with $[+]/[-] \sim 2$ are unable to incorporate additional drug molecules. The R_H and PDI values recorded for all DIM/CMD-PEG systems are listed in Table 2.3 for solutions containing 0.2 g/L of polymer and drug in amounts such that $[+]/[-] = 2.0$. The hydrodynamic size of DIM/85-CMD₄₀-PEG₁₄₀ micelles is slightly larger than that of DIM/80-CMD₄₀-PEG₆₄. This difference in size can be attributed to the difference in the length of the PEG segment of the two copolymers (140 EG units or M_n (PEG) ~ 6200 g/mol vs. 40 EG units or M_n (PEG) ~ 2800 g/mol). Diminazene/CMD-PEG micelles of low polydispersity index, such as those represented in Figure 2.2 for systems of $[+]/[-] > 1$ were prepared by dropwise addition of a drug solution to a magnetically stirred polymer solution. This method consistently led to micelles of identical size for a given $[+]/[-]$ ratio. However, when the drug solution was added in one shot to the polymer solution, the resulting micelles were significantly more polydisperse in size (PDI > 0.1). These PDI values are similar to those reported by Govender *et al.* in the case of DIM/poly(aspartic acid)-*block*-PEG systems which were prepared by a “one-shot” mixing.^[12] In order to ascertain reproducibility of the micellar properties, throughout this study diminazene/CMD-PEG nanoparticles were prepared via the dropwise addition of the drug solution to the polymer solution.

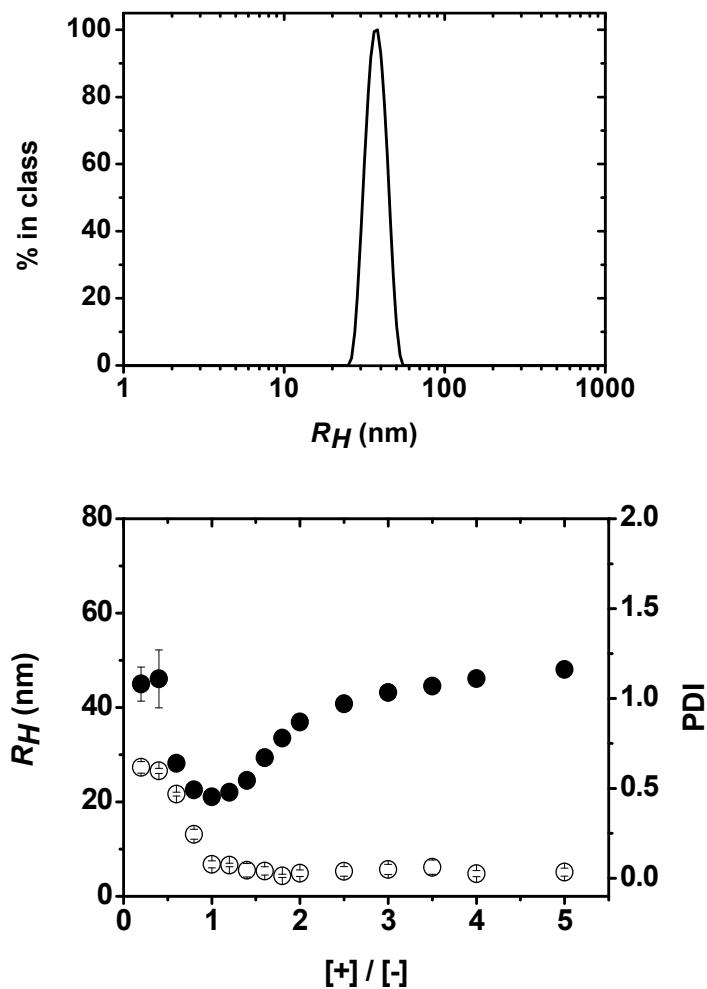


Figure 2.2. (top): Distribution of the hydrodynamic radius (R_H) of micelles in a solution of DIM/60-CMD₆₈-PEG₆₄ ($[+]/[-] = 2$; polymer concentration: 0.2 g/L; solvent: Tris-HCl buffer, 25 mM, pH 5.3; temperature: 25 °C; θ : 90 °C); (bottom): plots of the changes of R_H (●) and the polydispersity index (PDI, ○) as a function of $[+]/[-]$ in mixtures of DIM and 60-CMD₆₈-PEG₆₄; polymer concentration: 0.2 g/L; temperature: 25 °C; θ : 90 °C.

Table 2.3. Characteristics of DIM/CMD-PEG micelles ($[+]/[-] = 2$)^a in a Tris-HCl buffer (25 mM, pH 5.3) for four different diblock copolymers

Polymer	R_H (nm) ^b	PDI ^b	CAC (g/L)	$M_{w,app}$ ($\times 10^{-6}$ g/mol)	N_{DIM}	N_{agg}	% DIM ^c
85-CMD ₄₀ -PEG ₁₄₀	48.7 ± 0.6	0.05 ± 0.03	0.048	8.25	12300	363	64.3
80-CMD ₄₀ -PEG ₆₄	43.5 ± 0.7	0.01 ± 0.01	0.032	7.21	10400	348	62.0
60-CMD ₆₈ -PEG ₆₄	36.9 ± 0.5	0.02 ± 0.01	0.014	4.99	7300	174	60.1
30-CMD ₆₈ -PEG ₆₄	49.7 ± 0.6	0.10 ± 0.02	0.095	3.89	3700	178	41.4

^a: $[+]/[-]$: ratio of the molar concentration of positive charges provided by the drug to that of negative charges provided by the polymer.

^b: Mean of six measurements ± S.D.

^c: % DIM loading = weight of drug/(weight of micelles)×100.

In the case of DIM/30-CMD₆₈-PEG₆₄, micelles of uniform size distribution were obtained only for $[+]/[-] > 1.6$. The micelles were larger than DIM/60-CMD₆₈-PEG₆₄ micelles of identical $[+]/[-]$ ratio (Table 2.3). The backbone of the two copolymers (30-CMD₆₈-PEG₆₄ and 60-CMD₆₈-PEG₆₄) is the same, but 30-CMD₆₈-PEG₆₄ contains about half as many charges as 60-CMD₆₈-PEG₆₄. Consequently, the level of drug incorporation in 30-CMD₆₈-PEG₆₄ micelles is lower, for identical $[+]/[-]$, compared to the situation in DIM/60-CMD₆₈-PEG₆₄. With fewer drug molecules bound to the CMD segments, the micellar core remains more hydrated leading to the formation of larger micelles.

The apparent molecular weight ($M_{w,app}$) of DIM/CMD-PEG nanoparticles ($[+]/[-] = 2$) was obtained by a Zimm plot analysis of static light scattering measurements. From this value, and knowing the weight average molecular weight of individual chains determined by GPC (Table 2.2), it is possible to estimate (1) the aggregation number (N_{agg}) of the micelles, defined here as the number of CMD-PEG chains associated in each micelle and

(2) the number (N_{DIM}) of drug molecules incorporated in a micelle. In this calculation, it is assumed that there is no free drug in the mixed solutions and that each carboxylate substituent of the CMD block is bound to one diminazene molecule. Values of $M_{\text{w, app}}$, N_{DIM} and N_{agg} calculated for micelles formed by CMD-PEG samples of different block lengths and degrees of substitution are listed in Table 2.3. The N_{agg} value depends primarily on the length of the CMD block: it is the same for the two copolymers, 30-CMD₆₈-PEG₆₄ and 60-CMD₆₈-PEG₆₄, which differ greatly in DS but are of identical length. The N_{agg} and N_{DIM} of micelles formed by two polymers with similar DS and CMD block length, but different PEG segments (85-CMD₄₀-PEG₁₄₀ and 80-CMD₄₀-PEG₆₄) are similar, implying that the PEG segments play a passive role in directing the micellar composition, which is driven primarily by the CMD block. Control experiments using isothermal titration calorimetry confirmed the absence of interactions between PEG and DIM (Supporting information).

2.5.3. Determination of the [+]/[-] ratios corresponding to the onset of micellization and to the maximum drug loading capacity by ¹H NMR spectroscopy

Incorporation of drug molecules in the core of polymeric micelles restricts the motion of the protons linked to the drug as well as that of the polymer fragments directly bound to the drug. This loss of mobility is reflected by a significant line broadening and/or disappearance of the ¹H NMR signals due to the corresponding protons. We used this inherent property of solution NMR spectroscopy to detect the [+]/[-] ratio for which the drug is effectively entrapped into micelles (onset of micellization) as well as the [+]/[-] value for which the maximum loading capacity of a PIC micelle is attained. The method also allows one to ascertain the absence of free drug in a PIC-micelle formulation. It is described in detail, since it is applicable readily to other drug/diblock copolymer systems.

The ¹H NMR spectrum of diminazene diacetate in D₂O at room temperature (Figure 2.3, bottom) presents signals at δ 7.5 and 7.7 ppm, attributed to the aromatic protons, H_c and H_d , respectively^[24], as well as singlets at δ 1.92 and 3.63 ppm assigned, respectively, to the methyl (H_a) and methylene (H_b) protons of the acetate counterions.

Also shown in Figure 2.3 are the ^1H NMR spectra of drug/60-CMD₆₈-PEG₆₄ solutions of different $[+]/[-]$ ratios. Turning our attention first to the signals of these spectra corresponding to the drug, we note that (1) the signals at δ 1.92 and 3.63 ppm due to the drug counterion (acetate) are sharp and well resolved in all spectra, indicating that the acetates remain in solution, preserving their freedom of motion; (2) the signals in the aromatic region (δ 7.5 and 7.7 ppm) due to the protons of the drug are strongly affected by the presence of the polymer. They appear weak and broadened in the spectrum of the mixture with $[+]/[-] = 0.2$. Moreover, in the spectrum of this system, the signal attributed to the resonance of the protons H_d undergoes a significant upfield shift, implying a change in the local environment of these protons upon binding to the polymer linked carboxylates. Both signals in the aromatic region vanish in spectra of mixed solutions of $[+]/[-] = 1.0$ – 2.0 . They reappear in spectra of mixtures with $[+]/[-] > 2.0$, signaling the presence of free drug in the micellar solution, as seen in Figure 2.3 (right) where we present spectra of mixed systems with $[+]/[-] = 4$ and 10 .

In the ^1H NMR spectra of mixed systems, one notices also changes in the signals due to the resonance of protons linked to the polymer. Thus, signals at δ 4.08–4.15, 4.89 and 5.07 ppm ascribed to protons of the CMD block decrease in intensity with increasing $[+]/[-]$. They are still detectable in mixed solutions of $[+]/[-] = 0.8$, but disappear for mixed systems of $[+]/[-] > 1$, signaling severe loss of mobility of the CMD block under these conditions (Figure 2.3). In contrast, the signals due to the PEG protons ($-\text{CH}_2-\text{CH}_2-\text{O}-$, δ 3.61 ppm) remain unaffected by changes in $[+]/[-]$, an indication that the PEG chains preserve their mobility within the corona of the PIC micelles. As noted earlier, signals due to the DIM protons are visible in spectra of mixed systems with $[+]/[-] > 2$, yet the signals due to the CMD protons remain undetectable up to $[+]/[-] = 10$, the highest ratio tested. Thus the PIC micelles preserve their integrity even in the presence of a large excess of free drug.

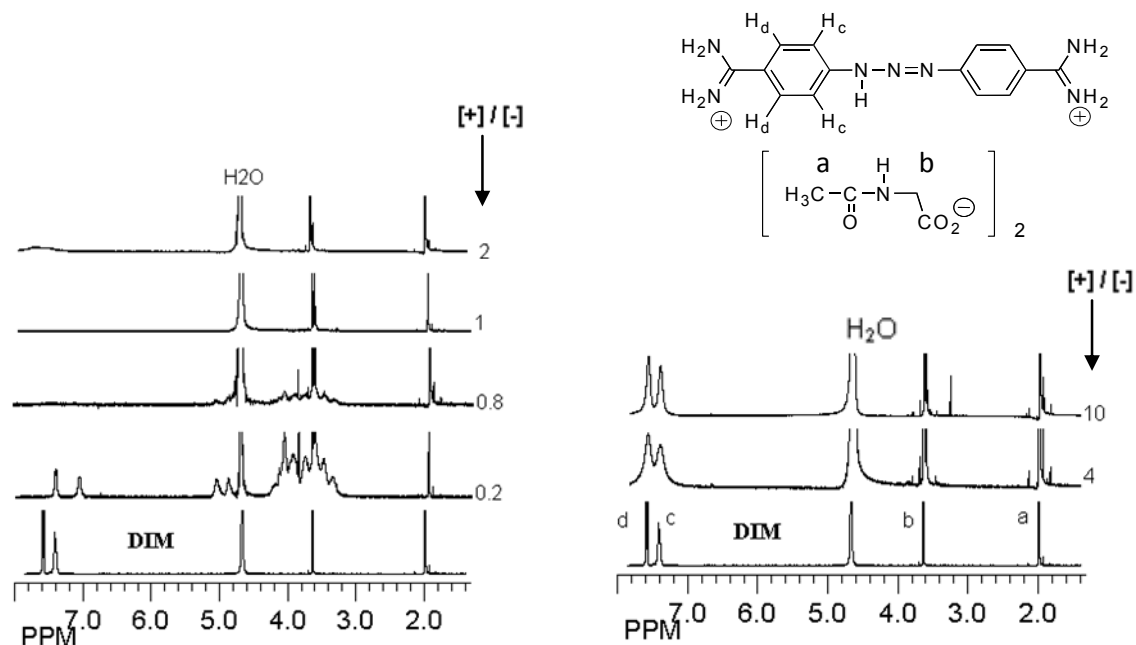


Figure 2.3. ^1H NMR spectra recorded for diminazene diacetate (DIM, lower spectra) and solutions of DIM and 60-CMD₆₈-PEG₆₄ of $0 < [+]/[-] < 2$ (left) and $[+]/[-] = 4, 10$ (right); polymer concentration: 3.0 g/L, solvent: D₂O; temperature : 25 °C.

Taken together, the results of ^1H NMR experiments suggest the formation of micelles with some ordered structure, presumably a core-corona system, where PEG segments form a highly hydrated corona surrounding a core composed of diminazene electrostatically bound to CMD segments. Remembering that each drug molecule possesses two cationic centres, the ^1H NMR data may be taken as an indication that micelles formed upon charge neutralization ($[+]/[-] \sim 1$), in which each drug molecule interacts with two polymer-bound carboxylates, are able to incorporate additional drug molecules, until only one of the two binding sites of the drug is involved in the complexation. This conclusion can be drawn from the combined facts that (i) signals ascribed to protons of the CMD block gradually decrease in intensity in spectra of mixed solutions of $0 < [+]/[-] < 1$ and (ii) in the same mixed systems, signals of protons linked to the drug cannot be detected, whereas

signals due to the drug protons reappear in mixtures of $[+]/[-] > 2$, a ratio corresponding to maximum drug loading in micelles of this copolymer. For this ratio, the weight percent loading of drug in the micelle ranges from ~ 40 to ~ 65 wt% depending on the type of CMD-PEG (Table 2.3). An identical spectroscopic analysis was performed also to monitor the interactions between DIM and the copolymer 30-CMD₆₈-PEG₆₄, which has a lower DS than 60-CMD₆₈-PEG₆₄, but has the same molar mass. The DIM/30-CMD₆₈-PEG₆₄ mixed system followed the same trends as those depicted in Figure 2.3, except that the signals due to the drug aromatic protons and the CMD protons remained detectable as long as $[+]/[-] < 1.6$, confirming the observation from DLS experiments (see above) that micelles of this copolymer only form in solutions of $[+]/[-] > 1.6$. In the case of the samples 85-CMD₄₀-PEG₁₄₀ and 80-CMD₄₀-PEG₆₄, the ¹H NMR experiments revealed trends similar to those exhibited by the DIM/60-CMD₆₈-PEG₆₄ system. The results of the ¹H NMR study go beyond mere structural information. They indicate that for *in vivo* applications it is crucial to use drug-loaded micelles of $1 \leq [+]/[-] \leq 2$ in order to ascertain the absence of free drug, which is easily accessible to the external harsh conditions, such as those found in the GIT.

2.5.4. Critical association concentration of diminazene/CMD-PEG micelles

The minimal polymer concentration for which PIC micelles can be detected for a given $[+]/[-]$ ratio, or critical association concentration (CAC), is an important parameter controlling the *in vivo* stability of a drug delivery system subjected to extensive dilution upon administration.^[25] The CAC value of diminazene/CMD-PEG micelles depends on the chemical composition of the ionic diblock copolymer and on the level of drug loading within the micelle. It was determined for micelles formed in Tris-HCl buffer, pH 5.3 by each of the four diblock copolymers in the presence of diminazene in amounts such that $[+]/[-] = 2.0$. Micellar solutions ranging from 5×10^{-3} g/L to 0.2 g/L were prepared by dilution of a stock micellar solution (CMD-PEG: 0.2 g/L). The intensity of the light scattered by each solution was measured. The CAC values (Table 2.3) were taken as the concentration corresponding to the onset of the increase in scattered light intensity,

determined graphically from plots of $I_C/I_{0.2}$ vs. CMD-PEG concentration, where I_C is the intensity of light scattered by a solution of CMD-PEG of concentration c and $I_{0.2}$ is the intensity of light scattered by a solution of CMD-PEG concentration = 0.2 g/L, as shown in Figure 2.4. The CAC value of all micelles is very low, (<0.1 g/L of polymer) vouching for the stability of the micelles against dilution. The lowest value was recorded for micelles formed by the copolymer of longest CMD block and highest DS (60-CMD₆₈-PEG₆₄), presumably as a consequence of their high drug loading capacity. The length of the PEG block has only a minor influence on the CAC value of the micelles, as seen by comparing the values determined for 85-CMD₄₀-PEG₁₄₀ and 80-CMD₄₀-PEG₆₄ (Table 2.3). Similar trends have been reported in previous studies of other micelles.^[26]

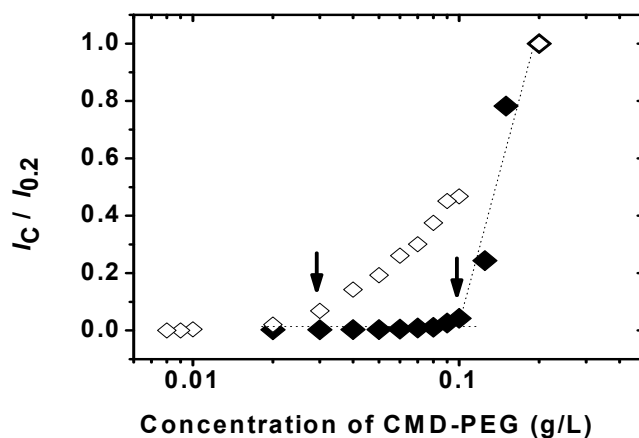


Figure 2.4. Plots of the changes as a function of polymer concentration of the ratio ($I_C/I_{0.2}$) of the intensity of light scattered by a solution of DIM and 60-CMD₆₈-PEG₆₄ (◇) or 30-CMD₆₈-PEG₆₄ (◆) of concentration c to that of a solution of DIM and polymer of concentration 0.2 g/L; solvent: Tris-HCl buffer, 25 mM, pH 5.3; the arrows indicate the critical association concentration.

2.5.5. Effect of salt (NaCl) on micelle formation and stability

Low molecular weight salts screen the charges of the ionic diblock copolymer, such that above a given salt concentration the micellar assemblies fall apart.^[27, 28] For *in vivo* applications it is crucial to ascertain that a specific drug/diblock copolymer system can resist the salinity of the biological milieu. Therefore we evaluated by light scattering measurements the salt concentration beyond which diminazene/CMD-PEG micelles do not form, using aqueous DIM/CMD-PEG solutions containing from 0 to 0.6 M [NaCl]. Figure 2.5, bottom, illustrates the dependence on salt concentration of the micellar R_H and the scattered light intensity in the case of the DIM/85-CMD₄₀-PEG₁₄₀ system (polymer concentration: 0.2 g/L; [+]/[-] = 2.0). The profile can be divided into three domains: (i) for $0 < [\text{NaCl}] \leq 0.2$ M, both R_H and the scattered light intensity (I_{Sc}) increase; (ii) for $0.2 < [\text{NaCl}] \leq 0.4$ M, R_H increases whereas I_{Sc} sharply decreases; and (iii) for $[\text{NaCl}] > 0.4$ M, R_H decreases while the scattering intensity remains weak and constant. The micelles of diminazene and 80-CMD₄₀-PEG₆₄ as well as the copolymer of lower DS (60-CMD₆₈-PEG₆₄) respond to changes in salinity according to the same three-zone pattern.

The increase of R_H and I_{Sc} in region I may be attributed to an overall increase in micellar size as a result of partial salt-induced dehydration of the PEG corona, which facilitates merging of micelles upon collision and promotes the formation of large micelles. In this region, the salinity is too low to disrupt the drug/CMD-PEG ionic interactions within the core of the micelle. Micelles begin to show signs of disintegration for $[\text{NaCl}] \sim 0.3$ M as detected by a decrease in scattered light intensity. This salt concentration corresponds to the beginning of region II. The disintegration of the micelles occurs gradually by progressive loosening of the core interactions and expansion of the micelle size. The breadth of region II is narrow, however, and in solutions of $[\text{NaCl}] > 0.4$ M the solution contains primarily isolated drug molecules and polymer chains, with possibly loose drug/polymer associates. Thus, all CMD-PEG micelles in which the DS of the CMD block was 60% or higher are able to resist salt-induced disintegration up to 0.4 M, a value significantly higher than the physiological salt concentration (0.15 M).

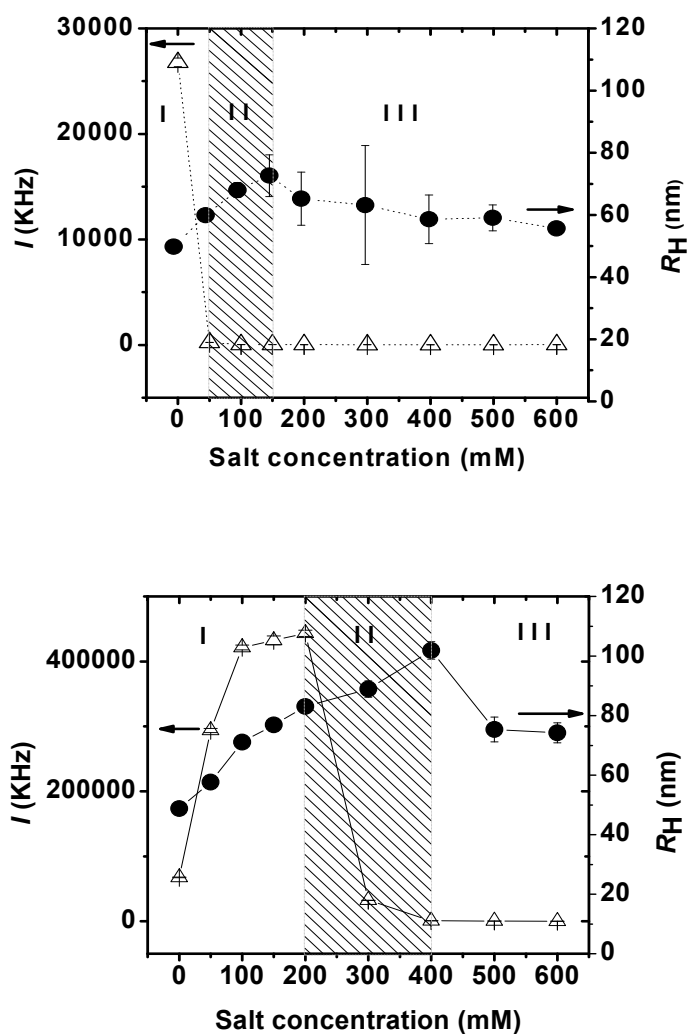


Figure 2.5. Plots of the changes of R_H of micelles (●) and the intensity of scattered light (I , △) as a function of NaCl concentration in mixtures of DIM and 30-CMD₆₈-PEG₆₄ (top) or 85-CMD₄₀-PEG₁₄₀ (bottom) in Tris-HCl buffer, 25 mM, pH5.3; polymer concentration: 0.2 g/L; $[+]/[-] = 2$; temperature: 25 °C; θ : 90°; the hatched area corresponds to region II (see text).

In contrast, micelles formed between diminazene and the copolymer 30-CMD₆₈-PEG₆₄, proved to be unable to withstand $[\text{NaCl}] > 0.1$ M, even under conditions of charge

neutralization ($[+]/[-] = 2$). For this system, a plot of I_{sc} vs. $[\text{NaCl}]$ (Figure 2.5, top) reveals that region I is limited to $0 < [\text{NaCl}] < 0.05$ M and region II spans from 0.05 to 0.15 M. Solutions of higher $[\text{NaCl}]$ exhibit low scattered light intensity ascribed to the presence of loosely bound objects with $R_H \sim 60$ nm. This observation leads us to conclude that the drug loading must be above a threshold value for charge neutralized PIC micelles to remain stable under physiological conditions. In the micelles studied here, this value is reached for diminazene/60-CMD₆₈-PEG₆₄ ($[+]/[-] = 2.0$) micelles, but not for diminazene/30-CMD₆₈-PEG₆₄ ($[+]/[-] = 2.0$). This result sets the lowest limit for the charge density of diblock copolymers useful in PIC-type drug delivery systems.

2.5.6. Zeta-potential studies

The interactions of nanoparticles with cells and cellular components are governed, at least in part, by their surface charge. The zeta (ζ) potential of DIM/85-CMD₄₀-PEG₁₄₀ micelles in Tris-HCl (25 mM, pH 5.3) ranged from ~ -7.6 mV for $[+]/[-] = 0.6$ to ~ -3.4 mV for $[+]/[-] = 2$, as expected since their charge is determined by that of the corona (PEG).

2.5.7. Effect of solution pH on the stability of diminazene/CMD-PEG micelles

Since the formation of polyion micelles relies on electrostatic interactions between oppositely charged drug and copolymer, there may exist pH conditions for which one of the interacting components will be neutral, triggering the disruption of the micellar core. In the case of the micelles described here, these conditions are attained when $\text{pH} < 4$ (neutralization of CMD-PEG) or $\text{pH} > 11$ (neutralization of diminazene). The pH dependence of the R_H of micelles and of the intensity of the light scattered by the solutions was monitored by DLS measurements which indicated that diminazene/85-CMD₄₀-PEG₁₄₀ micelles (polymer concentration: 0.2 g/L; $[+]/[-] = 2$, Figure 2.6) were of constant size ($R_H \sim 50$ nm) and scattering intensity for $4 < \text{pH} < 11$. Solutions brought to $\text{pH} < 4.0$ rapidly lost

their ability to scatter light, presumably as a consequence of the near complete destruction of the micellar assemblies. In the high pH region ($\text{pH} > 11$), similar changes in the scattering characteristics of the samples took place, although the decrease in scattering intensity was not as severe. Similar DLS measurements carried out with polymer solutions (0.2 g/L) in the absence of drug gave no evidence of polymer self-assembly.

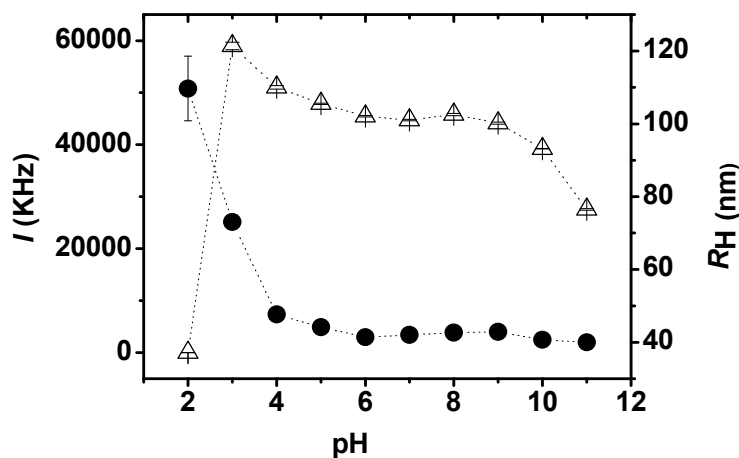


Figure 2.6. Plots of the changes of R_H of micelles (\bullet) and of the intensity of scattered light (I , \triangle) as a function of solution pH in mixtures of DIM and 85-CMD₄₀-PEG₁₄₀ in 25 mM Tris-HCl; polymer concentration: 0.2 g/L; $[+]/[-] = 2$; temperature: 25 °C; θ : 90°.

Interestingly, the pH-window of micellar stability reported in the case of DIM/poly(aspartic acid)-PEG micelles^[12] does not extend beyond 7.2 while in our study we ascertained that micellar systems formed by all CMD-PEG copolymers exhibit the same behavior as diminazene/85-CMD₄₀-PEG₁₄₀, independently on the charge density of the copolymer and of drug loading. The pH sensitivity of these PIC micelles, however, can be taken into advantage in the case of drug delivery systems targeted to cancerous tumors for which the drug must be kept protected under physiological conditions (pH 7.4) and must be released in the mild acidic environment of the extracellular spaces of tumors or in the acidic

environment of endosomes (pH~5–6) or lysosomes (pH ~ 4–5) following cellular uptake of the PIC micelles.^[29] Nonetheless, the pH window of micellar stability (4–11) prohibits the use of DIM/CMD-PEG micelles in oral formulations, unless care is taken to avoid premature drug release in the stomach, such as application of an appropriate enteric coating.^[30]

2.5.8. Storage stability of diminazene/CMD-PEG micelles

We assessed the stability of diminazene/CMD-PEG micelles ([+]/[-] = 2.0) in Tris–HCl buffer, pH 5.3 at room temperature by following the evolution of their R_H over a period of 2 months. In the case of diminazene/80-CMD₄₀-PEG₁₄₀, for instance, the micelle R_H increased slightly (from 48.5 to 60.1 nm) over the course of the first week and remained constant upon further storage. Tests carried out with micelles of diminazene/CMD-PEG of different composition yielded similar trends, confirming the stability of the micelles. A slight increase in size over the first few days after micelle preparation was noticed in all cases. Initial experiments carried out on micellar formulations in Tris–HCl buffer (pH 5.3, [+]/[-] = 2.0) indicated that redissolution of the lyophilized micelles was incomplete, even after treatment in a sonicator bath. Moreover, the size and size distribution of the micelles were significantly larger, compared to those of the micelles prior to freeze-drying, with an R_H approximately twice that of the original value and a PDI > 0.10. However, micellar solutions complemented with 5% (w/v) of the cryoprotectant trehalose readily dissolved in water after freeze drying, yielding diminazene/CMD-PEG micelles of size slightly larger than the original micelles. Thus, diminazene/85-CMD₄₀-PEG₁₄₀ micelles had R_H values of 50 and 75 nm, respectively, before and after freeze-drying/redissolution. The tendency of nanoparticulate formulations to agglomerate upon freeze-drying has been observed previously. Addition of cryoprotectants or cross linking of the micellar core are effective means to prevent agglomeration.^[31-33]

2.5.9. Drug release studies

The release of diminazene diacetate from DIM/CMD-PEG micelles ($[+]/[-] = 2.0$) was monitored *in vitro* by the dialysis bag method using micelles formed between the drug and 85-CMD₄₀-PEG₁₄₀, which were shown to be stable under physiological conditions, as well as micelles formed with 30-CMD₆₈-PEG₆₄ known to disintegrate under these conditions. The profile recorded under physiological conditions of pH and ionic strength ($[\text{NaCl}] = 0.15 \text{ M}$, Tris-HCl buffer 25 mM, pH 7.4) (Figure 2.7) reveals complete drug release after ~ 8 h. Nonetheless this profile differs significantly from that recorded for a drug solution used as control, especially in the initial part of the release experiment, implying that micelles sustain the drug release over 8 h. In salt-free conditions diminazene/85-CMD₄₀-PEG₁₄₀ micelles retained $\sim 40\%$ of the drug after 24 h (50% after 8 h, Figure 2.7), while diminazene/30-CMD₆₈-PEG₆₄ nanoparticles released $\sim 72\%$ drug after 8 h. These release profiles differ from observations of Prompruk *et al.* who noted that DIM/poly(aspartic acid)-PEG micelles undergo immediate DIM release upon dialysis.^[19] We suggest that the enhanced stability of DIM/CMD-PEG micelles, compared to DIM/poly(aspartic acid)-PEG micelles, may be due to the formation of hydrogen bonds between the drug and the CMD block which possesses a large number of hydroxyl groups able to interact with the drug. This synergistic effect of weak bonds is akin to the stabilizing effect of drug/polymer hydrophobic interactions taking place in DIM/poly(aspartic acid-stat-phenylalanine), which exhibits sustained drug release^[19] or between poly(L-aspartic acid)-PEG in its free acid form and $[\text{Arg}^8]$ -vasopressin.^[34] In our case, however, the enhanced stability is an inherent property of the charged copolymers.

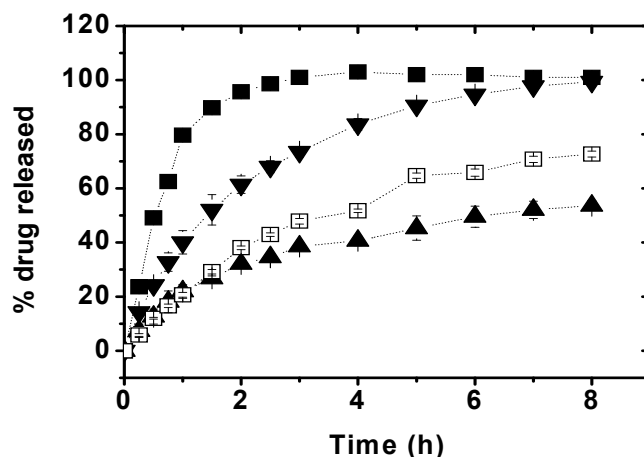


Figure 2.7. Release of DIM evaluated by the dialysis bag method from (■) DIM alone in Tris-HCl 25 mM, [NaCl] = 150 mM, pH 7.4; (▼) DIM/85-CMD₄₀-PEG₁₄₀ micelles, [+]/[-] = 2, in 25 mM Tris-HCl, [NaCl] = 150 mM, pH 7.4; (▲) DIM/85-CMD₄₀-PEG₁₄₀ micelles, [+]/[-] = 2, in 25 mM Tris-HCl [NaCl] = 0 mM, pH 5.3, and (□) DIM/30-CMD₆₈-PEG₆₄ at [+]/[-] = 2, in Tris-HCl, 25 mM [NaCl] = 0 mM, pH 5.3.

2.6. Conclusion

Four different CMD-PEG block copolymers have been tested for their ability to form PIC micelles with a cationic water soluble drug. The micelles formed were of small size (36–50 nm) and unimodal size distribution (PDI < 0.1). Properties of the micelles, such as their stability under different salt concentrations and drug release patterns depend primarily on the degree of substitution of the CMD block, which was readily adjusted by the synthesis protocol. Stable micelles with sustained drug release are formed if the DS of the CMD block exceeds a threshold value (~40%). ¹H NMR spectroscopy was used to determine the [+]/[-] molar ratio for which complete drug incorporation in the micelle core is achieved and the maximum drug loading attained. Further studies are aimed at widening the scope of drug/CMD-PEG micelles by assessing the characteristics of micelles formed by CMD-PEG and other cationic therapeutic agents, proteins and peptides. The *in vivo*

properties of drug/CMD-PEG micelles will be monitored next, since preliminary studies indicate that CMD-PEG samples present no toxicity towards several cell lines (Maysinger *et al.*, unpublished data).

2.7. Appendix A. Supplementary data

Supplementary data associated with this article can be found, in the online version, at doi:10.1016/j.ijpharm.2007.12.029.

2.8. Acknowledgments

The work was supported in part by a grant of the Natural Sciences and Engineering Research Council of Canada to FMW. GMS thanks the Ministry of Higher Education, Egypt for granting him a scholarship.

2.9. References

- [1] Skinner GW, Harcum WW, Barnum PE, Guo JH. The evaluation of fine-particle hydroxypropylcellulose as a roller compaction binder in pharmaceutical applications. *Drug Dev. Ind. Pharm.* **1999**, *25*: 1121-8.
- [2] Lee DY, Chen CM. Delayed pulse release hydrogel matrix tablet. U.S. Patent, 2000.
- [3] Payne GF. Biopolymer-based materials: The nanoscale components and their hierarchical assembly. *Curr. Opin. Chem. Biol.* **2007**, *11*: 214-9.
- [4] Francis MF, Cristea M, Yang Y, Winnik FM. Engineering polysaccharide-based polymeric micelles to enhance permeability of cyclosporin A across Caco-2 cells. *Pharm. Res.* **2005**, *22*: 209-19.
- [5] Francis MF, Piredda M, Winnik FM. Solubilization of poorly water soluble drugs in micelles of hydrophobically modified hydroxypropylcellulose copolymers. *J. Controlled Release* **2003**, *93*: 59-68.

- [6] Jeong YI, Kim SH, Jung TY, Kim IY, Kang SS, Jin YH, Ryu HH, Sun HS, Jin SG, Kim KK, Ahn KY, Jung S. Polyion complex micelles composed of all-trans retinoic acid and poly (ethylene glycol)-grafted-citosan. *J. Pharm. Sci.* **2006**, *95*: 2348-60.
- [7] Yang YL, Kataoka K, Winnik FM. Synthesis of diblock copolymers consisting of hyaluronan and poly(2-ethyl-2-oxazoline). *Macromolecules* **2005**, *38*: 2043-6.
- [8] Nomura Y, Ikeda M, Yamaguchi N, Aoyama Y, Akiyoshi K. Protein refolding assisted by self-assembled nanogels as novel artificial molecular chaperone. *FEBS Lett.* **2003**, *553*: 271-6.
- [9] Francis MF, Lavoie L, Winnik FM, Leroux J-C. Solubilization of cyclosporin A in dextran-g-polyethyleneglycolalkyl ether polymeric micelles. *Eur. J. Pharm. Biopharm.* **2003**, *56*: 337-46.
- [10] Hernandez OS, Soliman GM, Winnik FM. Synthesis, reactivity, and pH-responsive assembly of new double hydrophilic block copolymers of carboxymethyl dextran and poly(ethylene glycol). *Polymer* **2007**, *48*: 921-30.
- [11] Peregrine AS, Mamman M. Pharmacology of diminazene - a review. *Acta Trop.* **1993**, *54*: 185-203.
- [12] Govender T, Stolnik S, Xiong C, Zhang S, Illum L, Davis SS. Drug-polyionic block copolymer interactions for micelle formation: Physicochemical characterisation. *J. Controlled Release* **2001**, *75*: 249-58.
- [13] Thunemann AF, Schutt D, Sachse R, Schlaad H, Mohwald H. Complexes of poly(ethylene oxide)-block-poly(L-glutamate) and diminazene. *Langmuir* **2006**, *22*: 2323-8.
- [14] Harada A, Kataoka K. Novel polyion complex micelles entrapping enzyme molecules in the core. 2. Characterization of the micelles prepared at nonstoichiometric mixing ratios. *Langmuir* **1999**, *15*: 4208-12.
- [15] Tanodekaew S, Pannu R, Heatley F, Attwood D, Booth C. Association and surface properties of diblock copolymers of ethylene oxide and DL-lactide in aqueous solution. *Macromol. Chem. Phys.* **1997**, *198*: 927-44.

- [16] Harada A, Kataoka K. Novel polyion complex micelles entrapping enzyme molecules in the core: Preparation of narrowly-distributed micelles from lysozyme and poly(ethylene glycol)-poly(aspartic acid) block copolymer in aqueous medium. *Macromolecules* **1998**, *31*: 288-94.
- [17] Vamvakaki M, Palioura D, Spyros A, Armes SP, Anastasiadis SH. Dynamic light scattering vs H-1 NMR investigation of pH-responsive diblock copolymers in water. *Macromolecules* **2006**, *39*: 5106-12.
- [18] Li Y, Kwon GS. Methotrexate esters of poly(ethylene oxide)-block-poly(2-hydroxyethyl-L-aspartamide). Part I: Effects of the level of methotrexate conjugation on the stability of micelles and on drug release. *Pharm. Res.* **2000**, *17*: 607-11.
- [19] Prompruk K, Govender T, Zhang S, Xiong CD, Stolnik S. Synthesis of a novel PEG-block-poly(aspartic acid-stat-phenylalanine) copolymer shows potential for formation of a micellar drug carrier. *Int. J. Pharm.* **2005**, *297*: 242-53.
- [20] Nishiyama N, Okazaki S, Cabral H, Miyamoto M, Kato Y, Sugiyama Y, Nishio K, Matsumura Y, Kataoka K. Novel cisplatin-incorporated polymeric micelles can eradicate solid tumors in mice. *Cancer Res.* **2003**, *63*: 8977-83.
- [21] Huynh R, Chaubet F, Jozefonvicz J. Anticoagulant properties of dextranmethylcarboxylate benzylamide sulfate (DMCBSu); a new generation of bioactive functionalized dextran. *Carbohydr. Res.* **2001**, *332*: 75-83.
- [22] Rebizak R, Schaefer M, Dellacherie E. Polymeric conjugates of Gd³⁺-diethylenetriaminepentaacetic acid and dextran.1. Synthesis, characterization, and paramagnetic properties. *Bioconjugate Chem.* **1997**, *8*: 605-10.
- [23] Atsriku C, Watson DG, Tettey JNA, Grant MH, Skellern GG. Determination of diminazene aceturate in pharmaceutical formulations by HPLC and identification of related substances by LC/MS. *J. Pharm. Biomed. Anal.* **2002**, *30*: 979-86.
- [24] Lee SC, Cho JH, Mietchen D, Kim YS, Hong KS, Lee C, Kang DM, Park KD, Choi BS, Cheong C. Subcellular in vivo H-1 MR spectroscopy of *Xenopus laevis* oocytes. *Biophys. J.* **2006**, *90*: 1797-803.

- [25] Allen C, Maysinger D, Eisenberg A. Nano-engineering block copolymer aggregates for drug delivery. *Colloids Surf., B* **1999**, *16*: 3-27.
- [26] Alexandridis P, Holzwarth JF, Hatton TA. Micellization of poly(ethylene oxide)-poly(propylene oxide)-poly(ethylene oxide) triblock copolymers in aqueous-solutions - thermodynamics of copolymer association. *Macromolecules* **1994**, *27*: 2414-25.
- [27] Harada A, Kataoka K. Formation of stable and monodisperse polyion complex micelles in aqueous medium from poly(L-lysine) and poly(ethylene glycol)-poly(aspartic acid) block copolymer. *J. Macromol. Sci. Part A Pure Appl. Chem.* **1997**, *A34*: 2119-33.
- [28] Mao SR, Bakowsky U, Jintapattanakit A, Kissel T. Self-assembled polyelectrolyte nanocomplexes between chitosan derivatives and insulin. *J. Pharm. Sci.* **2006**, *95*: 1035-48.
- [29] Ulbrich K, Subr V. Polymeric anticancer drugs with pH-controlled activation. *Adv. Drug Deliv. Rev.* **2004**, *56*: 1023-50.
- [30] Sinha VR, Kumria R. Polysaccharides in colon-specific drug delivery. *Int. J. Pharm.* **2001**, *224*: 19-38.
- [31] Huh KM, Lee SC, Cho YW, Lee JW, Jeong JH, Park K. Hydrotropic polymer micelle system for delivery of paclitaxel. *J. Controlled Release* **2005**, *101*: 59-68.
- [32] Abdelwahed W, Degobert G, Fessi H. Investigation of nanocapsules stabilization by amorphous excipients during freeze-drying and storage. *Eur. J. Pharm. Biopharm.* **2006**, *63*: 87-94.
- [33] Miyata K, Kakizawa Y, Nishiyama N, Yamasaki Y, Watanabe T, Kohara M, Kataoka K. Freeze-dried formulations for in vivo gene delivery of PEGylated polyplex micelles with disulfide crosslinked cores to the liver. *J. Controlled Release* **2005**, *109*: 15-23.
- [34] Aoyagi T, Sugi K-i, Sakurai Y, Okano T, Kataoka K. Peptide drug carrier: studies on incorporation of vasopressin into nano-associates comprising poly(ethylene glycol)-poly(-aspartic acid) block copolymer. *Colloids Surf., B* **1999**, *16*: 237-42.

Appendix A. Supporting information (SI.2)

Isothermal titration calorimetry (ITC)

ITC Measurements were carried out with a VP-ITC instrument (from Microcal Inc) operated at 298 K. Samples of DIM and PEG 5000 were prepared in 25 mM Tris-HCl buffer adjusted to pH 5.3 ± 0.05 . Prior to measurements all the solutions were degassed under vacuum for about 10 min to eliminate any air bubbles. The drug solution (3 g/L, 5.8 mM) was placed in a 300 μ L continuously stirred (300-rpm) syringe and added to a 1.43 mL sample of PEG 5000 solution (0.092 g/L, 0.018 mM). The titration was performed by consecutive injections (10 μ L) of the drug solution into the PEG solution. Heats of dilution were determined in blank titrations by injecting aliquots (10 μ L) of the drug solution (3 g/L, 5.8 mM) into the same buffer solution (1.43 mL). A total of 28 aliquots were injected into the sample cell in intervals of 325 S. The calorimetric data were analyzed and converted to enthalpy change using Microcal ORIGIN 7.0.

PEG 5000 in its (-OH) form was chosen to be identical as the one in the block copolymers used in the study. Other experimental conditions, such as the drug and PEG concentrations were the same like those used in micelles preparation. Under the experimental conditions used, no interaction was detected between DIM and PEG since the ITC profiles of injecting DIM into PEG solution were not different from those of injecting DIM into the buffer (the blank) (Figure SI.2.1).

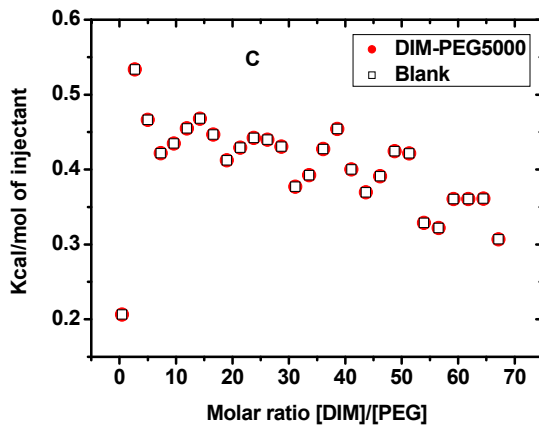
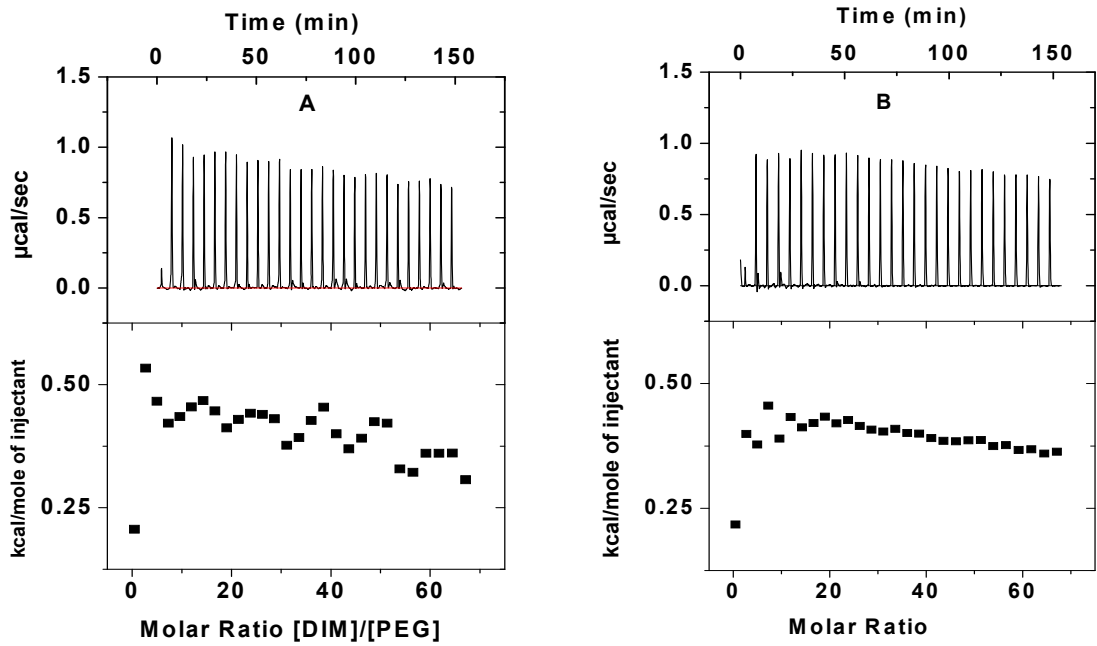


Figure SI.2.1. ITC profiles for titration of DIM into PEG solution in Tris-HCl buffer. A and B upper panel: raw power data, lower panel: integrated heats of interaction. A: titration of DIM into PEG, B: titration of DIM into the buffer, C: total energy exchanged as a function of the DIM/PEG molar ratio for titration of DIM into PEG and DIM into the buffer (blank).

CHAPTER THREE

RESEARCH PAPER

Minocycline Block Copolymer Micelles and Their Anti-Inflammatory Effects on Microglia²

**Ghareb Mohamed Soliman¹, Angela O. Choi², Dusica Maysinger²,
Françoise M. Winnik¹**

¹Faculty of Pharmacy and Department of Chemistry, Université de Montréal, CP 6128
Succursale Centre Ville, Montréal, QC, H3C 3J7, Canada.

²Department of Pharmacology and Therapeutics, McGill University, 3655 Promenade Sir-
William-Osler, Room 1314, McIntyre Medical Sciences Building, Montreal, QC, H3G
1Y6, Canada.

**Macromolecular Bioscience: In press, DOI: 10.1002/mabi.200900259
(Invited article)**

² My contribution included polymer synthesis, micelle preparation and characterization, interpreting the results and writing the paper, which was supervised by Dr. Françoise M. Winnik. Angela O. Choi contribution involved testing the polymers cytotoxicity and the anti-inflammatory properties of minocycline micelles, which was supervised by Dr. Dusica Maysinger.

3.1. Abstract

Minocycline hydrochloride (MH), a semisynthetic tetracycline antibiotic with promising neuroprotective properties, was encapsulated into polyion complex (PIC) micelles of carboxymethyldextran-*block*-PEG (CMD-PEG) as a potential new formulation of MH for the treatment of neuroinflammatory diseases. PIC micelles were prepared by mixing solutions of a Ca^{2+} /MH chelate and CMD-PEG copolymer in a Tris-HCl buffer. Light scattering and ^1H NMR studies confirmed that Ca^{2+} /MH/CMD-PEG core-corona micelles form at charge neutrality having a hydrodynamic radius ~ 100 nm and incorporating ~ 50 wt-% MH. MH entrapment in the micelles core sustained its release for up to 24 h under physiological conditions. The micelles protected the drug against degradation in aqueous solutions at room temperature and at 37 °C in the presence of fetal bovine serum. The micelles were stable in aqueous solution for up to one month, after freeze drying and in the presence of fetal bovine serum and bovine serum albumin. CMD-PEG copolymers did not induce cytotoxicity in human hepatocytes and murine microglia (N9) in concentrations as high as 15 mg/mL after incubation for 24 h. MH micelles were able to reduce the inflammation in murine microglia (N9) activated by lipopolysaccharides. These results strongly suggest that MH PIC micelles can be useful in the treatment of neuroinflammatory disorders.

3.2. Author Keywords

Dextran, drug delivery systems, calcium complexes, minocycline, neuroinflammation, polyion complex micelles.

3.3. Introduction

There is increasing evidence from studies in cell cultures, in animal models, and clinical trials that some antibiotics might have beneficial anti-inflammatory effects in the central nervous system.^[1, 2] For example, the tetracycline antibiotic minocycline exerts antioxidant and anti-inflammatory effects in hyperactivated microglia in animal models of

stroke, inhibiting their activation and proliferation.^[1, 3-5] Microglia comprise approximately 12% of cells in the brain and predominate in the gray matter.^[6] They typically exist in their surveyance state characterized by a ramified morphology and monitor the brain environment. Microglia are readily activated by a variety of stimuli, including pathogens producing pro-inflammatory cytokines and particulate matter (e.g. axonal debris). The microglial protective and destructive role depends on the degree of their activation and therefore agents which can modulate the activation process are clinically useful to shift the balance in favor of microglial protective state.^[7] Minocycline seems to be one such agent which has been explored as a monotherapy or in drug combinations. However, its poor stability and the numerous side effects related to the large doses required present serious limitations in terms of clinical applications.

Minocycline is routinely administered orally for the treatment of infectious and inflammatory diseases, such as acne vulgaris, rheumatoid arthritis, and some sexually transmitted diseases, in doses on the order of $3 \text{ mg kg}^{-1} \text{ day}^{-1}$.^[8] It was shown to induce neurorestoration in various animal models when applied intraperitoneally in doses of up to 200 mg kg^{-1} several times a day.^[9, 10]

Oral formulations for the treatment of bacterial infections contain minocycline hydrochloride (MH, Figure 3.1), which is an ionic compound very soluble in water.^[11, 12] MH is well absorbed when administered orally. However, due to its numerous side effects it is recommended to administer it intravenously (IV).^[10] It was noted, however, that after IV administration of MH, the levels of the drug in the brain were significantly lower than its concentration in the plasma, possibly as a consequence of the short MH lifetime in the bloodstream.^[10] MH is notoriously unstable in aqueous solution, especially in acidic or alkaline media where it undergoes epimerization at C₄.^[11, 13, 14] The resulting epi-MH is much less potent than MH and is prone to further degradation upon exposure to oxidants or to light.^[15]

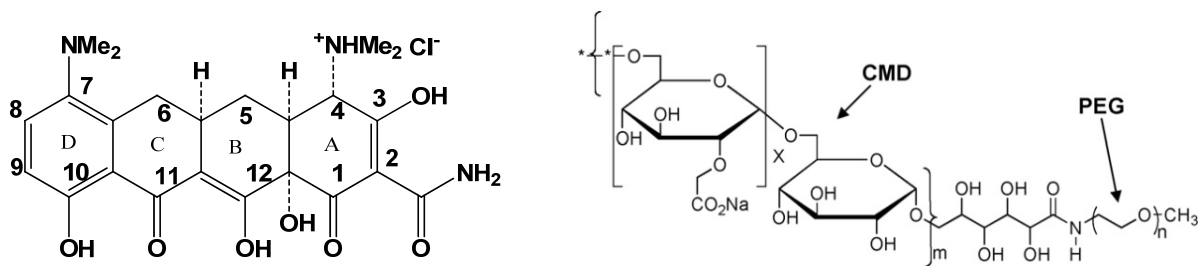


Figure 3.1. Chemical structures of minocycline hydrochloride (left panel) and CMD-PEG block copolymer (right panel).

The poor stability of MH in biological environment and serious side effects require new approaches for its administration in clinics. Thus, several research groups have developed and evaluated new means of MH delivery. For instance, Hu et al. have demonstrated that MH entrapped within PEGylated liposomes retained its activity and the effectiveness of IV injection of MH PEGylated liposomes every five days was comparable to that of daily intraperitoneal injection of MH alone.^[16] Core-shell nanoparticles with an inner core serving as nanocontainer for the drug and a shell providing both colloidal stability in aqueous media and stealth properties in the bloodstream were also assessed as delivery vehicles for MH. Thus, Liang et al. have prepared a micellar formulation of MH by entrapping it into octadecyl quaternized carboxymethyl chitosan nanoparticles.^[17] The MH-loaded nanoparticles were ~ 290 nm in size and contained up to 22 wt% MH. *In vitro* studies indicated that the drug could be released from the particles, but no further data on the effectiveness of the formulation were presented so far. Another promising approach consists in converting minocycline into alkanoyl-10-*O*-minocycline, a hydrophobic derivative of minocycline known to retain the antioxidant, anti-inflammatory, and antibiotic activities of minocycline. In aqueous media, alkanoyl-10-*O*-minocyclines self-assemble into nanoparticles expected to partition favorably in the blood-brain barrier and to possess enhanced stability, compared to minocycline.^[9] The encouraging results reported on the use of nanoparticles for the IV administration of MH prompted us to assess formulations of MH using polyion complex (PIC) micelles which also belong to the class of core-shell

nanoparticles.^[18-20] The solid core of PIC micelles contains an ionic drug neutralized by the ionic segment of an oppositely-charged hydrophilic diblock copolymer.^[19, 21] The shell of PIC micelles is formed by the second segment of the diblock copolymer, usually a PEG chain selected in view of its hydrophilic, non toxic properties and its outstanding stealth characteristics *in vivo*.^[22, 23] PIC micelles have found clinical applications in cancer chemotherapy and in gene delivery.^[24-26] The usefulness of PIC micelles in drug delivery derives from their small size (~ 100 nm), high drug loading, ease of fabrication and handling, thermodynamic stability, and design flexibility. Since MH is an amphoteric molecule with an isoelectric point of 6.4, it does not interact strongly with polyelectrolytes under physiological conditions.^[11] Consequently, MH is not suitable, per se, for incorporation into PIC micelles. It is important to recall here that, like all tetracycline antibiotics, MH is a metal-binding antibacterial agent, known to form complexes with divalent or trivalent cations by chelation of the C₁₁-C₁₂-C₁ carbonyl functionalities.^[27-29] Previous studies have shown that, in combination with the plasma protein-bound fraction of MH, the calcium -bound fraction represents more than 99% of MH concentration in the plasma.^[30] Depending on the metal salt to drug relative concentrations, MH can form 1:1 or 2:1 metal ion: drug chelates with calcium or magnesium ions. The 1:1 chelated form of MH is neutral under physiological conditions (pH 7.4), whereas the 2:1 metal ion: MH chelate is cationic, since the pK_as of MH are 5 and 9.5 for the C₇ and C₄ amino groups, respectively.^[31] This cationic form of MH should be able to undergo electrostatic interactions with polyanions and form PIC micelles with an appropriate hydrophilic anionic diblock copolymer. To test this hypothesis, we selected carboxymethyl-dextran-*block*-poly(ethylene glycol) (CMD-PEG, Figure 3.1), a diblock copolymer that consists of a neutral polyethylene glycol block linked to an anionic carboxymethyl-dextran block in which approximately 85 % of the glucose units bear carboxylate groups.^[32] This copolymer is known to be non-toxic and to form PIC micelles, 30-50 nm in radius, with cationic water soluble drugs, such as diminazene diaceturate, presenting high drug loading, sustained drug release and excellent stability.^[33] The Ca²⁺/MH/CMD-PEG micelles are not intended for oral administration since calcium is known to reduce the absorption of MH by 27%.^[34]

The objectives of the studies reported here were to prepare CMD-PEG based PIC micelles loaded with the 2:1 Ca^{2+} /MH chelate and to assess their anti-inflammatory activity in activated microglia cells. ^1H NMR spectroscopy was used to detect the formation of core-shell micelles in mixed solutions of CMD-PEG and 2:1 Ca^{2+} /MH. The size of the micelles and their stability under various conditions were assessed by dynamic light scattering (DLS) measurements. Since MH in aqueous media is prone to rapid degradation, we assessed the stability upon storage in ambient conditions and at 37 °C of MH entrapped into PIC micelles. The viability of human hepatocytes and murine microglia (N9) treated with CMD-PEG was assessed using several biochemical assays. The release of the drug from the micelles was determined and nitric oxide release was tested in the presence and absence of ternary Ca^{2+} /MH/CMD-PEG micelles in N9 microglia cells activated by lipopolysaccharides. The results of this study give strong indications that ternary Ca^{2+} /MH/CMD-PEG micellar formulations can act as effective delivery systems for MH to attenuate the excessive microglia activation commonly observed in several neurodegenerative disorders.

3.4. Experimental part

3.4.1. Materials

Water was deionized using a Millipore MilliQ system. Minocycline hydrochloride, trizma®hydrochloride, amberlite® IR-120, lipopolysaccharides, bovine serum albumin (BSA), and 3-(4,5-dimethylthiazol-2-yl)-2,5-diphenyl tetrazolium bromide (MTT) were purchased from Sigma Aldrich, St. Louis, MO. Dialysis membranes (Spectra/por, MWCO: 6-8 KDa, unless otherwise indicated) were purchased from Fisher Scientific (Rancho Dominguez, CA). The block copolymer CMD-PEG (Figure 3.1) was synthesized starting with dextran (Mn 6,000 g/mol) and α -amino- ω -methoxy-poly(ethylene glycol) (Mn 5,000 g/mol), as described previously.^[32] The degree of carboxymethylation of the dextran block, defined as the number of glucopyranose units having carboxymethyl groups per 100 glucopyranose units, was 85 %. The average number of glucopyranosyl and of $-\text{CH}_2-\text{CH}_2-$

O- repeat units of the CMD and PEG segments, were 40 and 140, respectively. Penicillin, streptomycin and Griess Reagent (1% sulphanilamide, 0.1% N-(1-naphthyl)-ethylenediamine dihydrochloride, 5% phosphoric acid) and fetal bovine serum were purchased from Invitrogen (Carlsbad, CA). Human hepatocytes and murine microglia (N9) cell lines were from ATCC. An alamar blue (7-hydroxy-3H-phenoxazin-3-one-10-oxide sodium salt) stock solution was purchased from Trek Diagnostic Systems, (Cleveland, Ohio).

3.4.2. Preparation of MH-loaded CMD-PEG micelles

Stock solutions of CaCl_2 (1.27 mg/mL, 8.63 mM), MH (2.33 mg/mL, 4.71 mM) and CMD-PEG (0.5 mg/mL, 1.74 mM -COONa) were prepared in Tris-HCl buffer (10 mM, pH 7.4). The solution pH was adjusted to 7.4 using 0.1 M NaOH if necessary. Specified volumes of the CaCl_2 solution were added to the MH solution to attain a Ca^{2+} /ligand molar ratio of 2/1. The CaCl_2 /MH solution was magnetically stirred for 10 min and added over a 10-min period to a magnetically stirred CMD-PEG solution, in amounts such that the $[+]/[-]$ ratio ranged from 0.5 to 2.0, where $[+]/[-]$ is the ratio of the molar concentrations of positive charges provided by the Ca^{2+} /drug complex to the negative charges provided by the polymer. In solutions of pH 7.4, the Ca^{2+} /MH complex has one positively charged group (C_4 dimethylammonium, Figure 3.1) while all the carboxylate groups of CMD-PEG are negatively charged (weak polyacid of $\text{pK}_a \sim 4.5$). The CMD-PEG concentration was 0.2 mg/mL in all samples. Samples were stirred overnight before measurements.

3.4.3. Characterization

^1H NMR spectra were recorded on a Bruker AV-400 MHz spectrometer operating at 400 MHz. Chemical shifts are given relative to external tetramethylsilane (TMS = 0 ppm). Samples for analysis were prepared by adding aliquots of a CaCl_2 solution (20.4 mg/mL, D_2O , pH 7.4) to a MH solution in D_2O (9.3 mg/mL, pH 7.4) such that the Ca^{2+} /drug molar ratio was 2:1. The resulting solutions were stirred for 10 min. They were added to a stirred solution of CMD-PEG in D_2O (pH 7.4,) in amounts such that the $[+]/[-]$ ratio ranged from

0.25:1 to 1.5:1. The final polymer concentration was 2.0 mg/mL in all the samples. Control solutions of MH, Ca²⁺/MH, and MH/CMD-PEG in D₂O were prepared keeping the same concentrations as the metal Ca²⁺/MH/CMD-PEG solutions. All samples were stirred for 1.0 h before measurements.

Dynamic light scattering (DLS) measurements were performed on a CGS-3 goniometer (ALV GmbH) equipped with an ALV/LSE-5003 multiple- τ digital correlator (ALV GmbH), a He-Ne laser ($\lambda = 632.8$ nm), and a C25P circulating water bath (Thermo Haake). The scattered light was measured at a scattering angle of 90°. A cumulant analysis was applied to obtain the diffusion coefficient (D) of the micelles in solution. The hydrodynamic radius (R_H) of the micelles was obtained using the Stokes-Einstein equation. The constrained regularized CONTIN method was used to obtain the particle size distribution. Samples were filtered through a 0.45 μ m Millex Millipore PVDF membrane prior to measurements. The data presented are the mean of six measurements \pm S.D.

HPLC analysis of MH was performed on an Agilent Technologies HP 1100 chromatography system equipped with a quaternary pump, a UV-visible diode array detector, a column thermostat and a HP Vectra computer equipped with the HP-Chemstation software. The assay was carried out at 25 °C using a 250 x 4.6 mm column filled with 5 μ m-reversed phase C₁₈ Hypersil® BDS (Thermo, Bellefonte, PA) eluted at a flow rate of 1.5 mL/min with a phosphate buffer (25 mM, pH 3.0)-methanol-acetonitrile, 85:10:5 v/v/v mixture.^[12] The injection volume was 40 μ L and the run time was 30 min. MH, monitored by its absorbance at 255 nm, had a retention time \sim 16 min. A calibration curve ($r^2 \geq 0.999$) of MH was prepared using standard solutions ranging in concentration from 20 to 80 μ g/mL prepared immediately prior to the assay.

3.4.4. Stability studies

To test the stability of MH-micelles in serum, Ca²⁺/MH/CMD-PEG micelles (CMD-PEG: 0.2 mg/mL, [+]/[-] = 1.0, [Ca²⁺]/[MH] = 2:1) in Tris-HCl buffer (10 mM, pH 7.4) were prepared as described above. One set of solutions was supplemented with BSA (0, 5, 10, 20, 30 and 40 mg/mL). Another set of samples was supplemented by 5 % fetal bovine

serum (FBS). Samples without serum were kept at room temperature for up to 30 days. Serum and BSA-containing solutions were incubated at 37 °C for 24 h. Samples were analyzed by DLS at various time intervals to determine the R_H and polydispersity index of the micelles.

The chemical stability upon storage of MH was tested using micelles (CMD-PEG: 0.1 mg/mL, $[Ca^{2+}]/[MH] = 2$, $[+]/[-] = 1.0$) prepared, as described above, with stock solutions of MH (1 mg/mL), CMD-PEG (0.53 mg/mL), $CaCl_2$ (0.54 mg/mL), in 10 mM Tris-HCl buffer, pH 7.4. The samples were kept at room temperature or at 37 ± 0.5 °C without protection against light. Samples containing 5 % fetal bovine serum were prepared as well and kept at 37 °C. At different time intervals, aliquots of the solutions were analyzed by HPLC. The data presented are the mean of three measurements \pm S.D.

To assess the micelle integrity upon freeze-drying, $Ca^{2+}/MH/CMD-PEG$ micellar solutions (3 mL, polymer concentration: 0.1 mg/mL; $[+]/[-] = 1.0$, $[Ca^{2+}]/[MH] = 2$) in a Tris-HCl buffer (10 mM, pH 7.4) were frozen in a dry ice/acetone bath. They were lyophilized for 48 h. The resulting powder was rehydrated with deionized water (3 mL) to reach a polymer concentration of 0.1 mg/mL. The resulting micellar solution was magnetically stirred for 10 min and the R_H and polydispersity index of an aliquot were determined by DLS.

3.4.5. Drug release studies

Identical measurements were performed with solutions (3.0 mL) in Tris-HCl buffer (10 mM, pH 7.4, $[NaCl] = 0$ or 150 mM) of MH, $CaCl_2/MH$, and $Ca^{2+}/MH/CMD-PEG$ micelles obtained as described above with a 2:1 $Ca^{2+}/drug$ ratio, a 1:1 $[+]/[-]$ ratio and $[MH] = 0.75$ mg/mL. The solutions were introduced in a dialysis tube (MWCO = 6-8 kDa). They were dialyzed against 150 mL of the same buffer at 37 °C. At predetermined time intervals, 3 mL aliquots were taken from the release medium and replaced by 3 mL of fresh buffer. The concentration of the drug was determined from the absorbance at 246 nm of the release medium samples and using a calibration curve. The cumulative percent of drug released was plotted as a function of dialysis time.

3.4.6. Cell survival and nitrite release determinations

Human hepatocytes were cultured in Human Hepatocyte Cell Culture Complete Media. Murine microglia (N9) cells were cultured in IMDM media containing 5% fetal bovine serum and 1% penicillin-streptomycin. Cells were maintained at 37°C (5% CO₂) in a humidified atmosphere. For the Alamar blue assay, human hepatocytes and N9 cells were seeded in black, clear bottom 96-well plates (Corning) at a density of 5x10⁴ cells/cm² and 1x10⁴ cells/cm², respectively. For the MTT assay and nitrite measurement, hepatocytes and N9 cells were seeded in 24-well plates (Sarstedt, Montreal, QC, Canada) at a density of 5x10⁴ cells/cm² and 2x10⁵ cells/cm², respectively.

Cells were given fresh media (IMDM, 5% FBS, 1% penicillin-streptomycin for N9 cells; Human Hepatocyte Complete Media for hepatocytes) 24 h after seeding. They were treated with free MH (50 µg/ml), the Ca²⁺/MH complex (dose equivalent to 50 µg/ml MH), Ca²⁺/MH/CMD-PEG micelles (dose equivalent to 50 µg/ml MH), or CMD-PEG (0.1 – 15 mg/ml) with or without concomitant addition of lipopolysaccharides (LPS; 10 µg/ml) for 24 hours (37°C, 5% CO₂, humidified atmosphere).

The alamar blue stock solution was diluted with fresh cell culture media to 10% v/v ratio. After cell treatment, media from each well were aspirated and 250 µL of the Alamar blue-media mixture were added to each well and incubated with the cells for 1 h at 37°C (5% CO₂, humidified atmosphere). The intensity of fluorescence at 590 nm of the reduced resazurin (excitation wavelength: 544 nm) was measured from the well bottom using a spectrofluorometer (FLUOstar OPTIMA). The percent viability was expressed as the fluorescence counts from treated samples over the untreated control. The colorimetric MTT assay was performed to assess the viability of N9 cells. One hour before the end of the treatment, MTT (12 µM, dissolved in sterile PBS) was added to the cells. Following a 1-h incubation at 37°C, media were removed, cells were lysed, and formazan was dissolved with dimethyl sulfoxide. The absorbance of the recovered formazan was measured at 595 nm using a Benchmark microplate reader (Bio-Rad, Mississauga, ON, Canada). All measurements were done in triplicates in three or more independent experiments. Nitrite

(NO₂⁻) release from N9 cells was measured using the Griess Reagent (1% sulphanilamide, 0.1% N-(1-naphthyl)-ethylenediamine dihydrochloride, 5% phosphoric acid). After treatment, 50 μL of the supernatant from each well were mixed with 50 μL of Griess reagent in a clear bottom 96-well plate, and incubated at room temperature for 15 min. Absorbance at 548 nm of each sample was measured in triplicates using the microplate reader.

3.5. Results and Discussion

3.5.1. Preparation, characterization, and stability of ternary Ca²⁺/MH/CMD-PEG nanoparticles

At the onset of the study, it was important to confirm that the 2:1 Ca²⁺/MH chelates interact electrostatically with the carboxylate groups of CMD-PEG to form core-shell nanoparticles and that competing electrostatic interactions between Ca²⁺ and the polymer carboxylates do not disrupt the Ca²⁺/drug chelation. ¹H NMR spectroscopy, DLS, and isothermal titration calorimetry (ITC) measurements were performed to address these issues. The ¹H NMR assay employed takes advantage of the fact that signals due to the resonance of low mobility protons broaden, and often cannot be detected at all, under conditions used to measure ¹H NMR spectra of soluble polymers.^[35] Thus, entrapment of the drug within the core of a micelle can be monitored readily by changes in the intensity and shape of ¹H NMR signals, as exemplified in Figure 3.2 which presents ¹H NMR spectra of solutions in D₂O (pH 7.4) of MH, with spectral assignments taken from literature data^[36], of the 2:1 Ca²⁺/MH chelate, of CMD-PEG, and of a mixture of CMD-PEG and the 2:1 Ca²⁺/MH chelate. The composition of this mixture was such that the molar ratio, [+]/[-], of positive charges provided by the 2:1 Ca²⁺/MH chelate to the negative charges provided by the diblock copolymer is equal to 1 (charge neutralization). Turning our attention first to the ¹H NMR spectrum of the chelate (Figure 3.2B), we note that upon binding of MH to Ca²⁺ the quartet due to the aromatic protons H₈ and H₉ decreases in intensity and new signals appear further downfield. The signal at 3.69 ppm due to H₄ is also affected

significantly. These spectral shifts reflect conformational changes of MH upon chelation of C₁₁-C₁₂-C₁ carbonyl functionalities by the cations.^[27] The ¹H NMR spectrum of CMD-PEG (Figure 3.2C) presents signals at δ 4.08-4.15, 4.89, and 5.07 ppm, ascribed to protons of the CMD block, and a broad strong singlet centered at δ 3.61 ppm due to the PEG methylene protons (-CH₂-CH₂-O-).^[33] The ¹H NMR spectrum of a mixed solution of the diblock copolymer and the drug chelate in amounts corresponding to charge neutralization (Figure 3.2D) is remarkably featureless: signals in the aromatic region due to the protons of chelated MH are undetectable. In the high field spectral range, one can observe a weak and broad signal ($\delta \sim 2.7 - 3.0$ ppm) that can be ascribed to MH protons with restricted motion and (ii) a strong singlet at δ 3.61 ppm due to the PEG methylene protons. Signals due to the protons of the CMD block are undetectable. The preservation of the PEG signals, together with the disappearance of signals due to the drug chelate and to the CMD block, are diagnostic in indentifying the formation of nanoparticles with a CMD/drug chelate rigid core and a shell made up of flexible hydrated PEG chains. Figure 3.2E presents the ¹H NMR spectrum of a mixture of MH and CMD-PEG of drug and polymer concentrations identical to those of the ternary Ca²⁺/MH/CMD-PEG system analyzed in Figure 3.2D. The signals of the drug and of the polymer are sharp and well resolved, confirming that, at pH 7.4, the drug does not interact with the polymer in the absence of Ca²⁺ ions.

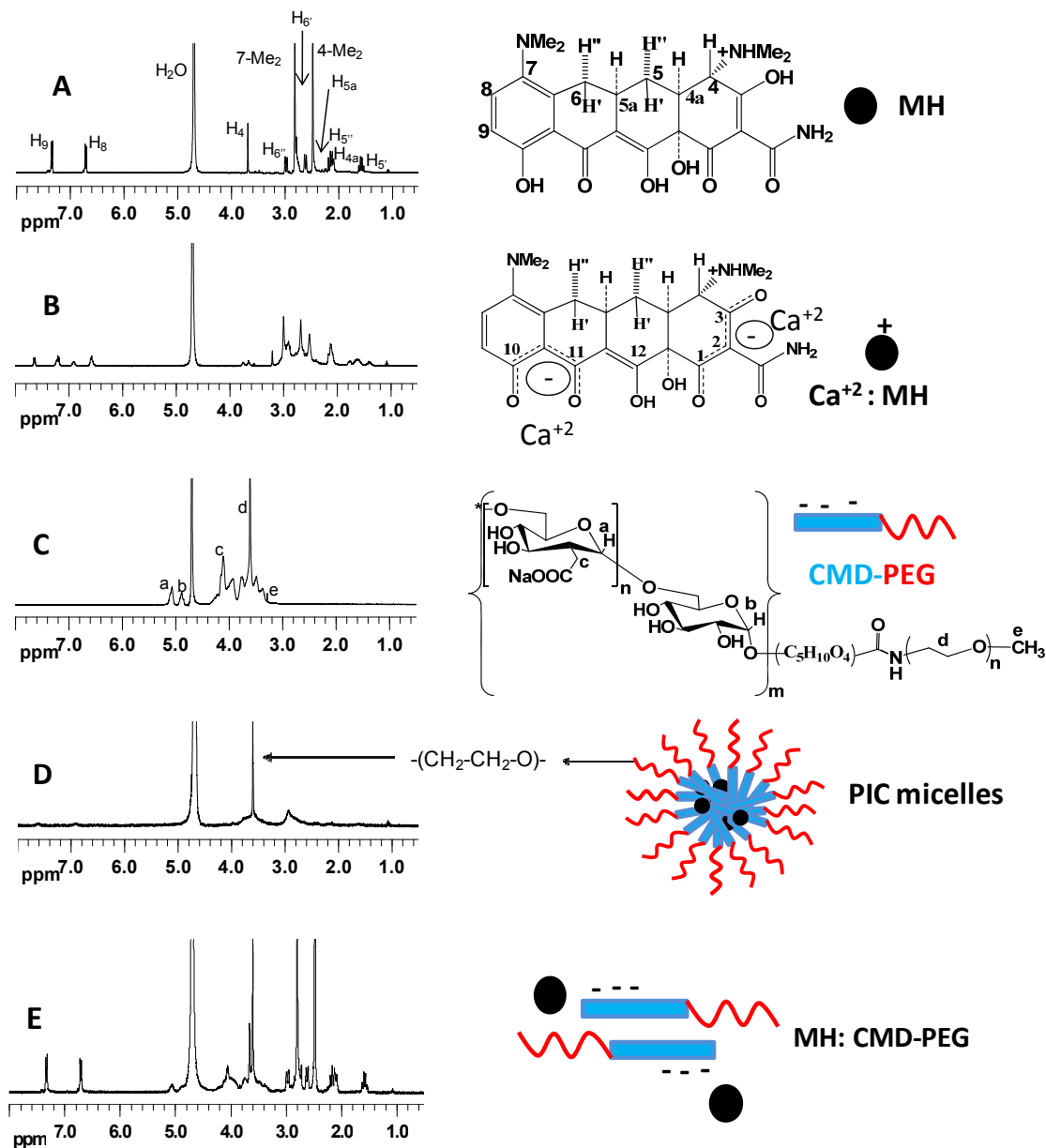


Figure 3.2. ^1H NMR spectra of MH (A), Ca^{2+}/MH , ($[\text{Ca}^{2+}]/[\text{MH}] = 2.0$) (B), CMD-PEG (C), $\text{Ca}^{2+}/\text{MH}/\text{CMD-PEG}$ (CMD-PEG concentration = 2.0 mg/mL, $[\text{+}]/[\text{-}] = 1.0$, $[\text{Ca}^{2+}]/[\text{MH}] = 2.0$) (D) and $\text{MH}/\text{CMD-PEG}$ ($[\text{+}]/[\text{-}] = 1.0$) (E) in D_2O , room temperature, pH 7.4 and representative illustrations of the species examined.

^1H NMR spectra of $\text{Ca}^{2+}/\text{MH}/\text{CMD-PEG}$ mixtures of $[+]/[-] > 1.0$ (i.e., $[+]/[-] = 1.25$ and 1.5) were recorded as well (Figure SI.3.1, supporting information). They present signals characteristic of the metal ion/MH complex in addition to signals due to the micelles, confirming that maximum drug loading is achieved at charge neutrality (i.e., $[+]/[-] = 1.0$). The actual drug loading of the micelles at charge neutrality is identical to the theoretical drug loading, or ~ 50 wt-% of the micelles, since no signals of the free drug were detectable in the ^1H NMR spectrum of the micelles at charge neutrality (Figure 3.2D). This drug loading capacity is significantly higher than the capacity of other nanoparticulate carriers, such as liposomes^[37] and poly(lactide-co glycolide) (PLGA) nanoparticles^[38], which usually have low encapsulation efficiencies for water soluble ionic drugs. High loading of drug delivery systems is highly desirable from the toxicological point of view, as it enhances the drug/excipients ratio and avoids overloading the body with unwanted chemicals.

To confirm the formation of nanoparticles upon mixing the 2:1 Ca^{2+}/MH chelate and CMD-PEG, we analyzed by DLS a series of solutions in which the polymer concentration was kept constant (0.2 mg/mL) while the 2:1 Ca^{2+}/MH chelate concentration was increased such that the charge ratio in the mixture covered the $0 < [+]/[-] \leq 2$ range. Mixed solutions of $[+]/[-] < 0.5$ did not scatter light. In mixed solutions with a $[+]/[-]$ ratio of 0.5, micellar objects were detected. They had a hydrodynamic radius (R_H) of ~ 100 nm and a polydispersity index (PDI) of ~ 0.2 (Figure 3.3A). In solutions of this composition, only part of the copolymer carboxylate groups is neutralized by the Ca^{2+}/MH chelate. The repulsion between residual carboxylates prevents the formation of tight micelles. The R_H value of the micelles decreases to ~ 80 nm as the $[+]/[-]$ ratio reaches 0.75, a consequence of the progressive neutralization of the carboxylate groups by added Ca^{2+}/MH chelate. For $[+]/[-] > 0.75$, the micelle size gradually increases, indicating that additional metal ion/drug complex is incorporated within the micelle core. The micelle R_H reaches ~ 105 nm in solutions of $[+]/[-] = 1.0$. For this composition, which will be used in further studies, the amount of MH incorporated in the micelles accounts for ~ 50 wt-% of the total micelles

weight. The polydispersity index (PDI) of the micelle population was ~ 0.1 for $[+]/[-] > 0.75$, indicating the formation of monodispersed nanoparticles.

The Ca^{2+} /MH/CMD-PEG micelles ($[+]/[-] = 1.0$, $\text{pH} = 7.4$) exhibited remarkable stability upon storage at room temperature for periods of 1 month, or longer. Their size and polydispersity index remained constant and no aggregation was detected. Moreover, micellar solutions of Ca^{2+} /MH/CMD-PEG were readily reconstituted after freeze drying by simple solubilization in water of the lyophilized powder, even in the absence of cryoprotectants. Upon re-dissolution, the micelles recovered their size ($R_H \sim 100$ nm) and colloidal stability. The micelles stability upon freeze drying and reconstitution is an important criterion for a pharmaceutically viable formulation, since the shelf life of a drug formulation in the powder form tends to be much longer than in solution. Also powders are easier to handle, store and transfer.

Control experiments were carried out to confirm that addition of Ca^{2+} to a solution of either CMD-PEG or MH does not trigger the formation of nanoparticles. The intensity of light scattered at an angle of 90° was determined as a function of added Ca^{2+} for solutions of increasing $[\text{Ca}^{2+}]$ in the ternary Ca^{2+} /MH/CMD-PEG system and in the binary systems Ca^{2+} /CMD-PEG and Ca^{2+} /MH (Figure 3.3B). For the ternary system, the scattered light intensity underwent a sharp increase for $[\text{Ca}^{2+}] > 0.15$ mg/mL ($[+]/[-] = 0.75$), an indication of the presence of micelles which, given their size, scatter light extensively. The intensity of scattered light for mixtures of either Ca^{2+} /CMD-PEG or Ca^{2+} /MH mixtures was weak, independently of $[\text{Ca}^{2+}]$. These results, together with the ^1H NMR results, confirm that PIC micelles incorporating MH only form in the presence of both the polymer and Ca^{2+} . The association constants of Ca^{2+} /MH and Ca^{2+} /CMD-PEG, $8.9 \pm 0.7 \times 10^4 \text{ M}^{-1}$ and $1.17 \pm 0.03 \times 10^4 \text{ M}^{-1}$, respectively, determined by isothermal titration calorimetry (ITC), indicate that the affinity of Ca^{2+} ions for MH is ~ 8 times higher than that for CMD-PEG (Supporting information). Therefore, in tertiary mixtures of Ca^{2+} /MH/CMD-PEG, Ca^{2+} ions preferentially bind to MH.

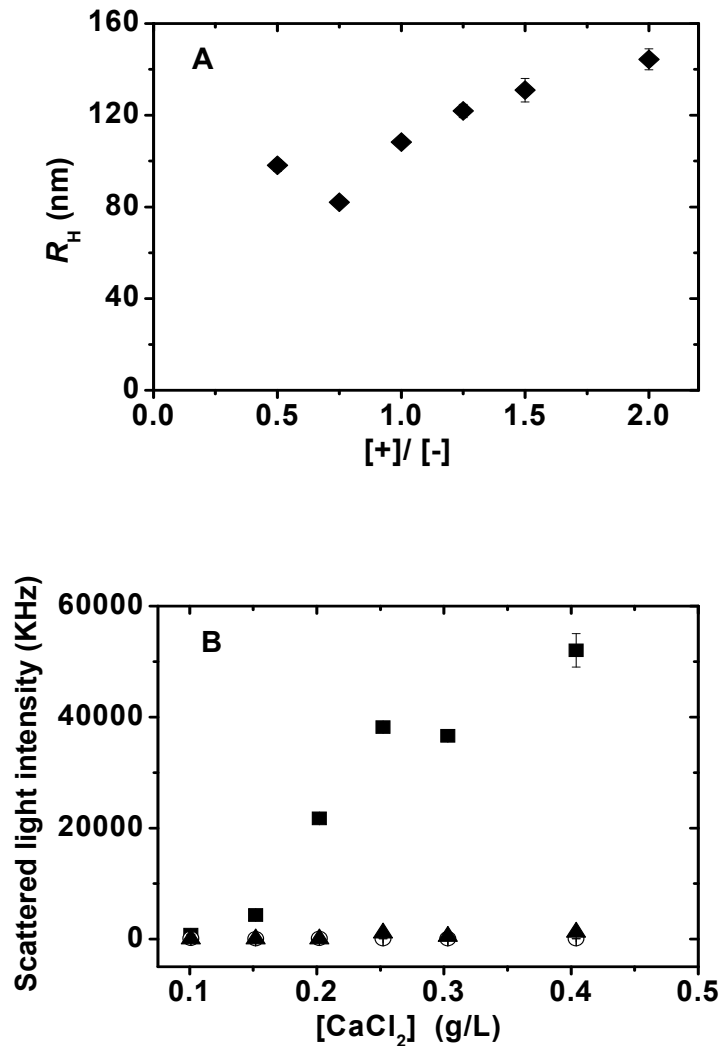


Figure 3.3. A: Hydrodynamic radius (R_H , \blacklozenge) of $Ca^{2+}/MH/CMD-PEG$ micelles as a function of the $[+]/[-]$ ratio; solvent: Tris-HCl buffer (10 mM, pH 7.4; CMD-PEG concentration: 0.2 mg/mL, $[Ca^{2+}]/[MH] = 2$).

B: Scattered light intensity as a function of calcium chloride concentration from solutions of $Ca^{2+}/MH/CMD-PEG$ micelles (\blacksquare), Ca^{2+}/MH (\blacktriangle) and $Ca^{2+}/CMD-PEG$ (\circ); solvent: Tris-HCl buffer (10 mM, pH 7.4), CMD-PEG concentration: 0.2 mg/mL.

3.5.2. Stability and release of MH entrapped in Ca^{2+} /MH/CMD-PEG nanoparticles ([+]/[-] = 1.0, pH 7.4)

Minocycline hydrochloride is known to degrade rapidly in aqueous solutions exposed to ambient light and temperature. A number of studies have shown that chelation of MH with Ca^{2+} significantly enhances the stability of the drug in solution.^[12, 29] It was important to confirm that the stabilizing effect of Ca^{2+} was preserved upon binding of the chelate to CMD-PEG and subsequent micellization. We set about to determine the changes, as a function of storage time, of the MH concentration in solutions of ternary Ca^{2+} /MH/CMD-PEG micelles ([+]/[-] = 1.0, pH = 7.4) and to compare it to [MH] in solutions of the drug alone, MH/CMD-PEG mixtures and the 2:1 Ca^{2+} /MH chelate stored under the same conditions. We used a standard HPLC assay for the quantitative analysis of MH.^[12] Representative chromatograms for samples stored at room temperature are depicted in Figure 3.4. From the chromatograms of the solution of MH alone recorded after various storage periods (Figures 3.4A), one can conclude that after ~ 2 weeks, nearly all the drug has degraded into several faster eluting derivatives, as reported previously.^[12] The same behavior was observed for the MH/CMD-PEG mixture (Figure 3.4B), confirming the NMR and DLS results that the polymer does not interact with MH in the absence of metal ions.

Chromatograms recorded for the Ca^{2+} /MH chelate solution (Figures 3.4C) display a band corresponding to MH, as the main component, even after 3 weeks of storage. Chromatograms of solutions stored for 2 weeks or more present in addition a weak slower eluting band, attributed to the MH C₄ epimer based on previous studies.^[12, 39] Chromatograms corresponding to solutions of Ca^{2+} /MH/CMD-PEG micelles ([+]/[-] = 1.0) are presented in Figure 3.4D. Their features are similar to those of the chromatograms recorded for the Ca^{2+} /MH chelate solutions, confirming that the enhanced stability provided to the drug by Ca^{2+} is not affected upon incorporation of the chelate in polymer micelles. We note that the intensity of the band ascribed to the elution of the MH C₄ epimer is slightly weaker in the chromatograms recorded for micellar solutions, compared to solutions of the Ca^{2+} /MH chelate. This observation gives some indication that the MH

epimerization at C₄ is somewhat slower when the Ca/MH chelate is entrapped within micelles, possibly as a consequence of CMD-PEG/MH chelate electrostatic interactions that may take place within the micellar core. The concentrations of MH in solutions of MH alone, of Ca²⁺ chelated MH, and the micellar formulation are listed in Table 3.1 for various times during a 3-month period of storage at room temperature.

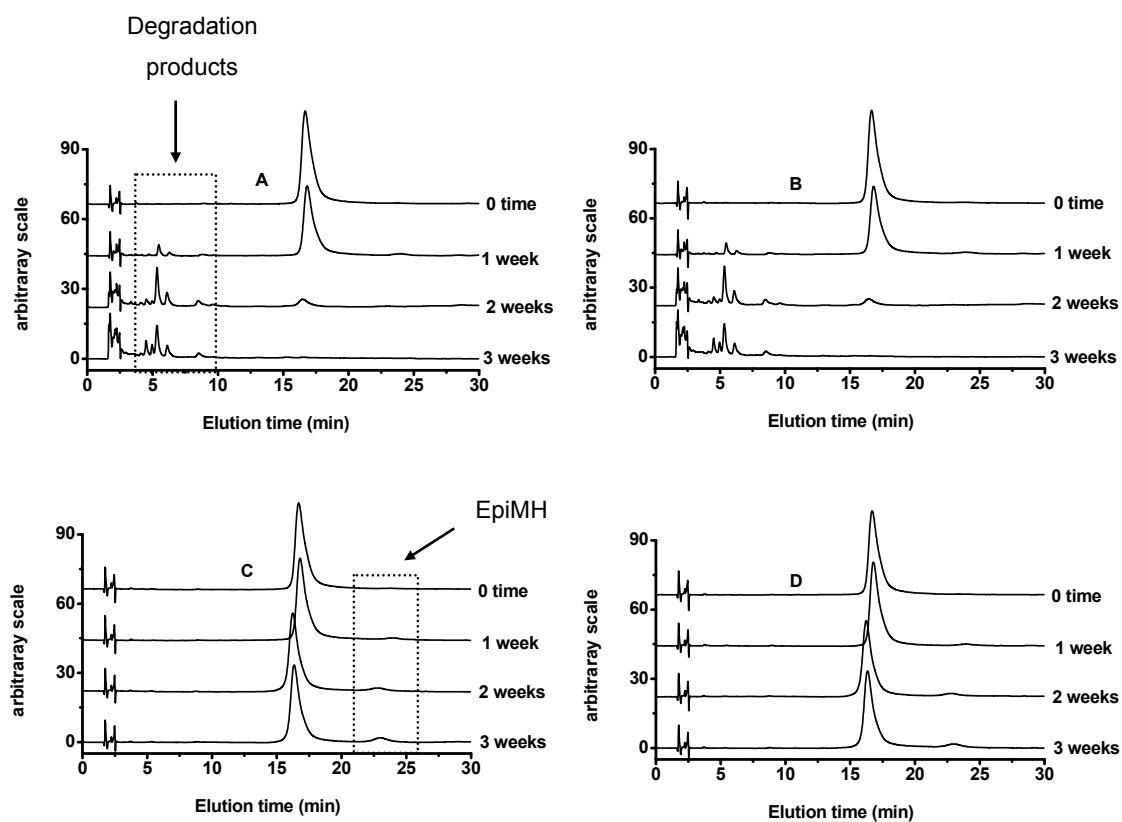


Figure 3.4. Chromatograms recorded upon storage at room temperature for up to 3 weeks of MH in Tris-HCl buffer (10 mM, pH 7.4) (A), MH/CMD-PEG (B), Ca²⁺/MH ([Ca²⁺]/[MH] = 2.0) (C), Ca²⁺/MH/CMD-PEG ([+]/ [-] = 1.0, [Ca²⁺]/[MH] = 2.0) (D), [CMD-PEG] = 0.1 mg/mL. For elution conditions: see experimental section.

Table 3.1. Residual amount of MH upon storage at room temperature of various formulations of the drug in Tris-HCl buffer of pH 7.4.^a

Time (days)	MH ^b	MH/CMD-PEG ^c	Ca ²⁺ /MH ^d	Ca ²⁺ /MH/CMD-PEG ^{d,e}
0	99.7 ± 1.9	100.5 ± 0.6	102 ± 0.5	98.4 ± 1.2
1	99.3 ± 1.4	101.1 ± 0.2	98 ± 1.2	98.9 ± 1.3
7	73.6 ± 0.4	72.6 ± 0.6	92.5 ± 0.6	98.3 ± 0.8
14	7.8 ± 0.6	7.6 ± 0.5	90.6 ± 1.4	96.3 ± 0.7
21			84.2 ± 0.9	90.9 ± 1.2
28			80.9 ± 1.1	86.3 ± 1.3
35			75.1 ± 0.9	81.5 ± 0.9
42			72.0 ± 0.1	77.3 ± 1.8
56			64.6 ± 1.4	73.4 ± 2.3
96			48.4 ± 3.0	68.2 ± 0.6

^a: amounts are expressed in percent of the initial MH concentration.

^b: solution of MH (0.3 mg/ mL).

^c: concentrations of MH and CMD-PEG are the same as those in Ca²⁺/MH/CMD-PEG micelles.

^d: [Ca²⁺]/[MH] = 2.0.

^e: [+]/[-] = 1.0.

The drug stability at 37 °C was lower than at room temperature. Nonetheless, the CMD-PEG copolymer still acts as a protective environment for the metal ion/drug complex. The concentrations of MH in solutions of MH alone, of Ca²⁺ chelated MH, and the micellar formulation are listed in Table 3.2 for various times of storage at 37 °C. Next, in an attempt to simulate the environment of the drug upon injection *in vivo*, we assessed the stability of MH in formulations incubated at 37°C in the presence of serum proteins. Addition of serum greatly enhances the stability of uncomplexed MH. Similar effects were reported previously in the case of drugs, such as curcumin and attributed to the formation of

protein/drug complexes.^[40] MH is known for its affinity to interact with serum proteins.^[41] The micellar constructs maintained their protective effects even in the presence of serum proteins: after a 7-day incubation at 37 °C with serum, ~ 75 % of the drug was intact when complexed within Ca²⁺/MH/CMD-PEG micelles, whereas only ~ 30 % of the drug was still present in a sample of free drug treated in the same conditions (Table 3.2).

Table 3.2. Residual amount of MH upon storage at 37 °C of various formulations of the drug in Tris-HCl buffer of pH 7.4 and in the same buffer containing 5% fetal bovine serum.^a

Time (days)	MH ^b		Ca ²⁺ /MH ^c		Ca ²⁺ /MH/CMD-PEG ^{c,d}	
	No serum	5% serum	No serum	5% serum	No serum	5% serum
0	102.3±1.3	97.1±1.3	98.9±1.6	98.3±1.4	98.1±1.3	96.6±0.5
1	96.8±0.7	95.0±0.7	92.9±0.9	92.6±1.5	90.5±0.8	89.5±1.7
7	3.5±0.0	31.5±0.8	64.9±2.4	76.4±0.6	66.6±1.0	74.0±2.9
16	-	20.6±0.0	59.0±3.7	65.5±1.7	67.9±5.7	69.7±2.4
22	-		56.6±1.6	60.7±0.5	66.6±0.5	66.6±0.3
29	-		47.6±1.0	61.5±0.7	60.4±0.7	63.3±0.6

^a: amounts are expressed in percent of the initial MH concentration.

^b: solution of MH (0.3 mg/ mL).

^c: [Ca²⁺]/[MH] = 2.0.

^d: [+]/[-] = 1.0.

We conducted also *in vitro* drug release studies in order to assess the suitability of the micelles to act as drug delivery systems. The release of MH from Ca²⁺/MH/CMD-PEG micelles was evaluated by the dialysis bag method, coupled with quantitative analysis of the drug using its UV absorbance at 246 nm (Figure 3.5).^[42] The micelles released ~ 50%

and 75 % drug after 8 h and 24 h, respectively. The drug release from the micelles was slightly faster under physiological salt concentrations (150 mM NaCl), which may be attributed to the weakening of the electrostatic interactions between Ca^{2+}/MH and CMD-PEG upon addition of salt.^[19, 33] Control experiments carried out with a solution of the Ca^{2+}/MH chelate revealed that drug release from this solution was significantly faster than from a $\text{Ca}^{2+}/\text{MH}/\text{CMD-PEG}$ micellar solution (Figure 3.5). After 8 h, ~ 88 % of the drug was released in the case of Ca^{2+}/MH solution, whereas for micellar solutions only 50 % drug was released after the same time. The sustained MH release from the micelles is expected to reduce the frequency of its administration, which results in fewer side effects and better patient compliance.

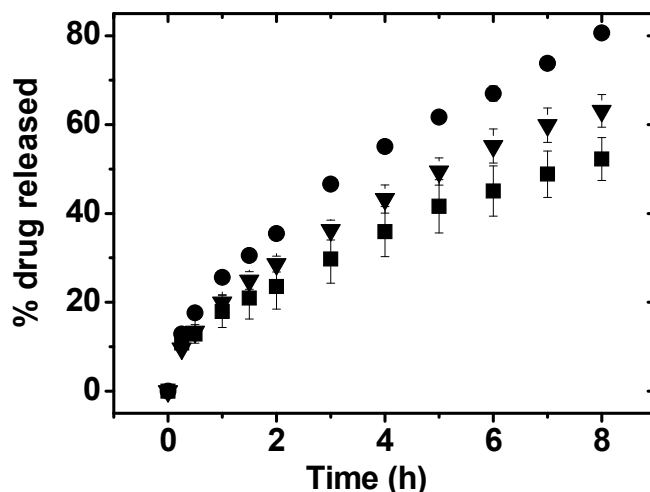


Figure 3.5. Release profiles for MH kept at 37 °C in Tris-HCl buffer (10 mM, pH 7.4) in the case of Ca^{2+}/MH (●), $\text{Ca}^{2+}/\text{MH}/\text{CMD-PEG}$ [NaCl] = 0 (■) and $\text{Ca}^{2+}/\text{MH}/\text{CMD-PEG}$ [NaCl] = 150 mM (▼). [+]/[-] for micelles = 1.0 and $[\text{Ca}^{2+}]/[\text{MH}] = 2.0$.

Next, we monitored by DLS the fate of $\text{Ca}^{2+}/\text{MH}/\text{CMD-PEG}$ micelles, first, in the presence of bovine serum albumin (BSA), and, second, in the presence of 5 % fetal bovine

serum. Although the interactions of the micelles with serum are the most relevant to the situation *in vivo*, BSA, which is the most abundant protein in serum, is often used as a model since its size and conformation are known precisely.^[43] The intensity fraction distribution of the R_H of Ca^{2+} /MH/CMD-PEG micellar solutions ([CMD-PEG]: 0.2 mg/mL, [+]/[-] = 1.0) and various amounts of BSA, from 0 to 40 mg/mL, are presented in Figure 3.6A. The R_H of BSA under the measurement conditions (5 mg/mL, pH 7.4) was 4.2 ± 0.1 nm, in agreement with reported values (Figure 3.6A, top trace).^[43, 44] The R_H value of Ca^{2+} /MH/CMD-PEG micelles in the absence of BSA was 84 ± 2 nm (Figure 3.6A, bottom trace). The presence of a signal ~ 4 nm in all BSA/micelle mixed systems, together with a signal ~ 90 nm indicates that the micelle integrity is preserved in the presence of BSA. The micellar size distribution in solutions of highest BSA concentration is slightly broader than in solutions devoid of BSA, possibly as a consequence of some level of BSA adsorption onto the micelles. BSA, which is negatively charged under physiological conditions (pH 7.4) could act as competing polyelectrolyte for PIC micelles and polyelectrolyte complexes.^[19, 45] The stability of Ca^{2+} /MH/CMD-PEG micelles in the presence of BSA concentration as high as 100 times the polymer concentration is probably a consequence of the limited access of negatively charged BSA to the positively charged Ca^{2+} /MH chelate due to its entrapment in the micelles' core.

DLS analysis of Ca^{2+} /MH/CMD-PEG micelles incubated for 24 h at 37 °C with 5% fetal bovine serum also revealed the presence of two size populations (Figure 3.6B): (i) small objects of $R_H \sim 7$ nm, identified as serum proteins by comparison with the serum DLS data (Figure 3.6B, top trace) and (ii) larger objects of R_H , identical, within experimental uncertainty, to the R_H of micelles incubated under the same conditions, but in the absence of serum (Figure 3.6B, bottom trace). These observations confirm that the micelles withstand the serum environment and that protein adsorption onto micelles occurs to a limited extent, if at all.^[46]

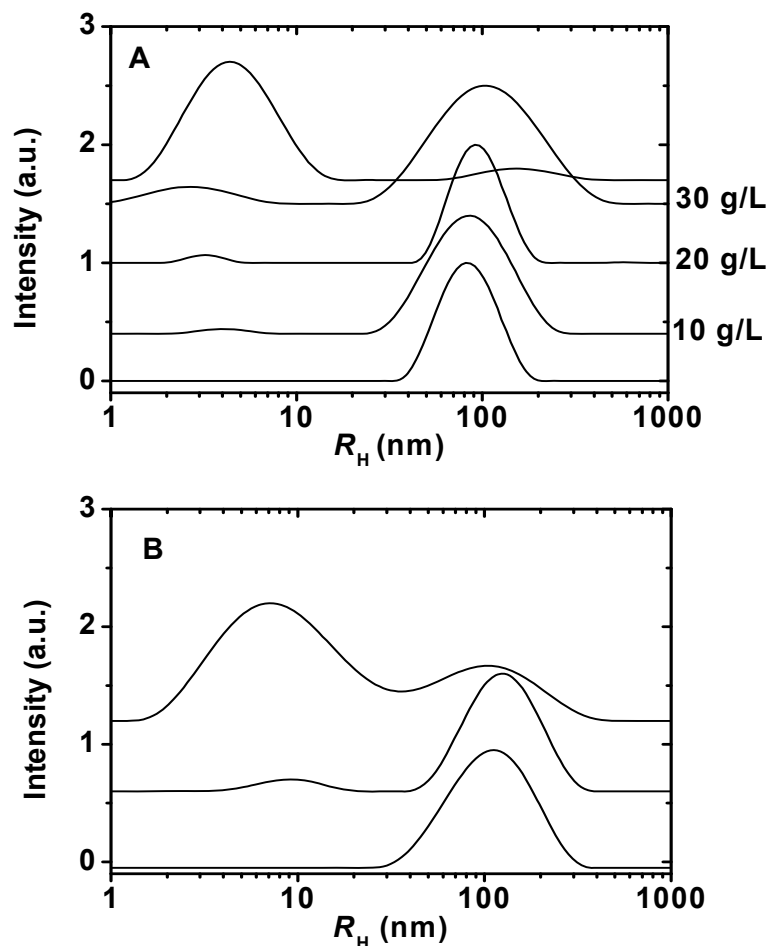


Figure 3.6. A: Normalized size distributions of Ca^{2+} /MH/CMD-PEG micelles upon incubation at 37 °C for 15 h with various amounts of BSA. Also shown are the size distributions recorded for micelles alone (bottom trace) and BSA alone (5 mg/mL) (top trace); $[+]/[-]$ for micelles = 1.0 and $[\text{Ca}^{2+}]/[\text{MH}] = 2.0$.

B: Normalized size distribution of Ca^{2+} /MH/CMD-PEG micelles upon incubation at 37 °C for 24 h with 5 % serum; also shown are the size distributions of micelles alone after incubation for 24 h at 37 °C (bottom trace) and of 5 % serum alone (top trace); $[+]/[-]$ for micelles = 1.0 and $[\text{Ca}^{2+}]/[\text{MH}] = 2.0$.

3.5.3. Cytotoxicity and anti-inflammatory effects of Ca²⁺/MH/CMD-PEG micelles

The cytotoxic effect of CMD-PEG on the viability of human hepatocytes and murine microglia was evaluated by the MTT and Alamar Blue assays and confirmed by cell counting. Hepatocytes were selected since the liver represents the main organ in which biotransformation of drugs and foreign substances takes place, while the inflamed microglia are the main targets of the drug in the central nervous system.^[47] Cell viability did not change significantly after a 24 h-incubation with CMD-PEG up to a concentration of 15 mg/mL (Figure SI.3.2, supporting information). The concentrations of CMD-PEG assessed were within the theoretical concentration range needed to achieve clinically relevant minocycline concentrations. It is anticipated that the PEG corona will prolong the micelles circulation in blood and reduce their uptake in the liver, as demonstrated previously with other PEGylated micelles.^[48]

The usefulness of micelle-entrapped MH for attenuation of microglia activity was tested in N9 microglia cells treated with lipopolysaccharides, (LPS), which are known inducers of microglia activation leading to the release of cytokines and nitric oxide.^[49] Minocycline can inhibit the LPS-induced microglia activation and, in turn, reduce the amount of nitric oxide (NO) released.^[50, 51] In the murine microglia (N9) model, a LPS dose of 10 µg/mL induced significant release of NO after 24 h (3.8 ± 0.1 a.u. compared to the untreated control (Figure 3.7)). The cells were subjected to concomitant treatments with 10 µg/mL LPS and 50 µg/mL MH in three formulations: MH, Ca²⁺/MH, and Ca²⁺/MH/CMD-PEG micelles or with 10 µg/mL LPS and 10 mg/mL CMD-PEG, in the absence of MH. As expected, MH alone greatly reduced the NO release (0.3 ± 0.01 a.u.). A similar effect was induced by Ca²⁺/MH/CMD-PEG micelles and by Ca²⁺/MH chelate at concentrations equivalent to 50 µg/mL (Figure 3.7). This result confirms that MH is released from the micelles in a pharmacologically active form and that the presence of the polymer or of CaCl₂ does not affect the drug activity. Unexpectedly, a control measurement that involved concomitant administration of LPS and CMD-PEG revealed that the polymer itself reduced

NO release by ~ 60%, compared to NO release level of the control measurement in the absence of CMD-PEG. If such an effect could be obtained in animal models and eventually in humans it could be of a significant relevance for improvement of minocycline effectiveness in an additive or even synergistic manner. We are currently pursuing these studies to assess if this polymer indeed does not only serve as a drug carrier but can also enhance beneficial anti-inflammatory effect of minocycline and other anti-inflammatory agents. The exact mechanism of this polymer-induced reduction in NO release is not clear and requires further investigations. .

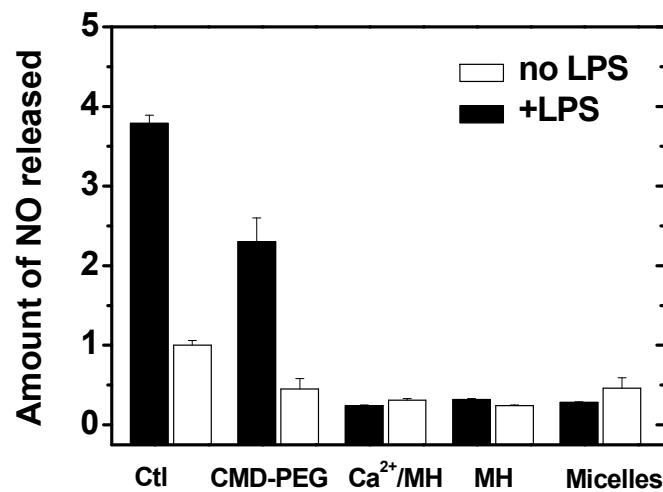


Figure 3.7. Amount of NO released in N9 microglia cells treated with MH alone, Ca²⁺/MH complex, Ca²⁺/MH/CMD-PEG micelles or CMD-PEG, all in the presence or absence of 10 µg/ml of lipopolysaccharide under normal cell culture conditions. Cells were treated for 24 h after which nitrite content in the media was measured using the Griess Reagent. All measurements were done in triplicates in three independent experiments. ** $p < 0.01$, *** $p < 0.001$

3.6. Conclusions

Complexation of the minocycline calcium chelate into CMD-PEG PIC micelles leads to a significant drug stabilization upon storage and in the presence of serum under physiological conditions. A similar approach may be suitable for other antibiotics and therapeutic agents whose stability can be increased in this manner. Preliminary *in vitro* results indicate that while encapsulating MH into Ca²⁺/MH/CMD-PEG micelles has its own merit in stabilizing the drug, controlling its release, and reducing protein adsorption, neither CaCl₂ nor the polymer negatively affect the anti-inflammatory activity of the drug. These observations need to be strengthened by *in vivo* investigations aimed at assessing if such formulations permit administration of MH in smaller but still effective doses which could significantly reduce the extent and severity of its undesirable side effects.

3.7. Appendix B. Supplementary data

Supporting information for this article is available at the bottom of the article's abstract page which can be accessed from the journal's homepage at <http://www.mbs-journal.de>.

3.8. Acknowledgements

The work was supported in part by a grant of the Natural Sciences and Engineering Research Council of Canada to FMW and DM and by a grant of the Canadian Institutes of Health Research to DM. GMS thanks the Ministry of Higher Education, Egypt for granting him a scholarship.

3.9. References

- [1] Blum D, Chtarto A, Tenenbaum L, Brotchi J, Levivier M. Clinical potential of minocycline for neurodegenerative disorders. *Neurobiol. Dis.* **2004**, *17*: 359-66.
- [2] Bernardino ALF, Kaushal D, Philipp MT. The antibiotics doxycycline and minocycline inhibit the inflammatory responses to the lyme disease spirochete *Borrelia burgdorferi*. *J. Infect. Dis.* **2009**, *199*: 1379-88.
- [3] Yrjanheikki J, Tikka T, Keinanen R, Goldsteins G, Chan PH, Koistinaho J. A tetracycline derivative, minocycline, reduces inflammation and protects against focal cerebral ischemia with a wide therapeutic window. *Proc. Natl. Acad. Sci. U. S. A.* **1999**, *96*: 13496-500.
- [4] Kim HS, Suh YH. Minocycline and neurodegenerative diseases. *Behav. Brain Res.* **2009**, *196*: 168-79.
- [5] Yenari MA, Xu LJ, Tang XN, Qiao YL, Giffard RG. Microglia potentiate damage to blood-brain barrier constituents - Improvement by minocycline in vivo and in vitro. *Stroke* **2006**, *37*: 1087-93.
- [6] Rio-Hortega P. Microglia. In: Penfield W, editor. *Cytology and cellular pathology of the nervous system*. New York: Hocker, 1932. p. 481-584.
- [7] Block ML, Zecca L, Hong J-S. Microglia-mediated neurotoxicity: Uncovering the molecular mechanisms. *Nat. Rev. Neurosci.* **2007**, *8*: 57-69.
- [8] Klein NC, Cunha BA. Tetracyclines. *Med. Clin. N. Am.* **1995**, *79*: 789-801.
- [9] Di Stefano A, Sozio P, Iannitelli A, Cerasa LS, Fontana A, Di Biase G, D'Amico G, Di Giulio M, Carpentiero C, Grumetto L, Barbato F. Characterization of alkanoyl-10-O-minocyclines in micellar dispersions as potential agents for treatment of human neurodegenerative disorders. *Eur. J. Pharm. Sci.* **2008**, *34*: 118-28.

- [10] Fagan SC, Edwards DJ, Borlongan CV, Xu L, Arora A, Feuerstein G, Hess DC. Optimal delivery of minocycline to the brain: Implication for human studies of acute neuroprotection. *Exp. Neurol.* **2004**, *186*: 248-51.
- [11] Zbinovsky V, Chrekian GP. Minocycline. In: Florey K, editor. *Analytical Profiles of Drug Substances*. New York: Academic Press, 1977. p. 323-39
- [12] Chow KT, Chan LW, Heng PWS. Formulation of hydrophilic non-aqueous gel: Drug stability in different solvents and rheological behavior of gel matrices. *Pharm. Res.* **2008**, *25*: 207-17.
- [13] Barry A, Badal R. Stability of minocycline, doxycycline, and tetracycline stored in agar plates and microdilution trays. *Curr. Microbiol.* **1978**, *1*: 33-6.
- [14] Jain N, Jain GK, Ahmad FJ, Khar RK. Validated stability-indicating densitometric thin-layer chromatography: Application to stress degradation studies of minocycline. *Anal. Chim. Acta* **2007**, *599*: 302-9.
- [15] Rasmussen B, Noller HF, Daubresse G, Oliva B, Misulovin Z, Rothstein DM, Ellestad GA, Gluzman Y, Tally FP, Chopra I. Molecular basis of tetracycline action: identification of analogs whose primary target is not the bacterial ribosome. *Antimicrob. Agents Chemother.* **1991**, *35*: 2306-11.
- [16] Hu W, Metselaar J, Ben L-H, Cravens PD, Singh MP, Frohman EM, Eagar TN, Racke MK, Kieseier BC, Stuve O. PEG minocycline-liposomes ameliorate CNS autoimmune disease. *PLoS ONE* **2009**, *4*: e4151.
- [17] Liang XF, Tian H, Luo H, Wang HJ, Chang J. Novel quaternized chitosan and polymeric micelles with cross-linked ionic cores for prolonged release of minocycline. *J. Biomater. Sci., Polym. Ed.* **2009**, *20*: 115-31.
- [18] Harada A, Kataoka K. Polyion complex micelles with core-shell structure: Their physicochemical properties and utilities as functional materials. *Macromol. Symp.* **2001**, *172*: 1-9.

- [19] Dautzenberg H, Konak C, Reschel T, Zintchenko A, Ulbrich K. Cationic graft copolymers as carriers for delivery of antisense-oligonucleotides. *Macromol. Biosci.* **2003**, 3: 425-35.
- [20] Talelli M, Pispas S. Complexes of cationic block copolymer micelles with DNA: Histone/DNA complex mimetics. *Macromol. Biosci.* **2008**, 8: 960-7.
- [21] Wang C-H, Wang W-T, Hsiue G-H. Development of polyion complex micelles for encapsulating and delivering amphotericin B. *Biomaterials* **2009**, 30: 3352-8.
- [22] Nishiyama N, Kataoka K. Current state, achievements, and future prospects of polymeric micelles as nanocarriers for drug and gene delivery. *Pharmacol. Ther.* **2006**, 112: 630-48.
- [23] Torchilin V. Multifunctional and stimuli-sensitive pharmaceutical nanocarriers. *Eur. J. Pharm. Biopharm.* **2009**, 71: 431-44.
- [24] Xiong X-B, Uludag H, Lavasanifar A. Biodegradable amphiphilic poly(ethylene oxide)-block-polyesters with grafted polyamines as supramolecular nanocarriers for efficient siRNA delivery. *Biomaterials* **2009**, 30: 242-53.
- [25] Jang WD, Nakagishi Y, Nishiyama N, Kawauchi S, Morimoto Y, Kikuchi M, Kataoka K. Polyion complex micelles for photodynamic therapy: Incorporation of dendritic photosensitizer excitable at long wavelength relevant to improved tissue-penetrating property. *J. Controlled Release* **2006**, 113: 73-9.
- [26] Osada K, Christie RJ, Kataoka K. Polymeric micelles from poly(ethylene glycol)-poly(amino acid) block copolymer for drug and gene delivery. *J. R. Soc. Interface* **2009**, 6: S325-S39.
- [27] Wessels JM, Ford WE, Szymczak W, Schneider S. The complexation of tetracycline and anhydrotetracycline with Mg^{2+} and Ca^{2+} : A spectroscopic study. *J. Phys. Chem. B* **1998**, 102: 9323-31.

- [28] Berthon G, Brion M, Lambs L. Metal-ion tetracycline interactions in biological-fluids.2. potentiometric study of magnesium complexes with tetracycline, oxytetracycline, doxycycline, and minocycline, and discussion of their possible influence on the bioavailability of these antibiotics in blood-plasma. *J. Inorg. Biochem.* **1983**, *19*: 1-18.
- [29] Devries T, Boissonneault R, Muldoon B. A tetracycline metal complex in a solid dosage form. Application: WO WO: (Warner Chilcott Company, Inc., USA). 2006. p. 24 pp.
- [30] Brion M, Berthon G, Fourtillan J-B. Metal ion-tetracyclines interactions in biological fluids. Potentiometric study of calcium complexes with tetracycline, oxytetracycline, doxycycline and minocycline and simulation of their distributions under physiological conditions. *Inorg. Chim. Acta* **1981**, *55*: 47-56.
- [31] Orti V, Audran M, Gibert P, Bougard G, Bressolle F. High-performance liquid chromatographic assay for minocycline in human plasma and parotid saliva. *J. Chromatogr. B* **2000**, *738*: 357-65.
- [32] Hernandez OS, Soliman GM, Winnik FM. Synthesis, reactivity, and pH-responsive assembly of new double hydrophilic block copolymers of carboxymethyl dextran and poly(ethylene glycol). *Polymer* **2007**, *48*: 921-30.
- [33] Soliman GM, Winnik FM. Enhancement of hydrophilic drug loading and release characteristics through micellization with new carboxymethyl dextran-PEG block copolymers of tunable charge density. *Int. J. Pharm.* **2008**, *356*: 248-58.
- [34] Leyden JJ. Absorption of minocycline hydrochloride and tetracycline hydrochloride: Effect of food, milk, and iron. *J. Am. Acad. Dermatol.* **1985**, *12*: 308-12.
- [35] Walderhaug H, Söderman O. NMR studies of block copolymer micelles. *Curr. Opin. Colloid Interface Sci.* **2009**, *14*: 171-7.

- [36] Nilges MJ, Enochs WS, Swartz HM. Identification and characterization of a tetracycline semiquinone formed during the oxidation of minocycline. *J. Org. Chem.* **1991**, *56*: 5623-30.
- [37] Ricci M, Giovagnoli S, Blasi P, Schoubben A, Perioli L, Rossi C. Development of liposomal capreomycin sulfate formulations: Effects of formulation variables on peptide encapsulation. *Int. J. Pharm.* **2006**, *311*: 172-81.
- [38] Lecaroz MC, Blanco-Prieto MJ, Campanero MA, Salman H, Gamazo C. Poly(D,L-lactide-co-glycolide) particles containing gentamicin: Pharmacokinetics and pharmacodynamics in *Brucella melitensis*-infected mice. *Antimicrob. Agents Chemother.* **2007**, *51*: 1185-90.
- [39] Nelis H, Deleenheer AP. Metabolism of minocycline in humans. *Drug Metab. Dispos.* **1982**, *10*: 142-6.
- [40] Ma ZS, Haddadi A, Molavi O, Lavasanifar A, Lai R, Samuel J. Micelles of poly(ethylene oxide)-b-poly(epsilon-caprolactone) as vehicles for the solubilization, stabilization, and controlled delivery of curcumin. *J. Biomed. Mater. Res., Part A* **2008**, *86A*: 300-10.
- [41] Bowles WH, Bokmeyer TJ. Staining of adult teeth by minocycline: Binding of minocycline by specific proteins. *J. Esthet. Restor. Dent.* **1997**, *9*: 30-4.
- [42] Aliabadi HM, Lavasanifar A. Polymeric micelles for drug delivery. *Expert Opin. Drug Deliv.* **2006**, *3*: 139-62.
- [43] Kelarakis A, Castelletto V, Krysmann MJ, Havredaki V, Viras K, Hamley IW. Interactions of bovine serum albumin with ethylene oxide/butylene oxide copolymers in aqueous solution. *Biomacromolecules* **2008**, *9*: 1366-71.
- [44] Martinez-Landeira P, Ruso JM, Prieto G, Sarmiento F, Jones MN. The interaction of human serum albumin with dioctanoylphosphatidylcholine in aqueous solutions. *Langmuir* **2002**, *18*: 3300-5.

- [45] Kakizawa Y, Harada A, Kataoka K. Glutathione-sensitive stabilization of block copolymer micelles composed of antisense DNA and thiolated poly(ethylene glycol)-block-poly(l-lysine): A potential carrier for systemic delivery of antisense DNA. *Biomacromolecules* **2001**, *2*: 491-7.
- [46] Liu J, Zeng F, Allen C. Influence of serum protein on polycarbonate-based copolymer micelles as a delivery system for a hydrophobic anti-cancer agent. *J. Controlled Release* **2005**, *103*: 481-97.
- [47] De Vocht C, Ranquin A, Willaert R, Van Ginderachter JA, Vanhaecke T, Rogiers V, Versées W, Van Gelder P, Steyaert J. Assessment of stability, toxicity and immunogenicity of new polymeric nanoreactors for use in enzyme replacement therapy of MNGIE. *J. Controlled Release* **2009**, *137*: 246-54.
- [48] Owens DE, Peppas NA. Opsonization, biodistribution, and pharmacokinetics of polymeric nanoparticles. *Int. J. Pharm.* **2006**, *307*: 93-102.
- [49] Nakamura Y, Si QS, Kataoka K. Lipopolysaccharide-induced microglial activation in culture: temporal profiles of morphological change and release of cytokines and nitric oxide. *Neurosci. Res.* **1999**, *35*: 95-100.
- [50] Kim S-S, Kong P-J, Kim B-S, Sheen D-H, Nam S-Y, Chun W. Inhibitory action of minocycline on lipopolysaccharide-induced release of nitric oxide and prostaglandin E2 in BV2 microglial cells. *Arch. Pharmacol Res.* **2004**, *27*: 314-8.
- [51] Ryan JH, Nancy N-M, Matthew SA, Joyce AD. Differential migration, LPS-induced cytokine, chemokine, and NO expression in immortalized BV-2 and HAPI cell lines and primary microglial cultures. *J. Neurochem.* **2008**, *107*: 557-69.

Appendix B. Supporting information (SI.3)

Isothermal titration calorimetry (ITC) studies

ITC Measurements were carried out with a Microcal VP-ITC instrument (Microcal Inc., Northampton, MA). The experiments were carried out in 10 mM Tris-HCL pH 7.4. Prior to measurements all the solutions were degassed under vacuum for about 10 min to eliminate any air bubbles. In a typical experiment, 10 μL aliquots of CaCl_2 solution (3.75 mM) were injected from a 300 μL continuously stirred (300-rpm) syringe into a 1.43 mL sample of MH solution (0.25 mM). In another set of experiments, CaCl_2 solution (7.5 mM) was injected into a 1.43 mL sample of CMD-PEG copolymer solution (1 mM carboxylates). Heats of dilution and mixing were determined in control experiments by injecting aliquots (10 μL) of CaCl_2 solution into the buffer (1.43 mL). A total of 28 aliquots were injected into the sample cell in intervals of 300 s. The calorimetric data were analyzed and converted to enthalpy change using Microcal ORIGIN 7.0. The enthalpy change for each injection was calculated by integrating the area under the peaks of the recorded time and then corrected with control experiments. The binding parameters (N , K , ΔH , ΔS) were determined by fitting the data using the fitting models available in Microcal ORIGIN 7.0 software.

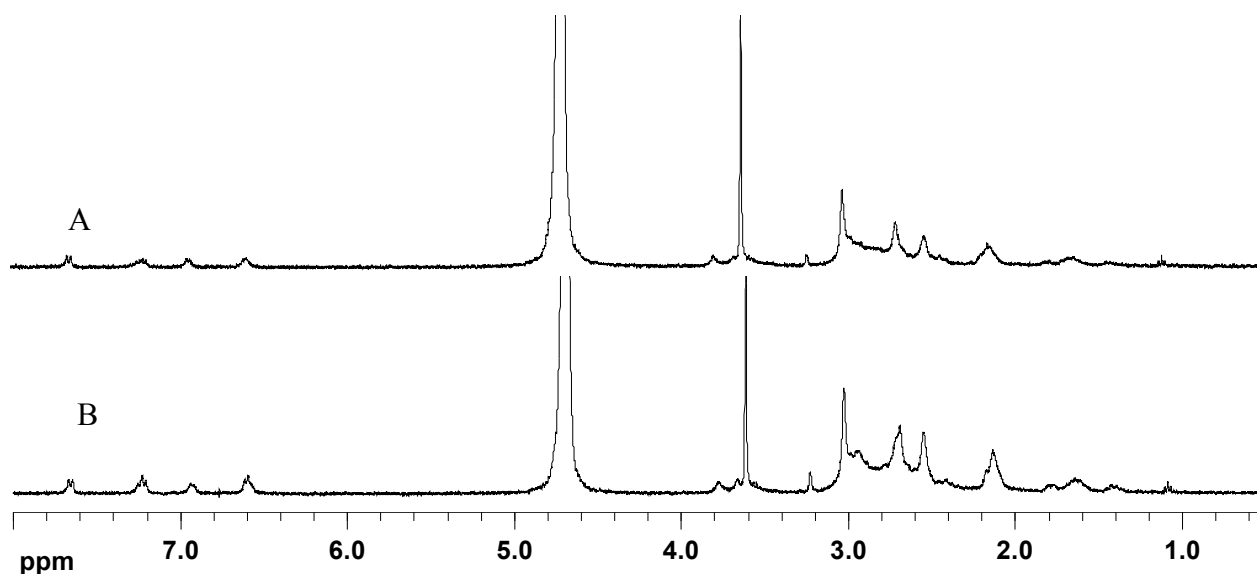


Figure SI.3.1. ^1H NMR spectra of $\text{Ca}^{2+}/\text{MH}/\text{CMD-PEG}$ micelles prepared in D_2O at [+]/[-] of 1.25 (A) and 1.5 (B).

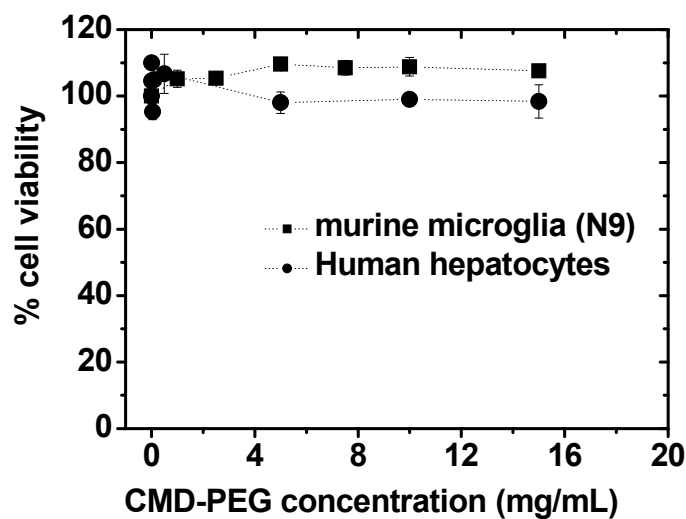


Figure SI.3.2. Cytotoxicity of CMD-PEG block polymer in human hepatocytes and murine microglia after treatment for 24 h with different polymer concentrations under normal cell culture conditions. Cell viability was assessed using the MTT and Alamar blue assays. All measurements were done in triplicates in three or more independent experiments.

CHAPTER FOUR

RESEARCH PAPER

Carboxymethyldextran-*b*-poly(ethylene glycol) Polyion Complex Micelles for the Delivery of Aminoglycoside Antibiotics³

**Ghareb Mohamed Soliman¹, Janek Szychowski², Stephen Hanessian²,
Françoise M. Winnik^{1,2}**

¹Faculty of Pharmacy and ²Department of Chemistry, Université de Montréal, CP 6128
Succursale Centre Ville, Montréal, QC, H3C 3J7, Canada

Pharmaceutical Research (To be submitted)

³ My contribution involved preparation and characterization of aminoglycosides micelles, synthesis of hydrophobically modified CMD-PEG polymers, interpreting the results and writing the paper, which was supervised by Dr. Françoise M. Winnik. Janek Szychowski contribution involved synthesis of guanidylated paromomycin, which was supervised by Dr. Stephen Hanessian.

4.1. Abstract

The aim of this study was to develop and characterize carboxymethyl-dextran-*b*-PEG (CMD-PEG) micelles as delivery systems for aminoglycoside antibiotics. Calorimetric studies showed that electrostatic interactions between different aminoglycosides and CMD-PEG were associated with proton uptake by the drugs from the buffers. The number of protons uptaken was temperature and pH dependent. CMD-PEG micelles incorporated up to 50 wt% drug and had a drug/CMD-PEG core and a PEG corona. Micelles incorporating neomycin were smaller in size and more resistant to salt-induced disintegration than those of paromomycin. However, both neomycin and paromomycin micelles were unstable under physiological conditions (pH 7.4, [NaCl] = 150 mM). Hydrophobically modified CMD-PEG (dodecyl-CMD-PEG) and guanidylated paromomycin were prepared to increase micelles stability under physiological conditions. Guanidylated paromomycin formed smaller and more stable micelles than paromomycin, though the micelles were unstable under physiological conditions. In contrast, micelles of neomycin/dodecyl-CMD-PEG resisted salt-induced disintegration for up to 200 mM NaCl, well above the physiological salt concentration. Different aminoglycosides were released from the micelles in a pharmacologically active form as indicated by their ability to kill a test micro-organism in culture. These results warrant *in vivo* evaluation of the optimal aminoglycoside/CMD-PEG micelle formulations.

4.2. Author Keywords

Aminoglycosides; Polyion complex micelles; Dextran; Isothermal titration calorimetry; Hydrophobic modification; Micelles stability.

4.3. Introduction

Aminoglycosides are a group of structurally diverse polyamines that have been frequently used in the treatment of serious infections caused by aerobic gram negative bacilli, such as pneumonia, urinary tract infections and peritonitis.^[1, 2] The antibacterial

activity of aminoglycosides results from their interaction with prokaryotic ribosomal RNA (rRNA).^[3] Aminoglycosides therapy is associated with a host of side effects due to drug accumulation in healthy non-target tissues. Nephrotoxicity and ototoxicity are the most common side effects of aminoglycosides and they are usually dose-limiting factors. Nephrotoxicity of aminoglycosides results from the accumulation in the kidney of a relatively high percentage (~ 10%) of the intravenously administered dose.^[4] Moreover, aminoglycosides are administered parenterally or locally, rather than orally due to their poor absorption in the gastro-intestinal tract as a consequence of their highly polar cationic nature.^[2, 5]

In view of the clinical importance of aminoglycosides, much effort has been directed towards their encapsulation into different drug delivery systems to modify their biodistribution, limit their toxicity and increase their oral bioavailability. Drug delivery systems tested include liposomes^[6-8], polymeric nanoparticles^[9], solid lipid nanoparticles^[10] and polyelectrolyte multilayers.^[11] Liposome-encapsulated aminoglycosides showed enhanced activity against resistant strains of *Pseudomonas aeruginosa* due to enhanced entry into the bacterial cell. Transmission electron microscope (TEM) confirmed that liposomes interact intimately with the outer membrane of *Pseudomonas aeruginosa*, leading to membrane deformation.^[7] Each of the nanocarriers tested so far, suffer from several drawbacks. Liposomes, for example, have limited stability in the presence of blood lipoproteins, low encapsulation efficiency, osmotic fragility and are unstable upon storage.^[9, 12, 13] Poly(lactic-co-glycolic acid) (PLGA) nanoparticles have limited drug loading efficiency (e.g. ~ 1 wt% for gentamicin). Gentamicin microspheres, although effective in reducing splenic infections in mice, triggered pulmonary embolism due to particles aggregation.^[14]

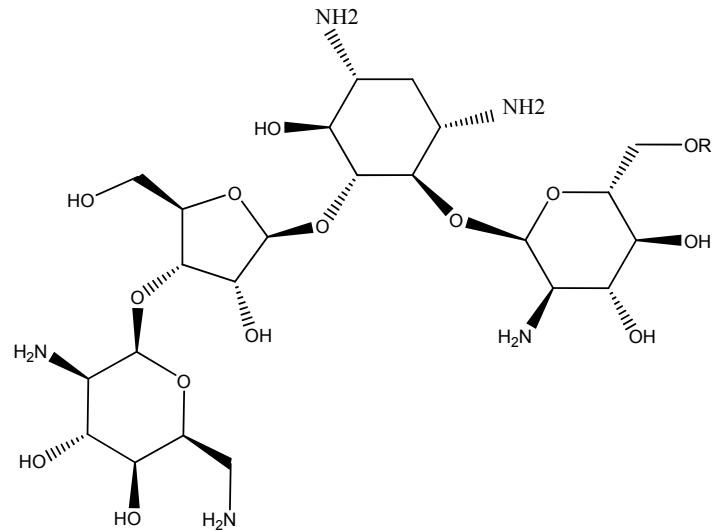
Polyion complex (PIC) micelles form by electrostatic interactions between an ionic dihydrophilic copolymer and an oppositely charged compound, such as drug, protein or nucleic acid.^[15-18] PIC micelles present a number of advantages for biomedical applications, including ease of fabrication, excellent colloidal stability in aqueous media, high drug loading capacity, small size and narrow size distribution. They are thermodynamically

stable and resist disintegration upon dilution as long as their concentration exceeds the critical association concentration (CAC), which usually is very low. PIC micelles usually have a poly(ethylene glycol) (PEG) corona, which prolongs their circulation time in the blood allowing them to accumulate passively in tissues of leaky vasculature, such as tumors and inflamed tissues.^[19] Carboxymethyl-dextran-*b*-PEG (CMD-PEG) copolymers are a new family of dextran-based anionic copolymers known to be non-toxic and to form PIC micelles with a number of cationic drugs.^[20, 21] CMD-PEG PIC micelles had small size, high drug loading capacity and were stable upon freeze drying and in presence of serum proteins. The shortcomings of the drug carriers used, so far to deliver aminoglycosides and the favorable properties of CMD-PEG micelles motivated us to exploit them for aminoglycosides encapsulation and delivery.

The objectives of this study were to formulate and characterize PIC micelles of CMD-PEG and two aminoglycoside antibiotics: neomycin sulfate and paromomycin sulfate (Figure 4.1). Neomycin and paromomycin are examples of 4, 5-disubstituted 2-deoxystreptamine aminoglycosides. Their structures differ by the 6' substituent: 6' hydroxyl group in paromomycin is replaced by an amino group in neomycin. Neomycin and paromomycin are positively charged at pH 7.4 making them suitable for PIC micelles formation with polyanions, such as CMD-PEG. The thermodynamics of the interaction between either neomycin or paromomycin and CMD-PEG were studied by isothermal titration calorimetry (ITC). Factors affecting the formation and stability of aminoglycosides/CMD-PEG micelles, as well as optimal conditions for their preparation were characterized by ¹H NMR spectroscopy and dynamic light scattering (DLS). Drug release from the micelles, as well as the ability of the released drugs to kill a test micro-organism in culture was also investigated.

One of the limitations of PIC micelles is their sensitivity to changes in ionic strength of the medium. Thus, small molecular weight salts screen the charges of oppositely charged species in the micelles core leading to micellar disassembly after certain salt concentration.^[22] Herein we proposed two approaches for CMD-PEG micelles stabilization against increase in salinity: (i) hydrophobic modification of CMD-PEG copolymers by

grafting dodecyl chains at different grafting densities and (ii) guanidylation of paromomycin.



Neomycin: R = NH₂
Paromomycin: R = OH

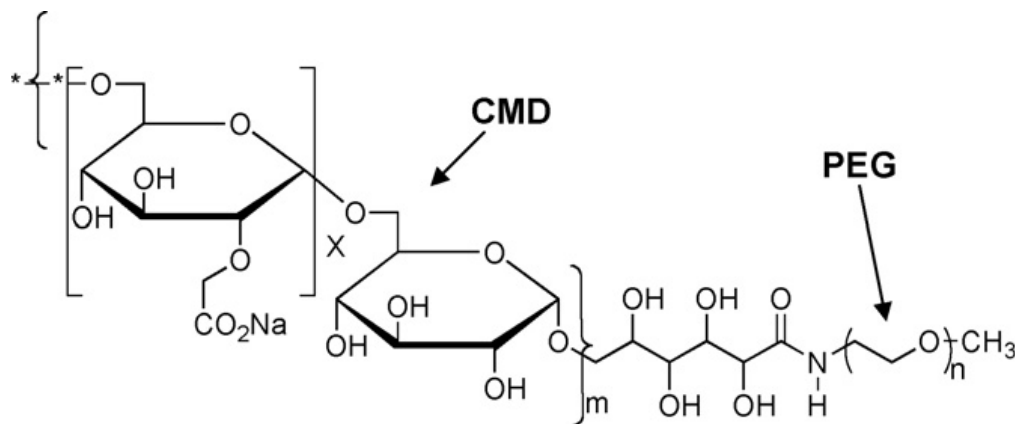


Figure 4.1. Chemical structures of neomycin, paromomycin (top) and CMD-PEG block copolymer (bottom).

4.4. Materials and methods

4.4.1. Materials

Trizma® hydrochloride (Tris-HCl), sodium cacodylate, HEPES, Tricine, Amberlite® IR-120, neomycin sulfate, paromomycin sulfate and all other chemicals were purchased from Sigma-Aldrich Chemicals (St. Louis, MO). Dextran was purchased from Fluka Chemical Co. (Buchs, Switzerland) and its number average molecular weight was determined to be 6400 g/mol by gel permeation chromatography. Dialysis tubing (SpectraPore, MWCO: 1,000 or 6,000-8,000 g/mol) was purchased from Fisher Scientific (Rancho Dominguez, CA). All solvents were reagent grade and used as received. The block copolymer CMD-PEG (Figure 4.1) was synthesized starting with dextran (M_n 6,000 g/mol) and α -amino- ω -methoxy-poly(ethylene glycol) (M_n 5,000 g/mol), as described previously.^[23] The degree of carboxymethylation of the dextran block, defined as the number of glucopyranose units having carboxymethyl groups per 100 glucopyranose units, was 85%. The average number of glucopyranosyl and of $-\text{CH}_2\text{-CH}_2\text{-O}-$ repeat units of the CMD and PEG segments, were 40 and 140, respectively. Detailed procedures for synthesis of guanidylated paromomycin are given as supplementary data (Figure SI.4.1).

4.4.2. Methods

4.4.2.1. General methods

^1H NMR spectra were recorded for solutions in D_2O (25 °C) using a Bruker AV-400 MHz spectrometer operating at 400 MHz. Chemical shifts are given relative to external tetramethylsilane (TMS = 0 ppm). Lyophilization was performed with a Virtis (Gardiner, NY) Sentry Benchtop (3L) freeze-dryer. UV-vis absorption spectra were recorded with an Agilent 8452A photodiode array spectrometer. Steady-state fluorescence spectra were recorded using a Varian Cary Eclipse fluorescence spectrophotometer.

4.4.2.2. Synthesis and characterization of hydrophobically modified CMD-PEG ^[24]

CMD-PEG (288 mg, 0.97 mmol carboxylate) was dissolved in deionized water (120 mL) and the pH was adjusted to 4.0 using 1.0 N HCl. *N*-Ethoxycarbonyl-2-ethoxy-1,2-dihydroquinoline (EEDQ) (216 mg, 0.87 mmol) was dissolved in absolute ethanol (120 mL) and the resulting solution was added gradually to CMD-PEG. The apparent pH of the water/ethanol mixture was adjusted to 4.0 and kept at this value for 30 min. Subsequently, dodecylamine (162 mg, 0.87 mmol) was added and the pH was increased to 9.0 by 1.0 N NaOH and the reaction mixture was stirred for 1.0 h at this pH. The ethanol was removed under reduced pressure at 50 °C and the product was recovered by freeze drying. The resulting dodecyl-CMD-PEG was purified by soxhlet extraction with hexane for 24 h to remove the unreacted dodecylamine and EEDQ. Dodecyl-CMD-PEG was converted to its free acid form by treatment with a cation exchange resin (Amberlite® IR 120). It was characterized by ¹H NMR spectroscopy of its solution in DMSO-*d*₆. The grafting density (defined as the number of dodecyl chains per 100 glycopyranose units) was determined from the ¹H NMR spectrum in DMSO-*d*₆ as the ratio between the area of the signal due to terminal methyl protons of the dodecyl chain (0.85 ppm) and the integral due to dextran anomeric protons (4.66 ppm) (Figure 4.2).

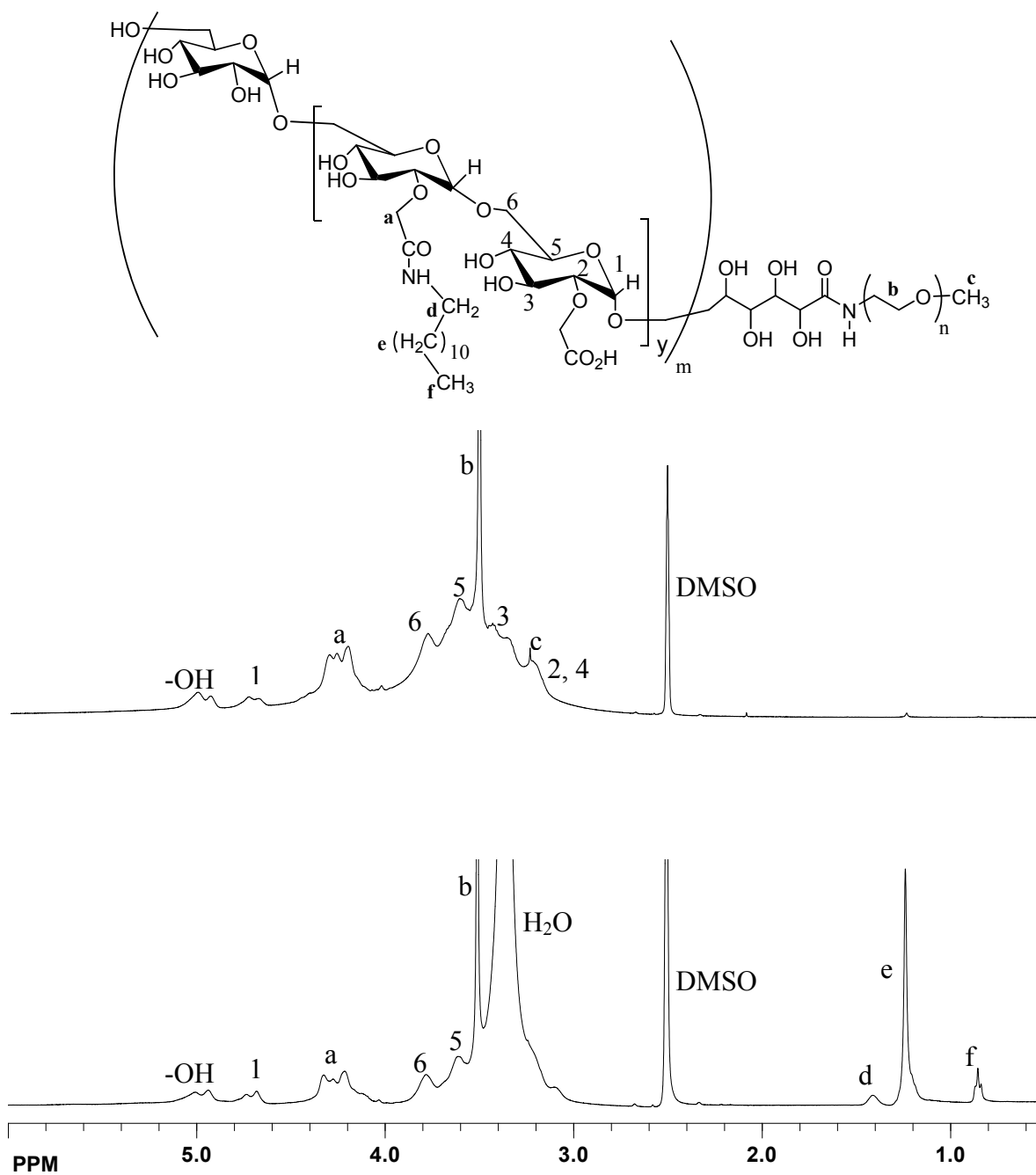


Figure 4.2. ^1H NMR spectra of CMD-PEG block copolymer (top spectrum) and dodecyl₃₈-CMD-PEG copolymer (bottom spectrum) recorded in $\text{DMSO-}d_6$ at room temperature.

Two water-soluble dodecyl-CMD-PEG copolymers were obtained by amide bond formation between dodecylamine and CMD-PEG carboxylate groups: dodecyl₁₈-CMD-PEG and dodecyl₃₈-CMD-PEG where 18 and 38 are the grafting densities of the dodecyl chains. FTIR spectrum of dodecyl₃₈-CMD-PEG copolymers (Figure SI.4.2) show bands at 1546 cm⁻¹ and 1644 cm⁻¹, attributed to the amide II and amide I vibration bands, respectively. Critical association concentration (CAC) was ~ 100 µg/mL for both dodecyl₁₈-CMD-PEG and dodecyl₃₈-CMD-PEG (Figure SI.4.3, supporting information).

4.4.2.3. Isothermal titration calorimetry (ITC)

ITC Measurements were carried out with a Microcal VP-ITC instrument (Microcal Inc., Northampton, MA). The experiments were carried out at pH 7.0 and 8.0. The buffer solutions used at pH 7.0 were 10 mM phosphate, 10 mM HEPES, 10 mM sodium cacodylate and 10 mM Tris-HCl while at pH 8.0 the buffers used were 10 mM phosphate, 10 mM HEPES, 10 mM Tricine and 10 mM Tris-HCl. Sufficient NaCl was added to each buffer solution to bring the total [Na⁺] to 50 mM. The experiments at pH 7.0 were carried out at 25 °C and 37 °C while those at pH 8.0 were carried out at 25 °C. The heat capacity change (ΔC_p) associated with the binding of either neomycin sulfate or paromomycin sulfate to CMD-PEG was determined in sodium cacodylate buffer (10 mM, pH 7.0) by performing additional experiments at 20 °C and 45 °C. Solutions of neomycin sulfate, paromomycin sulfate and CMD-PEG were prepared in the buffers and their pH values were adjusted as required. Prior to measurements all the solutions were degassed under vacuum for about 10 min to eliminate any air bubbles. In a typical experiment, 10 µL aliquots of neomycin sulfate solution (6.0 g/L, 6.6 mM, 39.6 mM amine) or paromomycin sulfate solution (5.65 g/L, 7.92 mM, 39.6 mM amine) were injected from a 300 µL continuously stirred (300-rpm) syringe into a 1.43 mL sample of CMD-PEG solution (0.75 g/L, 2.61 mM carboxylate). Heats of dilution and mixing were determined in control experiments by injecting aliquots (10 µL) of each drug solution into the same buffer (1.43 mL). A total of 28 aliquots were injected into the sample cell in intervals of 300 s. The calorimetric data were analyzed and converted to enthalpy change using Microcal ORIGIN 7.0. The enthalpy

change for each injection was calculated by integrating the area under the peaks of the recorded time and then corrected with control experiments. The binding parameters (N , K , ΔH , ΔS) were determined by fitting the data using the fitting models available in Microcal ORIGIN 7.0 software.

4.4.2.4. ^1H NMR spectra of aminoglycosides/CMD-PEG mixtures

Specified volumes of aminoglycosides stock solutions in D_2O were added dropwise to a magnetically stirred solution of CMD-PEG in D_2O over a period of 10 min in amounts such that $[\text{amine}]/[\text{carboxylate}]$ ranged from 1.0 to 5.0. The $[\text{amine}]/[\text{carboxylate}]$ is the ratio of the molar concentrations of amino groups provided by the drugs to that of carboxylate groups provided by the polymer. The effect of salt on different neomycin micelles was studied by preparing the micelles in D_2O at pH 7.4 and $[\text{NaCl}] = 150$ mM (polymer concentration: 2.0 g/L; $[\text{amine}]/[\text{carboxylate}] = 2.5$).

4.4.2.5. Light scattering studies

Dynamic light scattering experiments (DLS) were performed on a CGS-3 goniometer (ALV GmbH) equipped with an ALV/LSE-5003 multiple- τ digital correlator (ALV GmbH), a He-Ne laser ($\lambda = 632.8$ nm), and a C25P circulating water bath (Thermo Haake). A cumulant analysis was applied to obtain the diffusion coefficient (D) of the micelles in solution. The hydrodynamic radius (R_H) of the micelles was obtained using the Stokes-Einstein equation (1),

$$D = \frac{k_B T}{6\pi\eta_s R_H} \quad (1)$$

where η_s is the viscosity of the solvent, k_B is the Boltzmann constant, and T is the absolute temperature. The constrained regularized CONTIN method was used to obtain the particle size distribution. The data presented are the mean of six measurements \pm S.D. Solutions for analysis were filtered through a 0.45 μm Millex Millipore PVDF membrane prior to measurements.

4.4.2.6. Preparation and characterization aminoglycosides/CMD-PEG micelles

4.4.2.6.1. General method

Stock solutions of CMD-PEG or dodecyl-CMD-PEG (1.0 g/L) and aminoglycosides (4.96 and 5.27 g/L for paromomycin sulfate and neomycin sulfate, respectively) were prepared in phosphate buffer (10 mM, pH 7.0). Specified volumes of the drugs solutions were added dropwise to a magnetically stirred polymer solution over a 10-min period to obtain solutions with [amine]/[carboxylate] ratio ranging from 1.0 to 5.0. The volume of each sample was adjusted to 2.5 mL by the same buffer. CMD-PEG concentration was 0.2 g/L in all samples. Hydrodynamic radius (R_H), polydispersity index (PDI) and intensity of scattered light of an aliquot of the samples were determined by DLS.

4.4.2.6.2. pH studies

A micellar solution (polymer concentration: 0.2 g/L; [amine]/[carboxylate] = 2.5) was prepared in phosphate buffer (10 mM, pH 7.0) following the general procedures described above. Aliquots of this solution were treated with either 1.0 N NaOH or 1.0 N HCl to obtain solutions with pH values ranging from 9.0 to 2.0. After each pH adjustment, the sample was magnetically stirred for 5 min before measurements. Solutions of polymers alone (in absence of drugs) were treated in the same way described above and used as controls. R_H , PDI and intensity of scattered light were determined by DLS. The mean \pm S.D. of six measurements were determined.

4.4.2.6.3. Effect of salt (NaCl) on micelles formation and stability

Micellar solutions (polymer concentration: 0.5 g/L; [amine]/[carboxylate] = 2.5) were prepared in 10 mM phosphate buffer (10 mM, pH 7.0). Aliquots of a NaCl stock solution (2.5 M) in the same buffer were added to the micellar solutions in volumes such that [NaCl] in the sample ranged from 10 to 400 mM. The mixture was stirred for 5 min and the volume of each sample was adjusted to 2.5 mL with the same buffer. pH of solutions having [NaCl] = 150 mM was increased to 7.4 by the addition of 1.0 M NaOH,

followed by overnight stirring. R_H , PDI and intensity of scattered light were determined by DLS. The mean \pm S.D. of six measurements were determined.

4.4.2.7. Effect of freeze-drying on micelles integrity

Micellar solutions (polymer concentration: 0.2 g/L; [amine]/[carboxylate] = 2.5) in a phosphate buffer (10 mM, pH 7.0) were frozen by placing the glass vials containing the samples in a dry ice/acetone mixture (temperature: -78 °C). After 30 min the vials were placed in the freeze-dryer and lyophilized for 48 h. The resulting powder was rehydrated with deionized water to reach a polymer concentration of 0.2 g/L. The resulting mixture was stirred at room temperature for 10 min and analyzed by DLS.

4.4.2.8. Effect of dilution on micelles integrity

Micellar solutions were prepared as described above in phosphate buffer (10 mM, pH 7.0) with a polymer concentration of 0.5 g/L and [amine]/[carboxylate] = 2.5. The micelles were serially diluted to different polymer concentration using the same buffer and hydrodynamic radius and intensity of light scattered of aliquots were determined by DLS. The relative scattered light intensity (intensity of scattered light at certain polymer concentration/intensity at polymer concentration of 0.5 g/L) was plotted against polymer concentration. Critical association concentration (CAC) was determined from the plot following methods reported previously.^[20]

4.4.2.9. Drug release studies

The release of neomycin from micelles was evaluated by the dialysis bag method at 37 °C. The micellar solution (3.0 mL, neomycin: 2.0 g/L, [amine]/[carboxylate] = 2.5) was introduced into a dialysis membrane of MWCO = 6.0-8.0 kDa and dialyzed against 25 mL of 10 mM phosphate buffer containing either 0 mM NaCl (pH 7.0 or 7.4) or 150 mM NaCl (pH 7.0 or 7.4). A control experiment to determine the drug diffusion through the dialysis membrane was carried out in the absence of the polymer. At predetermined time intervals, 5 mL aliquots were taken from the release medium and replaced by equal volumes of fresh buffer. Neomycin concentration in the release samples was determined using the

derivatizing agent *o*-phthaldialdehyde following reported procedures.^[25] Briefly, 1 mL of each sample was mixed with 1 mL of *o*-phthaldialdehyde solution in isopropanol (1 mg/mL). Next, 1.5 mL isopropanol was added to prevent precipitation of neomycin/*o*-phthaldialdehyde complex and the volume of each sample was completed to 5.0 mL by borate buffer (50 mM, pH 9.0). The samples were allowed to stand for 1 h at room temperature. Subsequently, neomycin concentration was determined using a UV-visible spectrophotometer at the wavelength corresponding to maximum absorbance of neomycin/*o*-phthaldialdehyde complex ($\lambda_{\text{max}} = 335 \text{ nm}$). A calibration curve of neomycin was prepared before each determination.

4.4.2.10. Minimal inhibitory concentration (MIC) determination

Micelles of aminoglycosides/CMD-PEG were prepared in deionized water at drug concentration of 0.3 g/L and [amine]/[carboxylate] = 2.5. Micellar solutions were diluted using sterile Luria-Bertani media (LB) in a 96 wells plate to get drug concentrations of 0.25, 0.50, 0.75, 1.00, 2.00, 4.00, 8.00, 16.0 and 32.0 $\mu\text{g/ mL}$. *E. coli* X-1 blue strain was grown at 37 °C in 2 mL sterile LB to mid log phase (until absorbance at 595 nm reaches 0.6) and this suspension was shaken for homogeneity before adding 1 μL in each well. Blank samples were prepared without *E. coli* X-1 blue strain. After shaking the plate at 37 °C for 5 h, the absorbance at 595 nm of each well was monitored. The lowest concentration at which the absorbance at 595 nm was the same as the blank samples was considered to be the MIC. MIC determination was done in triplicate in all cases.

4.5. Results and discussion

4.5.1. Isothermal titration calorimetry (ITC) studies

PIC micelles formation relies on electrostatic interactions between an ionic copolymer and an oppositely charged drug.^[26-28] *In vitro* and *in vivo* performance of PIC micelles depends to a large extent on the strength of these electrostatic interactions.^[29] This

necessitates a thorough characterization of these interactions and understanding the factors affecting them.

4.5.1.1. Buffer and pH dependence of aminoglycosides and CMD-PEG interactions

We used ITC to study the binding of neomycin sulfate and paromomycin sulfate to CMD-PEG at 25 and 37 °C in four buffers with different ionization enthalpies (ΔH_{ion}) at pH 7.0 and 8.0. Figure 4.3 shows the corrected integrated heats for the titration of neomycin (panels A, B and E) and paromomycin (panels C, D and F) into CMD-PEG in four different buffers at pH 7.0 (panels A, C, E and F) and 8.0 (panels B and D). The integrated heats of the interaction were corrected by subtracting the corresponding dilution heats resulting from injecting identical amounts of drugs into buffers. The thermodynamic parameters resulting from the data fit are presented in Table 4.1, 4.2 and 4.3. By inspecting Figure 4.3 and Table 4.1, 4.2 and 4.3, one notices that at pH 7.0 and 8.0 at either 25 °C or 37 °C, the binding of neomycin and paromomycin to CMD-PEG was exothermic in the following buffers: cacodylate, HEPES, Tricine and phosphate and endothermic in Tris-HCl. The observed enthalpy change (ΔH_{obs}) was buffer dependent and its magnitude at pH 7.0 followed the following order: cacodylate > phosphate > HEPES > Tris-HCl whereas at pH 8.0 the order was: phosphate > HEPES > Tricine > Tris-HCl. This signifies that the observed enthalpy change (ΔH_{obs}) was not intrinsic to the binding of neomycin and paromomycin to CMD-PEG but it also contains contribution from the buffer ionization.

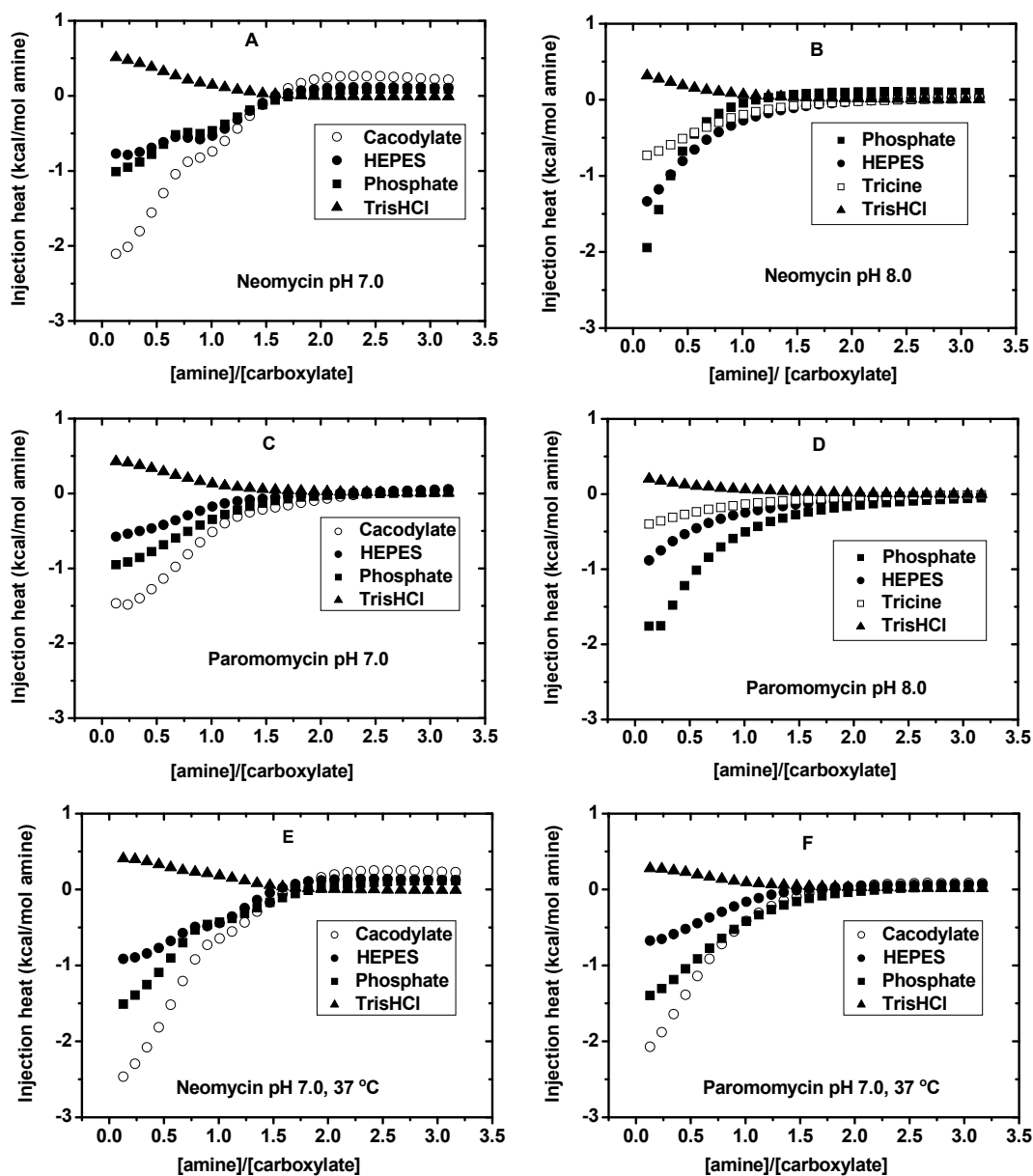


Figure 4.3. Corrected integrated injection heats plotted as a function of the [amine]/[carboxylate] ratio for the titration of either neomycin sulfate (A, B, E) or paromomycin sulphate (C, D, F) into CMD-PEG copolymer in different buffers at pH 7.0 (A, C, E, F) or 8.0 (B, D) at 25 °C (A, B, C, D) or 37 °C (E, F).

Table 4.1. Thermodynamic parameters for the binding of neomycin sulfate to CMD-PEG at pH 7.0 and 8.0, at 25 °C and a Na⁺ concentration of 50 mM.

Binding parameter	pH 7.0				pH 8.0			
	Cacodylate ^a	Phosphate ^a	HEPES ^a	Tris-HCl ^a	Phosphate ^b	HEPES ^b	Tricine ^b	Tris-HCl ^b
<i>N</i>	3	3	3	3	0.3± 0.02	0.52± 0.02	0.63±0.02	0.46± 0.009
<i>K</i> (X10 ³)(M ⁻¹)	6.02 ± 1.6	0.89 ± 0.57	59.9± 98	2.69±0.59	6.64± 2.4	2.49±0.34	2.59 ±0.3	1.54±0.06
ΔH_{obs} (kcal/mol)	-2.51±0.09	-1.25± 0.25	-0.77± 0.03	0.61 ±0.01	-2.45 ± 0.30	-1.81±0.10	-0.92±0.03	0.52±0.01
<i>T</i> ΔS_{obs} (kcal/mol)	2.63	2.77	5.75	5.30	2.75	2.81	3.72	4.88
ΔG (kcal/mol)	-5.15	-4.02	-6.52	-4.69	-5.2	-4.62	-4.64	-4.36

^a: Data was fitted using a model for three sequential binding sites.

^b: Data was fitted using a model for single set of binding sites.

Table 4.2. Thermodynamic parameters for the binding of paromomycin sulfate to CMD-PEG at pH 7.0 and 8.0, at 25 °C and a Na⁺ concentration of 50 mM.

Binding parameter	pH 7.0				pH 8.0			
	Cacodylate ^a	Phosphate ^a	HEPES ^a	Tris-HCl ^b	Phosphate ^b	HEPES ^b	Tricine ^b	Tris-HCl ^b
<i>N</i>	3	3	3	0.72±0.00	0.55± 0.02	0.40± 0.02	0.58±0.02	0.53± 0.04
<i>K</i> (X10 ³) (M ⁻¹)	14.1±4.2	1.83± 0.09	2.63±0.58	2.69±0.05	1.3±0.12	0.82 ±0.04	0.89±0.04	1.25 ±0.19
ΔH_{obs} (kcal/mol)	-1.53±0.01	-1.20±0.01	-0.66±0.02	0.53±0.00	-3.04±0.18	-2.06±0.12	-0.73±0.03	0.33 ±0.03
$T\Delta S_{obs}$ (kcal/mol)	4.11	2.97	3.65	5.21	1.2	1.91	3.27	4.55
ΔG (kcal/mol)	-5.64	-4.17	-4.31	-4.68	-4.24	-3.97	-4.00	-4.22

^a: Data was fitted using a model for three sequential binding sites.

^b: Data was fitted using a model for single set of binding sites.

Table 4.3. Thermodynamic parameters for the binding of neomycin sulfate and paromomycin sulfate to CMD-PEG at pH 7.0 and at 37 °C and a Na⁺ concentration of 50 mM.

Binding parameter	Neomycin				Paromomycin			
	Cacodylate ^a	Phosphate ^a	HEPES ^a	Tris-HCl ^a	Cacodylate ^a	Phosphate ^a	HEPES ^a	Tris-HCl ^b
<i>N</i>	3	3	3	3	3	3	3	0.73 ± 0.01
<i>K</i> (X10 ³)(M ⁻¹)	2.96± 1.3	0.93 ± 0.34	3.06± 0.98	1.87±0.41	1.67±0.08	2.05±0.07	3.63±0.6	1.72±0.14
ΔH_{obs} (kcal/mol)	-2.96 ±0.16	-2.27± 0.26	-1.02± 0.06	0.50 ±0.02	-2.69±0.02	-1.72±0.01	-0.77±0.01	0.39 ±0.01
$T\Delta S_{obs}$ (kcal/mol)	1.95	1.94	3.90	5.14	1.87	2.96	4.27	4.99
ΔG (kcal/mol)	-4.91	-4.21	-4.92	-4.64	-4.56	-4.68	-5.04	-4.60

^a: Data was fitted using a model for three sequential binding sites.

^b: Data was fitted using a model for single set of binding sites.

According to the proton linkage theory, the observed enthalpy change (ΔH_{obs}) is related to buffer ionization by the following relationship^[30]:

$$\Delta H_{\text{obs}} = \Delta H_{\text{int}} + \Delta n \Delta H_{\text{ion}} \quad (2)$$

Where ΔH_{int} is the intrinsic binding enthalpy (the enthalpy that is determined in a buffer with negligible ionization enthalpy), Δn is the number of protons released or uptaken during the binding and ΔH_{ion} is the buffer heat of ionization. Thus, by plotting ΔH_{obs} against ΔH_{ion} of different buffers, the slope of the straight line gives the number of protons linked to binding and the intercept gives the intrinsic binding enthalpy (ΔH_{int}). The binding is accompanied by proton release to the buffer if the slope is negative and by proton uptake from the buffer if the slope is positive. The relationship between ΔH_{obs} and ΔH_{ion} was linear with positive slopes in all cases signifying that the binding of neomycin and paromomycin to CMD-PEG was accompanied by proton uptake from the buffers (Figure SI 4.4). The numbers of protons uptaken during the binding, as well as the intrinsic thermodynamic parameters are listed in Table 4.4. The pK_a values of neomycin sulfate amino groups range from 6.92 to 9.51 while those of paromomycin sulfate range from 7.07 to 9.46.^[31] The pK_a values of the free base forms are 5.74-8.8 for neomycin^[32] and 6.5-9.13 for paromomycin.^[33] At pH 7.0, the fraction (f_{ion}) of a given drug amino group of known pK_a that exists in the protonated ($-\text{NH}_3^+$) state is given by the Henderson-Hasselbalch equation (Equation 3):

$$f_{\text{ion}} = \left(\frac{1}{1 + 10^{7 - pK_a}} \right) \quad (3)$$

Based on this equation, at pH 7.0 neomycin sulfate has 5.33 out of its 6 amino groups in ionized state while neomycin free base has 4.5 amino groups in ionized state. At the same pH, paromomycin sulfate has 4.41 out of its 5 amino groups in ionized state while paromomycin free base has 3.98 protonated amino groups. Thus, in order to be fully protonated at pH 7.0 and 25 °C, neomycin sulfate should uptake 0.67 protons from the buffer (0.11 proton/amino group) while neomycin free base needs 1.5 protons (0.25 protons/amino group). Paromomycin sulfate needs 0.59 protons (0.11 protons/amino group) while paromomycin free base needs 1.02 protons (0.20 protons/amino group) to attain full

ionization state. The protons needed to achieve full ionization state are uptaken from the buffers. Data in Table 4.4 shows that Δn uptaken by neomycin and paromomycin at pH 7.0 and 25 °C to attain full ionization is closer to the number of protons needed by the free base form and not the sulfate salt form for both drugs. This indicates that the complex formation takes place between CMD-PEG and the free base form of the drug, even though the sulfate forms were used in the experiments. Barbieri and Pilch^[33] reported similar findings for the binding of paromomycin sulfate to the 16S rRNA A-site. They attributed their findings to the dilute state of paromomycin sulfate in the experiments (drug concentration: 0 to 45 μM) or to the presence of 150 mM NaCl, which, according to the authors, breaks electrostatic bond between the drug amino groups and the sulfate anions.

Table 4.4. Intrinsic thermodynamic parameters and number of uptaken protons for the binding of paromomycin sulfate and neomycin sulfate to CMD-PEG at pH 7.0 (25 °C and 37 °C) and at pH 8.0 (25 °C) and a Na^+ concentration of 50 mM.

	pH	T (°C)	Δn^a	ΔH_{int}^b (kcal/mol)	$T\Delta S_{int}^c$ (kcal/mol)	ΔG^d (kcal/mol)
Neomycin	7.0	25	0.23 ± 0.10	-1.99 ± 0.15	3.1 ± 0.9	-5.09 ± 1.05
	7.0	37	0.29 ± 0.01	-2.68 ± 0.20	1.99 ± 0.13	-4.67 ± 0.33
	8.0	25	0.29 ± 0.02	-3.03 ± 0.29	1.67 ± 0.06	-4.70 ± 0.35
Paromomycin	7.0	25	0.17 ± 0.00	-1.45 ± 0.01	3.16 ± 0.49	-4.61 ± 0.50
	7.0	37	0.24 ± 0.00	-2.24 ± 0.01	2.48 ± 0.20	-4.72 ± 0.21
	8.0	25	0.34 ± 0.01	-3.54 ± 0.19	0.56 ± 0.05	-4.10 ± 0.14

^a: Number of protons uptaken per amino group.

^b: Obtained from equation 2.

^c: Calculated using the standard relationship $T\Delta S_{int} = \Delta H_{int} - \Delta G$

^d: Calculated using the standard relationship $\Delta G = -RT \ln K$

Similar behaviour observed in our experiments under relatively higher drug concentration (6.6 mM for neomycin and 7.92 mM for paromomycin) and lower salt

concentration (50 mM NaCl), warrants investigation into the reason behind this observation. Proton uptake has also been observed during the interaction between different cationic compounds and DNA and was attributed to shift of pK_a of the cationic species to higher values upon binding.^[34-36] The number of protons uptaken during the binding (Δn) of neomycin and paromomycin to CMD-PEG increased by increasing pH of the solution. Thus, pH increase from 7.0 to 8.0 resulted in increasing Δn from 0.23 to 0.29 protons/ NH_2 for neomycin and from 0.17 to 0.34 protons/ NH_2 for paromomycin (Table 4.4). The increased Δn resulted in more exothermic ΔH_{obs} since the proton uptake is an exothermic process (Figure 4.3).^[34] Similar observations were reported for the binding of neomycin and paromomycin to the A site of 16S rRNA.^[37] Similar increase in Δn was observed by increasing temperature from 25 to 37 °C at pH 7.0 (Table 4.4), which may be attributed to the temperature-induced decrease in pK_a . pK_a values of paromomycin amino groups were reported to decrease by an average of 0.026 pH units per 1 °C increase in temperature.^[33]

4.5.1.2. Intrinsic thermodynamic parameters for binding of neomycin and paromomycin to CMD-PEG

Thermodynamic parameters listed in Table 4.4 are intrinsic to the binding of neomycin and paromomycin to CMD-PEG and are independent of the buffers used. At pH 7.0 and 25 °C, the entropic contribution ($T\Delta S_{\text{int}}$) to the binding was 3.10 and 3.16 kcal/mol for neomycin and paromomycin, respectively. Thus, at pH 7.0 and 25 °C, the entropy change ($T\Delta S_{\text{int}}$) accounts for 61 and 68% of the driving force for the binding of neomycin and paromomycin to CMD-PEG, respectively. This observation is in good agreement with a report on the binding of the same drugs to the A site of 16S rRNA for which it was reported that 72% of the driving force for the binding of paromomycin to RNA was derived from entropic contributions.^[31] Electrostatic interactions between aminoglycosides and either RNA or CMD-PEG are associated with counter ions release, which results in entropy gain of the system.^[38, 39] A temperature increase from 25 to 37 °C at pH 7.0 reduced $T\Delta S_{\text{int}}$ for both neomycin and paromomycin (Table 4.4). A pH increase from 7.0 to 8.0 at 25 °C resulted in a more pronounced decrease of $T\Delta S_{\text{int}}$. The decrease in $T\Delta S_{\text{int}}$ as the temperature

or pH increases is attributed to the increase in the number of protons uptaken (Δn) during the binding of neomycin and paromomycin to CMD-PEG (Table 4.4). Being an enthalpically favoured process, proton uptake increases the enthalpic contribution and decreases the entropic contribution to the binding free energy. Entropy loss as a result of temperature or pH increase was nearly compensated for by the gain in enthalpy (ΔH_{int}) resulting in an average decrease of ΔG of around 0.4 kcal/mol with the increase in temperature or pH (Table 4.4). The data in Table 4.4 shows also that neomycin has more binding affinity to CMD-PEG than paromomycin at 25 °C and pH 7.0. The higher binding of neomycin is enthalpic in origin due to the difference in Δn , which was higher for neomycin (0.23 protons/ NH_2) compared to that of paromomycin (0.17 protons/ NH_2).

4.5.1.3. Heat capacity change (ΔC_p) determination

The heat capacity change (ΔC_p) upon binding of neomycin and paromomycin to CMD-PEG was determined by carrying out ITC experiments for solutions at different temperatures under identical pH and buffer conditions. The heat capacity change at constant pressure is the temperature derivative of the enthalpy change (equation 4).

$$\Delta C_p = \left(\frac{\partial \Delta H_{\text{obs}}}{\partial T} \right)_p \quad (4)$$

Plotting ΔH_{obs} versus temperature yields ΔC_p as the slope of the straight line. We determined ΔC_p for the binding of neomycin and paromomycin to CMD-PEG in sodium cacodylate buffer at pH 7.0 by carrying out ITC experiments at 20, 25, 37 and 45 °C. ΔC_p values were -243.3 and -324.95 cal.mol⁻¹.K⁻¹ for neomycin and paromomycin, respectively. These values are not attributed to electrostatic interactions only but should also contain contribution from hydrophobic and other interactions. Similar negative ΔC_p values were reported for the interaction between dextran sulfate and a series of positively charged drugs.^[40] Heat capacity changes reflect change in solvent accessible surfaces upon binding. Burial of non polar surfaces results in negative ΔC_p while burial of polar surfaces gives

positive ΔC_p .^[41, 42] Electrostatic interactions are also known to increase the magnitude of the negative values of ΔC_p .^[40, 43, 44]

4.5.2. ^1H NMR studies

We used ^1H NMR to probe the structure of the PIC micelles formed by electrostatic interactions between CMD-PEG and either neomycin sulfate or paromomycin sulfate. Previous studies showed that the formation in water of nanoparticles with core-corona structures can be detected by ^1H NMR spectroscopy.^[45, 46] This takes advantage of the fact that protons of the polymer segments forming the core have restricted movement and thus, their signals appear broad or did not appear at all. In contrast, protons of the polymer segments forming the corona maintain their mobility and their signals appear well resolved. ^1H NMR spectrum of neomycin sulfate (Figure 4.4A) shows three signals for the three anomeric protons on the three amino sugars at 5.2, 5.34 and 5.87 ppm. The axial and equatorial methylene protons on the substituted cyclohexane ring resonate at 1.66 and 2.2 ppm, respectively. The other neomycin protons show a series of signals between 3.16 to 4.45 ppm.^[47] Figure 4.4B shows the ^1H NMR spectrum of CMD-PEG, which presents signals at δ 4.08-4.15, 4.89, and 5.07 ppm, ascribed to protons of the CMD block, and a broad strong singlet centered at δ 3.61 ppm due to the PEG methylene protons (-CH₂-CH₂-O-).^[20] The spectrum of neomycin/CMD-PEG micelles ([amine]/[carboxylate] = 2.5, pH 7.4, [NaCl] = 0 mM) (Figure 4.4C) features only a strong signal at δ 3.61 ppm, ascribed to PEG protons. The signals due to the protons of neomycin and CMD segment of the polymer disappeared almost completely confirming the formation of PIC micelles with neomycin/CMD core and PEG corona (Figure 4.4C). Spectra of micelles prepared at $1.5 \leq [\text{amine}]/[\text{carboxylate}] \leq 2.5$ were similar to that presented in Figure 4.4C. Micelles having $[\text{amine}]/[\text{carboxylate}] < 1.5$ or > 2.5 showed signals characteristic of free drug. This confirms that maximum drug loading was achieved for mixture having $[\text{amine}]/[\text{carboxylate}] = 2.5$. Micelles of this composition have 50 wt% drug, which was taken as the actual drug loading since their NMR spectrum shows no signals of free drug (Figure 4.4C). The stability of these micelles was challenged by recording their ^1H NMR

spectrum under physiological conditions (pH 7.4, [NaCl] = 150 mM) (Figure 4.4D). Under these conditions, the micelles showed signs of disintegration as evidenced by the appearance of signals characteristic of neomycin protons (indicated by arrows in Figure 4.4D). The micelles disintegration is not complete, however since the intensity of neomycin peaks is much smaller than that of neomycin alone recorded under similar conditions (Figure 4.4A). Identical ^1H NMR experiments performed on the paromomycin/CMD-PEG micelles showed results similar to those of neomycin /CMD-PEG.

Salt-induced disintegration has been observed for several PIC micelles and was attributed to the weakening of electrostatic interactions in the micelles core.^[48] PIC micelles ability to resist salt-induced disintegration depends on many factors including strength of the electrostatic interactions, pK_a s of the interacting groups, presence of additional driving forces (e.g. hydrophobic interactions, hydrogen bonding) and polymer architecture. Hydrophobic modifications of polymers and cross linking of micelles core have been suggested for PIC micelles stabilization.^[49, 50] Yuan *et al.*, reported that PIC micelles of lysozyme/poly(ethylene glycol)-*b*-poly(aspartic acid) with hydrophobic groups (phenyl, naphthyl and pyrenyl) attached to the ω -end of the polymer had smaller critical association concentration and better tolerability to salt-induced disintegration.^[49] Herein we hypothesize that hydrophobically modified CMD-PEG could lead to more stable micelles. To test this hypothesis, we prepared two hydrophobically modified CMD-PEG polymers that differ in the grafting density of dodecyl chains: dodecyl₁₈-CMD-PEG and dodecyl₃₈-CMD-PEG. ^1H NMR spectrum of dodecyl₃₈-CMD-PEG in D₂O (Figure 4.4E) shows signals characteristic of CMD block (at δ 4.08-4.36, 4.89, and 5.07 ppm) and PEG (at δ 3.61 ppm), in addition to signals of dodecyl chains (at δ 1.18 ppm for $-(\text{CH}_2)_{10}\text{-CH}_3$ and at δ 0.78 ppm for $-(\text{CH}_2)_{10}\text{-CH}_3$).

To test the ability of dodecyl₃₈-CMD-PEG to stabilize the micelles, ^1H NMR spectra of its micelles with neomycin were recorded in absence (Figure 4.4F) and presence (Figure 4.4G) of 150 mM NaCl at pH 7.4. As expected the spectrum of the micelles prepared in the absence of salt shows only signals attributed to PEG corona of the micelles (Figure 4.4F). Interestingly, neomycin/dodecyl₃₈-CMD-PEG micelles prepared under physiological

conditions (pH 7.4, [NaCl] = 150 mM) (Figure 4.4G) did not show any signs of micelles disintegration. This confirms the ability of this copolymer to stabilize the micelles against salt-induced disintegration. These results were confirmed by other techniques, such as dynamic light scattering studies (see below).

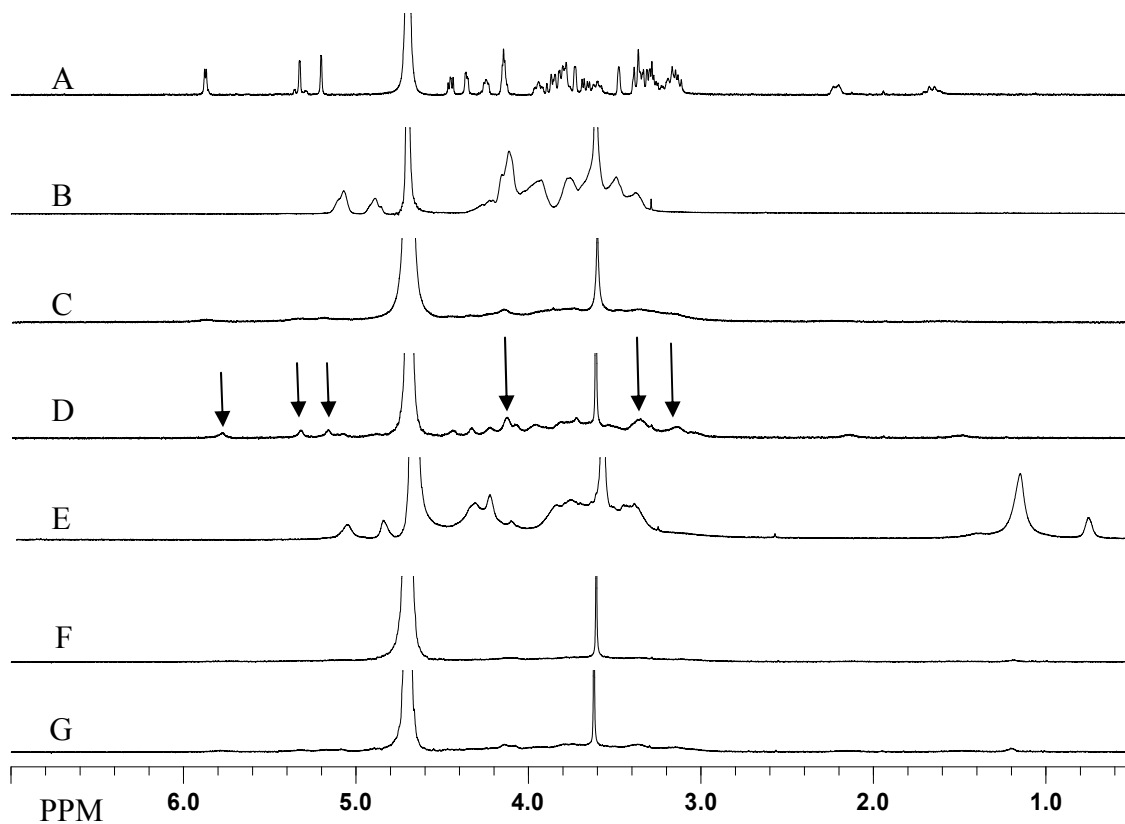


Figure 4.4. ^1H NMR spectra of neomycin sulfate (A), CMD-PEG (B), neomycin/CMD-PEG micelles (pH 7.4, 0 mM NaCl) (C), neomycin/CMD-PEG micelles (pH 7.4, 150 mM NaCl) (D), dodecyl₃₈-CMD-PEG (E), neomycin/dodecyl₃₈-CMD-PEG micelles (pH 7.4, 0 mM NaCl) (F) and neomycin/dodecyl₃₈-CMD-PEG micelles (pH 7.4, 150 mM NaCl) (G). All micelles were prepared in D_2O at polymer concentration of 2.0 g/L, neomycin concentration of 2.1 g/L and [amine]/[carboxylate] = 2.5.

Table 4.5. Characteristics of aminoglycosides/CMD-PEG micelles ([amine]/[carboxylate] = 2.5) in a phosphate buffer (10 mM, pH 7.0)

Micelle	R_H^a	PDI	% Drug ^b
Neomycin/CMD-PEG	74.9±1.8	0.03±0.03	50
Paromomycin/CMD-PEG	130.1±0.5	0.08±0.03	49.8
Neomycin/dodecyl ₁₈ -CMD-PEG	63.3±0.6	0.08±0.05	50
Paromomycin/dodecyl ₁₈ -CMD-PEG	48.5±0.4	0.02±0.03	49.8
Neomycin/ dodecyl ₃₈ -CMD-PEG	40.5±0.4	0.06±0.03	50
Paromomycin/dodecyl ₃₈ -CMD-PEG	54.5±1.2	0.03±0.02	49.8
6"-guanidino-paromomycin/CMD-PEG	110±2.2	0.08±0.02	50
5"-deoxy-5"-guanidino-paromomycin/CMD-PEG	83.8±2.6	0.04±0.05	50

^a: Mean of six measurements ± S.D.

^b: % drug loading = weight of drug/(weight of micelles)×100.

4.5.3. Size of aminoglycosides/CMD-PEG micelles

Neomycin and paromomycin micelles with different polymers were prepared in phosphate buffer (10 mM, pH 7.0) at different [amine]/[carboxylate] ratios. The R_H of micelles plotted as a function of [amine]/[carboxylate] are presented in Figure 4.5. All drug/polymer mixtures prepared at [amine]/[carboxylate] < 1.0 did not scatter enough light indicating the absence of nanoparticles. Paromomycin/CMD-PEG micelles at [amine]/[carboxylate] = 1.0 showed R_H ~100 nm and polydispersity index (PDI) ~ 0.3. Increasing [amine]/[carboxylate] to 1.5 resulted in a drop of R_H to ~ 70 nm and PDI to 0.2

(Figure 4.5A). R_H of the micelles gradually increased by further increase in $[\text{amine}]/[\text{carboxylate}]$ probably as a consequence of incorporating more drug in the micelles core. R_H levelled off at $[\text{amine}]/[\text{carboxylate}] = 2.5$, after which it remained constant confirming the NMR results that maximum drug loading was achieved at this point.

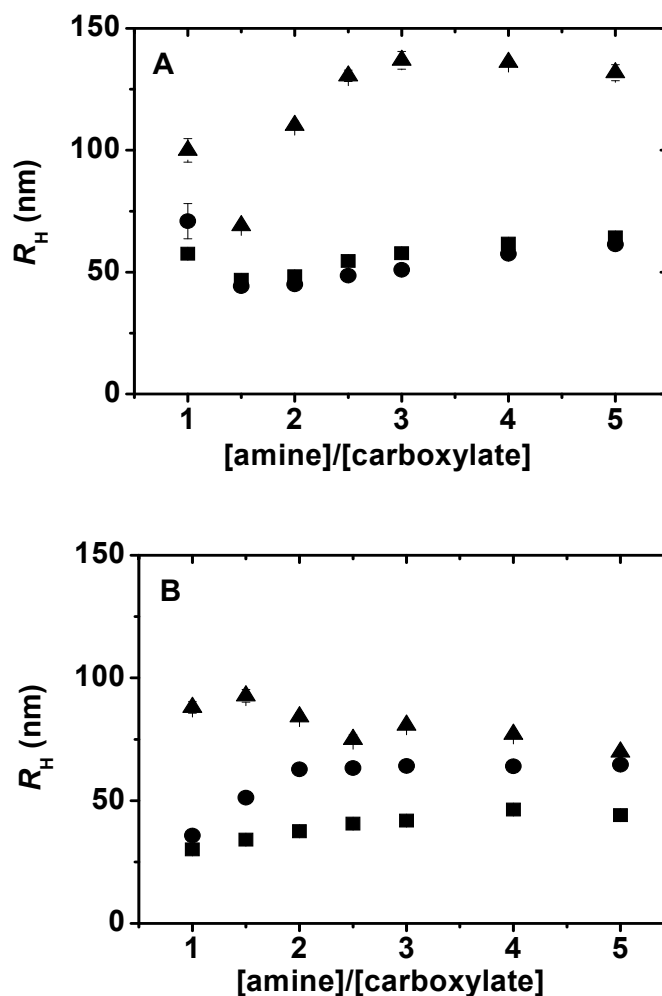


Figure 4.5. Effect of the $[\text{amine}]/[\text{carboxylate}]$ molar ratio on the hydrodynamic radius of paromomycin sulfate (panel A) and neomycin sulfate (panel B) micelles with different polymers: CMD-PEG (\blacktriangle), dodecyl₁₈-CMD-PEG (\bullet), dodecyl₃₈-CMD-PEG (\blacksquare). Micelles were prepared in phosphate buffer (10 mM, pH 7.0) at polymer concentration = 0.2 g/L.

R_H of neomycin/CMD-PEG micelles slightly decreased by increasing the [amine]/[carboxylate] ratio and levelled off at [amine]/[carboxylate] = 2.5, again reaching the maximum drug loading (Figure 4.5B). PDI was < 0.1 for both neomycin and paromomycin micelles prepared at [amine]/[carboxylate] > 1.5 indicating the narrow particle size distribution of the micelles.^[17] Neomycin micelles had smaller size than those of paromomycin (Table 4.5) presumably as a result of tighter electrostatic interactions in the core of neomycin micelles due to the presence of an additional amino group in neomycin (Figure 4.1). This amino group has pKa of 9.24, which makes it fully ionized at pH 7.0.^[31]

Figure 4.5 shows also the R_H of neomycin and paromomycin micelles prepared with dodecyl₁₈-CMD-PEG and dodecyl₃₈-CMD-PEG plotted as a function of [amine]/[carboxylate] ratio. Hydrophobic modification of CMD-PEG significantly affected the size of its micelles with paromomycin. Thus, paromomycin/CMD-PEG micelles were almost twice as big as those of paromomycin/dodecyl-CMD-PEG micelles at identical [amine]/[carboxylate] ratios and polymer concentration. Similar effect was observed for neomycin micelles (Figure 4.5B). No significant difference in size was detected between paromomycin micelles with either dodecyl₁₈-CMD-PEG or dodecyl₃₈-CMD-PEG copolymers (Figure 4.5A). Yet, neomycin/dodecyl₃₈-CMD-PEG micelles were smaller than those of neomycin/dodecyl₁₈-CMD-PEG (Table 4.5). PIC micelles have well-solvated core and corona.^[48] The core of aminoglycosides/CMD-PEG micelles is expected to be hydrated and swollen since it is formed by hydrophilic compounds (neomycin and paromomycin-electrostatically linked to CMD segment of the polymer). On the other hand, aminoglycosides/dodecyl-CMD-PEG micelles may have less hydrated core due to the presence of hydrophobic dodecyl chains. Less hydrated core together with hydrophobic interactions between dodecyl chains probably resulted in PIC micelles with tighter core and hence, a smaller size. Gao *et al.*, reported similar results where lysozyme /poly(1-tetradecene-alt-maleic acid) complexes were smaller than those of lysozyme/poly(isobutylene-alt-maleic acid), which was attributed to hydrophobic interactions in the case of poly(1-tetradecene-alt-maleic acid).^[18]

4.5.4. Effect of salt on micelles formation and stability

Figure 4.6 shows the effect of salt on the neomycin and paromomycin micelles integrity in terms of intensity of scattered light and micelles size. Micelles were prepared in phosphate buffer (10 mM, pH 7.0) with CMD-PEG and dodecyl-CMD-PEG polymers. Turning our attention first to aminoglycosides micelles with unmodified CMD-PEG, paromomycin/CMD-PEG micelles rapidly disintegrated upon increasing salt concentration (Figure 4.6A). They lost ~ 80% of their scattered light intensity at [NaCl] of 50 mM and disintegrated almost completely at [NaCl] of 100 mM. Neomycin/CMD-PEG micelles were more resistant to salt-induced disintegration. For instance, they maintained the same scattered light intensity for [NaCl] \leq 50 mM, after which the intensity rapidly decreased reaching ~ 30% of the initial value at [NaCl] = 100 mM (Figure 4.6C). The different salt tolerance for neomycin and paromomycin micelles may be attributed to stronger electrostatic interactions in the core of neomycin micelles due to the presence of an additional amino group. Salt had similar effect on the size of both neomycin/CMD-PEG and paromomycin/CMD-PEG micelles (Figure 4.6B and D). Size of both micelles increased upon increasing [NaCl] up to 50 and 150 mM for paromomycin and neomycin micelles, respectively. Further increase in [NaCl] led to decrease in micelles size, probably as a sign of micelle disintegration. Salt causes dehydration of the micelles PEG corona, which facilitates the formation of bigger micelles.^[20] These results of instability of aminoglycosides/CMD-PEG micelles under physiological salt concentration (150 mM NaCl) are in agreement with those shown by NMR studies (see above).

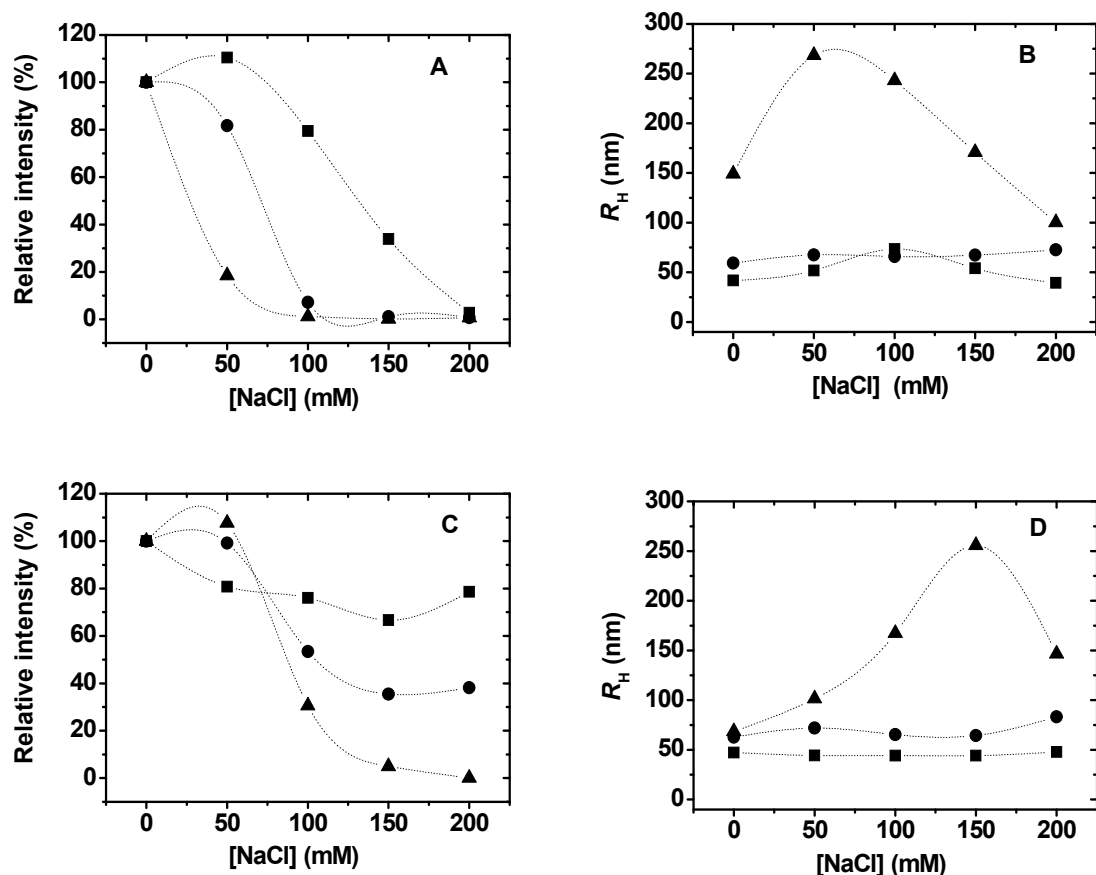


Figure 4.6. Effect of salt on the intensity of scattered light and hydrodynamic radius of paromomycin (panels A and B) and neomycin (panels C and D) micelles with different CMD-PEG copolymers: dodecyl₃₈-CMD-PEG (■), dodecyl₁₈-CMD-PEG (●), CMD-PEG (▲). Micelles were prepared in phosphate buffer (10 mM, pH 7.0) at final polymer concentration = 0.5 g/L and [amine]/[carboxylate] = 2.5. Relative scattering intensity = intensity at certain salt concentration/ intensity at salt concentration = 0.

Figure 4.6 shows also the effect of salt on the stability of aminoglycosides/dodecyl-CMD-PEG micelles. Hydrophobic modification of CMD-PEG copolymers greatly enhanced the stability of their micelles with aminoglycosides against increase in salinity. Thus, the neomycin/dodecyl₁₈-CMD-PEG micelles maintained their initial size and ~ 40 % of their scattering intensity at [NaCl] = 150 mM (Figure 4.6C and D). Better ability to resist

salt-induced disintegration was achieved by increasing the level of dodecyl modification of CMD-PEG. For instance, neomycin/dodecyl₃₈-CMD-PEG micelles maintained the same size and ~ 80% of their initial scattered light intensity for salt concentrations up to 200 mM, well above the physiological salt concentration. Hydrophobic modification of CMD-PEG had a less pronounced effect on paromomycin micelles stability against increase in salinity. Yet, the micelles of paromomycin/dodecyl₃₈-CMD-PEG maintained their initial size and ~ 80% of their initial scattered light intensity at [NaCl] = 100 mM, compared to negligible scattered light intensity for paromomycin/CMD-PEG micelles at the same [NaCl]. Interestingly, neomycin/dodecyl₃₈-CMD-PEG micelles prepared under physiological conditions ([NaCl] = 150 mM and pH 7.4) showed no signs of micelles disintegration even after three month of micelles storage at room temperature. From these results it can be concluded that the level of CMD-PEG hydrophobic modification, as well as the basicity of the aminoglycoside amino groups are major factors determining micelles stability against increase in salinity. Enhanced stability of neomycin/dodecyl₃₈-CMD-PEG against salt-induced disintegration is probably due to the participation of electrostatic and hydrophobic interactions in the formation of tighter micelles core. Similar results were reported previously for other PIC micelles.^[18, 49]

In addition to hydrophobic modification of CMD-PEG, we prepared guanidylated paromomycin as another approach to increase stability of PIC micelles against salt-induced disintegration. Guanidine groups are more basic than amino groups, planar and exhibit directionality in their hydrogen bonding interactions.^[51] Therefore, we hypothesize that guanidylated paromomycin could have stronger electrostatic interactions with CMD-PEG than paromomycin leading to more stable micelles. To test this hypothesis, we prepared 6'''-guanidino-paromomycin and 5''-deoxy-5''-guanidino-paromomycin (Figure SI.4.1, supporting information) and tested the stability of their micelles with CMD-PEG at different salt concentrations. Guanidylated paromomycin showed better ability to withstand salt-induced disintegration. Thus, 6'''-guanidino-paromomycin/CMD-PEG micelles retained ~ 40 % of their initial scattering intensity at 50 mM NaCl compared to ~ 20 % for paromomycin at the same salt concentration (Figure SI.4.3A, supporting information).

Replacement of paromomycin 5' hydroxyl group by a guanidine group (5'-deoxy-5'-guanidino-paromomycin) resulted in a much better stabilizing effect against salt. As illustrated in Figure SI.4.3A, 5'-deoxy-5'-guanidino-paromomycin/CMD-PEG micelles maintained the same scattered light intensity for $[\text{NaCl}] \leq 50 \text{ mM}$ and $\sim 30\%$ of their initial scattered light intensity at $[\text{NaCl}] = 100 \text{ mM}$. This enhanced stability of guanidylated paromomycin micelles might result from stronger interactions between guanidine groups of the drug and carboxylate groups of CMD-PEG.

4.5.5. pH studies

4.5.5.1. Effect of pH on the self assembly of CMD-PEG and dodecyl-CMD-PEG in aqueous solution

Figure 4.7 shows the effect of pH on the intensity of light scattered by different CMD-PEG polymeric solutions. Intensity of light scattered by unmodified CMD-PEG solutions was very small and almost constant over the 2-9 pH range. This indicates that CMD-PEG, under these conditions does not self-assemble into nanoparticles. In contrast, dodecyl-CMD-PEG showed pH-dependent self assembly. Thus, intensity of light scattered by dodecyl-CMD-PEG solutions was small and constant over the pH range 7-9. At $\text{pH} < 6.0$, intensity of scattered light increased for both dodecyl₁₈-CMD-PEG and dodecyl₃₈-CMD-PEG and continued to increase with further decrease in pH. Below pH 5.0, intensity of light scattered by dodecyl₁₈-CMD-PEG was less than that of dodecyl₃₈-CMD-PEG. At $\text{pH} > 6.0$, carboxylate groups of CMD-PEG are ionized leading to electrostatic repulsion that prevents self assembly. Dodecyl-CMD-PEG did not show self assembly at $\text{pH} > 6.0$ probably because electrostatic repulsions between ionized carboxylate groups offset hydrophobic attractions by dodecyl chains. Electrostatic repulsions were absent in acidic solutions due to neutralization of carboxylate groups, though CMD-PEG did not form nanoparticles due to lack of amphiphilicity. In contrast, dodecyl-CMD-PEG formed nanoparticles in acidic solutions due to absence of electrostatic repulsions and presence of

hydrophobic interactions between dodecyl chains. At pH 3.0, R_H of dodecyl₃₈-CMD-PEG and dodecyl₁₈-CMD-PEG were 99.72 ± 8.9 nm and 87.81 ± 7.7 nm, respectively.

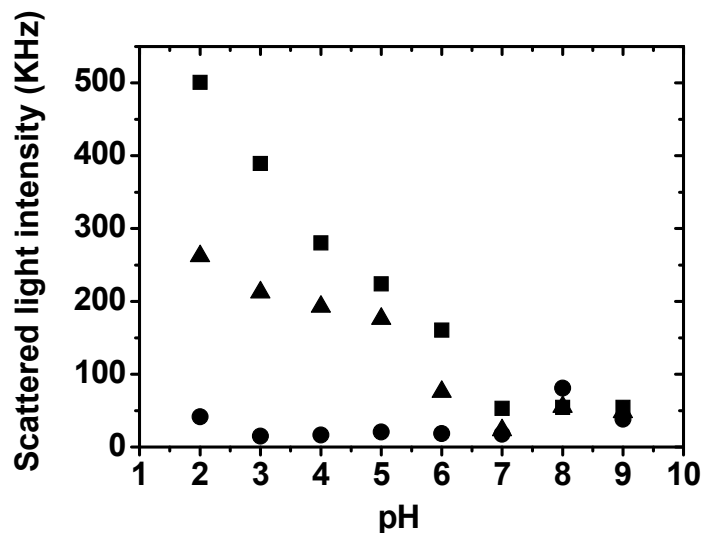


Figure 4.7. Effect of pH on the intensity of light scattered by polymeric solutions of dodecyl₃₈-CMD-PEG (■), dodecyl₁₈-CMD-PEG (▲), and CMD-PEG (●). Solutions were prepared in 10 mM phosphate buffer at polymer concentration of 0.2 mg/mL.

4.5.5.2. Aminoglycosides/CMD-PEG micelles

The solution pH affects the formation and stability of aminoglycosides/CMD-PEG PIC micelles since it affects the degree of ionization of both the drugs and the polymer. We examined by DLS the effect of pH on the integrity of different aminoglycosides/CMD-PEG micelles in terms of intensity of scattered light and hydrodynamic radius (Figure 4.8). One notices that both the intensity of scattered light and R_H were almost constant for $4.0 \leq \text{pH} \leq 7.0$ for all the drugs studied. This pH range corresponds to full ionization of both the drugs and polymer. Therefore, electrostatic interactions between the drugs amino groups and CMD-PEG carboxylate groups are most favourable. Scattered light intensity decreased by decreasing pH below 4.0 signalling the formation of loose drug/polymer associates due to

neutralization of CMD-PEG. Similar decrease in scattered light intensity was observed at pH values > 7.0 due to neutralization of the drugs.

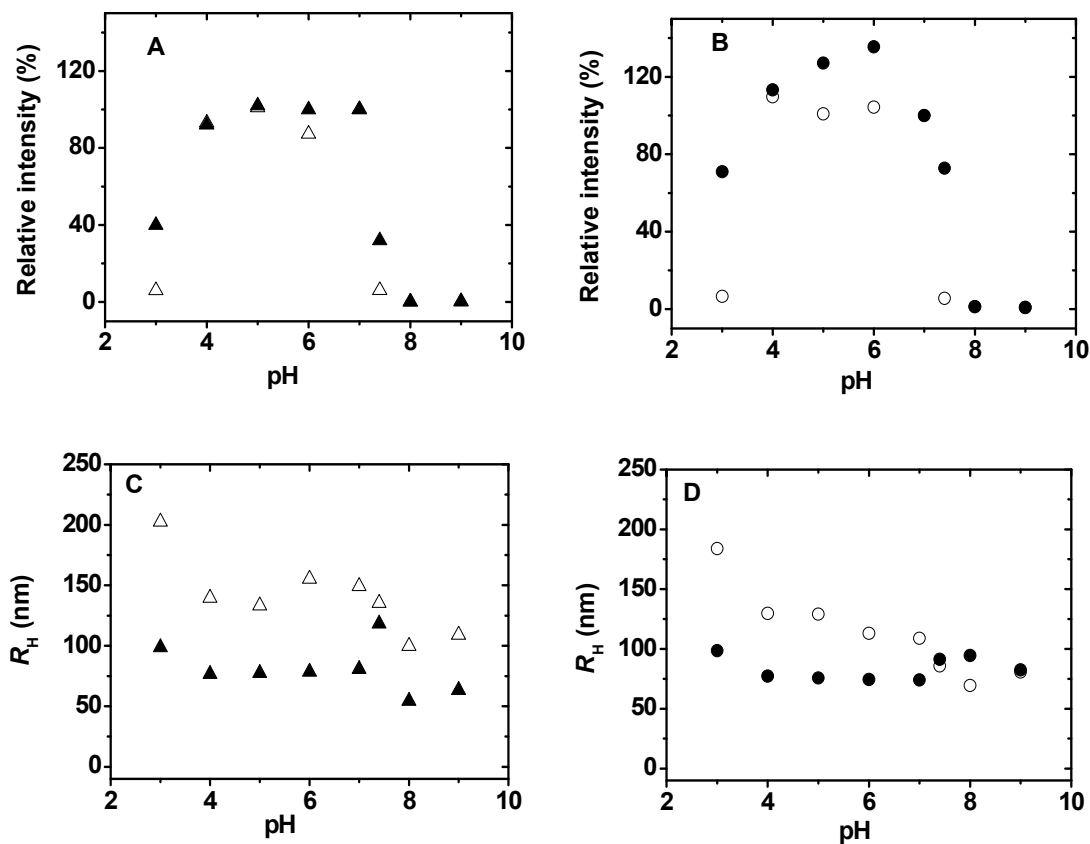


Figure 4.8. Effect of pH on the intensity of scattered light (A and B) and hydrodynamic radius (C and D) of CMD-PEG micelles with different aminoglycosides: neomycin (▲), paromomycin (△), 6''-guanidino-paromomycin (○) and 5''-deoxy-5''-guanidino-paromomycin (●). Micelles were prepared in phosphate buffer (10 mM, pH 7.0) at final [CMD-PEG] = 0.5 g/L. Relative scattering intensity = intensity at certain pH/ intensity at pH 7.0.

Scattered light intensity for neomycin and 5''-deoxy-5''-guanidino-paromomycin micelles at pH 7.4 was higher than that of paromomycin micelles (Figure 4.8). Moreover, the size of neomycin and 5''-deoxy-5''-guanidino-paromomycin was smaller than that of

paromomycin micelles. These observations may be attributed due to the presence of an additional amino group and a guanidine group in neomycin and 5''-deoxy-5''-guanidino-paromomycin, respectively. These groups are highly basic and are almost completely ionized at pH 7.4 resulting in stronger interactions with CMD-PEG carboxylate groups. Identical experiments carried out on the micelles of aminoglycosides/dodecyl-CMD-PEG showed similar effect of pH on the micelles formation and stability.

4.5.6. Effect of freeze drying on micelles integrity

Both neomycin/CMD-PEG and paromomycin/CMD-PEG micelles were readily dispersed in distilled water after freeze drying without the need of lyoprotectants. However, the freeze drying process increased the size of the micelles from 85.1 ± 1.5 to 118.48 ± 2.8 nm and from 149.0 ± 4.8 to 168.9 ± 5.4 nm for neomycin and paromomycin micelles, respectively. Size of neomycin/ dodecyl₁₈-CMD-PEG micelles also increased after freeze drying and reconstitution from 63.3 ± 0.7 nm to 78.8 ± 0.9 nm. In contrast, neomycin/ dodecyl₃₈-CMD-PEG micelles showed $R_H \sim 40$ nm both before and after freeze drying, in the absence of cryoprotectants showing the ability of these micelles to withstand the stresses of the freeze drying process.

4.5.7. Effect of dilution on micelles stability

Micelles used for *in vivo* applications are subjected to extensive dilution upon intravenous administration. Therefore, they should be stable against dilution for a period of time long enough to allow delivery of the encapsulated drug to its target.^[52] Figure 4.9 shows the hydrodynamic radius and scattered light intensity plotted as a function of polymer concentration for neomycin/CMD-PEG and paromomycin/CMD-PEG micelles. Both micelles were prepared in phosphate buffer (10 mM, pH 7.0) at [CMD-PEG] = 0.5 g/L and serially diluted to different polymer concentrations using the same buffers. Micelles dilution decreased the scattered light intensity due to a decrease in micelles concentration. Micelles critical association concentration (CAC) (the minimal polymer concentration for which micelles can be detected) was determined from the plot as the

concentration corresponding to the onset of the increase in the scattered light intensity (Figure 4.9).^[53]

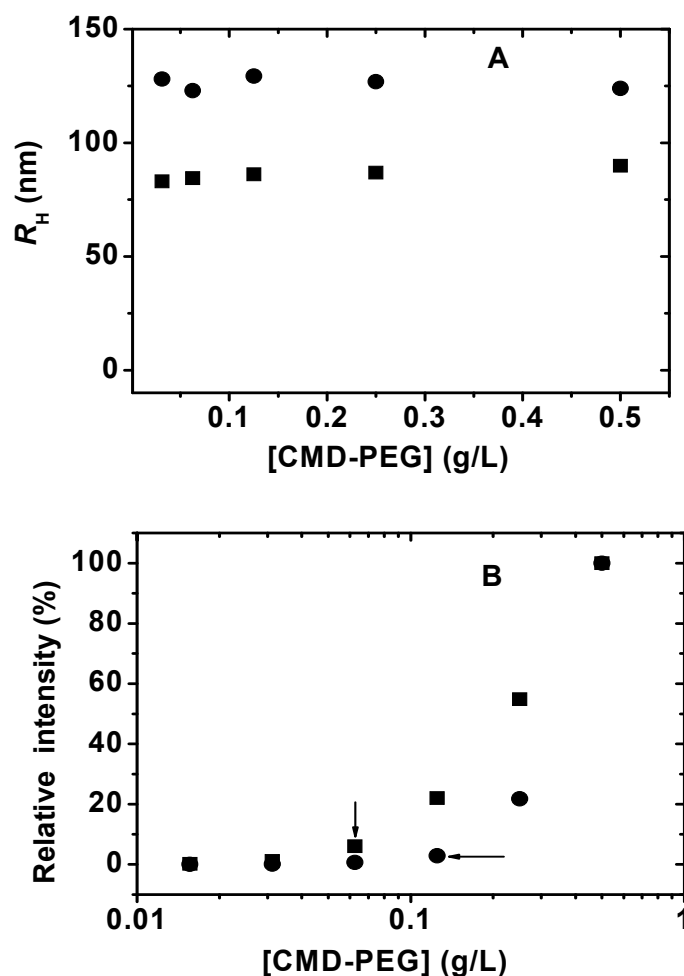


Figure 4.9. Effect of dilution on the hydrodynamic radius (A) and relative intensity of scattered light (B) for neomycin/CMD-PEG micelles (■) and paromomycin/CMD-PEG micelles (●). Relative scattering intensity = intensity at certain CMD-PEG concentration/intensity at CMD-PEG concentration of 0.5 g/L.

The CAC values were 0.0625 and 0.125 g/L for neomycin and paromomycin micelles, respectively. Neomycin micelles were more resistant to dilution than those of paromomycin as indicated by their lower CAC. This may be attributed to tighter

interactions in the core of neomycin micelles due to the presence of an additional amino group. The size of both micellar systems was not affected by the dilution and remained constant for polymer concentrations as low as 0.05 g/L.

4.5.8. Drug release studies

The release of neomycin from its PIC micelles with CMD-PEG and dodecyl₃₈-CMD-PEG was evaluated by the dialysis bag method (Figure 4.10). Neomycin release experiments were carried out in phosphate buffer at different pH values and different salt concentrations since these factors are known to affect drug release rate from PIC micelles.^[20, 28] Neomycin rapidly diffused out through the dialysis membrane in the absence of polymers and almost complete release was achieved after 4 h (Figure 4.10). In contrast, micelles-encapsulated neomycin showed slower release rate under all the conditions studied. Neomycin release rate from the micelles was strongly affected by ionic strength of the release medium. For instance, the slowest release rate was detected in phosphate buffer at pH 7.0-7.4 and 0 mM NaCl. Under these conditions neomycin was slowly released from the micelles where ~ 30% was released after 24 h. Neomycin release rate was significantly increased by increasing [NaCl] from 0 to 150 mM. Thus, after 24 h percent drug released increased from ~ 30 % at pH 7.4, [NaCl] = 0 mM to ~ 70% at pH 7.4, [NaCl] = 150 mM. Higher drug release rate in the presence of 150 mM NaCl confirms that drug is released by an ion exchange mechanism.^[54] Similar observations were reported for other PIC micelles.^[28] Despite higher neomycin release rate under physiological conditions (pH 7.4, [NaCl] = 150 mM), the micelles were still able to sustain drug release for more than 24 h (Figure 4.10). Neomycin release rate from the micelles was not affected by increasing pH from 7.0 to 7.4 neither in presence nor in absence of 150 mM NaCl. Neomycin/dodecyl₃₈-CMD-PEG micelles showed drug release rate that was not significantly different from that of neomycin/CMD-PEG micelles. It is noteworthy that no burst drug release was detected even in the presence of high salt concentration confirming that the drug is located in the micelles core. Drug located near nanoparticles surface rapidly diffuses out in the release medium giving a burst release effect.^[28]

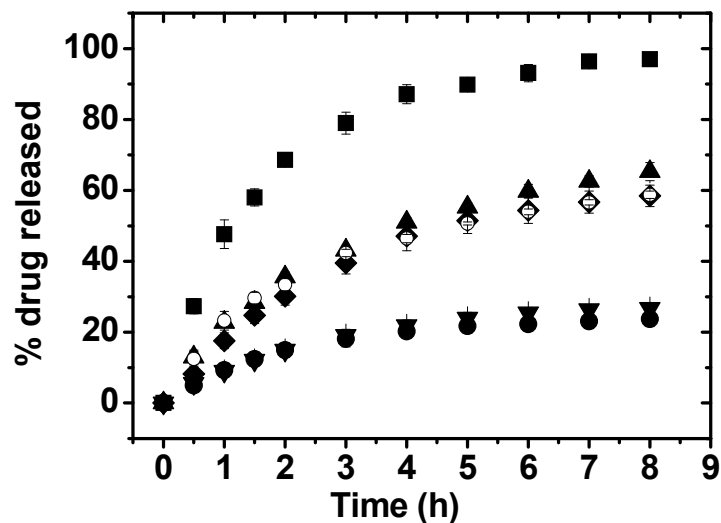


Figure 4.10. Release profiles at 37 °C in 10 mM phosphate buffer of neomycin from: neomycin alone (■); neomycin/CMD-PEG micelles, pH 7.0, [NaCl] = 0 mM (●); neomycin/CMD-PEG micelles, pH 7.4, [NaCl] = 0 mM (▼); neomycin/CMD-PEG micelles, pH 7.0, [NaCl] = 150 mM (◆); neomycin/CMD-PEG micelles, pH 7.4, [NaCl] = 150 mM (▲); neomycin/dodecyl₃₈-CMD-PEG micelles, pH 7.4, [NaCl] = 150 mM (○). ([neomycin] = 2.0 g/L, [amine]/[carboxylate] = 2.5).

4.5.9. Antibacterial activity of micelles-encapsulated aminoglycosides

ITC studies showed that neomycin sulfate and paromomycin sulfate bind to CMD-PEG in a pattern similar to their binding to the A site of 16S rRNA.^[31, 37] The reason behind this similarity may be that binding in both cases is triggered by electrostatic interactions between aminoglycosides amino groups and phosphate groups in rRNA or carboxylate groups in CMD-PEG. It should be recalled here that the antibacterial activity of aminoglycosides derives from their binding to 16S rRNA. Therefore, it was important to confirm that interactions between aminoglycosides and CMD-PEG did not affect their

ability to bind to 16S rRNA. Antibacterial activity of many aminoglycosides encapsulated in CMD-PEG micelles was evaluated by exposing a test organism (*E. coli* X-1 blue strain) to different drug concentrations and determining the lowest concentration that prevents detectable bacterial growth (minimal inhibitory concentration, MIC). Antibacterial activity of several aminoglycosides (neomycin, paromomycin, tobramycin and amikacin) was not altered by their encapsulation in CMD-PEG micelles. Thus, whether drugs were free or encapsulated in PIC micelles, MICs were 2-8, 4-8, 2.5-5 and 2-8 µg/mL for amikacin, neomycin, paromomycin and tobramycin, respectively. These results confirm that encapsulation of aminoglycosides in CMD-PEG micelles did not reduce their antibacterial activity. Similar results were reported for ciprofloxacin encapsulated in polyethylbutylcyanoacrylate nanoparticles and amphotericin B encapsulated in poly(lactic-co-glycolic acid) nanoparticles.^[55, 56]

4.6. Conclusion

PIC micelles were formed by electrostatic interactions between two aminoglycosides: neomycin sulfate and paromomycin sulfate and different CMD-PEG copolymers. ITC studies showed that interactions between either neomycin or paromomycin and CMD-PEG were accompanied by uptake of protons from the buffer, the number of which was pH and temperature dependent. PIC micelles of aminoglycosides/CMD-PEG had a core consisting of drug/CMD complex and a PEG corona. Aminoglycosides/CMD-PEG micelles were unstable under physiological conditions (pH 7.4, [NaCl] = 150 mM). Interestingly, micelles stability under these conditions was significantly improved by hydrophobic modification of CMD-PEG. Optimal micelle formation (neomycin/dodecyl₃₈-CMD-PEG) resisted salt-induced disintegration for up to 200 mM and sustained drug release under physiological conditions for more than 24 h. They maintained their integrity after freeze drying and upon storage at room temperature for up to 3 months. Favourable micelles properties (e.g. small size, ability to withstand increases in salinity and change in pH) were observed for drugs having more cationic groups (neomycin and 5"-deoxy-5"-guanidino-paromomycin rather than

paromomycin) and polymer having both carboxylate and dodecyl groups (dodecyl-CMD-PEG rather than CMD-PEG). Other aminoglycosides (e.g. gentamicin, amikacin and tobramycin) were also successfully encapsulated in CMD-PEG micelles. Further *in vivo* evaluation of micelles-encapsulated aminoglycosides is under way since preliminary experiments indicated that drugs encapsulated in the micelles retained their antimicrobial activity.

4.7. Acknowledgments

The work was supported in part by a grant of the Natural Sciences and Engineering Research Council of Canada to FMW. GMS acknowledges financial support by the Ministry of Higher Education, Egypt.

4.8. References

- [1] Daniel SP, Malvika K, Christopher MB, John EK. Thermodynamics of aminoglycoside-rRNA recognition. *Biopolymers* **2003**, *70*: 58-79.
- [2] Hombach J, Hoyer H, Bernkop-Schnürch A. Thiolated chitosans: Development and in vitro evaluation of an oral tobramycin sulphate delivery system. *Eur. J. Pharm. Sci.* **2008**, *33*: 1-8.
- [3] Moazed D, Noller HF. Interaction of antibiotics with functional sites in 16s ribosomal-RNA. *Nature* **1987**, *327*: 389-94.
- [4] Nagai J, Takano M. Molecular aspects of renal handling of aminoglycosides and strategies for preventing the nephrotoxicity. *Drug Metabol. Pharmacokinet.* **2004**, *19*: 159-70.
- [5] Roberta C, Alessandro B, Valerio P, Elisabetta M, Gian Paolo Z, Maria Rosa G. Duodenal administration of solid lipid nanoparticles loaded with different percentages of tobramycin. *J. Pharm. Sci.* **2003**, *92*: 1085-94.
- [6] Halwani M, Mugabe C, Azghani AO, Lafrenie RM, Kumar A, Omri A. Bactericidal efficacy of liposomal aminoglycosides against *Burkholderia cenocepacia*. *J. Antimicrob. Chemother.* **2007**, *60*: 760-9.
- [7] Mugabe C, Halwani M, Azghani AO, Lafrenie RM, Omri A. Mechanism of enhanced activity of liposome-entrapped aminoglycosides against resistant strains of *Pseudomonas aeruginosa*. *Antimicrob. Agents Chemother.* **2006**, *50*: 2016-22.
- [8] Abraham AM, Walubo A. The effect of surface charge on the disposition of liposome-encapsulated gentamicin to the rat liver, brain, lungs and kidneys after intraperitoneal administration. *Int. J. Antimicrob. Agents* **2005**, *25*: 392-7.
- [9] Lecaroz MC, Blanco-Prieto MJ, Campanero MA, Salman H, Gamazo C. Poly(D,L-lactide-co-glycolide) particles containing gentamicin: Pharmacokinetics and

- pharmacodynamics in *Brucella melitensis*-infected mice. *Antimicrob. Agents Chemother.* **2007**, *51*: 1185-90.
- [10] Cavalli R, Gasco MR, Chetoni P, Buralassi S, Saettone MF. Solid lipid nanoparticles (SLN) as ocular delivery system for tobramycin. *Int. J. Pharm.* **2002**, *238*: 241-5.
- [11] Chuang HF, Smith R, xe, C, Hammond PT. Polyelectrolyte multilayers for tunable release of antibiotics. *Biomacromolecules* **2008**, *9*: 1660-8.
- [12] Mugabe C, Azghani AO, Omri A. Preparation and characterization of dehydration-rehydration vesicles loaded with aminoglycoside and macrolide antibiotics. *Int. J. Pharm.* **2006**, *307*: 244-50.
- [13] Bridges PA, Taylor KMG. The effects of freeze-drying on the stability of liposomes to jet nebulization. *J. Pharm. Pharmacol.* **2001**, *53*: 393-8.
- [14] Prior S, Gander B, Irache JM, Gamazo C. Gentamicin-loaded microspheres for treatment of experimental *Brucella abortus* infection in mice. *J. Antimicrob. Chemother.* **2005**, *55*: 1032-6.
- [15] Otsuka H, Nagasaki Y, Kataoka K. PEGylated nanoparticles for biological and pharmaceutical applications. *Adv. Drug Deliv. Rev.* **2003**, *55*: 403-19.
- [16] Merdan T, Kopecek J, Kissel T. Prospects for cationic polymers in gene and oligonucleotide therapy against cancer. *Adv. Drug Deliv. Rev.* **2002**, *54*: 715-58.
- [17] Bontha S, Kabanov AV, Bronich TK. Polymer micelles with cross-linked ionic cores for delivery of anticancer drugs. *J. Controlled Release* **2006**, *114*: 163-74.
- [18] Gao G, Yao P. Structure and activity transition of lysozyme on interacting with and releasing from polyelectrolyte with different hydrophobicity. *J. Polym. Sci. Pol. Chem.* **2008**, *46*: 4681-90.

- [19] Matsumura Y, Maeda H. A new concept for macromolecular therapeutics in cancer-chemotherapy - mechanism of tumorotropic accumulation of proteins and the antitumor agent smancs. *Cancer Res.* **1986**, *46*: 6387-92.
- [20] Soliman GM, Winnik FM. Enhancement of hydrophilic drug loading and release characteristics through micellization with new carboxymethyl-dextran-PEG block copolymers of tunable charge density. *Int. J. Pharm.* **2008**, *356*: 248-58.
- [21] Soliman GM, Choi AO, Maysinger D, Winnik FM. Minocycline block copolymer micelles and their anti-inflammatory effects on microglia. *Macromol. Biosci.* *In press.*
- [22] Matsumoto S, Christie RJ, Nishiyama N, Miyata K, Ishii A, Oba M, Koyama H, Yamasaki Y, Kataoka K. Environment-responsive block copolymer micelles with a disulfide cross-linked core for enhanced siRNA delivery. *Biomacromolecules* **2009**, *10*: 119-27.
- [23] Hernandez OS, Soliman GM, Winnik FM. Synthesis, reactivity, and pH-responsive assembly of new double hydrophilic block copolymers of carboxymethyl-dextran and poly(ethylene glycol). *Polymer* **2007**, *48*: 921-30.
- [24] Mauzac M, Jozefonvicz J. Anticoagulant activity of dextran derivatives. Part I: Synthesis and characterization. *Biomaterials* **1984**, *5*: 301-4.
- [25] Suchitra S, Sampath, Robinson DH. Comparison of new and existing spectrophotometric methods for the analysis of tobramycin and other aminoglycosides. *J. Pharm. Sci.* **1990**, *79*: 428-31.
- [26] Kawamura A, Harada A, Kono K, Kataoka K. Self-assembled nano-bioreactor from block ionomers with elevated and stabilized enzymatic function. *Bioconjugate Chem.* **2007**, *18*: 1555-9.
- [27] Chelushkin PS, Lysenko EA, Bronich TK, Eisenberg A, Kabanov VA, Kabanov AV. Polyion complex nanomaterials from block polyelectrolyte micelles and linear

- polyelectrolytes of opposite charge: 1. Solution Behavior. *J. Phys. Chem. B* **2007**, *111*: 8419-25.
- [28] Yang KW, Li XR, Yang ZL, Li PZ, Wang F, Liu Y. Novel polyion complex micelles for liver-targeted delivery of diammonium glycyrrhizinate: *In vitro* and *in vivo* characterization. *J. Biomed. Mater. Res. Part A* **2009**, *88A*: 140-8.
- [29] Gaucher G, Dufresne M-H, Sant VP, Kang N, Maysinger D, Leroux J-C. Block copolymer micelles: Preparation, characterization and application in drug delivery. *J. Controlled Release* **2005**, *109*: 169-88.
- [30] Baker BM, Murphy KP. Evaluation of linked protonation effects in protein binding reactions using isothermal titration calorimetry. *Biophys. J.* **1996**, *71*: 2049-55.
- [31] Kaul M, Barbieri CM, Kerrigan JE, Pilch DS. Coupling of drug protonation to the specific binding of aminoglycosides to the A site of 16 S rRNA: Elucidation of the number of drug amino groups involved and their identities. *J. Mol. Biol.* **2003**, *326*: 1373-87.
- [32] Botto RE, Coxon B. Nitrogen-15 nuclear magnetic resonance spectroscopy of neomycin B and related aminoglycosides. *JACS* **1983**, *105*: 1021-8.
- [33] Barbieri CM, Pilch DS. Complete thermodynamic characterization of the multiple protonation equilibria of the aminoglycoside antibiotic paromomycin: A calorimetric and natural abundance ¹⁵N NMR study. *Biophys. J.* **2006**, *90*: 1338-49.
- [34] Ehtezazi T, Rungsardthong U, Stolnik S. Thermodynamic analysis of polycation-DNA interaction applying titration microcalorimetry. *Langmuir* **2003**, *19*: 9387-94.
- [35] Lobo BA, Koe GS, Koe JG, Middaugh CR. Thermodynamic analysis of binding and protonation in DOTAP/DOPE (1:1): DNA complexes using isothermal titration calorimetry. *Biophys. Chem.* **2003**, *104*: 67-78.
- [36] Takahashi M, Maraboeuf F, Morimatsu K, Selmane T, Fleury F, Norden B. Calorimetric analysis of binding of two consecutive DNA strands to RecA protein

- illuminates mechanism for recognition of homology. *J. Mol. Biol.* **2007**, *365*: 603-11.
- [37] Kaul M, Pilch DS. Thermodynamics of aminoglycoside-rRNA recognition: The binding of neomycin-class aminoglycosides to the A site of 16S rRNA. *Biochemistry* **2002**, *41*: 7695-706.
- [38] Ou Z, Muthukumar M. Entropy and enthalpy of polyelectrolyte complexation: Langevin dynamics simulations. *J. Chem. Phys.* **2006**, *124*: 154902-11.
- [39] Hofs B, Voets IK, Keizer Ad, Stuart MAC. Comparison of complex coacervate core micelles from two diblock copolymers or a single diblock copolymer with a polyelectrolyte. *PCCP* **2006**, *8*: 4242-51.
- [40] Santos HA, Manzanares JA, Murtomäki L, Kontturi K. Thermodynamic analysis of binding between drugs and glycosaminoglycans by isothermal titration calorimetry and fluorescence spectroscopy. *Eur. J. Pharm. Sci.* **2007**, *32*: 105-14.
- [41] Mazur S, Tanious FA, Ding D, Kumar A, Boykin DW, Simpson IJ, Neidle S, Wilson WD. A thermodynamic and structural analysis of DNA minor-groove complex formation. *J. Mol. Biol.* **2000**, *300*: 321-37.
- [42] Privalov PL, Makhatadze GI. Contribution of hydration and non-covalent interactions to the heat capacity effect on protein unfolding. *J. Mol. Biol.* **1992**, *224*: 715-23.
- [43] Lee C-F, Allen MD, Bycroft M, Wong K-B. Electrostatic interactions contribute to reduced heat capacity change of unfolding in a thermophilic ribosomal protein L30e. *J. Mol. Biol.* **2005**, *348*: 419-31.
- [44] Goncalves E, Kitas E, Seelig J. Structural and thermodynamic aspects of the interaction between heparan sulfate and analogues of melittin. *Biochemistry* **2006**, *45*: 3086-94.

- [45] Hrkach JS, Peracchia MT, Bomb A, Lotan n, Langer R. Nanotechnology for biomaterials engineering: Structural characterization of amphiphilic polymeric nanoparticles by ¹H NMR spectroscopy. *Biomaterials* **1997**, *18*: 27-30.
- [46] Jeong YI, Kim SH, Jung TY, Kim IY, Kang SS, Jin YH, Ryu HH, Sun HS, Jin SG, Kim KK, Ahn KY, Jung S. Polyion complex micelles composed of all-trans retinoic acid and poly(ethylene glycol)-grafted-citosan. *J. Pharm. Sci.* **2006**, *95*: 2348-60.
- [47] Reid DG, Gajjar K. A proton and carbon 13 nuclear magnetic resonance study of neomycin B and its interactions with phosphatidylinositol 4,5-bisphosphate. *J. Biol. Chem.* **1987**, *262*: 7967-72.
- [48] Voets IK, de Keizer A, Stuart MAC. Complex coacervate core micelles. *Adv. Colloid Interface Sci.* **2009**, *147-148*: 300-18.
- [49] Yuan X, Harada A, Yamasaki Y, Kataoka K. Stabilization of lysozyme-incorporated polyion complex micelles by the ω-end derivatization of poly(ethylene glycol)-poly(α,β-aspartic acid) block copolymers with hydrophobic groups. *Langmuir* **2005**, *21*: 2668-74.
- [50] Yuan X, Yamasaki Y, Harada A, Kataoka K. Characterization of stable lysozyme-entrapped polyion complex (PIC) micelles with crosslinked core by glutaraldehyde. *Polymer* **2005**, *46*: 7749-58.
- [51] Luedtke NW, Baker TJ, Goodman M, Tor Y. Guanidinoglycosides: A novel family of RNA ligands. *JACS* **2000**, *122*: 12035-6.
- [52] Torchilin VP. Structure and design of polymeric surfactant-based drug delivery systems. *J. Controlled Release* **2001**, *73*: 137-72.
- [53] Li Y, Kwon GS. Methotrexate esters of poly(ethylene oxide)-block-poly(2-hydroxyethyl-L-aspartamide). Part I: Effects of the level of methotrexate conjugation on the stability of micelles and on drug release. *Pharm. Res.* **2000**, *17*: 607-11.

- [54] Aliabadi HM, Lavasanifar A. Polymeric micelles for drug delivery. *Expert Opin. Drug Deliv.* **2006**, *3*: 139-62.
- [55] Page-Clisson ME, Pinto-Alphandary H, Ourevitch M, Andremont A, Couvreur P. Development of ciprofloxacin-loaded nanoparticles: Physicochemical study of the drug carrier. *J. Controlled Release* **1998**, *56*: 23-32.
- [56] Bang J-Y, Song C-E, Kim C, Park W-D, Cho K-R, Kim P-I, Lee S-R, Chung W-T, Choi K-C. Cytotoxicity of amphotericin B-incorporated polymeric micelles composed of poly(DL-lactide-co-glycolide)/dextran graft copolymer. *Arch. Pharmacol Res.* **2008**, *31*: 1463-9.

Appendix C. Supporting information (SI.4)

SI.4.1. Synthesis and characterization of guanidylated paromomycin

SI.4.1.1. Synthesis of compound 3 (6'''-guanidino-paromomycin) (Figure SI.4.1)

NaOH (0.80 g, 20 mmol) was dissolved in H₂O (5 mL) and this solution was added to a solution of compound **1** (0.50 g, 0.26 mmol) in 1,4-dioxane (15 mL). After 16 h, a TLC indicated a complete consumption of the starting material and showed the formation of a new baseline product (mobile phase: CHCl₃:AcOH:MeOH, 20:5:3). A MS analysis confirmed the formation of the 6'''-NH₂ product. *m/z* calcd for C₆₅H₇₇N₅O₂₂ g⁺: 1280.5, MS found: 1280.6. Dioxane was evaporated under reduced pressure, and the free amino compound was decanted in the remaining water as a white gum (0.33 g). A minimum of MeOH (3 mL) was added to this white gum and this solution was transferred in water (50 mL) to obtain a white precipitated that was recovered by filtration. Lyophilization afforded a dry product to which CHCl₃ (20 mL), Et₃N (0.11 mL, 0.78 mmol) and reagent **2** (0.21 g, 0.47 mmol) were added and the solution was refluxed for 18 h. After evaporation of the solvent under reduced pressure, the residue was dissolved in a minimum CH₂Cl₂ and loaded onto a silica gel column. The elution was done with 0 to 5% MeOH in CH₂Cl₂ to obtain the desired N-Cbz protected guanidylated paromomycin (0.41 g, 72%). *m/z* calcd for C₇₂H₈₄N₇O₂₆ [M+H]⁺: 1462.5, MS found: 1462.7. This N-Cbz protected guanidylated paromomycin (0.41 g, 0.28 mmol) was dissolved in MeOH (5 mL) and H₂O was added until the solution became cloudy. 20% Pd(OH)₂/C (80 mg) and few drops of AcOH were added and the suspension was stirred under hydrogen atmosphere (hydrogen balloon) until the conversion of the starting material into the product was completed as indicated by MS analysis (6 h). The mixture was filtered through a layer of Celite on cotton, concentrated under vacuum, washed with CH₂Cl₂ twice, dissolved in water and lyophilized to afford compound **3** (240 mg, 90%) as a per acetate salt. *m/z* calcd for C₂₄H₄₈N₇O₁₄ [M+H]⁺: 658.3, MS found: 658.4.

Compound **1** was treated with aqueous NaOH to selectively unprotect the 6'''-NH₂ group via a 6 member cyclic carbamate. The resulting free amino group was guanidylated

with reagent **2** and *N*-Cbz hydrogenolysis afforded the desired 6'''-guanidino-paromomycin (**3**).

SI.4.1.2. Synthesis of compound **5** (5''-deoxy-5''-guanidino-paromomycin)

Compound **4** (1.2 g, 0.86 mmol) was dissolved in THF (30 mL), few drops of H₂O (0.1 mL) and PPh₃ (0.27 g, 1.0 mmol) were added. 18 h later, the solvent was evaporated under reduced pressure and the residue was taken in a minimum of CH₂Cl₂ and loaded on a silica gel column. The elution was done with 4 to 8 % MeOH in CH₂Cl₂ to obtain the pure 5''-amino compound (0.20 g, 17%). *m/z* calcd for C₇₀H₈₁N₆O₂₃ [M+H]⁺: 1373.5, MS found: 1373.8. This 5''-amino compound (0.20 g, 0.15 mmol) was dissolved in CHCl₃ (20 mL), Et₃N (0.041 mL, 0.30 mmol) and reagent **2** (0.80 mg, 0.18 mmol) were added and the solution was refluxed for 18 h. After evaporation of the solvent under reduced pressure, the residue was dissolved in a minimum CH₂Cl₂ and loaded onto a silica gel column. The elution was done with 2 to 7% MeOH in CH₂Cl₂ to obtain the desired *N*-Cbz protected guanidylated paromomycin (0.20 g, 83%). *m/z* calcd for C₈₇H₉₅N₈O₂₇ [M+H]⁺: 1683.6, MS found: 1684.0. This *N*-Cbz protected guanidylated paromomycin (0.20 g, 0.12 mmol) was dissolved in 80% aqueous acetic acid (5 mL) and the solution was heated at 60 °C until a MS analysis showed total conversion of the starting material into the benzylidene deprotected product (5 h). The solution was evaporated under reduced pressure and the residue was dissolved in MeOH (3 mL) and H₂O was added until the solution became cloudy. 20% Pd(OH)₂/C (40 mg) and few drop of AcOH were added and the suspension was stirred under hydrogen atmosphere (hydrogen balloon) until the conversion of the starting material into the product was completed as indicated by MS analysis (6 h) *m/z* calcd for C₈₀H₉₁N₈O₂₇ [M+H]⁺: 1595.6, MS found: 1595.9. The mixture was filtered through a layer of Celite on cotton, concentrated under vacuum, washed with CH₂Cl₂ twice, dissolved in water and lyophilized to afford compound **5** (105 mg, 87%) as a per acetate salt. *m/z* calcd for C₂₄H₄₉N₈O₁₃ [M+H]⁺: 657.3, MS found: 657.4.

In order to obtain a different guanidylated paromomycin, the known compound **4** was treated with PPh₃ under Staudinger conditions and the resulting amine was

guanidylated with reagent **2**. Benzylidene deprotection with aqueous AcOH followed by *N*-Cbz hydrogenolysis afforded the desired 5''-deoxy-5''-guanidino-paromomycin (**5**).

SI.4.2. Steady-state fluorescence spectroscopy

Pyrene (1 X10⁻⁶ M) was used as a probe to investigate the micropolarity sensed in its solubilization site from measurement of the pyrene polarity index (I_1/I_3), which is the ratio of the intensities of the first and third vibronic peaks in the fluorescence spectrum. Pyrene was excited at 334 nm and the emission spectra were scanned from 350 to 550 nm. The samples studied were dodecyl-CMD-PEG. I_1/I_3 ratios were plotted versus polymer concentration and the critical association concentration (CAC) values were determined from the graph as the concentration corresponding to the first drop in I_1/I_3 .

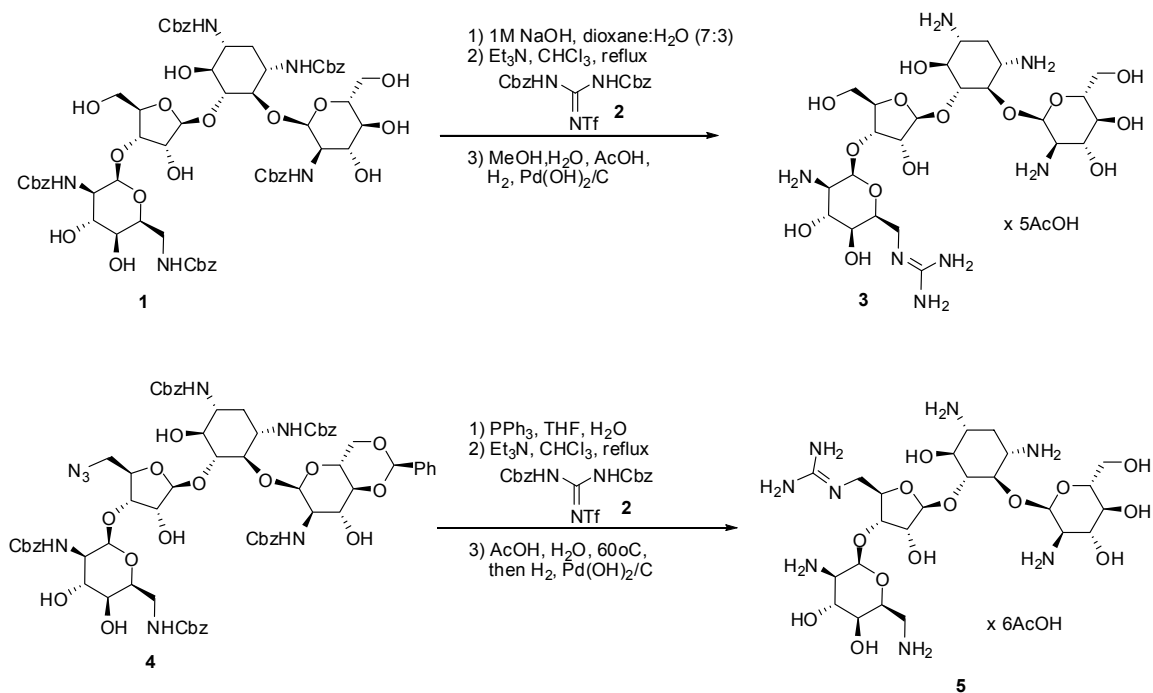


Figure SI.4.1. Synthesis of 6''-guanidino-paromomycin (**3**) and 5''-deoxy-5''-guanidino-paromomycin (**5**).

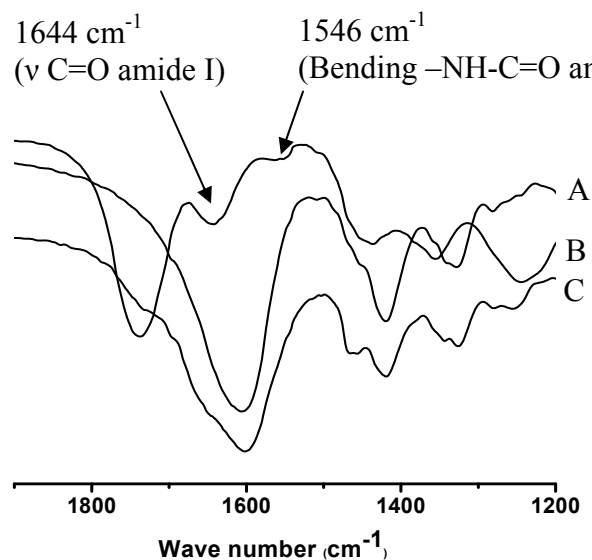


Figure SI.4.2. FTIR spectra of CMD-PEG sodium salt (A), dodecyl₃₈-CMD-PEG free acid (B), and dodecyl₃₈-CMD-PEG sodium salt (C) (powder sample) in the region of 1200-1900 cm^{-1} .

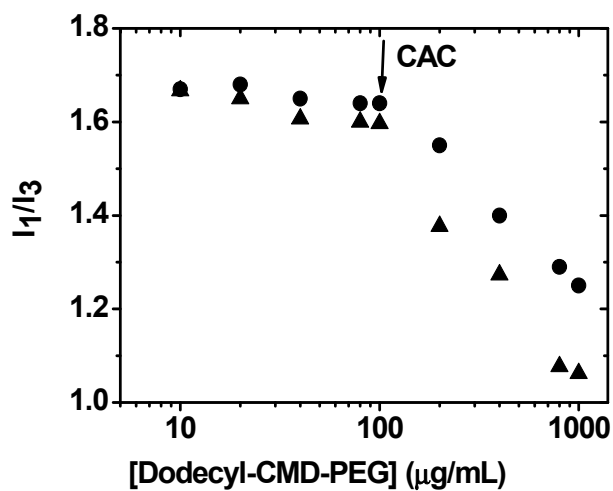


Figure SI.4.3. Plot of intensity ratio (I_1/I_3) of pyrene emission spectra ($\lambda_{\text{ex}} = 335 \text{ nm}$) versus concentration of dodecyl₁₈-CMD-PEG (●) and dodecyl₃₈-CMD-PEG (▲) in water.

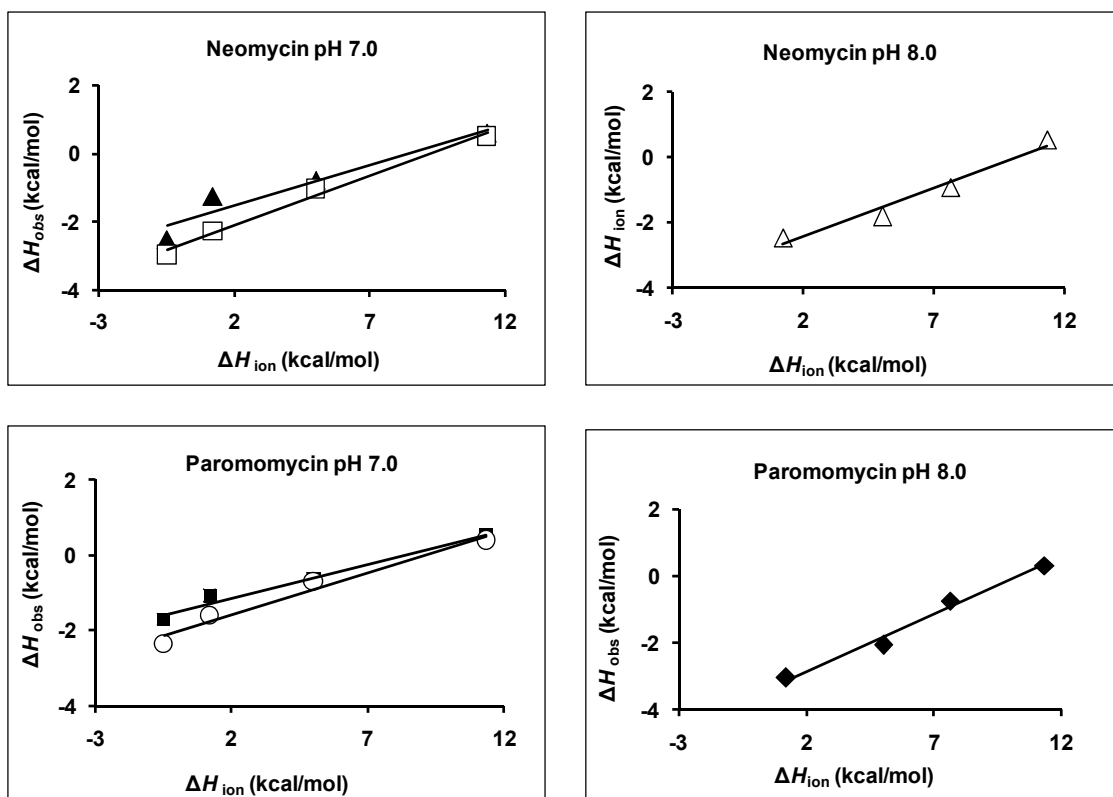


Figure SI.4.4. Observed enthalpy change (ΔH_{obs}) plotted as a function of the buffer heat of ionization for the titration of either neomycin sulfate (\blacktriangle : pH 7.0, 25 °C, $R^2 = 0.923$; \square : pH 7.0, 37 °C, $R^2 = 0.989$; \triangle : pH 8.0, 25 °C, $R^2 = 0.962$) or paromomycin sulfate (\blacksquare : pH 7.0, 25 °C, $R^2 = 0.978$; \circ : pH 7.0, 37 °C, $R^2 = 0.969$; \blacklozenge : pH 8.0, 25 °C, $R^2 = 0.984$) into CMD-PEG in different buffers. The solid lines represent the linear regression fit of the experimental data.

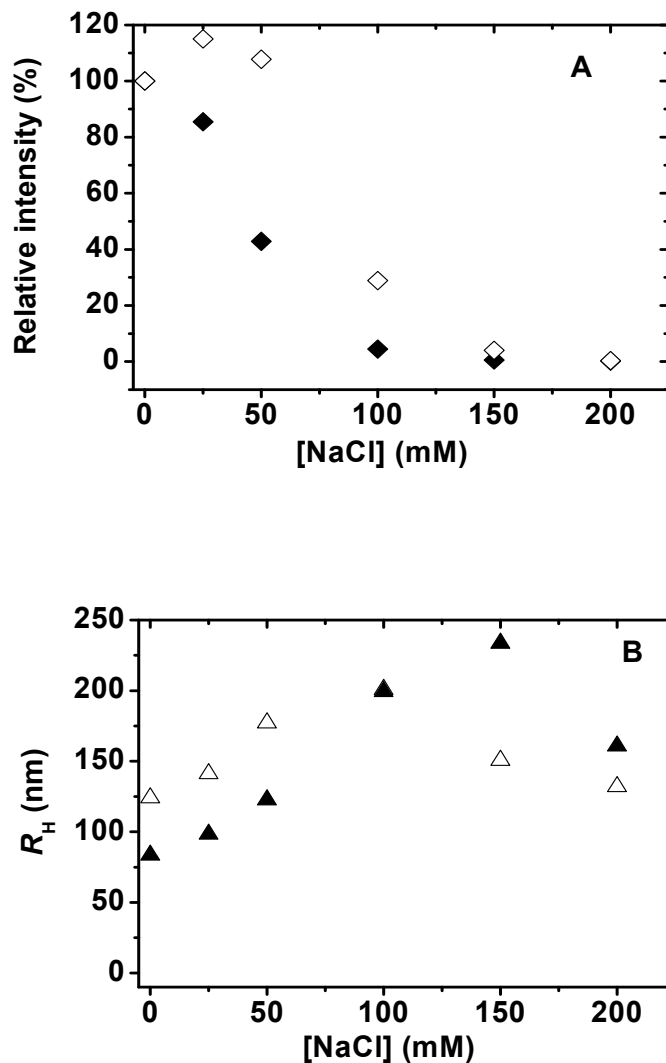


Figure SI.4.5. Effect of salt on the intensity of scattered light (A) and hydrodynamic radius (B) of 6''-guanidino-paromomycin/CMD-PEG micelles (\blacklozenge) and 5''-deoxy-5''-guanidino-paromomycin/CMD-PEG micelles (\diamond) prepared in phosphate buffer (10 mM, pH 7.0) at [CMD-PEG] = 0.5 g/L. Relative scattering intensity = intensity at certain salt concentration/ intensity at salt concentration = 0.

CHAPTER FIVE

GENERAL DISCUSSION

The design and evaluation of new drug delivery systems remain an active area of research both in academia and industry.^[1] The aim of these new drug carriers is to maximize efficacy of existing and new drugs and to minimize side effects and toxicity associated with their administration.^[2] To reach this goal, many new delivery systems have been devised, amongst which, polymeric nanoparticles are by far the most promising ones. Polymers have been a conventional *passive* component of many drug formulations and it is only recently that polymers become *active* drug carriers. This development was made possible by advances in polymer synthesis and polymer physico-chemistry, which resulted in custom-made polymers with diverse structures and functionalities.^[3] Micelles of amphiphilic copolymers, polyion complex (PIC) micelles, dendrimers, polymersomes, nanospheres and nanocapsules are examples of polymeric nanoparticles that are being currently under extensive investigation. The extraordinary performance of these nanoparticles in terms of maximizing drug efficacy, improving patient compliance and reducing drug adverse effects have resulted in their appreciation by the pharmaceutical industry. A number of successful nanoparticulate drug formulations are already on the market while many other are undergoing clinical trials.^[4, 5]

Although polymeric nanoparticles have been widely used for site specific delivery of various drugs, their use for the delivery of ionic water soluble drugs is limited due to poor encapsulation efficiency. This limitation has been overcome by the advent of a relatively new class of polymeric micelles called PIC micelles that opened a new avenue for the encapsulation of ionic drugs.^[6] PIC micelles enjoy high drug loading efficiency since drug encapsulation relies on electrostatic interactions between the ionic drug and an oppositely charged copolymer. Other features of PIC micelles that make them attractive drug carriers include ease of fabrication, ability to encapsulate a wide range of ionic drugs, excellent colloidal and thermodynamic stability, small size and narrow size distribution. PIC micelles have been adopted for several applications including gene therapy, cancer therapy and many others due to their exciting properties.

The present project is an attempt to devise PIC micelles formulations that could provide effective delivery of two important classes of antibiotics: aminoglycosides and

tetracyclines. Aminoglycosides and tetracyclines are broad spectrum antibiotics that need new means of their formulation and delivery. For instance, efficacy of aminoglycosides is limited by the nephrotoxicity and ototoxicity associated with their use. These side effects could be avoided by proper selection of a PIC micelles formulation that selectively maximizes drug concentration in diseased tissue and minimizes it in healthy tissues. Furthermore, tetracycline antibiotics, such as minocycline have shown new promising neuroprotective properties in several animal models.^[7] However, minocycline clinical use is limited by its instability in aqueous solutions and its poor pharmacokinetics, which could be improved by its encapsulation into a suitable PIC micelles formulation. Thus, a novel family of carboxymethyl-dextran-PEG (CMD-PEG) block copolymers suitable for PIC micelles formation with cationic drugs, such as aminoglycosides and tetracyclines was developed in this project. Dextran was selected partly due to its well known safety and biodegradability and partly due to its structural features that allow introduction of different functional groups.^[8, 9] PEG was selected in view of its hydrophilicity, biocompatibility and ability to prolong circulation time of several nanoparticulate drug delivery systems.^[10]

5.1. Synthesis of CMD-PEG block copolymers

Carboxymethyl-dextran-*block*-PEG (CMD-PEG) (Figure 2.1, Chapter 2) is an anionic dihydrophilic block copolymer having carboxymethyl (-CH₂COONa) groups grafted on the dextran chain. The synthesis protocol of DEX-PEG copolymers involved a straightforward end-to-end coupling of DEX-lactone and PEG-amine via a lactone aminolysis reaction under mild conditions. Conversion of the neutral DEX-PEG copolymers into the corresponding polyanionic CMD-PEG copolymers was achieved by carboxymethylation of the dextran block. The degree of substitution (DS) of the dextran block, defined here as the molar percent of glucopyranose rings bearing -CH₂COONa groups was readily controlled by varying the reaction conditions. Thus, CMD-PEG copolymers with high carboxylate contents were obtained by treating solutions of DEX-PEG in an isopropanol/water (85/15 v/v) mixture with aqueous NaOH solution (9.0 M) at 60 °C followed by addition of monochloroacetic acid.^[11] CMD-PEG with moderate

carboxylate contents were obtained by carrying out the carboxymethylation reaction in aqueous solution.^[12] CMD-PEG copolymers have a random distribution of carboxymethyl groups along the dextran chain.

5.2. CMD-PEG copolymers candidates

Electrostatic interactions between polyanionic CMD-PEG copolymers and cationic drugs trigger formation of PIC micelles with a drug/CMD ionic complex core and a PEG corona. Relative block length of CMD and PEG segments and charge density of the CMD block can affect the properties of the resulting PIC micelles.^[13-15] To address this issue, four CMD-PEG copolymers were prepared: (i) two copolymers identical in terms of the length of CMD and PEG blocks, but different in terms of the charge density of the CMD block (30-CMD₆₈-PEG₆₄ and 60-CMD₆₈-PEG₆₄); and (ii) two copolymers in which the charged block is the same, but the PEG block is of different molecular weight (80-CMD₄₀-PEG₆₄ and 85-CMD₄₀-PEG₁₄₀). To select a CMD-PEG copolymer with optimal properties in terms of high drug loading, controlled drug release and micelles stability, the micellization of these copolymers and a model cationic drug, diminazene diacetate (DIM) was studied. DIM has two amidino groups with pK_a of 11 (Figure 2.3, Chapter 2), which makes them fully ionized at physiological pH of 7.4.^[16] DIM was selected to characterize the micelles of different CMD-PEG copolymers since it formed PIC micelles with other polyanionic copolymers, such as PEG-*b*-PAsp and PEG-*b*-PGlu.^[17, 18] Micelles of 85-CMD₄₀-PEG₁₄₀ showed the most satisfactory results in terms of drug loading efficiency, controlled drug release and micelles stability (Table 5.1). Therefore, this copolymer was selected for encapsulation of other cationic drugs, such as aminoglycosides and minocycline.

5.3. Preparation of CMD-PEG PIC micelles

PIC micelles are generally prepared by simple mixing of aqueous solutions of the oppositely charged polymer and drug. PIC micelles of DIM/CMD-PEG were prepared by either drop-wise or “one shot” addition of DIM solution to CMD-PEG solution. Average size was almost the same for micelles obtained by both methods. In contrast, micelles

prepared by the drop-wise addition method had much smaller polydispersity index (PDI) confirming their unimodal size distribution. DIM/PEG-*b*-PAsp micelles prepared by the “one shot” addition method were polydisperse in size (PDI \sim 0.2).^[18] Thus, the drop-wise addition method was used for the preparation of CMD-PEG micelles encapsulating minocycline and aminoglycosides (AGs) and resulted in monodispersed micelles (PDI < 0.1).

5.4. Formation, structure and drug loading of CMD-PEG micelles

CMD-PEG copolymers have carboxylic acid groups with $pK_a \sim 4.5$ while the investigated drugs have cationic groups with different pK_a s: ~ 11 for DIM amidino groups, 9.5 for minocycline C₄ amino group (Figure 3.1, Chapter 3) and 7.0-9.5 for neomycin and paromomycin amino groups (Figure 4.1, Chapter 4). At pH 7.4, these drugs and CMD-PEG copolymers have oppositely charged groups that interact together leading to formation of PIC micelles. It is noteworthy that electrostatic interactions between DIM and CMD (in the absence of PEG) led to phase separation and precipitation. Replacement of CMD with CMD-PEG endowed the system with the amphiphilicity required for PIC micelle formation (Figure 5.1). ¹H NMR studies confirmed that CMD-PEG copolymers formed PIC micelles with PEG corona and CMD/drug core with all the studied drugs (i.e., DIM, MH and AGs) (Figure 5.1). The entrapment of a drug in the core of nanoparticles is of prime importance since this protects the drug against degradation in harsh physiological environments, controls the drug release and modifies its pharmacokinetics.^[19] For example, MH encapsulated in the core of CMD-PEG micelles was significantly more stable against degradation in aqueous solutions than the free drug (Figure 3.4, Chapter 3).

¹H NMR was also used to determine the onset of micellization (the [+]/[-] ratio at which the micelles form) and [+]/[-] ratio for maximum drug loading. These two properties were dependent on the drug and the CMD-PEG copolymer used to formulate the micelles. In the case of DIM micelles, the onset of micellization was affected by the molecular weight of neither CMD nor PEG. In contrast, it was dependent on the degree of substitution

(DS) of the CMD block. Thus, core-corona micelles were observed at $[+]/[-] \geq 0.8$ for copolymer having $DS \geq 60\%$ and at $[+]/[-] \geq 1.6$ for copolymer with $DS \leq 30\%$. It should be recalled here that CMD-PEG copolymers do not form PIC micelles by themselves and that a certain number of DIM molecules should be ionically-linked to the polymer chains to create the hydrophobic domains necessary for micelles formation. Consequently, the polymers having lower DS (i.e., fewer carboxylate groups) needs higher $[+]/[-]$ ratio to achieve the same drug concentration obtained at certain $[+]/[-]$ for polymer with high DS.

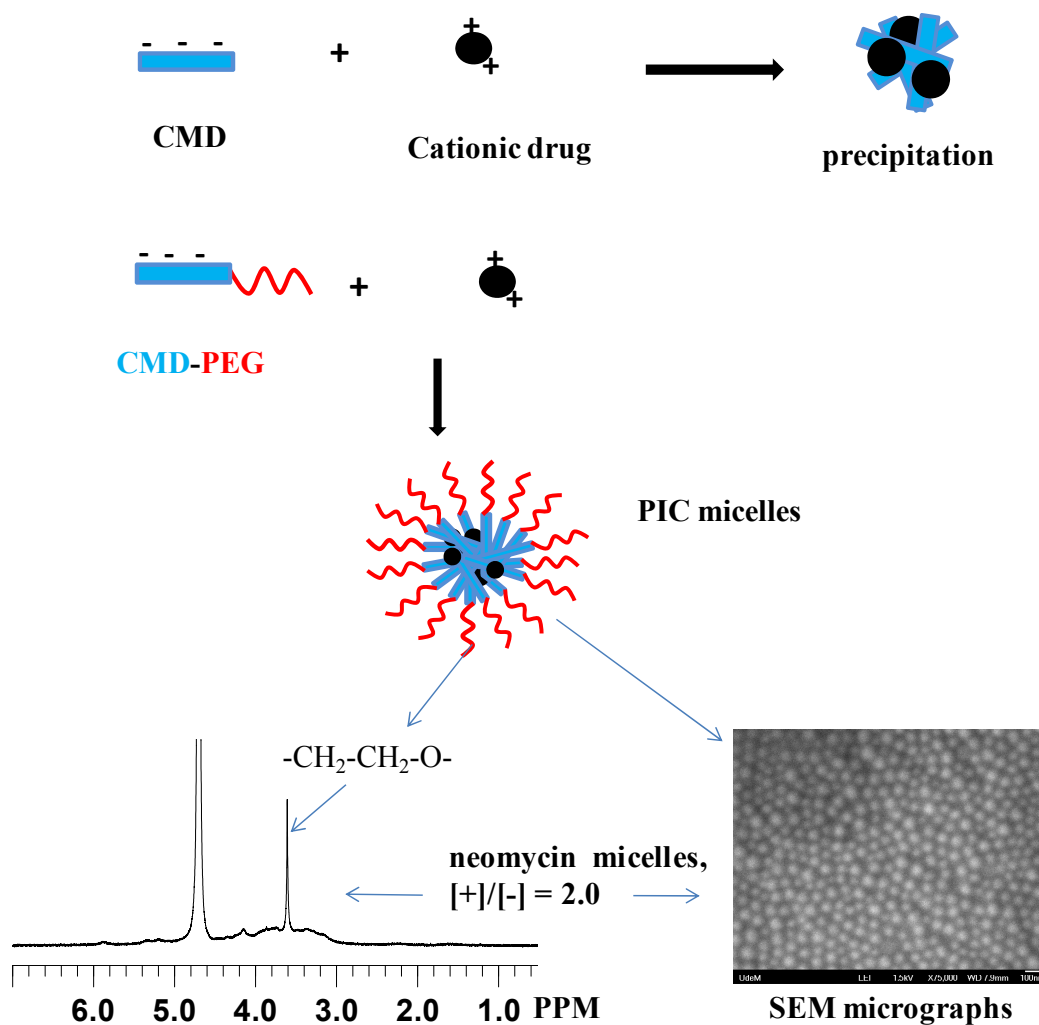


Figure 5.1. Formation and structure of drug-loaded CMD-PEG PIC micelles.

The drugs used in this project have different physicochemical properties, which affected the properties of the resulting micelles. Thus, for the same polymer (i.e., 85-CMD₄₀-PEG₁₄₀), micelles form at $[+]/[-] \sim 1.0$ for DIM and MH and at $[+]/[-] \sim 2.0$ for neomycin and paromomycin. This difference is presumably attributed to the presence of aromatic rings in DIM (Figure 2.3, Chapter 2) and MH (Figure 3.1, Chapter 3), which assist in creating the hydrophobic domains needed for micelles formation. Neomycin and paromomycin are very hydrophilic molecules (Figure 4.1, Chapter 4), therefore more drug molecules need to be neutralized to achieve the required amphiphilicity. Maximum drug loading was also dependent on the drug and the copolymer (Table 5.1). For all the studied copolymers and drugs, maximum drug loading was achieved at charge ratios corresponding to CMD-PEG neutralization, after which free drug was detectable in solution. This confirms that drug encapsulation takes place primarily by electrostatic interactions. Interestingly, 85-CMD₄₀-PEG₁₄₀ copolymer had drug loading capacity ≥ 50 wt% for all the studied drugs showing its potential as a drug delivery system.

Table 5.1. Characteristics of different CMD-PEG micelles.

Drug	Polymer	% Drug ^a	R_H ^b	CAC (g/L)
DIM	85-CMD ₄₀ -PEG ₁₄₀ ^c	64.3	48.7 ± 0.6	0.048
DIM	80-CMD ₄₀ -PEG ₆₄	62.0	43.5 ± 0.7	0.032
DIM	60-CMD ₆₈ -PEG ₆₄	60.1	36.9 ± 0.5	0.014
DIM	30-CMD ₆₈ -PEG ₆₄	41.4	49.7 ± 0.6	0.095
MH	85-CMD ₄₀ -PEG ₁₄₀	50	99.0 ± 2.7	ND
Neomycin	85-CMD ₄₀ -PEG ₁₄₀	50	74.9±1.8	0.060
Neomycin	dodecyl ₁₈ -CMD-PEG	50	63.3±0.6	ND
Neomycin	dodecyl ₃₈ -CMD-PEG	50	40.5±0.4	ND
Paromomycin	85-CMD ₄₀ -PEG ₁₄₀	49.8	130.1±0.5	0.120
Paromomycin	dodecyl ₁₈ -CMD-PEG	49.8	48.5±0.4	ND
Paromomycin	dodecyl ₃₈ -CMD-PEG	49.8	54.5±1.2	ND

^a: % maximum drug loading = weight of drug/(weight of micelles)×100.

^b: Mean of six measurements ± S.D. R_H measured for micelles prepared at [+]/[-] = 2.0 for DIM, 1.0 for MH and 2.5 for neomycin and paromomycin.

^c: In this nomenclature, the prefix denotes the degree of carboxymethylation of the dextran block; the subscripts designate the average number of glucopyranosyl and -CH₂-CH₂-O- repeat units of the CMD and PEG segments, respectively.

ND: not determined.

5.5. Size and polydispersity of CMD-PEG micelles

The size and polydispersity of nanoparticles affect their *in vivo* fate, effectiveness and safety. For instance, oral absorption of nanoparticles ~ 100 nm in diameter was reported to be 15 to 250-fold higher than that of micro-sized particles.^[20] The diameter of all CMD-PEG micelles was ≤ 200 nm, except those of paromomycin/85-CMD₄₀-PEG₁₄₀ (Table 5.1). This sub-200 nm size and biocompatibility of CMD-PEG copolymers are expected to increase the circulation time of the micelles in the blood.^[21, 22] The size of CMD-PEG micelles was dependent on the drug and copolymer used in micelle formation (Table 5.1). For the same copolymer (i.e., 85-CMD₄₀-PEG₁₄₀), micelles size increased in this order: DIM micelles < neomycin micelles < MH micelles < paromomycin micelles. The exact mechanism behind this size difference is not clear. However, since the copolymer and experimental conditions (polymer concentration, pH and ionic strength) are identical, the difference in micelles size could be attributed to different physicochemical properties of the encapsulated drugs (e.g. pKa, hydrophilicity/lipophilicity balance and molecular weight). Thus, DIM micelles had the smallest size probably due to high basicity of the drug amidino groups (pKa = 11), and the presence of hydrophobic aromatic groups (Figure 2.3, Chapter 2). Neomycin micelles were smaller than those of paromomycin probably because neomycin has an additional amino group (Figure 4.1, Chapter 4). Higher basicity of the drugs cationic groups might lead to tighter electrostatic interactions in the micelles core, which resulted in smaller micelles.

The presence of hydrophobic groups along CMD-PEG copolymer chains affected the size of their PIC micelles with neomycin and paromomycin (Table 5.1). Thus, dodecyl-CMD-PEG micelles encapsulating neomycin or paromomycin were significantly smaller than those of the corresponding CMD-PEG. Polymeric micelles of amphiphilic copolymers have a so-called “solid core” in aqueous solutions due to the generally high glass transition temperature, T_g , of the core forming segments and the almost complete absence of solvent in the micellar core. In contrast, PIC micelles have a hydrated core since they are formed by electrostatic interactions, a relatively weak driving force compared to hydrophobic interactions.^[15] PIC micelles of dodecyl-CMD-PEG may have hydrophobic interactions

between dodecyl chains in the micelles core leading to less hydrated core and thus, smaller micelles. Less hydrated core might also be the reason behind smaller size of DIM/60-CMD₆₈-PEG₆₄ micelles compared to those of DIM/30-CMD₆₈-PEG₆₄ (Table 5.1).

5.6. Micelles critical association concentration (CAC)

Compared to surfactant micelles, polymeric micelles have lower CAC, which guarantees their thermodynamic stability against extensive dilution *in vivo*.^[23] CAC of DIM micelles with different CMD-PEG copolymers was dependent on the degree of substitution (DS) and the length of the dextran block (Table 5.1). The lowest CAC was recorded for micelles formed by the copolymer of longest CMD block and highest DS (60-CMD₆₈-PEG₆₄), presumably as a consequence of their high drug content. The length of the PEG block has only a minor influence on the CAC of the micelles, as seen by comparing the values determined for 85-CMD₄₀-PEG₁₄₀ and 80-CMD₄₀-PEG₆₄ (Table 5.1). The CAC was also affected by the drug used to formulate the micelles. Thus, CAC of neomycin micelles was half that of paromomycin micelles, probably due to stronger electrostatic interactions between neomycin and CMD-PEG.

5.7. Effect of salt on CMD-PEG micelles stability

Small molecular weight salts weaken electrostatic interactions in PIC micelles core leading to micellar dissociation after certain salt concentration.^[24] For DIM micelles with different CMD-PEG copolymers, micelles ability to withstand salinity was dependent on the DS of the dextran block. Thus, micelles of DIM and copolymers of DS $\geq 60\%$ remained stable at NaCl concentrations as high as 300 mM, a value significantly higher than the physiological salt concentration (150 mM). This was in contrast with micelles of DIM and copolymers of DS $\leq 30\%$, which disintegrated at NaCl concentrations ≥ 100 mM. Aminoglycosides micelles were generally less resistant to increase in salinity than DIM micelles with the same CMD-PEG copolymer. Moreover, neomycin micelles were more resistant to salt-induced disintegration than those of paromomycin probably due to stronger interactions in the core of neomycin micelles. Nevertheless, stability of neomycin micelles

at physiological salt concentration was not enough to permit *in vivo* application. To increase stability of aminoglycosides micelles, two approaches were devised: hydrophobic modification of CMD-PEG by grafting dodecyl chains to the CMD backbone and guanidylation of paromomycin. Interestingly, neomycin and paromomycin micelles with dodecyl-CMD-PEG were more tolerable to increase in salinity than those with CMD-PEG, probably due to participation of hydrophobic interactions between dodecyl chains in micelle stabilization. Stability of dodecyl-CMD-PEG micelles was dependent on the drug and grafting density of dodecyl chains: more stable micelles were observed for neomycin and copolymers having higher dodecyl content. Neomycin/dodecyl₁₃₈-CMD-PEG micelles resisted salt-induced disintegration for NaCl concentration up to 200 mM. Furthermore, guanidylated paromomycin/CMD-PEG micelles were more resistant against salt-induced disintegration than those of paromomycin, probably because guanidine groups are more basic than amino groups.^[25] Therefore, stability of CMD-PEG PIC micelles against increase in salinity was dependent on the forces that trigger micelle formation (i.e., whether electrostatic interactions only or combination electrostatic and hydrophobic interactions) and on the ionic charge density of the cationic drug used to form the micelles.

5.8. Effect of pH on micelle formation and stability

Solution pH affects the degree of ionization of CMD-PEG carboxylate groups and the drugs cationic groups. Thus, there was a pH range for which the drug and CMD-PEG had adequate charge density to form stable PIC micelles. For the same polymer (i.e., 85-CMD₄₀-PEG₁₄₀), this pH range was dependent on the drug, probably because the studied drugs have different pK_as. DIM showed the widest pH range of micelles stability: micelles were stable in the pH range 4.0-11.0. In contrast, neomycin and paromomycin micelles were stable over a narrower pH range (4.0-7.4 and 4.0-7.0 for neomycin and paromomycin, respectively). This may be attributed to the presence of two amidino groups in DIM (pK_a ~ 11), which remain positively charged at higher pH values compared to the amino groups of neomycin (highest pK_a ~ 9.5) and paromomycin (highest pK_a ~ 9.4).^[16, 26]

5.9. Stability of CMD-PEG micelles

Nanoparticulate drug delivery system should be colloiddally stable for periods of time long enough to permit accurate dosing, *in vitro* and to allow safe delivery of the drug to its target, *in vivo*. Furthermore, nanoparticles should maintain their integrity during freeze drying and recover their size after reconstitution in a suitable solvent. CMD-PEG micelles encapsulating different drugs were colloiddally stable in solutions kept at room temperature without phase separation or aggregation for periods longer than two months. Moreover, all the micelles maintained their size and stability after freeze drying and reconstitution in the absence of cryoprotectants, except DIM micelles which needed the presence of 5% (w/v) trehalose.

5.10. Drug release from CMD-PEG micelles

Following characterization of different drug delivery aspects of CMD-PEG micelles, it was necessary to confirm that the micelles can sustain the release of different drugs. For DIM micelles, CMD-PEG copolymers of higher DS showed better control over the drug release rate. Thus, micelles of copolymers having high DS (e.g., 85-CMD₄₀-PEG₁₄₀) released ~ 50% DIM after 8 h, compared to ~ 72% after the same time for micelles of copolymers having low DS (e.g., 30-CMD₆₈-PEG₆₄). Different drugs encapsulated in CMD-PEG micelles were released in a sustained fashion when compared to free drugs. For instance, *in vitro* testing demonstrated that neomycin was slowly released from the micelles where ~ 25% drug was released after 8 h, compared to ~ 100% in the case of drug alone. CMD-PEG micelles of different drugs showed higher drug release rate in the presence of physiological salt concentration, probably as a consequence of weakening of electrostatic interactions in the micelles core. Nevertheless, CMD-PEG micelles sustained the release of minocycline and neomycin for up to 24 h under physiological conditions (i.e., pH 7.4, 150 mM NaCl). This confirms the potential of these micelles to reduce the frequency of drug administration.

5.11. Cytotoxicity of CMD-PEG copolymers

Since CMD-PEG copolymers were designed for drug delivery applications, it was imperative to evaluate their cytotoxicity in different cell line. Thus, CMD-PEG cytotoxicity was evaluated in two cell lines: human hepatocytes and murine microglia. The liver represents the main organ in which biotransformation of drugs and foreign substance takes place while the inflamed microglia are the main target for minocycline micelles in the central nervous system.^[27] CMD-PEG did not reduce the viability of both cell lines when treated for 24 h at polymer concentrations as high as 15 mg/mL. This confirms the biocompatibility of CMD-PEG copolymers. Indeed, these polymers will be diluted in the blood stream following IV injection and local concentrations in the liver tissues are not expected to reach such high levels. Moreover, the PEG corona of the micelles is expected to prolong the micelles circulation in blood and reduce their uptake in the liver, as demonstrated previously with other PEGylated nanoparticles.^[28]

5.12. Pharmacological activity of micelles-encapsulated drugs

The biocompatibility and other favorable properties of CMD-PEG micelles warranted biological evaluation of micelles-encapsulated drugs. Thus, anti-inflammatory activity of micelles-encapsulated MH was evaluated in murine microglia (N9) cells activated by lipopolysaccharides (LPS). Micelles-encapsulated MH reduced inflammation in microglia cells to levels similar to those observed for the free drug. Preliminary experiments showed that CMD-PEG copolymer (in the absence of MH) reduced LPS-induced inflammation in N9 microglia, which could enhance the anti-inflammatory activity of MH in either additive or even synergistic manner. Furthermore, the minimal inhibitory concentration (MIC) in *E. coli* of different aminoglycosides encapsulated in CMD-PEG micelles was comparable to that of free aminoglycosides. These results confirmed that different drugs were released from CMD-PEG micelles in a pharmacologically active form. Furthermore, the presence of CMD-PEG copolymers did not reduce the pharmacological activity of encapsulated drugs.

5.13. References

- [1] Devalapally H, Chakilam A, Amiji MM. Role of nanotechnology in pharmaceutical product development. *J. Pharm. Sci.* **2007**, *96*: 2547-65.
- [2] Bawarski WE, Chidlowsky E, Bharali DJ, Mousa SA. Emerging nanopharmaceuticals. *Nanomed. Nanotechnol. Biol. Med.* **2008**, *4*: 273-82.
- [3] Sakuma S, Hayashi M, Akashi M. Design of nanoparticles composed of graft copolymers for oral peptide delivery. *Adv. Drug Deliv. Rev.* **2001**, *47*: 21-37.
- [4] Matsumura Y, Kataoka K. Preclinical and clinical studies of anticancer agent-incorporating polymer micelles. *Cancer Sci.* **2009**, *100*: 572-9.
- [5] Karmali PP, Kotamraju VR, Kastantin M, Black M, Missirlis D, Tirrell M, Ruoslahti E. Targeting of albumin-embedded paclitaxel nanoparticles to tumors. *Nanomed.-Nanotechnol. Biol. Med.* **2009**, *5*: 73-82.
- [6] Harada A, Kataoka K. Formation of polyion complex micelles in an aqueous milieu from a pair of oppositely-charged block copolymers with poly(ethylene glycol) segments. *Macromolecules* **1995**, *28*: 5294-9.
- [7] Zemke D, Majid A. The potential of minocycline for neuroprotection in human neurologic disease. *Clin. Neuropharmacol.* **2004**, *27*: 293-8.
- [8] de Jonge E, Levi M. Effects of different plasma substitutes on blood coagulation: A comparative review. *Crit. Care Med.* **2001**, *29*: 1261-7.
- [9] Heinze T, Liebert T, Heublein B, Hornig S. Functional Polymers Based on Dextran. Polysaccharides II, 2006. p. 199-291.
- [10] Kakizawa Y, Kataoka K. Block copolymer micelles for delivery of gene and related compounds. *Adv. Drug Deliv. Rev.* **2002**, *54*: 203-22.
- [11] Huynh R, Chaubet F, Jozefonvicz J. Anticoagulant properties of dextranmethylcarboxylate benzylamide sulfate (DMCBSu); a new generation of bioactive functionalized dextran. *Carbohydr. Res.* **2001**, *332*: 75-83.
- [12] Rebizak R, Schaefer M, Dellacherie E. Polymeric conjugates of Gd³⁺-diethylenetriaminepentaacetic acid and dextran.1. Synthesis, characterization, and paramagnetic properties. *Bioconjugate Chem.* **1997**, *8*: 605-10.

- [13] Harada A, Kataoka K. Effect of charged segment length on physicochemical properties of core-shell type polyion complex micelles from block ionomers. *Macromolecules* **2003**, *36*: 4995-5001.
- [14] Adams DJ, Rogers SH, Schuetz P. The effect of PEO block lengths on the size and stability of complex coacervate core micelles. *J. Colloid Interface Sci.* **2008**, *322*: 448-56.
- [15] Voets IK, de Keizer A, Stuart MAC. Complex coacervate core micelles. *Adv. Colloid Interface Sci.* **2009**, *147-148*: 300-18.
- [16] Atsriku C, Watson DG, Tettey JNA, Grant MH, Skellern GG. Determination of diminazene acetate in pharmaceutical formulations by HPLC and identification of related substances by LC/MS. *J. Pharm. Biomed. Anal.* **2002**, *30*: 979-86.
- [17] Thunemann AF, Schutt D, Sachse R, Schlaad H, Mohwald H. Complexes of poly(ethylene oxide)-block-poly(L-glutamate) and diminazene. *Langmuir* **2006**, *22*: 2323-8.
- [18] Govender T, Stolnik S, Xiong C, Zhang S, Illum L, Davis SS. Drug-polyionic block copolymer interactions for micelle formation: Physicochemical characterisation. *J. Controlled Release* **2001**, *75*: 249-58.
- [19] Torchilin V. Multifunctional and stimuli-sensitive pharmaceutical nanocarriers. *Eur. J. Pharm. Biopharm.* **2009**, *71*: 431-44.
- [20] Desai MP, Labhsetwar V, Amidon GL, Levy RJ. Gastrointestinal uptake of biodegradable microparticles: Effect of particle size. *Pharm. Res.* **1996**, *13*: 1838-45.
- [21] Stolnik S, Illum L, Davis SS. Long circulating microparticulate drug carriers. *Adv. Drug Deliv. Rev.* **1995**, *16*: 195-214.
- [22] Nishiyama N, Kataoka K. Current state, achievements, and future prospects of polymeric micelles as nanocarriers for drug and gene delivery. *Pharmacol. Ther.* **2006**, *112*: 630-48.
- [23] Lavasanifar A, Samuel J, Kwon GS. Poly(ethylene oxide)-block-poly(-amino acid) micelles for drug delivery. *Adv. Drug Deliv. Rev.* **2002**, *54*: 169-90.

- [24] Yan Y, de Keizer A, Cohen Stuart MA, Drechsler M, Besseling NAM. Stability of complex coacervate core micelles containing metal coordination polymer. *J. Phys. Chem. B* **2008**, *112*: 10908-14.
- [25] Luedtke NW, Baker TJ, Goodman M, Tor Y. Guanidinoglycosides: A novel family of RNA ligands. *JACS* **2000**, *122*: 12035-6.
- [26] Kaul M, Barbieri CM, Kerrigan JE, Pilch DS. Coupling of drug protonation to the specific binding of aminoglycosides to the A site of 16 S rRNA: Elucidation of the number of drug amino groups involved and their identities. *J. Mol. Biol.* **2003**, *326*: 1373-87.
- [27] De Vocht C, Ranquin A, Willaert R, Van Ginderachter JA, Vanhaecke T, Rogiers V, Versées W, Van Gelder P, Steyaert J. Assessment of stability, toxicity and immunogenicity of new polymeric nanoreactors for use in enzyme replacement therapy of MNGIE. *J. Controlled Release* **2009**, *137*: 246-54.
- [28] Owens DE, Peppas NA. Opsonization, biodistribution, and pharmacokinetics of polymeric nanoparticles. *Int. J. Pharm.* **2006**, *307*: 93-102.

CHAPTER SIX

CONCLUSIONS AND PERSPECTIVES

6.1. Conclusions

Different carboxymethyl-dextran-PEG block copolymers (CMD-PEG) of *tunable charge density* were developed for the enhanced delivery for cationic drugs. CMD-PEG PIC micelles encapsulating different cationic drugs demonstrated several favorable properties: high drug loading capacity, small size and colloidal stability in solution and after freeze drying. CMD-PEG micelles had a PEG corona and a drug/CMD core. Drug encapsulation in the micelles core sustained its release and protected it against degradation in aqueous solutions. Different drugs were released from CMD-PEG micelles in a pharmacologically active form. Micelles properties were greatly affected by ionic charge density of CMD-PEG copolymers and the type of encapsulated drug. To obtain stable PIC micelles, ionic charge density and chemical composition of PIC micelles components need to be carefully considered. Physiological conditions (pH 7.4 and 0.15 M NaCl) compromised stability of some aminoglycosides micelle formulations, which was greatly enhanced by hydrophobic modification of CMD-PEG copolymers. A similar strategy may be appropriate to stabilize PIC micelles of other ionic copolymers. By virtue of their biocompatibility, small size and ability to reduce adsorption of plasma proteins, CMD-PEG micelles are expected to be viable delivery systems for cationic drugs. Collectively, the results presented in this thesis will assist in understanding the relationship between structural features of ionic drugs and polymers and properties of the resulting PIC micelles. This will help in the preparation of PIC micelles with optimized properties that can improve therapeutic efficacy and reduce side effects of many ionic drugs.

6.2. Future work

The encouraging results obtained in this thesis justify *in vivo* evaluation of a number of CMD-PEG formulations. Thus, minocycline and neomycin micelles will be evaluated, *in vivo* to determine their pharmacokinetics and biodistribution. Furthermore, neuroprotective effects of minocycline micelles will be evaluated in mice having unilateral cortical cerebral ischemia. Micelles of hydrophobically modified CMD-PEG need to be evaluated more in depth for better understanding of the mechanism of micelle stabilization. Other ionic

copolymers that form unstable PIC micelles will be modified and their stability against increase in salinity will be investigated. This will determine whether the observed stabilization effect is specific to CMD-PEG or general phenomena.

When it comes to the usefulness of DEX-PEG copolymers as delivery systems for drugs other than the cationic ones, a number of experiments may be suggested. Firstly, CMD-PEG copolymers will be exploited as delivery vehicles for hydrophobic drugs (e.g., anticancer drugs) by increasing the grafting density of dodecyl chains or using more hydrophobic moieties (e.g., PCL). Secondly, DEX-PEG copolymer will be converted into a polycation by attachment of positively charged moieties (e.g., arginine) to the dextran block. The resulting positively charged polymers will be used as non-viral gene vectors for the encapsulation and delivery of DNA, siRNA or oligonucleotides.

Appendix D. Supporting information (SI.5): Properties of the drugs used in this thesis

1. Diminazene diacetate (DIM)

1.1. Indications

DIM (Figure SI.5.1) is a cationic molecule belongs to the group of aromatic diamidines. DIM is used in tropical countries for the effective treatment of trypanosomiasis in cattle, sheep and goats.^[1] It is given as an intramuscular injection of 3-5 mg/kg.

1.2. Physicochemical properties

DIM contains two benzamidine moieties linked via a triazene at the 4 position of each ring. The triazene link is susceptible to cleavage resulting in the formation of 4-aminobenzamidine and a 4-amidinophenyldiazonium salt.^[2] DIM is unstable under acidic conditions where its half-life at pH 3, is 35 min, decreasing to 1.5 min at pH 1.75. The pH-rate profile of DIM showed a region (pH 1–4) where specific acid catalysis was dominant, followed by a transitional region (pH 5–7), and finally a region (pH > 7) where uncatalysed degradation was most important.^[2] In this thesis DIM was used as a model cationic drug to study the effect of relative block length of CMD-PEG copolymer segments and charge density of the CMD block on the properties of the resulting PIC micelles. DIM is water soluble, readily available and inexpensive. DIM was shown previously to form PIC micelles with other anionic block copolymers such as poly(ethylene glycol)-*block*-poly(aspartic acid)^[3] and poly(ethylene glycol)-*block*-poly(L-glutamate).^[4]

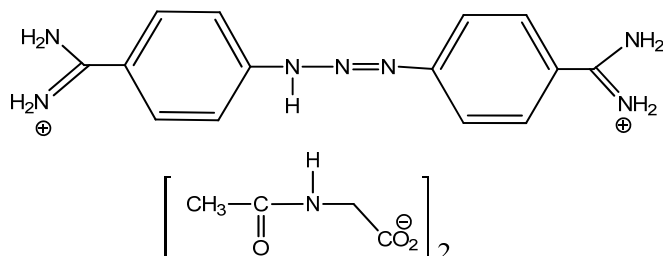


Figure SI.5.1. Chemical structure of diminazene diacetate

2. Minocycline hydrochloride (MH)

2.1. Indications

Minocycline hydrochloride (MH) (Figure SI.5.2) is a semisynthetic tetracycline antibiotic with a broad spectrum activity against a wide range of microbes including both Gram negative and Gram positive bacteria and both aerobes and anaerobes.^[5] MH acts by binding to the 30S ribosomal subunit of bacterial ribosomes and interferes with protein translation, thereby inhibiting bacterial protein synthesis.^[6] Minocycline is routinely administered orally for the treatment of infectious and inflammatory diseases, such as acne, rheumatoid arthritis, and some sexually transmitted diseases, in doses on the order of 3 mg kg⁻¹ day⁻¹.^[8] In addition to its antimicrobial activity, recent studies have shown that minocycline is effective as a neuroprotective agent in animal models of many diseases such as Huntington's disease^[7], Parkinson disease^[8], stroke^[9], amyotrophic lateral sclerosis^[10], traumatic brain injury^[11], spinal cord injury^[12], focal cerebral ischemia^[13] and global cerebral ischemia.^[14] The mechanisms underlying this neuroprotective effect have been shown to involve the inhibition of enzymes linked with cytokine production, such as nitric oxide synthase and interleukin-1 β converting enzyme. More importantly, minocycline was shown to have strong, acute anti-inflammatory effects in the brain, as it can penetrate the blood brain barrier and inhibit activation of immune cells and microglia, limiting the release of cytokines, and reducing the overall neuroinflammation.^[15]

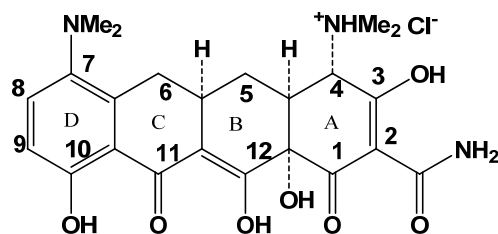


Figure SI.5.2. Chemical structure of minocycline hydrochloride

2.2. Physicochemical properties

Tetracyclines have in common a fused 4-ring structure, and differ in the chemical groups at the 5, 6, and 7 positions. MH was first isolated in 1967, and it contains a dimethylamino group at the 7 position (Figure SI.5.2).^[16] MH, like other tetracycline antibiotics, is stable in the dry powder state for at least 3-4 years.^[17] In aqueous solutions, however, it is unstable and undergoes a number of degradative changes including epimerization and oxidation.^[18] MH is more susceptible to oxidation than other tetracyclines since its D ring (Figure SI.5.2) is a substituted *p*-amino phenol. The absence of hydroxyl groups at both C₅ and C₆ prevents the formation of anhydro, or iso compounds, which are the common degradation products of other tetracyclines. The stability of tetracyclines in solution is dependent on the solution pH, being more stable in acidic solutions.^[18] The most common transformation reaction of MH is epimerization, a steric rearrangement in the configuration of the dimethylamino group at C₄ leading to the formation of epi-MH.^[19] The pharmacological activity of MH epimer is less than 5 % of the parent compound. After 24 h storage at room temperature, MH solutions (10 mg/mL) in 5 % sucrose and phosphate buffered-saline (PBS) pH 7.4 were discoloured and precipitated.^[15] MH solutions kept at pH 4.2 and 6.2 maintained 90 and 76 % of their initial potency after storage for one week at room temperature, respectively.^[18]

2.3. Biopharmaceutical properties

MH has a broader antimicrobial activity compared to other tetracyclines.^[5] The recommended dosage of minocycline is 100 to 200 mg/day.^[16] Oral administration of 200 mg MH results in almost complete absorption, producing a peak serum concentration of 3 to 5 µg/mL with a half-life of 11 to 13 h.^[6] Tetracyclines are ion chelators and compounds containing iron, aluminum hydroxide, sodium bicarbonate, calcium or magnesium salts can reduce their absorption. For instance, administration of MH with milk reduces its oral absorption by 27%.^[20] Intravenous administration of 200 mg MH produces peak serum concentrations of about 6 µg/mL.^[21] Intravenous doses of minocycline in rats producing serum concentrations of both 3.6 µg/mL and 13 µg/mL have been shown to reduce infarct size in a model of stroke.^[22] Therefore, standard MH doses in human are expected to have

neuroprotective effects. MH has an isoelectric point of 6.4, which is about one pH unit higher than that of other tetracyclines. This allows MH to diffuse more easily into lipid tissues at physiological pH, including brain, thyroid and fat tissues.^[17] Therapy with MH is well tolerated when it is used for short durations in doses up to 200 mg/day.^[9] Long-term treatment, although recognized as generally safe, has resulted in serious side effects in some cases. These include gastrointestinal adverse effects and dizziness^[23], staining of teeth^[24], autoimmune hepatitis^[25, 26], lupus^[27], hypersensitivity syndrome and serum sickness^[28]. MH is not recommended for use in young children, pregnant women, patients who are hypersensitive to tetracyclines, or patients with renal insufficiency.

3. Aminoglycosides

3.1. Indications

Aminoglycosides (Figure SI.5.3) are a group of structurally diverse polyamines either derived from *Streptomyces* spp. (streptomycin, neomycin and tobramycin) or *Micromonospora* spp. (gentamicin) or synthesised in vitro (netilmicin, amikacin, arbekacin and isepamicin).^[29] Aminoglycosides are active against a wide spectrum of microorganisms, including Gram-positive and Gram-negative bacteria, mycobacteria and protozoa. They have been frequently used in the treatment of serious infections caused by aerobic Gram negative bacilli such as pneumonia, urinary tract infections and peritonitis.^[30, 31] Today most frequently used aminoglycosides are gentamicin, tobramycin and amikacin, whilst streptomycin remains an important drug in the treatment of tuberculosis, brucellosis, tularaemia and plague. Paromomycin and spectinomycin have been used to treat intestinal protozoal pathogens and *Neisseria gonorrhoeae* infections, respectively.^[29] The antibacterial activity of aminoglycosides results from their interaction with the aminoacyl site of 16S ribosomal RNA (rRNA) within the 30S ribosomal subunit.^[32]

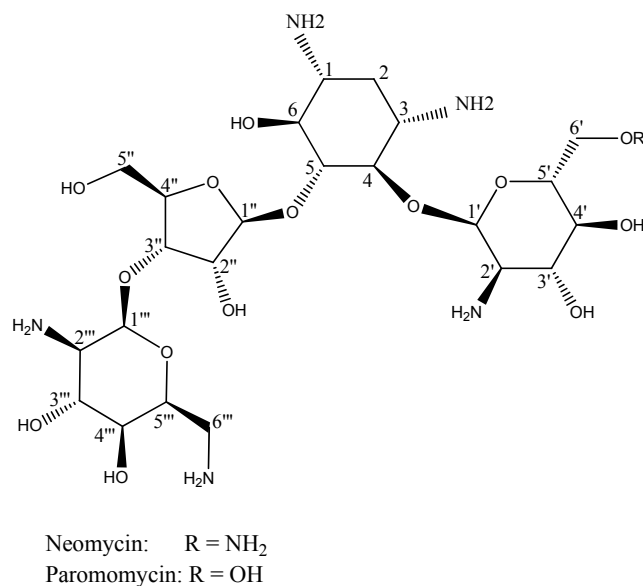


Figure SI.5.3. Chemical structure of neomycin and paromomycin.

3.2. Physicochemical properties

Aminoglycosides are polycationic molecules highly soluble in water. Chemically there are two major classes of aminoglycosides that contain a central aminocyclitol moiety (2-deoxystreptamine (2-DOS)), with one class consisting of 4,5-disubstituted 2-DOS compounds and the other consisting of 4,6-disubstituted 2-DOS compounds. Examples of the 4,6-disubstituted 2-DOS class include tobramycin, kanamycins A and B, and amikacin, while examples of the 4,5-disubstituted 2-DOS class include neomycin B, paromomycin I, and lividomycin A.

3.3. Biopharmaceutical properties

Aminoglycosides are administered parenterally or locally, rather than orally due to their poor absorption in the gastro-intestinal tract as a consequence of their polar cationic nature.^[31, 33] The poor cellular penetration of aminoglycosides limit their activity against intracellular pathogens.^[34] Aminoglycoside antimicrobial activity is mostly concentration-

dependent, which means that higher concentration of the antibiotic (relative to the minimal inhibitory concentration (MIC) against a given organism) induces more efficient killing of the organism. High peak concentrations enhance efficacy whilst lower trough concentrations reduce the incidence of nephrotoxicity. Therefore, aminoglycosides should be given as once-daily administration to achieve these optimal concentrations and results in improved efficacy and toxicity outcomes.^[35] Nephrotoxicity and ototoxicity are the most common side effects of aminoglycosides and they are usually dose-limiting factors in the successful therapy using aminoglycosides. The nephrotoxicity of aminoglycosides results from the accumulation of a relatively high percentage (~ 10 %) of the intravenously administered dose in the kidney.^[36]

References

- [1] Peregrine AS, Mamman M. Pharmacology of diminazene - a review. *Acta Trop.* **1993**, *54*: 185-203.
- [2] Campbell M, Prankerd RJ, Davie AS, Charman WN. Degradation of berenil (diminazene aceturate) in acidic aqueous solution. *J. Pharm. Pharmacol.* **2004**, *56*: 1327-32.
- [3] Govender T, Stolnik S, Xiong C, Zhang S, Illum L, Davis SS. Drug-polyionic block copolymer interactions for micelle formation: Physicochemical characterisation. *J. Controlled Release* **2001**, *75*: 249-58.
- [4] Thunemann AF, Schutt D, Sachse R, Schlaad H, Mohwald H. Complexes of poly(ethylene oxide)-block-poly(L-glutamate) and diminazene. *Langmuir* **2006**, *22*: 2323-8.
- [5] Zemke D, Majid A. The potential of minocycline for neuroprotection in human neurologic disease. *Clin. Neuropharmacol.* **2004**, *27*: 293-8.
- [6] Klein NC, Cunha BA. Tetracyclines. *Med. Clin. N. Am.* **1995**, *79*: 789-801.
- [7] Chen M, Ona VO, Li MW, Ferrante RJ, Fink KB, Zhu S, Bian J, Guo L, Farrell LA, Hersch SM, Hobbs W, Vonsattel JP, Cha JHJ, Friedlander RM. Minocycline

- inhibits caspase-1 and caspase-3 expression and delays mortality in a transgenic mouse model of Huntington disease. *Nat. Med.* **2000**, *6*: 797-801.
- [8] Du YS, Ma ZZ, Lin SZ, Dodel RC, Gao F, Bales KR, Triarhou LC, Chernet E, Perry KW, Nelson DLG, Luecke S, Phebus LA, Bymaster FP, Paul SM. Minocycline prevents nigrostriatal dopaminergic neurodegeneration in the MPTP model of Parkinson's disease. *Proc. Natl. Acad. Sci. U. S. A.* **2001**, *98*: 14669-74.
- [9] Blum D, Chtarto A, Tenenbaum L, Brotchi J, Levivier M. Clinical potential of minocycline for neurodegenerative disorders. *Neurobiol. Dis.* **2004**, *17*: 359-66.
- [10] Lin SZ, Zhang YQ, Dodel R, Farlow MR, Paul SM, Du YS. Minocycline blocks nitric oxide-induced neurotoxicity by inhibition p38 MAP kinase in rat cerebellar granule neurons. *Neurosci. Lett.* **2001**, *315*: 61-4.
- [11] Mejia ROS, Ona VO, Li MW, Friedlander RM. Minocycline reduces traumatic brain injury-mediated caspase-1 activation, tissue damage, and neurological dysfunction. *Neurosurgery* **2001**, *48*: 1393-9.
- [12] Wells JEA, Hurlbert RJ, Fehlings MG, Yong VW. Neuroprotection by minocycline facilitates significant recovery from spinal cord injury in mice. *Brain* **2003**, *126*: 1628-37.
- [13] Wang CX, Yang T, Shuaib A. Effects of minocycline alone and in combination with mild hypothermia in embolic stroke. *Brain Res.* **2003**, *963*: 327-9.
- [14] Arvin KL, Han BH, Du YS, Lin SZ, Paul SM, Holtzman DM. Minocycline markedly protects the neonatal brain against hypoxic-ischemic injury. *Ann. Neurol.* **2002**, *52*: 54-61.
- [15] Fagan SC, Edwards DJ, Borlongan CV, Xu L, Arora A, Feuerstein G, Hess DC. Optimal delivery of minocycline to the brain: Implication for human studies of acute neuroprotection. *Exp. Neurol.* **2004**, *186*: 248-51.
- [16] Allen JC. Drugs Five Years Later: Minocycline. *Ann. Intern. Med.* **1976**, *85*: 482-7.
- [17] Zbinovsky V, Chrekian GP. Minocycline. In: Florey K, editor. Analytical Profiles of Drug Substances. New York: Academic Press, 1977. p. 323-39

- [18] Barry A, Badal R. Stability of minocycline, doxycycline, and tetracycline stored in agar plates and microdilution trays. *Curr. Microbiol.* **1978**, *1*: 33-6.
- [19] Chow KT, Chan LW, Heng PWS. Formulation of hydrophilic non-aqueous gel: Drug stability in different solvents and rheological behavior of gel matrices. *Pharm. Res.* **2008**, *25*: 207-17.
- [20] Leyden JJ. Absorption of minocycline hydrochloride and tetracycline hydrochloride: Effect of food, milk, and iron. *J. Am. Acad. Dermatol.* **1985**, *12*: 308-12.
- [21] Saivin S, Houin G. Clinical pharmacokinetics of doxycycline and minocycline. *Clin. Pharmacokinet.* **1988**, *15*: 355-66.
- [22] Xu L, Fagan S, Waller J, Edwards D, Borlongan C, Zheng J, Hill W, Feuerstein G, Hess D. Low dose intravenous minocycline is neuroprotective after middle cerebral artery occlusion-reperfusion in rats. *BMC Neurol.* **2004**, *4*: 7.
- [23] Kloppenburg M, Breedveld FC, Terwiel JP, Mallee C, Dijkmans BAC. Minocycline in active rheumatoid-arthritis - a double-blind, placebo-controlled trial. *Arthritis Rheum.* **1994**, *37*: 629-36.
- [24] Good ML, Hussey DL. Minocycline: stain devil? *Br. J. Dermatol.* **2003**, *149*: 237-9.
- [25] Davies MG, Kersey PJW. Acute hepatitis and exfoliative dermatitis associated with minocycline. *Br. Med. J.* **1989**, *298*: 1523-4.
- [26] Teitelbaum JE, Perez-Atayde AR, Cohen M, Bousvaros A, Jonas MM. Minocycline-related autoimmune hepatitis - Case series and literature review. *Arch. Pediatr. Adolesc. Med.* **1998**, *152*: 1132-6.
- [27] Lawson TM, Amos N, Bulgen D, Williams BD. Minocycline-induced lupus: clinical features and response to rechallenge. *Rheumatology* **2001**, *40*: 329-35.
- [28] Harel L, Amir J, Livni E, Straussberg RS, Varsano I. Serum-sickness-like reaction associated with minocycline therapy in adolescents. *Ann. Pharmacother.* **1996**, *30*: 481-3.
- [29] Durante-Mangoni E, Grammatikos A, Utili R, Falagas ME. Do we still need the aminoglycosides? *Int. J. Antimicrob. Agents* **2009**, *33*: 201-5.

- [30] Daniel SP, Malvika K, Christopher MB, John EK. Thermodynamics of aminoglycoside-rRNA recognition. *Biopolymers* **2003**, *70*: 58-79.
- [31] Hombach J, Hoyer H, Bernkop-Schnürch A. Thiolated chitosans: Development and in vitro evaluation of an oral tobramycin sulphate delivery system. *Eur. J. Pharm. Sci.* **2008**, *33*: 1-8.
- [32] Moazed D, Noller HF. Interaction of antibiotics with functional sites in 16s ribosomal-RNA. *Nature* **1987**, *327*: 389-94.
- [33] Roberta C, Alessandro B, Valerio P, Elisabetta M, Gian Paolo Z, Maria Rosa G. Duodenal administration of solid lipid nanoparticles loaded with different percentages of tobramycin. *J. Pharm. Sci.* **2003**, *92*: 1085-94.
- [34] Belyi IF. Actin machinery of phagocytic cells: Universal target for bacterial attack. *Microsc. Res. Tech.* **2002**, *57*: 432-40.
- [35] Freeman CD, Nicolau DP, Belliveau PP, Nightingale CH. Once-daily dosing of aminoglycosides: review and recommendations for clinical practice. *J. Antimicrob. Chemother.* **1997**, *39*: 677-86.
- [36] Nagai J, Takano M. Molecular aspects of renal handling of aminoglycosides and strategies for preventing the nephrotoxicity. *Drug Metabol. Pharmacokinet.* **2004**, *19*: 159-70.